FINITE DEFORMATIONS OF A GENERALIZED BLATZ-KO MATERIAL

by

YI WANG

A thesis submitted to the University of Plymouth

in partial fulfillment for the degree of

DOCTOR OF PHILOSOPHY

School of Mathematics and Statistics

Faculty of Technology

July 1996

To my mother and my son

ABSTRACT

FINITE DEFORMATIONS OF A GENERALIZED BLATZ-KO MATERIAL

YI WANG

In this dissertation, the finite deformations of a certain class of compressible, isotropic elastic materials are investigated. The class is characterized by a two-parameter family of strain energy functions which includes the well-known Blatz-Ko material model for foam rubbers. The Blatz-Ko material, which has been arrived at by experiment and whose deformations have been studied previously, is obtained from the considered class of materials by specifying one of the two parameters involved in the definition of the class. On employing the semi-inverse method, according to which the form of the solution is given at the outset in terms of functions which are then determined from the equilibrium equations and boundary conditions, closed-form solutions to the equilibrium equations are obtained for the non-homogeneous deformations describing the straightening of a sector of a circular tube, the bending of a rectangular block into a sector of a circular tube, the eversion of cylindrical and spherical shells, and the cylindrical and spherical expansions, and a number of associated boundary value problems are investigated using both analytical and numerical methods. Certain situations in which solutions of the pre-assigned form cannot exist are identified and cases of non-uniqueness are dealt with by discriminating between the different solutions on physical grounds. The homogeneous deformations of the materials in this class are also examined and, throughout, comparison is being made with the behaviour of the Blatz-Ko material. For the whole range of deformations examined, it is found that the materials for which one of the parameters is greater than, or equal to, two (the case when this parameter equals to two corresponds to the Blatz-Ko material) become harder as this parameter increases, but that otherwise they all behave in a similar manner. Consequently, it is concluded that the materials in this particular subclass will also represent foam rubbers of the type described by the Blatz-Ko material. In order to describe the situations in which the solutions become unstable, the conditions for the strong ellipticity of the equilibrium equations for non-linearly elastic materials are reformulated so as to be expressible in terms of the derivatives of the strain-energy function regarded as a function of the principal stretches. Use of these conditions reveals that the solutions to the considered boundary value problems become unstable at certain critical values of the applied loads.

ACKNOWLEDGMENTS

I would like to express my sincerest thanks to my supervisor Dr. Marian Aron for his constructive supervision and support throughout this study and also to my second supervisor Dr. David Wilton for his encouragement and support in many ways.

I would like to thank the University of Plymouth for providing me the studentship and funding to attend conferences. Special thanks go to the School of Mathematics and Statistics for providing such a nice research and study environment.

I wish to thank my fellow researchers in the School of Mathematics and Statistics, particularly Hazel, Jenny, and Christine for their help.

Finally I must thank my mother for her encouragement and moral support and also my son for the busy and colourful life that we share together.

AUTHOR'S DECLARATION

At no time during the registration for the degree of Doctor of Philosophy has the author been registered for any other University award.

This study was financed with the aid of a studentship from the University of Plymouth.

The work was partially presented at a number of national and international conferences and several papers have been published or will be published in the near future.

Publications:

- Y. Wang, M. Aron; A reformulation of the strong ellipticity conditions for unconstrained hyperelastic media, to appear in *J. Elasticity.*
- Y. Wang, M. Aron; Radial deformations of cylindrical and spherical shells composed of a generalized Blatz-Ko material, to appear in *J. Applied Mathematics and Mechanics(ZAMM).*
- M. Aron, Y. Wang; Remarks concerning the flexure of a compressible non-linearly elastic rectangular block, *J. Elasticity*, 1995, Vol.40, pp99-106.
- M. Aron, Y. Wang; On deformations with constant modified stretches describing the bending of rectangular blocks, *Quarterly Journal of Mechanics and applied Mathematics*, 1995, Vol.48, Pt.3, pp375-386.

Presentations:

- M. Aron, Y. Wang; On deformations with constant modified stretches describing the bending of rectangular blocks, the British Applied Mathematics Colloquium, April, 1994, Sheffield.
- Y. Wang, M. Aron; Some deformations of a generalized Blatz-Ko material, the British Applied Mathematics Colloquium, April, 1995, Birmingham. Awarded as the second Eric Watson prize for the best postgraduate talk.
- Y. Wang, M. Aron; Radial deformations of cylindrical and spherical shells composed of a generalized Blatz-Ko material, the Third International Congress on Industrial and Applied Mathematics, July, 1995, Hamburg.
- Y. Wang, M. Aron; The bending of a rectangular block into a sector of a circular tube composed of a generalized Blatz-Ko material, the British Applied Mathematics Colloquium, April, 1996, Loughborough.

Signed....Yi Wang.....

Date..2nd July 1996

Contents

List of Tables

List of Figures

Chapter 1

Introduction

1.1 Motivation and aim

Since the early 1940's, there has been enormous progress in the development of the theory of finite elasticity. Significant theoretical results, many confirmed by experiments, have projected considerable light on the physical behaviour of rubber-like materials such as synthetic elastomers, polymers, and biological tissues, in addition to natural rubber. This success has since brought numerous interdisciplinary publications in other important areas of physical science, which include thermomechanics, electromechanics, etc. and the foundations laid for the theory of finite elasticity now support new fields of study, such as couple stress and multipolar continuum theories. Consequently, the finite elasticity theory has attracted an intensive attention from many researchers.

As is well known, one of the conceptual differences between problems of the clas-

sical linear theory of elasticity and those of the theory of finite elasticity is that the specification of the form of the strain energy function, which represents the constitutive relation of a specific material, is generally an inherent part of problems of the finite elasticity theory, whereas in the classical theory one need only specify the material constants occurring in the generalized Hooke's Law. This is not a trivial difficulty since the rubber-like materials considered in the finite elasticity theory each behave differently and both the form and parameters of the material model (strain energy function) need to be determined experimentally. Unfortunately, there is relatively little experimental work reported in the open literature. Such work is reported by Rivlin & Saunders [1], Fung [2], Blatz & Ko [3], Veronda & Westman [4], Christensen [5], Fong & Penn [6], Flory & Tatara [7], Ogden [8], Peng & Landel [9], and reviews have been given by Treloar [10] and Ogden [11]. By combining theoretical and experimental results some material models have been proposed, which include the neo-Hookean material, the Mooney-Rivlin material, and the Blatz-Ko material (cf. [12, Section 2.9]). It is known that the latter is used to describe foam rubbers, which belong to the category of compressible isotropic elastic materials. Nevertheless, new forms of the strain energy function are still needed to suit the wide diversity of rubber-like materials, and this need provides the motivation for the present study. Accordingly, the aim of this study is to assess the suitability of a certain theoretical material model (which generalizes the Blatz-Ko material) to represent foam rubbers.

1.2 The Blatz-Ko material

With the intention to include the effect of compressibility of rubbery materials, in 1962, Blatz & Ko proposed a strain energy function W in the form [3]:

$$W = \frac{1}{2}\mu f\{i_1 - 1 - \frac{1}{\nu} + \frac{1-2\nu}{\nu} i_3^{\frac{-2\nu}{1-2\nu}}\} + \frac{1}{2}\mu(1-f)\{i_2 - 1 - \frac{1}{\nu} + \frac{1-2\nu}{\nu} i_3^{\frac{2\nu}{1-2\nu}}\} \quad (1.1)$$

where μ, f, ν are constants and

$$\begin{aligned} i_1 &= \lambda_1^2 + \lambda_2^2 + \lambda_3^2, \\ i_2 &= \lambda_1^{-2} + \lambda_2^{-2} + \lambda_3^{-2}, \\ i_3 &= \lambda_1\lambda_2\lambda_3. \end{aligned} \quad (1.2)$$

Here λ_i are the principal stretches and μ, ν are material constants corresponding to the ground state shear modulus and the Poisson's ratio respectively (see Chapter 2 of this thesis for notations of the theory of finite elasticity). With a view toward determining the material constants in the material model (1.1), Blatz & Ko also reported their experimental results on a batch of polyurethane foam rubber in [3]. The foam rubber was prepared by leaching out salt from a filled composite. The resultant foams have 47 vol. % voids, about 40 μ in diameter, and was tested in uniaxial, strip biaxial, and homogeneous biaxial tension on an Instron machine. A summary of their experimental results is presented in Table 1.1. Thus, it follows that in the case of a 47 vol. % foamed polyurethane rubber the material model (1.1) reduces to

$$W = \frac{1}{2}\mu\{\lambda_1^{-2} + \lambda_2^{-2} + \lambda_3^{-2} + 2\lambda_1\lambda_2\lambda_3 - 5\}. \quad (1.3)$$

Type Test	μ (p.s.i.)	f	ν
Simple tension	38	0.13	1/4
Strip-biaxial tension	29	0.07	1/4
Homogeneous-biaxial tension	27	-0.19	1/4
Average value	32	0	1/4

Table 1.1: Experimental results.

It is of interest to note that two of the samples in Blatz & Ko's uniaxial test fractured at 140% strain (the corresponding stretch is 2.4) and that they observed that these are the values beyond which the sample is caused to snap by a slight increase in load. According to their comments, although these so-called ultimate values say nothing about the details of the fracture mechanics, they give an upper bound to the strain level beyond which fracture initiates in a given sample. Also we realize that the above mentioned experimental result imposes a restriction upon the material model (1.3) in practice. This material model (1.3) is well known as the *Blatz-Ko material* and has attracted an intensive attention from many researchers [13, 14, 15, 16, 17, 18, 19].

In 1975, Knowles & Sternberg reported their results on the ellipticity of the equations of finite elastostatics for the Blatz-Ko material, in which they have obtained explicit necessary and sufficient conditions, in terms of restrictions upon the principal stretches, for the strong ellipticity of the material [13]. In their following work [20], they discussed the failure of ellipticity and the emergence of discontinuous deformation

gradients in plane finite elastostatics for the Blatz-Ko material, in which it was revealed that "Elastostatic shocks" exist when the governing equations of equilibrium suffer a loss of ellipticity. Knowles & Sternberg's work also imposes restrictions upon the material model (1.3) in the sense that it provides us with upper and lower bounds for the ratio of the principal stretches which when violated, imply that the corresponding solutions are unstable (see [47, Section 68b]).

In their work on the Poisson function of finite elasticity, Beatty & Stalnaker [21] derived the Poisson function for the Blatz-Ko material and the relations of the Poisson function to the classical Poisson's ratio were discussed in details. Also they have shown that the material model (1.1) is the unique hyperelastic material for which the coefficients in the Cauchy stress response relation depend on i_3 alone.

Since 1985 systematical research in finding closed-form equilibrium solutions for non-homogeneous deformations of elastic solids composed of the Blatz-Ko material has been carried out. This work was initiated by Abeyaratne and Horgan [15] who have obtained closed-form solutions describing the expansion of a cavity in an infinite body. Using the substitution employed in [15] for solving the radial equilibrium equation, closed-form solutions describing the radial deformation of hollow spheres and cylinders have been obtained in [22, 16] (see also [23]). Discussions on the radial expansion problem in the case of uniform pressure, either internal or external, reveal that (i) these axisymmetric solutions only exists when the pressures are within a certain interval, (ii) the strong ellipticity condition is violated for certain critical values of the applied

pressures, and (iii) non-uniqueness of the solution exists for the boundary value problem. In 1990, several closed-form equilibrium solutions for the Blatz-Ko material were presented by Carroll & Horgan in [17], which include deformations that describe the bending of a cylindrical sector into another cylindrical sector, the straightening of a cylindrical sector, the bending of a block into a cylindrical sector, the expansion, compaction and the eversion of cylinders or spheres, and the torsion with axial extension of circular cylinders or tubes. The torsion problem for this material is also investigated in [24] and [25]. In [24] it is shown that axisymmetric anti-plane shear is not possible in the material (1.3) (see also [26]) and in [27] and [30] it is shown that pure azimuthal shear is also not possible in this material.

The Blatz-Ko material model also has appeared in other researchers' publications, such as [28] and [29].

It is noted that the Blatz-Ko material model is a successful example in finding the constitutive relation for a specific material. But more material models are still needed to fit the wide diversity in the characteristics of compressible elastic materials. To this end, similar combinative experimental and theoretical work has been done for other compressible elastic materials and various material models have been proposed, such as the compressible neo-Hookean material (cf. [31, 32]), the compressible Varga material [33, 34], the harmonic material [35], *etc.* Also a great deal work has been done in generalizing existing material models to widen the use of these known successful models. The various generalizations of the Blatz-Ko material will be discussed in the

next section.

1.3 Various generalizations

In 1988, Willson and Myers considered a strain energy function of the form [36]

$$W = \mu[\frac{n}{2}(\lambda_1^{-2} + \lambda_2^{-2} + \lambda_3^{-2}) + \frac{n-1}{2}(\lambda_1^2 + \lambda_2^2 + \lambda_3^2) + \frac{1}{2} + \lambda_1\lambda_2\lambda_3 - 3n] \qquad (1.4)$$

where n is a material constant and the constraint $n \geq 1$ was imposed upon (1.4) so as to secure a physical response. It is readily checked that the material model (1.4) reduces to the Blatz-Ko material model in the case when $n = 1$. This material model was used in their further work [37].

In 1991, Silling used a specific strain energy function in his research on the creasing singularity problem, which, in plane strain, is in the form [38]

$$W = a(\lambda_1^{-k}\lambda_2^{-l} + \lambda_2^{-k}\lambda_1^{-l} - 2) + a(k+l)(\lambda_1\lambda_2 - 1), \qquad (1.5)$$

where k, l, and a are material constants, $a > 0$. He assumed that $k \geq l$, $k + l > 0$. This material model is related to the Blatz-Ko material by replacing k with 2 and l with zero.

In 1978, based on principal stretches λ_i, Hill proposed a particular isotropic form of strain energy function [39] as

$$W = \sum \frac{c^{(m)}}{m}\{\lambda_1^m + \lambda_2^m + \lambda_3^m - 3 + \frac{1}{n}[(\lambda_1\lambda_2\lambda_3)^{-mn} - 1]\} \qquad (1.6)$$

where the summation extends over associated pairs $m, c^{(m)}$ of constitutive parameters, n being an additional material constant. The ground state shear modulus is by (1.6)

$$\mu = \frac{1}{2}\sum mc^{(m)} \tag{1.7}$$

and the corresponding bulk modulus is

$$\kappa = (n + \frac{1}{3})\sum mc^{(m)}. \tag{1.8}$$

Thus, for a stable stress-free ground state to exist, it is required that

$$\sum mc^{(m)} > 0 \tag{1.9}$$

and

$$n > -\frac{1}{3}. \tag{1.10}$$

It is noted that the material model (1.6) reduces to the Blatz-Ko material (1.3) when $m_1 = -2, n = 1/2$. The material constants in the Hill's material model were determined by Storakers' experiments for two vulcanized foam rubbers [40]. For the selected natural rubber in their experiment, which is considered to be highly compressible, the material constants are

$$m_1 = -m_2 = 4.5, \quad c^{(1)} = 1.85, c^{(2)} = -9.20, \quad n = 0.92 \tag{1.11}$$

and for the synthetic ethylenepropylendiene rubber, which is considered to be slightly compressible, the material constants are

$$m_1 = -m_2 = 3.6, \quad c^{(1)} = 2.04, c^{(2)} = -0.51, \quad n = 25 \tag{1.12}$$

in which the constants $c^{(i)}$ being expressed in $10^{-2}N\,mm^{-2}$.

In Haughton's research work on the cavitation in compressible elastic membranes [41], Haughton used a certain form of strain energy function to represent a class of compressible elastic materials:

$$W = \frac{\mu}{\beta}(\lambda_1^{-\beta} + \lambda_2^{-\beta} + \lambda_3^{-\beta} + \beta\lambda_1\lambda_2\lambda_3 - \beta - 3),\ \mu > 0,\ \beta > 0, \tag{1.13}$$

where μ and β are positive material constants. This is a one-term specialization of Hill's strain energy function ($n = 1/\beta$, cf. (1.6)) and this material model represents the Blatz-Ko material (1.3) when $\beta = 2$. This material model has also been used by Biwa in 1995 in his work on the critical stretch for formation of a cylindrical void [42].

According to the work of Aron & Aizicovici [43], the restriction of (1.13) to plane strain belongs to a class of strain energies for which the (in-plane) mean Cauchy stress corresponding to any purely distortional deformation originating from a given ground state is dominated by the (in-plane) mean Cauchy stress in that ground state. It is noticed in [43] that solid rubbers satisfy the opposite inequalities and thus, despite lack of experimental evidence, for $\beta \neq 2$, we have reason to believe that (1.13) may also be capable of describing foam rubbers.

The above mentioned generalized forms of the Blatz-Ko material have provided us with more flexibility and wider choices of material models. We note that, in particular, the strain energy function (1.13) was obtained by specialization from a family of strain energy functions which were supported by experiments and moreover, that (1.13) is expected to represent foam rubbers by theoretical analysis. Therefore, we will use this

material model in this study and we call it the *generalized Blatz-Ko material.*

1.4 Methods and results

In this study we investigate the mechanical features of the materials in the class (1.13) with $\beta \neq 2$ and comparison is being made with the mechanical features of the Blatz-Ko material. Such comparative method has been used in literature (see [31, 13]). To this end, we need to find closed-form solutions in the context of finite elasticity. As it is well known, another conceptual difference between the problems of the classical linear theory of elasticity and those of the theory of finite elasticity is the inherent non-lineality of the governing equations. This adds considerable difficulty to the problem of finding exact solutions for problems of finite elasticity, which are very valuable and useful in understanding mechanical features of materials and in the design of mechanical experiments. In 1954 and 1955, Ericksen has examined the problems of finding all of the deformations which can be supported, in the absence of body force, in all homogeneous, isotropic incompressible elastic solids [44], or in all homogeneous, isotropic compressible elastic solids [45]. The first category consists of all isochoric homogeneous deformations and five families of non-homogeneous deformations, the so called controllable or universal deformations (see [44] and [46]). The second category consists of homogeneous deformations only, i.e., there is no non-homogeneous deformation which can be supported in every compressible isotropic elastic material without applying a body force. This latter result implies that non-homogeneous deformations

can be discussed for compressible elastic solids, only in the context of a particular strain energy function, or a class of strain energy functions. For compressible elastic solids, in particular, the analysis of such deformations is usually very complicated even for simple forms of the strain energy function and very few closed form solutions have been obtained. In this study, we first compare the material characteristics of the materials (1.13) with $\beta \neq 2$ with those of the Blatz-Ko material by considering homogeneous deformations. Specifically, we discuss the isotropic extension, the isotropic plane stress, the uni-axial tension, the isotropic plane strain, the plane-strain uni-axial tension, and the simple shear deformation. From the analysis of these deformations we have obtained the following conclusions:

(i) For all values of $\beta > 0$, the distributions of Cauchy and Piola stresses are qualitatively similar in the isotropic extension, the uni-axial tension, the isotropic plane strain, and the plane-strain uni-axial tension and they indicate that the material hardens as β increases.

(ii) For all values of $\beta > 1$, the distributions of Piola stresses in isotropic plane stress are qualitatively similar and they indicate that the material hardens as β increases. For $\beta \leq 1$, however, the distributions of Piola stresses corresponding to this deformation are qualitatively different from the distributions in the case when $\beta > 1$, although they still indicate that the material hardens as β increases.

(iii) For all values of $\beta \geq 2$, the distributions of Cauchy stresses in the simple shear deformation are qualitatively similar and they indicate that the material hardens as β

increases. For $\beta < 2$, however, the distributions of Piola stresses corresponding to this deformation are qualitatively different from the distributions in the case when $\beta \geq 2$. In particular for $\beta < 2$, we can no longer conclude that the material hardens as β increases.

Next, we carry out the comparison by considering non-homogeneous deformations. We use the semi-inverse method, according to which the form of the solution is given at the outset in terms of functions which are then determined from the equilibrium equations and boundary conditions and, by generalizing the work of Carroll & Horgan [17], Abeyarante & Horgan [15], and Chung, Horgan & Abeyaratne [16], we obtain closed-form solutions to the equilibrium equations for the non-homogeneous deformations describing the straightening of a sector of a circular tube, the bending of a rectangular block into a sector of a circular tube, the eversion of cylindrical and spherical shells, and the cylindrical and spherical expansions. Additionally, also following these authors and using both analytical and numerical methods, we investigate a number of associated boundary value problems and, by means of a qualitative analysis, conclude that in respect of these deformations the materials in this class become harder as the material parameter β increases, but that otherwise they all behave in a similar manner.

Also, in this dissertation we pay special attention to considerations of stability, non-existence and non-uniqueness of solutions since these are incorporated inherently with problems in finite elasticity. In order to describe the situations in which the solutions become unstable, we reformulate the conditions for the strong ellipticity of

the equilibrium equations for non-linearly elastic materials so as to be expressible in terms of the derivatives of the strain-energy function regarded as a function of the principal stretches. By using these conditions we obtain necessary and sufficient conditions, in terms of restrictions upon the principal stretches, for the strong ellipticity of the material (1.13) (thereby generalizing the results arrived at in [13]) and find that for the six considered non-homogeneous deformations, the solutions become unstable for certain values of boundary conditions. (Consequently, we expect that solutions of a form different from those assigned initially will describe the deformations in these circumstances.) Conditions, in terms of boundary data in which solutions of the pre-assigned form do not exist, are also described here and instances of non-uniqueness of solution are dealt with by selecting on physical grounds the solution which appears to be the most plausible.

On the basis of the qualitative analysis involving both homogeneous and non-homogeneous deformations we conclude that all of the materials (1.13) for which $\beta \geq 2$ behave in the same manner and, consequently, that the materials (1.13) for which $\beta > 2$ also represent foam rubbers of the type described by the Blatz-Ko material ($\beta = 2$), the Blatz-Ko material being the softest material in the subclass defined by $\beta \geq 2$.

Chapter 2

Basic concepts and preliminaries

In this chapter we give an outline of the theory of continuum mechanics and discuss some preliminaries. In Section 2.1 we describe the kinematics of particles, in Section 2.2 we discuss the stress and equilibrium equations, in Section 2.3 we deal with the constitutive equations, and Section 2.4 is devoted to a discussion of various restrictions which are imposed upon the constitutive equations including the stability restriction. Lastly, Section 2.5 will describes briefly the basic formulas which are pertinent to plane strain. These notations can be found in many books (e.g., Truesdell & Noll [47], Truesdell [48], Atkin & Fox [12], Spencer [49], Ogden [50], etc.).

2.1 Kinematics of particles

Let $\{\mathbf{O}; \mathbf{e}_i\}$ be a fixed Cartesian coordinate system with an origin point $\mathbf{O}$ and an orthonormal vector basis$\{\mathbf{e}_i\}$ in an Euclidean space of three dimensions. A *place* is a

point in the Euclidean space, denoted by a set of coordinates (X_1, X_2, X_3), or position vector $\mathbf{X}$. A *body* $\Re$ is a set of material points, called *particles*, each particle of the set occupies a place in the Euclidean space, and is identified uniquely by its position vector at each instant of time t. At some reference time t_0, a typical particle occupies a unique point in the Euclidean space, denoted by its position vector $\mathbf{X}$. The position vector $\mathbf{X}$ is regarded as a label of the particle. We refer to such a particle as the particle $\mathbf{X}$. The domain $\Omega_0 = \{\mathbf{X}\}$ in the Euclidean space occupied by the body at time t_0 is called *a reference configuration.* At time t, the particle moves to a position, denoted by its present position vector $\mathbf{x}$,

$$\mathbf{x} = \mathbf{x}(\mathbf{X}, t), \ \mathbf{X} \in \Omega_0, \tag{2.1}$$

or, in component form,

$$x_1 = x_1(X_1, X_2, X_3, t), \ x_2 = x_2(X_1, X_2, X_3, t), \ x_3 = x_3(X_1, X_2, X_3, t),$$

which means that a particle with position vector $\mathbf{x}$ at time t was the particle with position vector $\mathbf{X}$ at the reference time t_0. The domain $\Omega = \{\mathbf{x}\}$ in the Euclidean space occupied by the body at time t is called *a configuration of the body at time* t, or *a current configuration* (see Figure 2.1). We assume that the function $\mathbf{x}(\mathbf{X}, t)$ are differentiable with respect to $\mathbf{X}$ and t as many times as required.

We restrict our attention to equilibrium problems only. Thus, we consider only two configurations of a body, an initial configuration and a final configuration. We refer to the mapping from the initial configuration to the final configuration as a *deformation* of

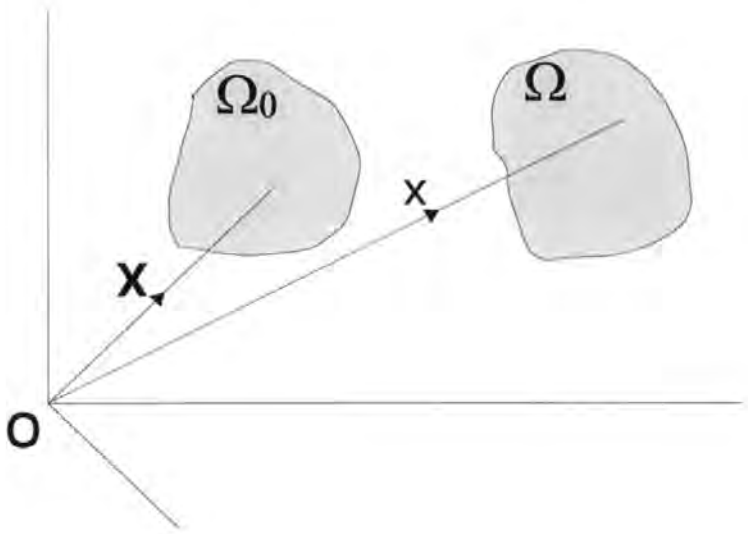

Figure 2.1: A body in the Euclidean space

the body. Therefore, the two configurations may be called the *undeformed configuration* and the *deformed configuration*, respectively. Thus we can omit the time t in (2.1), which is now in form

$$\mathbf{x} = \mathbf{x}(\mathbf{X}),\ \mathbf{X} \in \Omega_0. \tag{2.2}$$

We assume that the Jacobian

$$J \equiv \det[\partial x_i / \partial X_j]^* \tag{2.3}$$

exists at each point of Ω and that

$$J > 0. \tag{2.4}$$

*Letters in boldface denote vectors, second-order tensors, and matrices. Latin and Greek subscripts have the respective ranges (1,2,3) and (1,2). We employ the usual summation convention.

The physical significance of these assumptions is that the material of the body cannot penetrate itself, and that material occupying a finite non-zero volume in Ω_0 cannot be compressed to a point or expanded to infinite volume during the deformation. Mathematically (2.4) implies that (2.2) can be inverted uniquely.

We denote

$$\mathbf{F} \equiv \nabla \mathbf{x} = [\partial x_i / \partial X_j] \tag{2.5}$$

and call $\mathbf{F}$ the *deformation gradient.* In view of (2.3) and (2.4), tensor $\mathbf{F}$ is non-singular and can be decomposited uniquely into

$$\mathbf{F} = \mathbf{RU}, \quad \mathbf{F} = \mathbf{VR}, \tag{2.6}$$

where $\mathbf{U}$ and $\mathbf{V}$ are positive-definite symmetric tensors and $\mathbf{R}$ is a proper orthogonal tensor (see the polar decomposition theorem, cf. Spencer [49], Section 2.5, etc.). The physical significance of the decomposition (2.6) is that the deformation (2.5) may be split into two parts, i.e., a rigid rotation by $\mathbf{R}$ followed by a local stretching by $\mathbf{U}$, or a local stretching by $\mathbf{V}$ followed by the same rigid rotation of $\mathbf{R}$. The tensors $\mathbf{U}$ and $\mathbf{V}$ are known as the *right* and *left stretching tensors* respectively. Since the calculation of the tensors $\mathbf{U}$ and $\mathbf{V}$ may be awkward, i.e., may require irrational operations, it is customary to use their squares

$$\mathbf{C} \equiv \mathbf{F}^T\mathbf{F} = \mathbf{U}^2, \ \mathbf{B} \equiv \mathbf{F}\mathbf{F}^T = \mathbf{V}^2.^{\dagger} \tag{2.7}$$

---

†The superscript T will always indicate transposition.

These are also positive-definite symmetric tensors and are known as the *right* and *left Cauchy-Green strain tensors*, respectively. Since $\mathbf{V}$ ($\mathbf{U}$) is a positive-definite symmetrical tensor, there exists a set of axes $\{\mathbf{v}^i\}$ ($\{\mathbf{u}^i\}$), known as the *principal axes of stretch*, referred to which $\mathbf{V}$ ($\mathbf{U}$) is diagonal

$$\mathbf{V} = \sum_{i=1}^{3} \lambda_i \mathbf{v}^i \otimes \mathbf{v}^i, \ \mathbf{U} = \sum_{i=1}^{3} \lambda_i \mathbf{u}^i \otimes \mathbf{u}^i; \tag{2.8}$$

and the diagonal values $\{\lambda_i\}$ of $\mathbf{U}$ ($\mathbf{V}$) are called the *principal stretches*. $\mathbf{U}$ and $\mathbf{V}$ ($\mathbf{C}$ and $\mathbf{B}$) have the same principal stretches λ_i (λ_i^2) but different principal axes, and $\mathbf{R}$ is the rotation which carries the principal axes of $\mathbf{U}$ into the principal axes of $\mathbf{V}$, that is, $\mathbf{v}^i = \mathbf{R}\mathbf{u}^i$. The *principal invariants* $\{I_i\}$ of the strain tensor $\mathbf{C}$ ($\mathbf{B}$) are given by

$$\left.\begin{aligned} I_1 = \mathrm{tr}\mathbf{C} = \lambda_1^2 + \lambda_2^2 + \lambda_3^2, \\ I_2 = \tfrac{1}{2}[(\mathrm{tr}\mathbf{C})^2 - \mathrm{tr}(\mathbf{C}^2)] = \lambda_1^2\lambda_2^2 + \lambda_1^2\lambda_3^2 + \lambda_2^2\lambda_3^2, \\ I_3 = \det\mathbf{C} = \lambda_1^2\lambda_2^2\lambda_3^2. \end{aligned}\right\} \tag{2.9}$$

2.2 Stress and the equilibrium equation

Now we turn to another important factor in continuum mechanics – force. The forces acting on a part $\wp$ of a body $\Re$ in a configuration Ω at time t are of two kinds: *body forces* $\mathbf{f}_b$, which are continuous function of the volume V of $\wp$, and the *contact force* $\mathbf{f}_c$, which is a continuous function of the surface area A of the boundary $\partial\wp$ of $\wp$. The two densities $\mathbf{b}$ and $\mathbf{t}$, defined as

$$\mathbf{b} = \lim_{\delta V \to 0} \frac{\delta \mathbf{f}_b}{\rho \delta V}, \ \mathbf{t} = \lim_{\delta A \to 0} \frac{\delta \mathbf{f}_c}{\delta A},$$

are called the *specific body force* and the *traction*, respectively. Here ρ denotes the density of mass. The *Euler-Cauchy stress principle* assumes that the traction $\mathbf{t}$ can be expressed as

$$\mathbf{t} = \mathbf{t}(\mathbf{x}, \mathbf{n}),$$

where $\mathbf{n}$ is the outer normal to $\partial\wp$ in the deformed configuration. Clearly $\mathbf{t}$ depends on the position of $\wp$ and the direction of $\mathbf{n}$. It follows through Cauchy's *fundamental lemma* that there exists a tensor $\mathbf{T}(\mathbf{x})$, called the *Cauchy stress tensor*, such that

$$\mathbf{t}(\mathbf{x}, \mathbf{n}) = \mathbf{T}(\mathbf{x})\mathbf{n}. \tag{2.10}$$

We consider a body $\mathfrak{R}$ in a configuration Ω in equilibrium. The *Cauchy first law of continuum mechanics* gives the *equations of equilibrium* as

$$\mathrm{div}\mathbf{T} + \rho\mathbf{b} = \mathbf{0}, \text{ on } \Omega. \tag{2.11}$$

We regard the body force $\mathbf{b}$ as negligible and omit it henceforward. Thus, in the absence of body forces, the equilibrium equation (2.11) reduces to

$$\mathrm{div}\mathbf{T} = \mathbf{0}, \text{ on } \Omega. \tag{2.12}$$

The *Cauchy second law of continuum mechanics* yields

$$\mathbf{T} = \mathbf{T}^T, \tag{2.13}$$

that is, $\mathbf{T}$ is confined to the space of symmetric tensors. The component form of the equilibrium equation (2.12), in terms of the physical components of $\mathbf{T}$ in a Cartesian

coordinate system, is

$$\begin{aligned}
&\frac{\partial T_{xx}}{\partial x}+\frac{\partial T_{xy}}{\partial y}+\frac{\partial T_{xz}}{\partial z}=0,\\
&\frac{\partial T_{xy}}{\partial x}+\frac{\partial T_{yy}}{\partial y}+\frac{\partial T_{yz}}{\partial z}=0,\\
&\frac{\partial T_{xz}}{\partial x}+\frac{\partial T_{yz}}{\partial y}+\frac{\partial T_{zz}}{\partial z}=0,
\end{aligned} \tag{2.14}$$

and, in a cylindrical polar coordinate system, is

$$\begin{aligned}
&\frac{\partial T_{rr}}{\partial r}+\frac{1}{r}\frac{\partial T_{r\theta}}{\partial \theta}+\frac{\partial T_{rz}}{\partial z}+\frac{1}{r}(T_{rr}-T_{\theta\theta})=0,\\
&\frac{\partial T_{\theta r}}{\partial r}+\frac{1}{r}\frac{\partial T_{\theta\theta}}{\partial \theta}+\frac{\partial T_{\theta z}}{\partial z}+\frac{2}{r}T_{\theta r}=0,\\
&\frac{\partial T_{zr}}{\partial r}+\frac{1}{r}\frac{\partial T_{z\theta}}{\partial \theta}+\frac{\partial T_{zz}}{\partial z}+\frac{1}{r}T_{zr}=0,
\end{aligned} \tag{2.15}$$

where (r,θ,z) are cylindrical polar coordinates. In a spherical polar coordinate system, the component form of equation (2.12) is given by

$$\begin{aligned}
&\frac{\partial T_{rr}}{\partial r}+\frac{1}{r}\frac{\partial T_{r\theta}}{\partial \theta}+\frac{1}{r\sin\theta}\frac{\partial T_{r\phi}}{\partial \phi}+\frac{1}{r}(2T_{rr}-T_{\theta\theta}-T_{\phi\phi}+\cot\theta T_{r\theta})=0,\\
&\frac{\partial T_{\theta r}}{\partial r}+\frac{1}{r}\frac{\partial T_{\theta\theta}}{\partial \theta}+\frac{1}{r\sin\theta}\frac{\partial T_{\theta\phi}}{\partial \phi}+\frac{1}{r}[3T_{r\theta}+\cot\theta(T_{\theta\theta}-T_{\phi\phi})]=0,\\
&\frac{\partial T_{\phi r}}{\partial r}+\frac{1}{r}\frac{\partial T_{\phi\theta}}{\partial \theta}+\frac{1}{r\sin\theta}\frac{\partial T_{\phi\phi}}{\partial \phi}+\frac{1}{r}(3T_{r\phi}+2\cot\theta T_{\theta\phi})=0,
\end{aligned} \tag{2.16}$$

in which (r,θ,ϕ) are spherical polar coordinates.

As the consequence of symmetry of the Cauchy stress tensor $\mathbf{T}$, there exists a set of orthonormal axes $\{\mathbf{t}^i\}$, known as the *principal axes of stress*, referred to which, the tensor $\mathbf{T}$ is diagonal. The principal values $\{\tau_i\}$ of $\mathbf{T}$ are known as the *principal stresses* and we can write

$$\tau=\tau_i\mathbf{t}^i. \tag{2.17}$$

It is seen that the Cauchy stress tensor $\mathbf{T}$ enables us to calculate stress vectors measured per unit area of the surface in the current configuration Ω. In some situations it is more convenient to calculate the stress vectors in Ω measured per unit area of the corresponding element of surface in the reference configuration Ω_0. Therefore, the stress tensor $\mathbf{S}$, known as the *Piola stress tensor*, is introduced to describe the stress tensors measured per unit area of the surface in the reference configuration Ω_0, and this is related to the Cauchy stress through the rule

$$\mathbf{S} = J\mathbf{T}\mathbf{F}^{-T}. \tag{2.18}$$

In terms of $\mathbf{S}$ the equilibrium equation (2.12) and the symmetry condition (2.13) become

$$\mathrm{Div}\mathbf{S} = \mathbf{0}, \text{ on } \Omega_0, \tag{2.19}$$

and

$$\mathbf{S}\mathbf{F}^T = \mathbf{F}\mathbf{S}^T, \tag{2.20}$$

respectively. It is known that the Piola stress $\mathbf{S}$ is not symmetric in general.

2.3 Constitutive equations and the formulation of problems

A material is specified by its constitutive equation which relates the stress with deformation. The basic assumption of elasticity is that the stress depends upon the

deformation only through the deformation gradient $\mathbf{F}$, i.e.,

$$\mathbf{T} = \varphi(\mathbf{F}),\ T_{ij} = \varphi_{ij}(F_{kl}),\ \varphi_{ij} = \varphi_{ji}. \tag{2.21}$$

The theory of elasticity based on (2.21) is usually referred to as *Cauchy elasticity*. It is further assumed that there exists a single-valued scalar potential function $W(\mathbf{F})$, known as the *strain energy function*, such that

$$\mathbf{S} = \frac{\partial W(\mathbf{F})}{\partial \mathbf{F}},\ \text{or}\ \ \mathbf{T} = J^{-1}\frac{\partial W(\mathbf{F})}{\partial \mathbf{F}}\mathbf{F}^T. \tag{2.22}$$

This assumption was given by the justification on physical grounds by Sternberg & Knowles [51]. An elastic material which satisfies this assumption is called a *hyperelastic material*, and the theory of elasticity incorporating this further assumption is known as *Green elasticity* or *hyperelasticity*. The utilization of the *principle of material frame indifference* to the strain energy function W reveals that for hyperelastic materials the strain energy function W depends on the deformation gradient $\mathbf{F}$ only through the strain tensor $\mathbf{C}$, i.e.,

$$W(\mathbf{F}) = W(\mathbf{U}) = \tilde{W}(\mathbf{C}), \tag{2.23}$$

in which case, the stress tensors $\mathbf{T}$ and $\mathbf{S}$ are given by

$$\mathbf{S} = 2\mathbf{F}\frac{\partial \tilde{W}(\mathbf{C})}{\partial \mathbf{C}},\ \text{or}\ \ \mathbf{T} = 2J^{-1}\mathbf{F}\frac{\partial \tilde{W}(\mathbf{C})}{\partial \mathbf{C}}\mathbf{F}^T. \tag{2.24}$$

For an *isotropic*, hyperelastic material, the strain energy function W is a function of the principal invariants $\{I_i\}$ of $\mathbf{C}$ (or $\mathbf{B}$) alone and we have

$$\tilde{W}(\mathbf{C}) = \hat{W}(I_1, I_2, I_3) = W(\lambda_1, \lambda_2, \lambda_3). \tag{2.25}$$

Hence, the use of (2.25) in the last of (2.24) yields the following two useful forms of the general *constitutive equation for an isotropic, hyperelastic material*

$$\mathbf{T} = \alpha_0\mathbf{1} + \alpha_1\mathbf{B} + \alpha_2\mathbf{B}^2, \tag{2.26}$$

or, by use of the Cayley-Hamilton theorem,

$$\mathbf{T} = \beta_0\mathbf{1} + \beta_1\mathbf{B} + \beta_{-1}\mathbf{B}^{-1}. \tag{2.27}$$

The scalar coefficients α_i and β_i are given in terms of the strain energy function by

$$\begin{aligned}
\beta_0 &= \alpha_0 - I_2\alpha_2 = \frac{2}{\sqrt{I_3}}[I_2\frac{\partial\hat{W}}{\partial I_2} + I_3\frac{\partial\hat{W}}{\partial I_3}],\\
\beta_1 &= \alpha_1 + I_1\alpha_2 = \frac{2}{\sqrt{I_3}}\frac{\partial\hat{W}}{\partial I_1},\\
\beta_{-1} &= I_3\alpha_2 = -2\sqrt{I_3}\frac{\partial\hat{W}}{\partial I_2}.
\end{aligned} \tag{2.28}$$

We confine our attention to compressible, isotropic, hyperelastic materials in this thesis. Thus, for compressible, isotropic, hyperelastic materials, the constitutive equation (2.27) based on the principal axes $\{\mathbf{v}^i\}$, defined in (2.8), gives a simple expression for the principal stresses $\{\tau_i\}$ in terms of the partial derivatives of the strain energy function (cf. Ogden [50], Section 4.3.4)

$$\tau_i = \frac{\lambda_i}{\lambda_1\lambda_2\lambda_3}\cdot\frac{\partial W}{\partial\lambda_i}, \quad \text{no sum.} \tag{2.29}$$

The substitution of (2.18) into (2.26) and (2.27) leads to the constitutive relationship for the Piola stress $\mathbf{S}$

$$\mathbf{S} = J\mathbf{F}^{-1}(\alpha_0\mathbf{1} + \alpha_1\mathbf{B} + \alpha_2\mathbf{B}^2), \tag{2.30}$$

and

$$\mathbf{S} = J\mathbf{F}^{-1}(\beta_0\mathbf{1} + \beta_1\mathbf{B} + \beta_{-1}\mathbf{B}^{-1}). \tag{2.31}$$

In some situations it is convenient to express the coefficients $\beta_0, \beta_1, \beta_{-1}$ in terms of W regarded as a function of principal stretches. From the chain rule for differentiation, we have

$$\frac{\partial W}{\partial \lambda_i} = \frac{\partial \hat{W}}{\partial I_k} \cdot \frac{\partial I_k}{\partial \lambda_i}. \tag{2.32}$$

We denote

$$D_{ij} \equiv \frac{\partial I_j}{\partial \lambda_i} \tag{2.33}$$

which, in view of (2.9), are given by

$$\mathbf{D} = 2\begin{bmatrix} \lambda_1 & \lambda_1(\lambda_2^2 + \lambda_3^2) & \lambda_1\lambda_2^2\lambda_3^2 \\ \lambda_2 & \lambda_2(\lambda_1^2 + \lambda_3^2) & \lambda_1^2\lambda_2\lambda_3^2 \\ \lambda_3 & \lambda_3(\lambda_1^2 + \lambda_2^2) & \lambda_1^2\lambda_2^2\lambda_3 \end{bmatrix}. \tag{2.34}$$

Therefore, from (2.32) and (2.33), one establishes the relation between $\partial\hat{W}/\partial I_i$ and $\partial W/\partial\lambda_i$ as

$$\frac{\partial \hat{W}}{\partial I_i} = D_{ij}^{-1}\frac{\partial W}{\partial \lambda_j}, \tag{2.35}$$

where $\mathbf{D}^{-1}$ denotes the inverse matrix of $\mathbf{D}$. The substitution of (2.35) into (2.29) leads to

$$\begin{aligned} \beta_0 &= \frac{2(\lambda_1^2\lambda_2^2 + \lambda_1^2\lambda_3^2 + \lambda_2^2\lambda_3^2)}{\lambda_1\lambda_2\lambda_3} D_{2j}^{-1}\frac{\partial W}{\partial \lambda_j} + 2\lambda_1\lambda_2\lambda_3 D_{3j}^{-1}\frac{\partial W}{\partial \lambda_j}, \\ \beta_1 &= \frac{2}{\lambda_1\lambda_2\lambda_3} D_{1j}^{-1}\frac{\partial W}{\partial \lambda_j}, \\ \beta_{-1} &= -2\lambda_1\lambda_2\lambda_3 D_{2j}^{-1}\frac{\partial W}{\partial \lambda_j}. \end{aligned} \tag{2.36}$$

It is noted that the determinant of $\mathbf{D}$ will be zero if any two of the principal stretches are equal. Therefore, it should be borne in mind that (2.36) is only valid for the deformations with distinct principal stretches.

(2.12) and (2.26) are the governing equations for the finite deformations of compressible, isotropic, hyperelastic materials. These governing equations should be supplemented by suitable *boundary conditions*. Three kinds of boundary conditions are introduced, first of them is the *traction boundary condition*, in which the surface traction $\mathbf{t}$ is given on the boundary $\partial\Omega$ of a body $\Re$ in the deformed configuration Ω

$$\mathbf{t} = \bar{\mathbf{t}}, \text{ on } \partial\Omega, \tag{2.37}$$

the second is the *place boundary condition*, i.e., the position vector $\mathbf{x}$ on the boundary $\partial\Omega$ of a body $\Re$ in the deformed configuration Ω is prescribed by

$$\mathbf{x} = \bar{\mathbf{x}}, \text{ on } \partial\Omega. \tag{2.38}$$

The mixture of the above two kinds of boundary conditions forms the third kind of boundary condition, which is called the *mixed boundary condition*.

The major problem of the finite elasticity theory, known as the *Truesdell's problem* consists in finding restrictions that are to be imposed upon the strain energy function in order to ensure in analysis a meaningful characterization of physical response, and to guarantee appropriate smoothness and existence of solutions. We will come to it in the next section. In 1955, Ericksen [45] proved that in the absence of body forces, the homogeneous deformations are the only deformations possible in every compressible,

homogeneous and isotropic hyperelastic material. The *homogeneous deformations* are described as

$$\mathbf{x} = \mathbf{\Phi X} + \mathbf{\Xi}, \tag{2.39}$$

where $\mathbf{\Phi}$ is a constant tensor and $\mathbf{\Xi}$ is a constant vector. This result implies that non-homogeneous deformations can be discussed, for compressible elastic solids, only in the context of a particular strain energy function, or class of strain energy functions. Ericksen's result has had a very important effect on the study of non-homogeneous finite deformations. Nevertheless, for compressible solids, the analysis of such deformations is usually very complicated even for simple forms of the strain energy function and very few closed form solutions have been obtained.

For compressible, isotropic and hyperelastic materials, various kinds of strain energy function have been proposed. In Section 1.2 of this thesis we have discussed the Blatz-Ko material model in details, which represents compressible foam rubber. The harmonic materials proposed by John [35] have the form of strain energy function

$$W \equiv 2\mu[\hbar(\lambda_1 + \lambda_2 + \lambda_3) - J]$$

where μ is a positive constant and $\hbar$ is a twice continuously differentiable function. The material model is known to simplify the nonlinear partial differential equations governing the finite elasticity and has attracted many authors' attention [50, 52, 53, 54, 23, 55].

Generalizing from his model for incompressible material, Ogden proposed a strain energy function in the form [56]

$$W = \sum_n \frac{\mu_n}{\alpha_n}[(\lambda_1^{\alpha_n} + \lambda_2^{\alpha_n} + \lambda_3^{\alpha_n} - 3) + \zeta(\lambda_1\lambda_2\lambda_3)] \tag{2.40}$$

in which, μ_n, α_n are material constants, and the compressibility of the material is accounted for by the additive function ζ.

It is known that each of the material models listed here could describe a certain restricted class of materials. Therefore, new appropriate forms of the strain energy function are still needed to suit the wide diversity of properties of compressible, elastic materials.

2.4 Constitutive restrictions and stability

In order to ensure a physically realistic response, analytical restrictions are to be imposed upon the constitutive equations. The determination of such restrictions is known as the *Truesdell's problem* and will be discussed in what follows.

The *tension-extension inequality* (T-E) is expressed as

$$(\tau_i^* - \tau_i)(\lambda_i^* - \lambda_i) > 0 \text{ if } \lambda_i^* \neq \lambda_i,\ i = 1,2,3,\ \text{no sum}, \tag{2.41}$$

which is the requirement that when two principal stretches are held fixed, the third should increase with the application of tension, and decrease with pressure.

The *Baker-Ericksen inequality* (B-E) asserts that

$$(\tau_i - \tau_j)(\lambda_i - \lambda_j) > 0 \text{ if } \lambda_i \neq \lambda_j,\ i \neq j,\ i,j = 1,2,3,\ \text{no sum}, \tag{2.42}$$

which is the expectation that a greater stretch should correspond to a greater stress.

Let $\lambda_1 = \lambda_2 = \lambda_3 = \lambda$ so that $\tau_1 = \tau_2 = \tau_3 \equiv \tau(\lambda)$ (see (2.29)). The requirement that the volume should increase with tension ($\tau > 0$) and decrease with pressure ($\tau < 0$) leads to the *pressure-compression inequality* (P-C)

$$\tau(\lambda - 1) > 0 \text{ if } \lambda \neq 1. \tag{2.43}$$

A more restrictive form of P-C inequality is given as

$$\frac{\mathrm{d}\tau(\lambda, \lambda, \lambda)}{\mathrm{d}\lambda} > 0 \text{ if } \lambda \neq 1. \tag{2.44}$$

For compressible, hyperelastic materials, the substitution of $(2.22)_1$ into the equilibrium equation (2.19) leads to the *displacement equation of equilibrium*

$$A_{ijkl}(\mathbf{F})x_{k,lj} = 0 \text{ on } \Omega_0, \tag{2.45}$$

where

$$A_{ijkl} = \partial^2 W / \partial F_{ij} \partial F_{kl}. \tag{2.46}$$

Here $\mathbf{A}$ is a fourth-order tensor, called the *elasticity tensor*. The system of displacement-equations of equilibrium (2.45) is *strongly elliptic (S-E) at the deformation* $\mathbf{x}$ *if and only if*

$$A_{ijkl}(\mathbf{F}(\mathbf{X}))m_i m_k n_j n_l > 0 \tag{2.47}$$

for every pair of unit vectors $\mathbf{m}$ *and* $\mathbf{n}$. It can be shown that (2.47) implies (2.41) and (2.42) and it has an interpretation within the theory of the propagation of waves in hyperelastic materials (see Truesdell [48], Lecture 18).

Now we consider an infinitesimal displacement imposed upon a finite deformation $\mathbf{x}$. Let $\mathbf{u}$ be the infinitesimal displacement which is compatible with the boundary conditions of place and traction satisfied by $\mathbf{x}$. The gradient $\boldsymbol{\Upsilon}$ of $\mathbf{u}$ is defined by

$$\boldsymbol{\Upsilon} \equiv \nabla \mathbf{u}. \tag{2.48}$$

Let $\mathbf{S}_0$ be the Piola stress corresponding to the finite deformation $\mathbf{x}$, and $\mathbf{S}_R$ be the Piola stress for the deformation after the imposed infinitesimal displacement. As the consequence of being infinitesimal, the linearly approximate expression of $\mathbf{S}_R$ is

$$\mathbf{S}_R = \mathbf{S}_0 + \mathbf{A}\boldsymbol{\Upsilon}, \tag{2.49}$$

where $\mathbf{A}$ is defined in (2.46).

A static deformation of a body subject to boundary conditions of place and traction is said to be *infinitesimally stable* if the work done in every further infinitesimal deformation compatible with the boundary conditions is not less than that required to effect the same infinitesimal deformation subject to "dead loading", i.e., at the same state of stress as in the ground state of strain. That is

$$\int_{\Omega_0} \mathrm{tr}[(\mathbf{S}_R - \mathbf{S}_0)\boldsymbol{\Upsilon}^T] dv \geq 0, \tag{2.50}$$

where the integration is extended over the body in the deformed state of $\mathbf{x}$. On substituting (2.49) into (2.50) we obtain the condition for infinitesimal stability

$$\int_{\Omega_0} \mathrm{tr}[\mathbf{A}\boldsymbol{\Upsilon}\boldsymbol{\Upsilon}^T] dv = \int_{\Omega_0} A_{ijkl}\Upsilon_{ij}\Upsilon_{kl} dv \geq 0. \tag{2.51}$$

The following **Basic stability theorem** was found by Hadamard: *In order that a configuration of an elastic body be infinitesimally stable for boundary conditions of place and traction, it is necessary that the inequality*

$$A_{ijkl}m_i m_k n_j n_l \geq 0 \tag{2.52}$$

hold for all vectors $\mathbf{m}$ *and* $\mathbf{n}$ *at each particle.* This is referred to as *Hadamard inequality.* Comparison with (2.47) shows that Hadamard's inequality (2.52) is only slightly weaker than the S-E condition (2.47). Hadamard's inequality is only a local necessary condition for infinitesimal stability, for, if (2.52) fails to hold, the equilibrium configuration can not be stable. But in general, however, Hadamard's equality, like the S-E inequality, may be very difficult to analyze.

Many authors have worked in finding appropriate expressions for the S-E condition. For compressible, isotropic and non-linearly elastic solids, conditions for the strong ellipticity of the equilibrium equations were given by Simpson & Spector [57] and alternative formulations were provided by Rosakis [58] and Zubov & Rudev [59]. In contrast with the criteria obtained by Knowles &Sternberg [20] and Hill [60] (see also [61, 62]) for the case of plain strain, however, the conditions in [57] and [58] are not given in terms of the strain energy function expressed as a function of the principal stretches and consequently, their application is limited. Similarly, the formalism in [59] which is based upon the verification of certain conditional inequalities may also prove to be unsuitable in certain circumstances and thus, for three-dimensional deformations, there is a clear need for strong-ellipticity conditions which are as flexible as those that are

available in plane elastostatics. In what follows we obtain strong-ellipticity conditions for compressible, isotropic, hyperelastic solids that, in the three-dimensional setting, are the analogous of those arrived at in [20, 60, 61, 62], which is useful in application.

As it is well-known that, for a homogeneous isotropic hyperelastic material with strain energy function $W(\lambda_1, \lambda_2, \lambda_3)$, there exists a function $\sigma = \sigma(Q^1, Q^2, Q^3)$, where

$$Q^1 \equiv \frac{1}{2}(\lambda_1^2 + \lambda_2^2 + \lambda_3^2),\ Q^2 \equiv \frac{1}{4}(\lambda_1^4 + \lambda_2^4 + \lambda_3^4),\ Q^3 \equiv \lambda_1\lambda_2\lambda_3, \tag{2.53}$$

such that

$$W = W(\lambda_1, \lambda_2, \lambda_3) = \sigma(Q^1, Q^2, Q^3). \tag{2.54}$$

Simpson and Spector [57] introduce the notations

$$\sigma_i \equiv \frac{\partial \sigma}{\partial Q^i},\ \sigma_{i,j} \equiv \frac{\partial \sigma_i}{\partial Q^j}, \tag{2.55}$$

$$\mathbf{M}(M_{ij}) \equiv \begin{bmatrix} \lambda_1 & \lambda_2 & \lambda_3 \\ \lambda_1^3 & \lambda_2^3 & \lambda_3^3 \\ \lambda_2\lambda_3 & \lambda_1\lambda_3 & \lambda_1\lambda_2 \end{bmatrix}, \tag{2.56}$$

$$BE_i \equiv \sigma_1 + \sigma_2(\lambda_1^2 + \lambda_2^2 + \lambda_3^2 - \lambda_i^2), \tag{2.57}$$

$$TE_i \equiv \sigma_1 + 3\lambda_i^2\sigma_2 + M_{ki}\sigma_{k,j}M_{ji},\ \text{no sum over index i}, \tag{2.58}$$

$$\Psi_1 \equiv \lambda_2\lambda_3\sigma_2 + M_{k2}\sigma_{k,j}M_{j3}, \tag{2.59}$$

$$\Psi_2 \equiv \lambda_1\lambda_3\sigma_2 + M_{k1}\sigma_{k,j}M_{j3}, \tag{2.60}$$

$$\Psi_3 \equiv \lambda_1\lambda_2\sigma_2 + M_{k1}\sigma_{k,j}M_{j2}, \tag{2.61}$$

and show that the strong-ellipticity condition is satisfied at a deformation, with prin-

cipal stretches $\lambda_1, \lambda_2, \lambda_3$, if and only if for all choices of $\theta_1, \theta_2 = \pm 1$ we have

$$BE_i > 0,\ TE_i > 0, \tag{2.62}$$

$$E_i \equiv BE_i + (TE_1 TE_2 TE_3 TE_i^{-1})^{\frac{1}{2}} > |\Psi_i|, \tag{2.63}$$

and

$$TE_1^{\frac{1}{2}}(BE_1 + \theta_1\Psi_1) + TE_2^{\frac{1}{2}}(BE_2 + \theta_2\Psi_2) + TE_3^{\frac{1}{2}}(BE_3 + \theta_1\theta_2\Psi_3)$$

$$+[2(E_1 + \theta_1\Psi_1)(E_2 + \theta_2\Psi_2)(E_3 + \theta_1\theta_2\Psi_3)]^{\frac{1}{2}} + (TE_1 TE_2 TE_3)^{\frac{1}{2}} > 0. \tag{2.64}$$

As remarked in [57], if $\Psi_1\Psi_2\Psi_3 > 0$, then three of the four inequalities (2.64) are independent while the fourth, obtained by choosing θ_1, θ_2 so that

$$\Psi_1\theta_1 > 0,\ \Psi_2\theta_2 > 0,\ \Psi_3\theta_1\theta_2 > 0, \tag{2.65}$$

is implied by the other three.

Our aim here is to express the S-E conditions (2.62)-(2.64) in terms of the derivatives

$$W_i \equiv \frac{\partial W}{\partial \lambda_i},\ W_{ij} \equiv \frac{\partial^2 W}{\partial \lambda_i \partial \lambda_j}, \tag{2.66}$$

and to this end we note that

$$M_{ji} = \frac{\partial Q^j}{\partial \lambda_i}. \tag{2.67}$$

Thus

$$W_i = \sigma_k \frac{\partial Q^k}{\partial \lambda_i} = \sigma_k M_{ki}, \tag{2.68}$$

and

$$W_{ij} = \frac{\partial}{\partial \lambda_j}[\sigma_k M_{ki}] = M_{rj}\sigma_{k,r}M_{ki} + \sigma_k \frac{\partial M_{ki}}{\partial \lambda_j}. \tag{2.69}$$

On assuming that $\lambda_1 \neq \lambda_2 \neq \lambda_3$ and on making use of (2.68) and (2.69), it can be readily checked that we have

$$\left.\begin{aligned} BE_1 &= (\lambda_2 W_2 - \lambda_3 W_3)/(\lambda_2^2 - \lambda_3^2), \\ BE_2 &= (\lambda_1 W_1 - \lambda_3 W_3)/(\lambda_1^2 - \lambda_3^2), \\ BE_3 &= (\lambda_1 W_1 - \lambda_2 W_2)/(\lambda_1^2 - \lambda_2^2), \end{aligned}\right\} \tag{2.70}$$

$$TE_i = W_{ii}, \text{ no sum}, \tag{2.71}$$

and

$$\left.\begin{aligned} \Psi_1 &= (W_2\lambda_3 - W_3\lambda_2)/(\lambda_2^2 - \lambda_3^2) + W_{23}, \\ \Psi_2 &= (W_1\lambda_3 - W_3\lambda_1)/(\lambda_1^2 - \lambda_3^2) + W_{13}, \\ \Psi_3 &= (W_1\lambda_2 - W_2\lambda_1)/(\lambda_1^2 - \lambda_2^2) + W_{12}. \end{aligned}\right\} \tag{2.72}$$

On combining (2.62)-(2.64) with (2.70)-(2.72) we now find that for a hyperelastic material the strong-ellipticity condition holds at a state of deformation with distinct principal stretches *if* and *only if*, for all choices of $\theta_1, \theta_2 = \pm 1$, the following conditions are satisfied:

$$(\lambda_i W_i - \lambda_j W_j)/(\lambda_i - \lambda_j) > 0, \; W_{ii} > 0, \; i \neq j, \text{ no sum}, \tag{2.73}$$

$$\left.\begin{aligned} &(W_i - W_j)/(\lambda_i - \lambda_j) + W_{ij} + (W_{ii}W_{jj})^{\frac{1}{2}} > 0, \; i \neq j, \text{ no sum}, \\ &(W_i + W_j)/(\lambda_i + \lambda_j) - W_{ij} + (W_{ii}W_{jj})^{\frac{1}{2}} > 0, \; i \neq j, \text{ no sum}, \end{aligned}\right\} \tag{2.74}$$

and

$$W_{11}^{\frac{1}{2}}\left[\frac{(\lambda_2 + \theta_1\lambda_3)W_2 - (\lambda_3 + \theta_1\lambda_2)W_3}{\lambda_2^2 - \lambda_3^2} + \theta_1 W_{23}\right]$$
$$+W_{22}^{\frac{1}{2}}\left[\frac{(\lambda_1 + \theta_2\lambda_3)W_1 - (\lambda_3 + \theta_2\lambda_1)W_3}{\lambda_1^2 - \lambda_3^2} + \theta_2 W_{13}\right]$$

$$+W_{33}^{\frac{1}{2}}\left[\frac{(\lambda_1+\theta_1\theta_2\lambda_2)W_1-(\lambda_2+\theta_1\theta_2\lambda_1)W_2}{\lambda_1^2-\lambda_2^2}+\theta_1\theta_2W_{12}\right] \tag{2.75}$$
$$+\left\{2\left[\frac{(\lambda_2+\theta_1\lambda_3)W_2-(\lambda_3+\theta_1\lambda_2)W_3}{\lambda_2^2-\lambda_3^2}+\theta_1W_{23}+(W_{22}W_{33})^{\frac{1}{2}}\right]\right.$$
$$\cdot\left[\frac{(\lambda_1+\theta_2\lambda_3)W_1-(\lambda_3+\theta_2\lambda_1)W_3}{\lambda_1^2-\lambda_3^2}+\theta_2W_{13}+(W_{11}W_{33})^{\frac{1}{2}}\right]$$
$$\left.\cdot\left[\frac{(\lambda_1+\theta_1\theta_2\lambda_2)W_1-(\lambda_2+\theta_1\theta_2\lambda_1)W_2}{\lambda_1^2-\lambda_2^2}+\theta_1\theta_2W_{12}+(W_{11}W_{22})^{\frac{1}{2}}\right]\right\}^{\frac{1}{2}}$$
$$+(W_{11}W_{22}W_{33})^{\frac{1}{2}}>0.$$

The strong-ellipticity conditions for the case when two of the principal stretches are equal can be obtained from (2.73)-(2.75) by employing a limiting process based on the l'Hospital rule. If $\lambda_1\neq\lambda_2=\lambda_3$, for instance, we find that the necessary and sufficient conditions for strong ellipticity are

$$\tilde{W}_{11}>0,\ \tilde{W}_{22}=\tilde{W}_{33}>0, \tag{2.76}$$

$$(\lambda_1\tilde{W}_1-\lambda_2\tilde{W}_2)/(\lambda_1-\lambda_2)>0, \tag{2.77}$$

$$\tilde{W}_{22}-\tilde{W}_{23}+\tilde{W}_2/\lambda_2>0, \tag{2.78}$$

$$(\tilde{W}_1-\tilde{W}_2)/(\lambda_1-\lambda_2)+\tilde{W}_{12}+(\tilde{W}_{11}\tilde{W}_{22})^{\frac{1}{2}}>0, \tag{2.79}$$

$$(\tilde{W}_1+\tilde{W}_2)/(\lambda_1+\lambda_2)-\tilde{W}_{12}+(\tilde{W}_{11}\tilde{W}_{22})^{\frac{1}{2}}>0, \tag{2.80}$$

where $\tilde{W}_i$ and $\tilde{W}_{ij}$ stand for $W_i(\lambda_1,\lambda_2,\lambda_2)$ and $W_{ij}(\lambda_1,\lambda_2,\lambda_2)$ respectively. We note that the conditions (2.76)-(2.80) have been obtained by letting $\lambda_3\to\lambda_2$ in (2.73)-(2.74) and that the conditions that are obtained from (2.75) by this limiting process, which can be written as

$$\tilde{W}_{11}^{\frac{1}{2}}\left[\frac{(1-\theta_1)\tilde{W}_2}{2\lambda_2}+\frac{1}{2}(\theta_1+3)\tilde{W}_{22}+\frac{1}{2}(\theta_1-1)\tilde{W}_{23}\right]$$

$$+\tilde{W}_{22}^{\frac{1}{2}}\left\{\frac{[2\lambda_1+(1+\theta_1)\theta_2\lambda_2]\tilde{W}_1-[2\lambda_2+(1+\theta_1)\theta_2\lambda_1]\tilde{W}_2}{\lambda_1^2-\lambda_2^2}+(1+\theta_1)\theta_2\tilde{W}_{23}\right\}$$

$$+\left\{2\left[\frac{(1-\theta_1)\tilde{W}_2}{2\lambda_2}+\frac{1}{2}(\theta_1+3)\tilde{W}_{22}+\frac{1}{2}(\theta_1-1)\tilde{W}_{23}\right]\right. \tag{2.81}$$

$$\cdot\left[\frac{(\lambda_1+\theta_2\lambda_2)\tilde{W}_1-(\lambda_2+\theta_2\lambda_1)\tilde{W}_2}{\lambda_1^2-\lambda_2^2}+\theta_2\tilde{W}_{12}+(\tilde{W}_{11}\tilde{W}_{22})^{\frac{1}{2}}\right]$$

$$\left.\cdot\left[\frac{(\lambda_1+\theta_1\theta_2\lambda_2)\tilde{W}_1-(\lambda_2+\theta_1\theta_2\lambda_1)\tilde{W}_2}{\lambda_1^2-\lambda_2^2}+\theta_1\theta_2\tilde{W}_{12}+(\tilde{W}_{11}\tilde{W}_{22})^{\frac{1}{2}}\right]\right\}^{\frac{1}{2}}>0,$$

are consequences of (2.76)-(2.80).

In a similar manner, it follows from (2.76)-(2.80) that if $\lambda_1=\lambda_2=\lambda_3=\lambda$ the strong-ellipticity condition reduces to the following pair of inequalities:

$$W_{11}(\lambda,\lambda,\lambda)>0, \tag{2.82}$$

and

$$W_{11}(\lambda,\lambda,\lambda)-W_{12}(\lambda,\lambda,\lambda)+W_1(\lambda,\lambda,\lambda)/\lambda>0. \tag{2.83}$$

2.5 Plane strain

Now we turn to the special case of *plane strain* (plane deformation), we assume that a body occupies a domain Ω_0 in the reference configuration and that Ω_0 is a cylindrical domain symmetric about the coordinate plane $X_3=0$. The generators of the boundary $\partial\Omega_0$ are parallel to the X_3-axis and are subject the deformation (2.2) to the restriction

$$\partial x_\alpha/\partial X_3=0,\ x_3=X_3,\ \alpha=1,2,\ \text{on}\ \Omega_0. \tag{2.84}$$

Consequently,

$$x_\alpha = x_\alpha(\mathbf{X}) \text{ for all } \mathbf{X} = (X_1, X_2) \in \Pi_0 \tag{2.85}$$

where Π_0 is the middle cross-section of Ω_0. From (2.84), (2.5) and (2.7), in the present circumstances one concludes that $\mathbf{F}$, $\mathbf{C}$ and $\mathbf{B}$ are independent of X_3 such that

$$\begin{aligned} &F_{\alpha 3} = F_{3\alpha} = C_{\alpha 3} = C_{3\alpha} = B_{3\alpha} = B_{\alpha 3} = 0,\ F_{33} = C_{33} = B_{33} = 1, \\ &F_{\alpha\beta} = \frac{\partial x_\alpha}{\partial X_\beta},\ J = \det[F_{\alpha\beta}] = \lambda_1\lambda_2,\ C_{\alpha\beta} = F_{\rho\alpha}F_{\rho\beta},\ \ B_{\alpha\beta} = F_{\alpha\rho}F_{\beta\rho} \text{ on } \Pi_0, \end{aligned} \tag{2.86}$$

and the principal stretch λ_3 is

$$\lambda_3 = 1. \tag{2.87}$$

Further, in view of (2.86), the invariants given by (2.9) reduce to

$$I_1 = 1 + C_{\alpha\alpha},\ I_2 = \frac{1}{2}(2C_{\alpha\alpha} + C_{\alpha\alpha}C_{\beta\beta} - C_{\alpha\beta}C_{\alpha\beta}),\ I_3 = J^2 = \det[C_{\alpha\beta}]. \tag{2.88}$$

We define

$$I = F_{\rho\alpha}F_{\rho\alpha} = C_{\alpha\alpha} = \lambda_1^2 + \lambda_2^2, \tag{2.89}$$

and, from (2.86) and (2.88) one draws that I_1, I_2, I_3 in the case of plane deformation are linked by I, J as

$$I_1 = I + 1,\ I_2 = I_1 - 1 + I_3 = I + J^2,\ I_3 = J^2. \tag{2.90}$$

Then the strain energy function W becomes

$$W = \hat{W}(I, J). \tag{2.91}$$

Next we consider the implication of the assumption of plain strain on the constitutive law (2.30). From (2.30) and (2.86) one infers that $\mathbf{S}$ is independent of X_3 with

$$S_{3\alpha} = S_{\alpha 3} = 0,\ S_{33} = J(\beta_0 + \beta_1 + \beta_{-1}) \text{ on } \Pi_0. \tag{2.92}$$

The computation on (2.30) with (2.86), (2.89) and (2.90) leads to

$$S_{\alpha\beta} = 2\frac{\partial \hat{W}}{\partial I}F_{\alpha\beta} + J\frac{\partial \hat{W}}{\partial J}F^{-T}_{\alpha\beta}. \tag{2.93}$$

Thus, the equilibrium equations (2.19) at present evidently reduce to

$$\partial S_{\alpha\beta}/\partial X_\beta = 0 \text{ on } \Pi_0. \tag{2.94}$$

From (2.84) and (2.86), the Cauchy stress field $\mathbf{T}$ (see (2.27)) for plane strain is found to obey

$$T_{3\alpha} = T_{\alpha 3} = 0,\ T_{33} = \beta_0 + \beta_1 + \beta_{-1},\ T_{\alpha\beta} = T_{\beta\alpha} = \frac{\partial \hat{W}}{\partial J}\delta_{\alpha\beta} + \frac{2}{J}\frac{\partial \hat{W}}{\partial I}B_{\alpha\beta}. \tag{2.95}$$

And the equilibrium equations (2.12) for plane strain are of the form

$$\partial T_{\alpha\beta}/\partial x_\beta = 0 \text{ on } \Pi, \tag{2.96}$$

where Π is the middle cross-section of the domain occupied by the body in the deformed configuration. The component form of the equilibrium equation (2.96), in terms of the physical components of $\mathbf{T}$ in a Cartesian coordinate system, is

$$\begin{aligned} &\frac{\partial T_{xx}}{\partial x} + \frac{\partial T_{xy}}{\partial y} = 0, \\ &\frac{\partial T_{xy}}{\partial x} + \frac{\partial T_{yy}}{\partial y} = 0. \end{aligned} \tag{2.97}$$

In a cylindrical polar coordinate system, equation (2.96) takes the form:

$$\frac{\partial T_{rr}}{\partial r} + \frac{1}{r}\frac{\partial T_{r\theta}}{\partial \theta} + \frac{1}{r}(T_{rr} - T_{\theta\theta}) = 0,$$
$$\frac{\partial T_{\theta r}}{\partial r} + \frac{1}{r}\frac{\partial T_{\theta\theta}}{\partial \theta} + \frac{2}{r}T_{\theta r} = 0, \tag{2.98}$$

where (r, θ) are cylindrical polar coordinates.

For hyperelastic materials, in plane strain, the T-E inequality (2.41) reduces to

$$W_{11} > 0,\ W_{22} > 0, \tag{2.99}$$

and the B-E inequality (2.42) is of the form

$$\frac{(\lambda_1 W_1 - \lambda_2 W_2)}{(\lambda_1 - \lambda_2)} > 0. \tag{2.100}$$

The P-C inequality (2.44) can be rewritten as

$$\mathrm{d}\tau(\lambda, \lambda)/\mathrm{d}\lambda > 0, \quad \lambda \neq 1. \tag{2.101}$$

The S-E conditions (2.73)-(2.75) now have the form

$$(\lambda_1 W_1 - \lambda_2 W_2)/(\lambda_1 - \lambda_2) > 0,\ W_{11} > 0,\ W_{22} > 0, \tag{2.102}$$

together with

$$\frac{W_1 - W_2}{\lambda_1 - \lambda_2} + W_{12} + (W_{11}W_{22})^{\frac{1}{2}} > 0, \quad \frac{W_1 + W_2}{\lambda_1 + \lambda_2} - W_{12} + (W_{11}W_{22})^{\frac{1}{2}} > 0. \tag{2.103}$$

Chapter 3

The generalized Blatz-Ko material and homogeneous deformations

In this chapter, we examine a specific material by making use of the theory of continuum mechanics described in Chapter 2. In Section 3.1 we give a brief description of the material, and in Section 3.2 we discuss the strong-ellipticity condition for the material. The homogeneous deformations are then studied in Section 3.3.

3.1 The generalized Blatz-Ko material

In our present work, we consider a strain energy function of the form (1.13), which, for the sake of convenience, is cited as

$$W = \frac{\mu}{\beta}(\lambda_1^{-\beta} + \lambda_2^{-\beta} + \lambda_3^{-\beta} + \beta\lambda_1\lambda_2\lambda_3 - \beta - 3),\ \mu > 0,\ \beta > 0, \tag{3.1}$$

where μ and β are positive constants.

The partial derivatives of the strain energy function (3.1) with respect to the principal stretches are given by

$$W_i = \mu(\frac{J}{\lambda_i} - \lambda_i^{-\beta-1}),\ W_{ii} = \mu(\beta+1)\lambda_i^{-\beta-2},\ W_{ij} = \mu\frac{J}{\lambda_i\lambda_j},\ i \neq j,\ \text{no sum}, \quad (3.2)$$

and the ground-state elastic moduli associated with (3.1) are shown in Table 3.1 below. It is readily to verify that the material satisfies

Parameters	the generalized Blatz-Ko	the Blatz-Ko
Shear Modulus $[W_{11}(1,1,1) - W_{12}(1,1,1)]/2$	$\beta\mu/2$	μ
Lame coefficient $W_{12}(1,1,1)$	μ	μ

Table 3.1: The ground-state elastic moduli.

$$W(1,1,1) = 0,\ W_i(1,1,1) = 0 \quad (3.3)$$

which ensures that the reference configuration is unstressed and that the energy is zero in the reference configuration. $W = W(\lambda_1, \lambda_2, \lambda_3)$ has an absolute minimum at $\lambda_1 = \lambda_2 = \lambda_3 = 1$ and thus we have

$$W(\lambda_1, \lambda_2, \lambda_3) \geq 0, \quad (3.4)$$

the equality being possible if and only if $\lambda_1 = \lambda_2 = \lambda_3 = 1$.

3.2 The strong-ellipticity condition

For the material (3.1), it is easy to check that the P-C inequality (2.44), T-E and B-E inequalities ((2.41) and (2.42)) are satisfied for any $\beta, \mu > 0$. The S-E condition for the case of $\beta = 2$ was investigated in [13] and we note that the restriction of (3.1) to plane strain ($\lambda_3 = 1$) was considered in [38] where it was shown that for plane deformations of the material, the S-E condition prevails if and only if the principal stretches satisfies

$$t_{_E} < \lambda_1/\lambda_2 < 1/t_{_E}, \tag{3.5}$$

where $t_E \in (0,1)$ is a solution to the equation

$$f(x) \equiv (\beta+1)(x+1)x^{\frac{\beta}{2}} - (1+x^{\beta+1}) = 0. \tag{3.6}$$

(see [38], eq.(31) where t should be replaced by $\sqrt{t}$). As $f(1)f(0) = -2\beta < 0$ and $f'(x) > 0$ for $x \in (0,1]$, it follows that the equation (3.6) has exactly one root in the interval [0,1], and thus, since f satisfies the identity $f(x) = x^{\beta+1}f(1/x)$, we infer that this equation has exactly two roots in the interval $[0,\infty)$, namely t_E and $1/t_E$. The variation of $t_{_E}$ *vs.* β is illustrated in Figure 3.1 (cf. Figure 5 of [38]), which shows that $t_{_E}$ increases with β and tends to unity when β tends to infinity.

It is easily seen that the material (3.1) satisfies (2.73) and $(2.74)_1$ at all states of deformations with distinct principal stretches and that $(2.74)_2$ reduces to

$$(\beta+1)(d_{ij}+1)d_{ij}^{\frac{\beta}{2}} - (1+d_{ij}^{\beta+1}) > 0, \; d_{ij} = \lambda_i/\lambda_j. \tag{3.7}$$

In view of the previous discussion we conclude that the conditions

$$t_{_E} < d_{ij} < 1/t_{_E}, \tag{3.8}$$

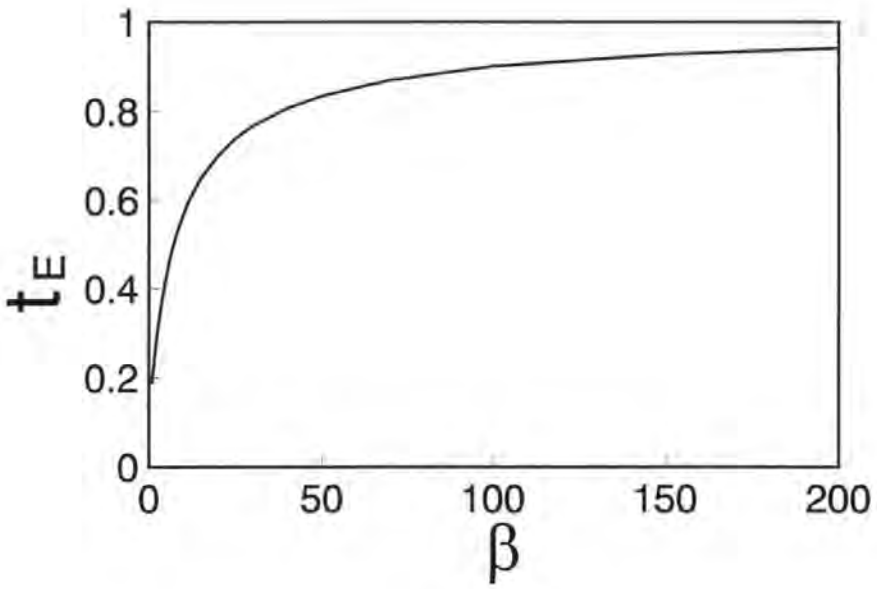

Figure 3.1: t_E *vs.* β

(which are equivalent to (3.7)) are necessary for the strong ellipticity to hold. In what follows we show that (3.8) are also sufficient for strong ellipticity. To this end, we assume that $\lambda_1 \neq \lambda_2 \neq \lambda_3$ (the sufficiency of (3.8) in the case when two, or all three, of the principal stretches coalesce follows immediately from (2.76)-(2.80) and (2.82)-(2.83)) and note that substitution of (3.1) into (2.72) reveals that we have $\Psi_i > 0$. Thus, according to the remark following (2.64), we infer that the inequality obtained from (2.75) by setting $\theta_1 = \theta_2 = 1$ is implied by the remaining three inequalities in (2.75). By inspection, it is readily found that, when (3.8) hold, the relevant inequalities in (2.75) are implied by the following triad of inequalities

$$W_{11}^{\frac{1}{2}}[(W_2 - W_3)/(\lambda_2 - \lambda_3) + W_{23}] + W_{33}^{\frac{1}{2}}[(W_1 + W_2)/(\lambda_1 + \lambda_2) - W_{12}] > 0,$$

$$W_{22}^{\frac{1}{2}}[(W_1 - W_3)/(\lambda_1 - \lambda_3) + W_{13}] + W_{33}^{\frac{1}{2}}[(W_1 + W_2)/(\lambda_1 + \lambda_2) - W_{12}] > 0, \quad (3.9)$$

$$W_{33}^{\frac{1}{2}}[(W_1 - W_2)/(\lambda_1 - \lambda_2) + W_{12}] + W_{22}^{\frac{1}{2}}[(W_1 + W_3)/(\lambda_1 + \lambda_3) - W_{13}] > 0.$$

The inequalities (3.9) can be re-written as

$$\begin{aligned} &d_{32}^{-\beta/2}(1 - d_{32}^{\beta+1})/(1 - d_{32}) > d_{12}^{-\beta/2}(1 + d_{12}^{\beta+1})/(1 + d_{12}), \\ &d_{31}^{-\beta/2}(1 - d_{31}^{\beta+1})/(1 - d_{31}) > d_{12}^{-\beta/2}(1 + d_{12}^{\beta+1})/(1 + d_{12}), \\ &d_{21}^{-\beta/2}(1 - d_{21}^{\beta+1})/(1 - d_{21}) > d_{13}^{-\beta/2}(1 + d_{13}^{\beta+1})/(1 + d_{13}), \end{aligned} \tag{3.10}$$

and, since (3.7) are assumed to hold, they will be satisfied if

$$x^{-\beta/2}(1 - x^{\beta+1})/(1 - x) > \beta + 1, \; x \in (0, \infty) - \{1\}. \tag{3.11}$$

To prove (3.11) we write

$$F(x) \equiv 1 - x^{\beta+1} - (1 - x)x^{\beta/2}(\beta + 1), \tag{3.12}$$

and note that

$$F'(x) = -(\beta + 1)x^{(\beta-2)/2}G(x), \tag{3.13}$$

where

$$G(x) = x^{(\beta+2)/2} - (1 + \beta/2)x + \beta/2. \tag{3.14}$$

Since the function G satisfies $G(1) = G'(1) = 0$ and $G'(x)(x - 1) > 0$ for $x \in (0, \infty) - \{1\}$, it follows that $G(x) > 0$ for $x \in (0, \infty) - \{1\}$ and that $F'(x) < 0$ for $x \in (0, \infty) - \{1\}$. Since $F(0) = 1$ and $F(1) = 0$, we have $F(x)(x-1) < 0$ for $x \in (0, \infty) - \{1\}$ which is equivalent to (3.11). The conditions (3.8) therefore, are both necessary and sufficient for the strong ellipticity to hold at a deformation of the material (3.1).

3.3 Homogeneous deformations

We consider now a homogeneous deformation of the form

$$x_i = \lambda_i X_i, \text{ no sum}, \tag{3.15}$$

in which the coefficients λ_i are positive constants and are recognized as the principal stretches of such a deformation. From (3.15) together with (2.5) and (2.7) through (2.27) one readily confirms that at present

$$S_{ii} = \frac{\partial W}{\partial \lambda_i}, \; S_{ji} = S_{ij} = 0, \; T_{ii} = \frac{\lambda_i}{J} \cdot \frac{\partial W}{\partial \lambda_i}, \; T_{ij} = 0, \text{ no sum}, \; i \neq j. \tag{3.16}$$

From (3.1) we find that

$$T_{ii} = J^{-1}\lambda_i S_{ii} = \mu(1 - \lambda_i^{-\beta} J^{-1}), \text{ no sum}. \tag{3.17}$$

The relations (3.17), which imply

$$T_{ii} < \mu, \text{ no sum}, \tag{3.18}$$

are explicitly invertible and lead to

$$\lambda_i = (1 - \frac{T_{ii}}{\mu})^{-\frac{1}{\beta}}[(1 - \frac{T_{11}}{\mu})(1 - \frac{T_{22}}{\mu})(1 - \frac{T_{33}}{\mu})]^{\frac{1}{\beta(\beta+3)}}, \text{ no sum}. \tag{3.19}$$

For our purposes it is essential to examine the consequences of (3.17), as far as these homogeneous deformations are concerned.

For the case of *isotropic extension* (or contraction) we have

$$\lambda_2 = \lambda_3 = \lambda_1, \; T_{ii} = \mu(1 - \lambda_1^{-\beta-3}), \; S_{ii} = \mu(\lambda_1^2 - \lambda_1^{-\beta-1}), \text{ no sum}. \tag{3.20}$$

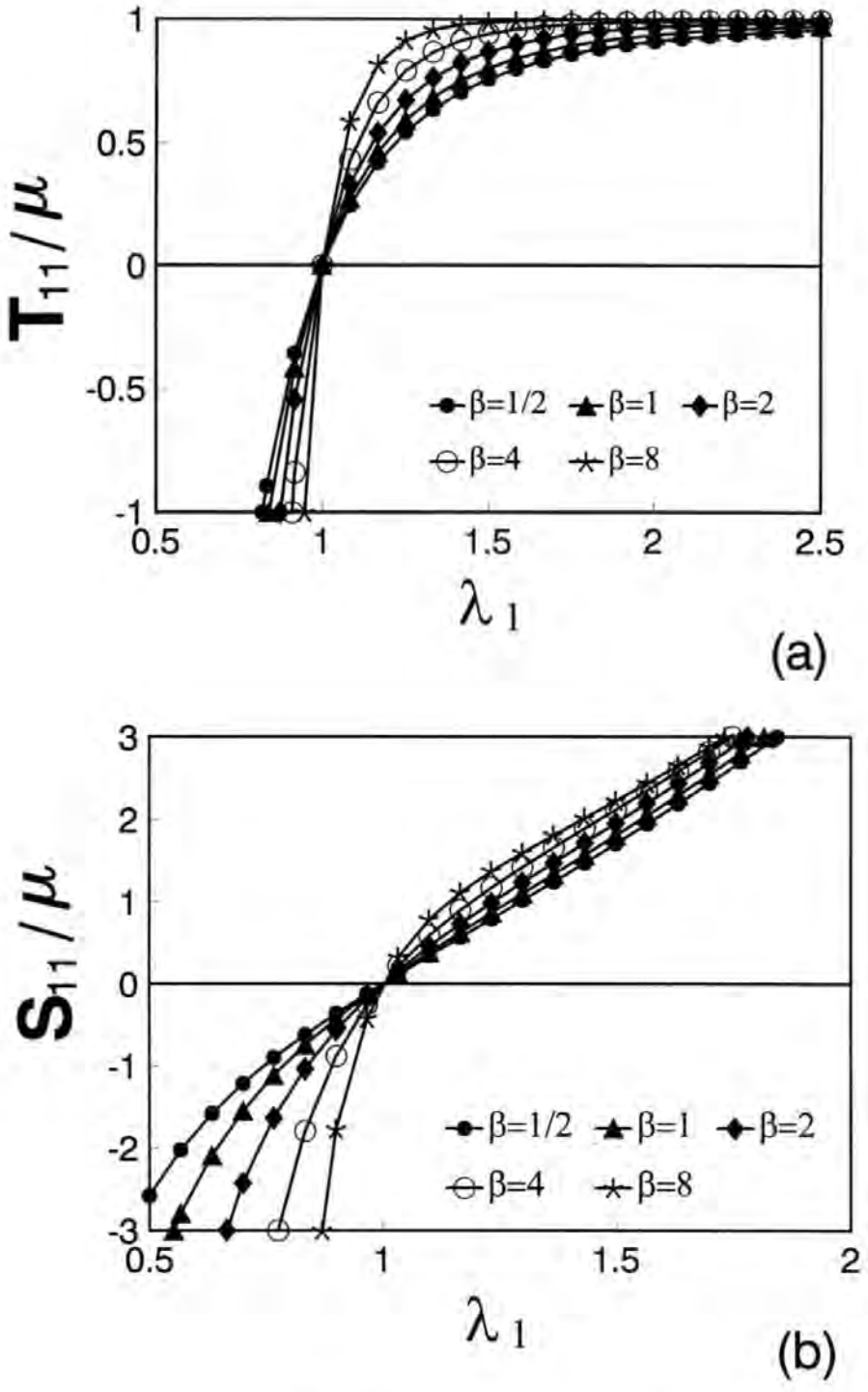

Figure 3.2: Isotropic extension

As is apparent from (3.20), for isotropic extension (see Figure 3.2a), $T_{11}(\lambda_1)$ is a steadily increasing concave function and $T_{11} \to \mu$ as $\lambda_1 \to \infty$, while $T_{11} \to -\infty$ as $\lambda_1 \to 0$. In Figure 3.2b, $S_{11}(\lambda_1)$ is monotone increasing, but $S_{11} \to \infty$ as $\lambda_1 \to \infty$ and the corresponding stress-stretch curve exhibits a reversal in curvature at $\lambda_1 = [(1+\beta)(1+\beta/2)]^{1/(\beta+3)}$. It is noted that for larger values of β, the Cauchy stress and Piola stress increase faster and that, otherwise, the distributions both the Cauchy and the Piola stresses are similar for all values of $\beta > 0$. Since greater magnitudes of the Cauchy stresses and the Piola stresses correspond to larger values of β, thus we conclude that the material becomes harder as β increases.

For a state of *isotropic plane stress* parallel to the plane $X_3 = 0$, there results

$$T_{33} = S_{33} = 0,\ \lambda_2 = \lambda_1,\ \lambda_3 = \lambda_1^{-2/(\beta+1)},$$

$$T_{11} = T_{22} = \mu[1 - \lambda_1^{-\beta(\beta+3)/(\beta+1)}],\ S_{11} = S_{22} = \mu[\lambda_1^{(\beta-1)/(\beta+1)} - \lambda_1^{-\beta-1}]. \qquad (3.21)$$

Variations of the Cauchy stress and the Piola stress with principal stretch are illustrated in Figure 3.3. From (3.21) it is seen that the Cauchy stress T_{11} has the same qualitative behaviour as in the case of the isotropic extension (see Figure 3.2), that is, T_{11} increases monotonically with λ_1 and $T_{11} \to \mu$ as $\lambda_1 \to \infty$, while $T_{11} \to -\infty$ when $\lambda_1 \to 0$. For all values of $\beta > 0$, the distributions of Cauchy stress are qualitatively similar and they indicate that the material hardens as β increases since greater magnitudes of the Cauchy stress correspond to larger values of β. In contrast, the variation of the Piola stress S_{11} with λ_1 depends on the parameter β. For all values of $\beta > 1$, $S_{11}(\lambda_1)$ is an monotonic and concave increasing function and $S_{11} \to \infty$ as $\lambda_1 \to \infty$. The distributions

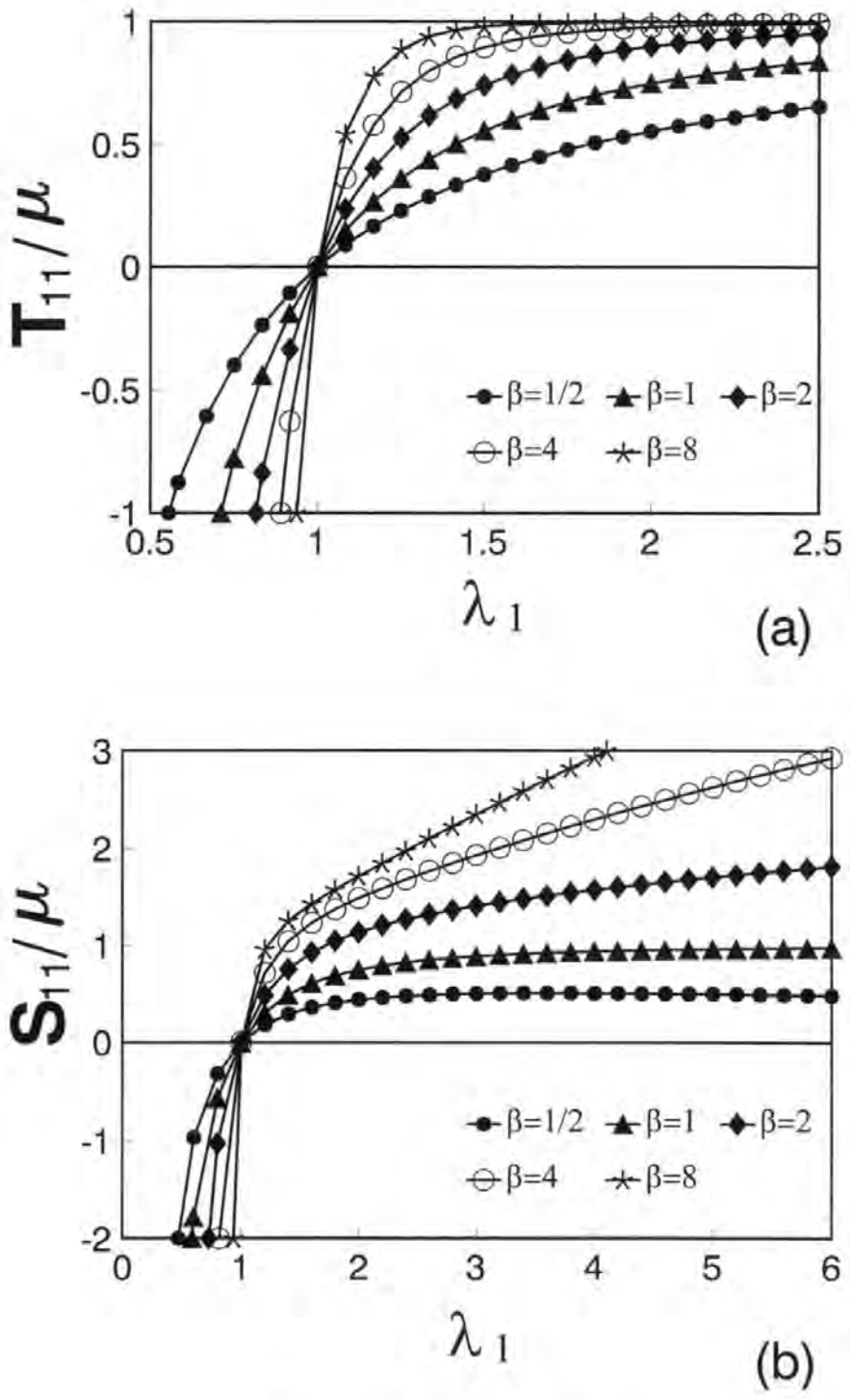

Figure 3.3: Isotropic plane stress

of S_{11} are qualitatively similar in the present circumstance and they indicate that the material become harder as β increases. In the case when $\beta = 1$ $S_{11}(\lambda_1)$ is an monotonic and concave increasing function and $S_{11} \to \mu$ as $\lambda_1 \to \infty$. For $\beta < 1$, however, $S_{11}(\lambda_1)$ increases steadily to its positive maximum value at $[(\beta+1)^2/(1-\beta)]^{(\beta+1)/[\beta(\beta+3)]}$ and then decreases monotonically to zero, with a reversal in curvature at $\{(\beta+1)^3(\beta+2)/[2(1-\beta)]\}^{(\beta+1)/[\beta(\beta+3)]}$. The distributions of the Piola stress corresponding to this circumstance are qualitatively different from the those in the case when $\beta > 1$, although they still indicate that the material hardens as β increases.

Further, in a special instance of *uni-axial tension* (or compression) parallel to the X_1-axis, one has

$$T_{22} = T_{33} = S_{22} = S_{33} = 0,\ \lambda_2 = \lambda_3 = \lambda_1^{-1/(\beta+2)},$$
$$T_{11} = \mu[1 - \lambda_1^{-\beta(\beta+3)/(\beta+2)}],\ S_{11} = \mu[\lambda_1^{-2/(\beta+2)} - \lambda_1^{-\beta-1}]. \tag{3.22}$$

In uni-axial tension (see Figure 3.4), according to (3.22), $T_{11}(\lambda_1)$ is likewise monotone increasing and concave; further $T_{11} \to \mu$ as $\lambda_1 \to \infty$ and $T_{11} \to -\infty$ as $\lambda_1 \to 0$. Also the inspection of Figure 3.4 reveals that the distributions of the Cauchy stress are qualitatively similar for all values of $\beta > 0$ and that they imply that the material becomes harder as β increases. It is of interest to note that these features of T_{11} are likely the same as in the cases of the isotropic extension and the isotropic plane stress. In contrast, $S_{11}(\lambda_1)$ in this case rises steadily to its positive maximum value at $[(1+\beta)(1+\beta/2)]^{(\beta+2)/\beta(\beta+3)}$ and then decreases monotonically to zero, with a reversal in curvature at $[(1+\beta)(2+\beta)^3/2]^{(\beta+2)/\beta(\beta+3)}$. The transverse stretch $\lambda_2(\lambda_1) = \lambda_3(\lambda_1)$

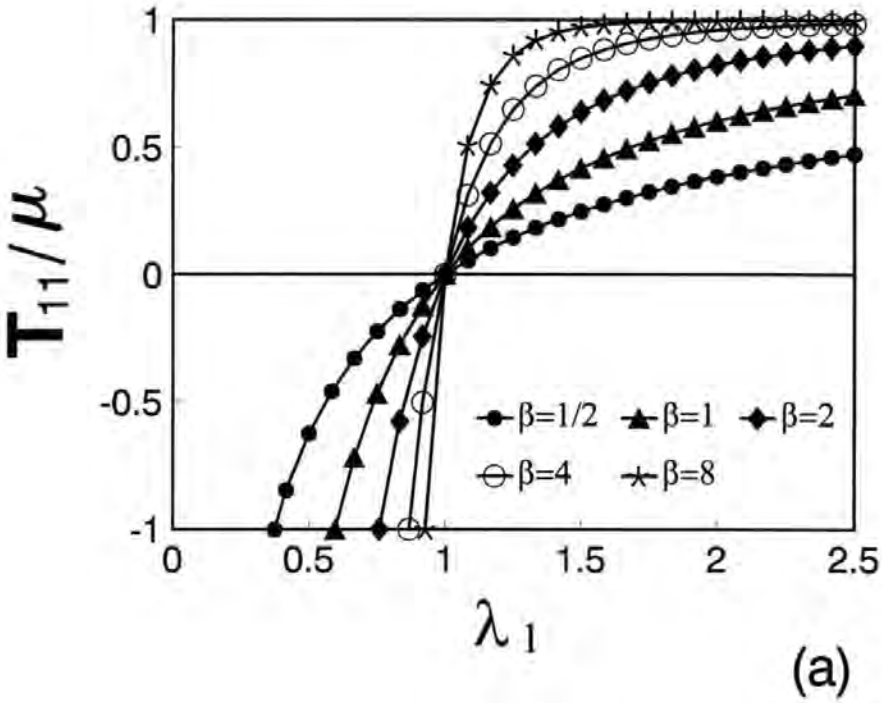

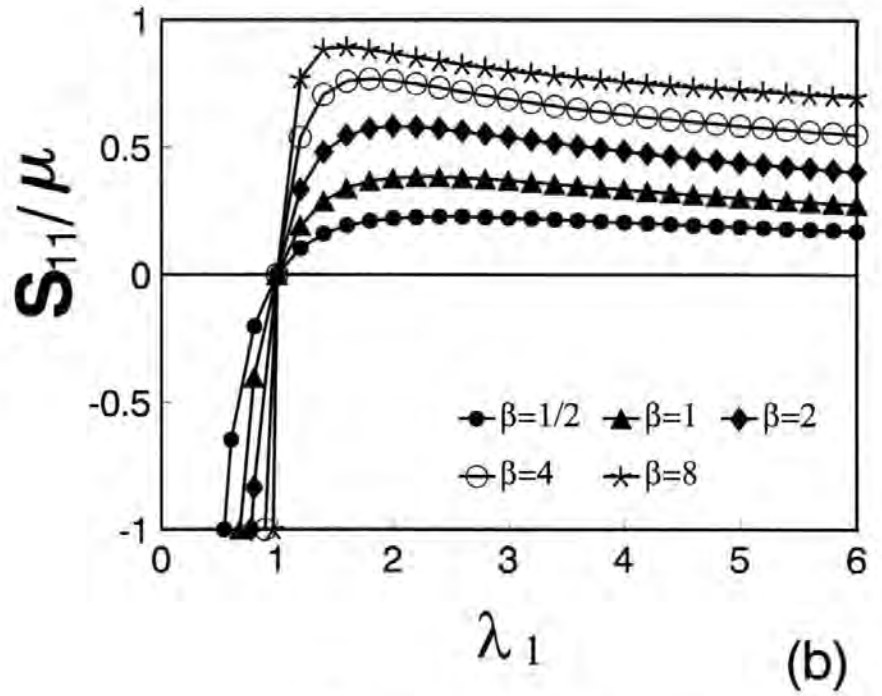

Figure 3.4: Uni-axial tension

is a decreasing convex function of the axial stretch λ_1, and $\lambda_2(\lambda_1) \to \infty$ as $\lambda_1 \to 0$, $\lambda_2(\lambda_1) \to 0$ as $\lambda_1 \to \infty$. From Figure 3.4 we note that the distributions of the Piola stresses are similar for all values of $\beta > 0$ and moreover, that the greater stress is needed for a fixed stretch as β increases. Therefore, we can conclude that the material hardens as β increases, which is the same as that drawn from the distributions of Cauchy stress corresponding to this deformation.

In the case of *isotropic plane strain* parallel to the plane $X_3 = 0$, we have

$$\lambda_3 = 1,\ \lambda_2 = \lambda_1,\ T_{11} = T_{22} = \mu(1 - \lambda_1^{-\beta-2}),\ T_{33} = \mu(1 - \lambda_1^{-2}),$$

$$S_{11} = S_{22} = \mu(\lambda_1 - \lambda_1^{-\beta-1}),\ S_{33} = \mu(\lambda_1^2 - 1). \tag{3.23}$$

In the case of isotropic plane strain (Figure 3.5), T_{11}, regarded as a function of λ_1, behaves qualitatively the same as in the above three cases. The Piola stress $S_{11}(\lambda_1)$ is a concave, monotone increasing function that tends to $-\infty$ as $\lambda_1 \to 0$ and $S_{11} = S_{22} \to \infty$ as $\lambda_1 \to \infty$. The transverse Piola stress S_{33} is convex and steadily increasing, with $S_{33}(0^+) = -\mu$, $S_{33}(\lambda_1) \to \infty$ as $\lambda_1 \to \infty$. It is shown by Figure 3.5 that for all values of $\beta > 0$, the distributions both Cauchy stress and Piola stress are qualitatively similar and that they indicate that the material becomes harder as β increases since the greater magnitudes both Cauchy and Piola stresses are corresponding to larger values of β.

In the event of *plane-strain uni-axial tension* (or compression) parallel to the X_1-axis, we get

$$\lambda_3 = 1,\ \lambda_2 = \lambda_1^{-1/(\beta+1)},$$

$$T_{11} = \mu[1 - \lambda_1^{-\beta(\beta+2)/(\beta+1)}],\ T_{22} = 0,\ T_{33} = \mu[1 - \lambda_1^{-\beta/(\beta+1)}], \tag{3.24}$$

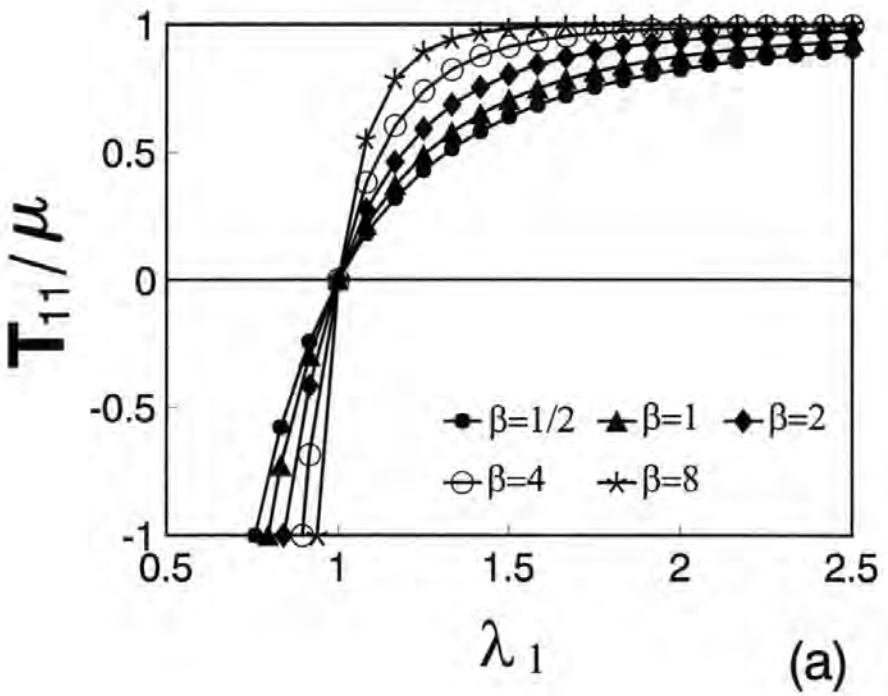

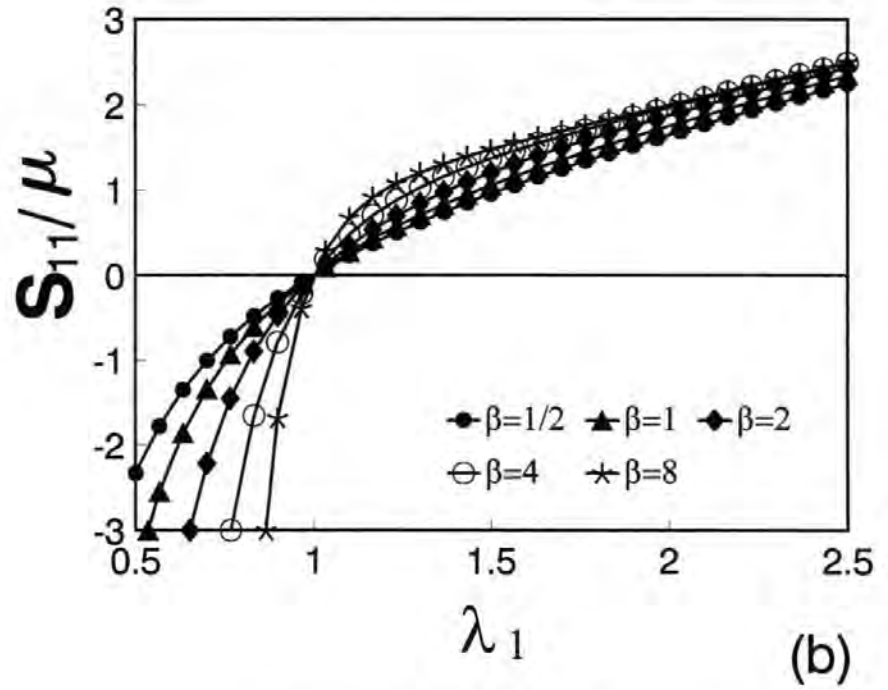

Figure 3.5: Isotropic plane strain

$$S_{11} = \mu[\lambda_1^{-1/(\beta+1)} - \lambda_1^{-\beta-1}],\ S_{22} = 0,\ S_{33} = \mu[\lambda_1^{\beta/(\beta+1)} - 1].$$

Equation (3.24), which pertains to plane-strain uni-axial tension (Figure 3.6), reveals that in this instance T_{11} is concave monotone increasing and that $T_{11} \to -\infty$ as $\lambda_1 \to 0$, $T_{11} \to \mu$ as $\lambda_1 \to \infty$; these properties are shared by the transverse Cauchy stress T_{33}. We note that the Cauchy stresses T_{11} and T_{33} behave qualitatively similar with the Cauchy stress T_{11} in the above four cases of homogeneous deformations and we can also conclude that the material becomes harder as β increases. On the other hand, the axial Piola stress S_{11} and the transverse stretch λ_2 exhibit the same qualitative behaviour as in the case of three-dimensional uni-axial tension discussed above. Further, S_{33} is concave and steadily increasing, $S_{33}(0^+) = -\mu$, $S_{33}(\lambda_1) \to \infty$ as $\lambda_1 \to \infty$. Also, we can draw the conclusion that for all values of $\beta > 0$, the material becomes harder as β increases from the distributions of the Piola stress S_{11}.

Finally, we consider a homogeneous plane deformation corresponding to a state of *simple shear*, parallel to the plane $X_3 = 0$. Thus, the deformation has the form

$$x_1 = X_1 + kX_2,\ x_2 = X_2,\ x_3 = X_3, \tag{3.25}$$

in which k is a constant, $\tan^{-1}k$ being the angle of shear. The principal stretches of (3.25) are related to k through

$$\lambda_1 = \sqrt{1 + \frac{k^2}{2} + \sqrt{k^2 + \frac{k^4}{4}}},\ \lambda_2 = \frac{1}{\lambda_1},\ \lambda_3 = 1. \tag{3.26}$$

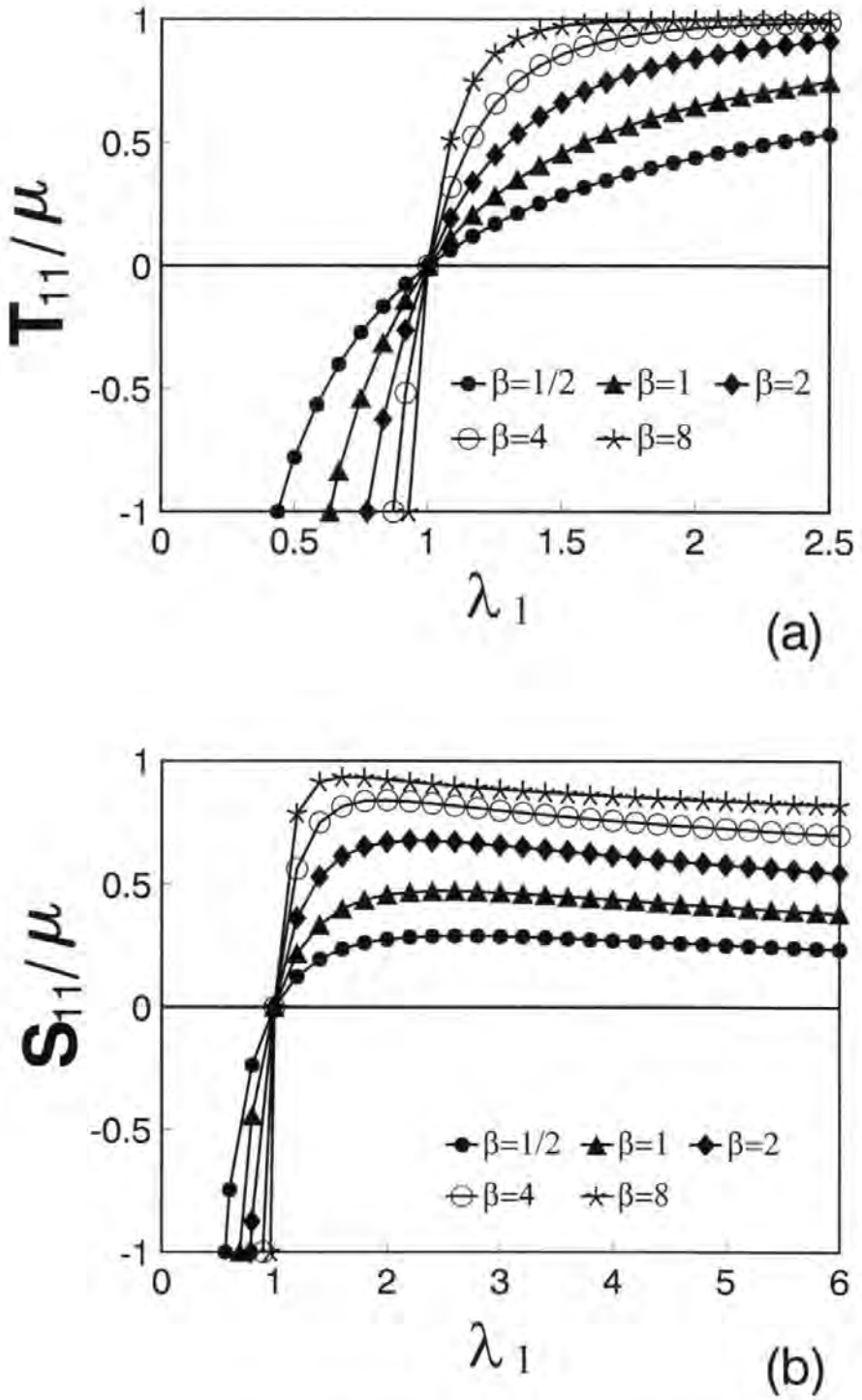

Figure 3.6: Plane strain uni-axial tension

In view of (3.26), matrix $\mathbf{D}$ (see (2.34)) reduces to

$$\mathbf{D} = 2\begin{bmatrix} \lambda_1 & \lambda_1^{-1}+\lambda_1 & \lambda_1^{-1} \\ \lambda_1^{-1} & \lambda_1^{-1}+\lambda_1 & \lambda_1 \\ 1 & \lambda_1^2+\lambda_1^{-2} & 1 \end{bmatrix}. \tag{3.27}$$

The determinant and the inverse matrix of $\mathbf{D}$ are

$$\det\mathbf{D} = 2(\lambda_1+\lambda_1^{-1})(\lambda_1^{-1}-\lambda_1)^3 \tag{3.28}$$

and

$$\mathbf{D}^{-1} = \frac{(\lambda_1^{-1}-\lambda_1)}{\det\mathbf{D}}\begin{bmatrix} \lambda_1^2 & \lambda_1^{-2} & -(\lambda_1^{-1}+\lambda_1) \\ -1 & -1 & \lambda_1^{-1}+\lambda_1 \\ \lambda_1^{-2} & \lambda_1^2 & -(\lambda_1^{-1}+\lambda_1) \end{bmatrix}. \tag{3.29}$$

From (2.27), (2.36), (3.2), (3.27) and (3.29) we find following expressions of stresses in the case of simple shear:

$$\begin{aligned}
T_{11} &= \frac{2\mu(\lambda_1^{-1}-\lambda_1)}{\det\mathbf{D}}[\lambda_1^{-3}+\lambda_1^3-\lambda_1^{-1}-\lambda_1 \\
&\quad +2\lambda_1^{1-\beta}+2\lambda_1^{\beta-1}-\lambda_1^{\beta+1}-\lambda_1^{-\beta-1}-\lambda_1^{3-\beta}-\lambda_1^{\beta-3}], \\
T_{12} &= T_{21} = \frac{2\mu k(\lambda_1^{-1}-\lambda_1)}{\det\mathbf{D}}[\lambda_1^{-\beta-1}+\lambda_1^{\beta+1}-\lambda_1^{\beta-1}-\lambda_1^{1-\beta}], \\
T_{22} &= \frac{2\mu(\lambda_1^{-1}-\lambda_1)}{\det\mathbf{D}}[\lambda_1^{-3}+\lambda_1^3-\lambda_1^{-1}-\lambda_1 \\
&\quad +2\lambda_1^{\beta+1}+2\lambda_1^{-\beta-1}-\lambda_1^{\beta-1}-\lambda_1^{1-\beta}-\lambda_1^{\beta+3}-\lambda_1^{-\beta-3}],
\end{aligned} \tag{3.30}$$

$$T_{3i} = T_{i3} = 0,\ S_{11} = S_{22} = T_{22},\ S_{12} = T_{12},\ S_{3i} = S_{i3} = 0,$$

$$\begin{aligned}
S_{21} &= T_{12} - kT_{22} = \frac{2\mu k(\lambda_1^{-1}-\lambda_1)}{\det\mathbf{D}}[\lambda_1^{-1}+\lambda_1-\lambda_1^{-3}-\lambda_1^3 \\
&\quad +\lambda_1^{\beta+3}+\lambda_1^{-\beta-3}-\lambda_1^{\beta+1}-\lambda_1^{-\beta-1}].
\end{aligned}$$

Variations of Cauchy stresses in the case of simple shear deformation are plotted in Figure 3.7. It is of interest to note on the basis of (3.30) that, in general, for the state of simple shear described by (3.25), the shear stresses T_{12}, S_{12} and S_{21} are non-linear (odd) steadily increasing functions of the shear parameter k; T_{12} and S_{12} depend linearly on the shear parameter k only in the case when $\beta = 2$. Observe that the normal stresses T_{22}, S_{11} (S_{22}) are compressive for all values of $\beta > 0$. But the normal stress T_{11} is tensile when $\beta < 2$, compressive when $\beta > 2$ and equal to zero only when $\beta = 2$. All non-vanishing stress components associated with the coordinate frame underlying (3.25) become unbounded as $k \to \infty$. We note from Figure 3.7 that for all values of $\beta \geq 2$, the distributions of the Cauchy stresses are qualitatively similar and that they indicate that the material hardens as β increases. For $\beta < 2$, however, the distributions of the Cauchy stresses are qualitatively different from those in the case when $\beta \geq 2$ and we can no longer conclude that the material becomes harder as β increases.

Thus, from the analysis on the above six cases of homogeneous deformations, see Figure 3.2 - Figure 3.7, we can draw the following conclusions:

(i) For all values of $\beta > 0$, the distributions of Cauchy and Piola stresses are qualitatively similar in the isotropic extension, the uni-axial tension, the isotropic plane strain, and the plane-strain uni-axial tension and they indicate that the material hardens as β increases.

(ii) For all values of $\beta > 1$, the distributions of Piola stresses in isotropic plane stress are qualitatively similar and they indicate that the material hardens as β increases. For

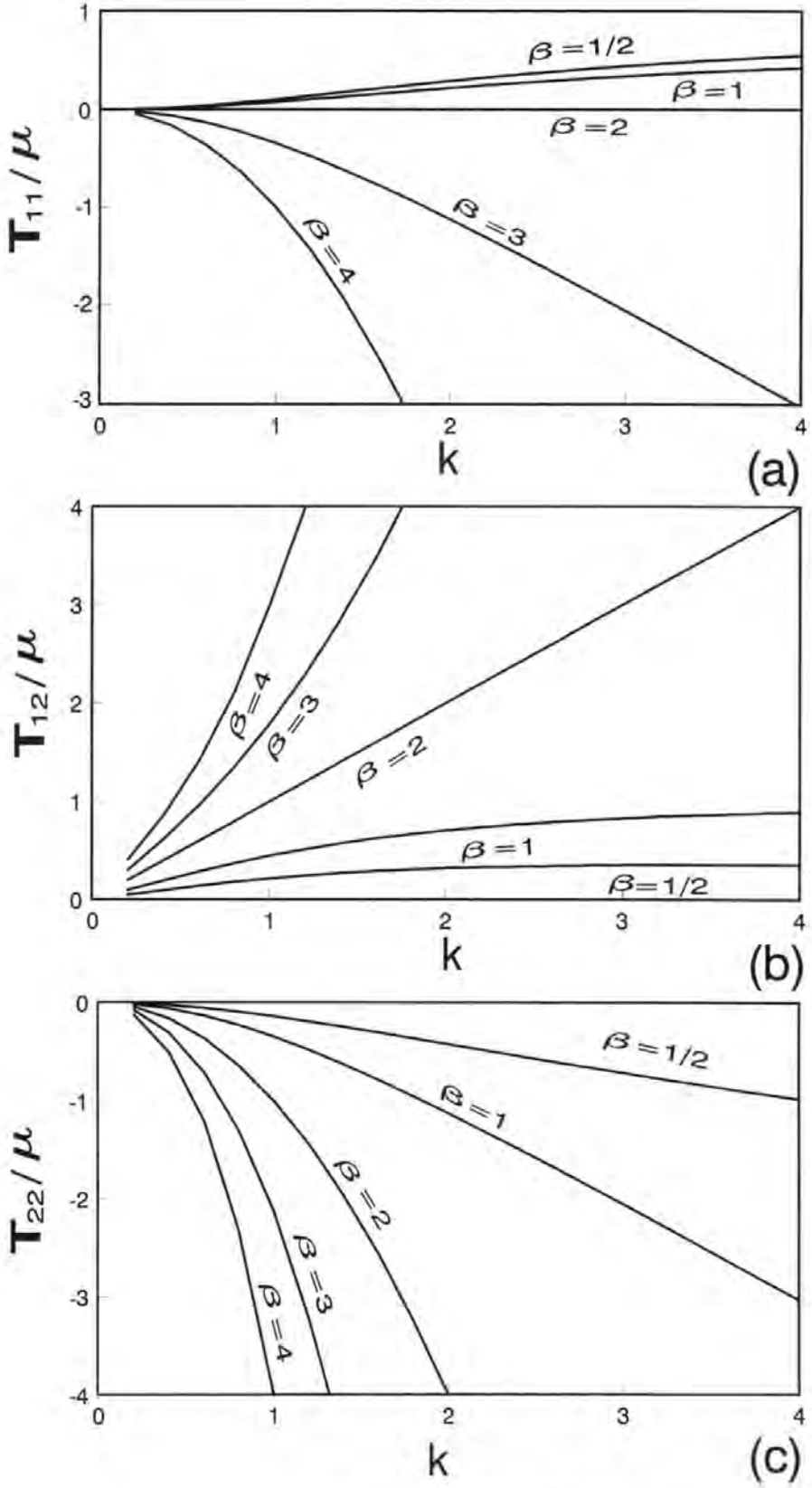

Figure 3.7: Simple shear

$\beta \leq 1$, however, the distributions of Piola stresses corresponding to this deformation are qualitatively different from the distributions in the case when $\beta > 1$, although they still indicate that the material hardens as β increases.

(iii) For all values of $\beta \geq 2$, the distributions of Cauchy stresses in the simple shear deformation are qualitatively similar and they indicate that the material hardens as β increases. For $\beta < 2$, however, the distributions of Piola stresses corresponding to this deformation are qualitatively different from the distributions in the case when $\beta \geq 2$. In particular for $\beta < 2$, we can no longer conclude that the material hardens as β increases.

Chapter 4

Straightening of a sector of a circular tube

In this chapter, we consider a simple non-homogeneous deformation in plane strain framework, namely the straightening of a sector of a circular tube. The chapter is presented in two parts: in the first part (section 4.1) we give the solution of the considered problem, and the analysis of the solution will be completed in the second part (section 4.2).

4.1 Solution of the problem

The non-homogeneous deformation with which we are concerned here is the straightening of a sector of a circular tube in plane strain. The deformation is given as (illustrated in Figure 4.1)

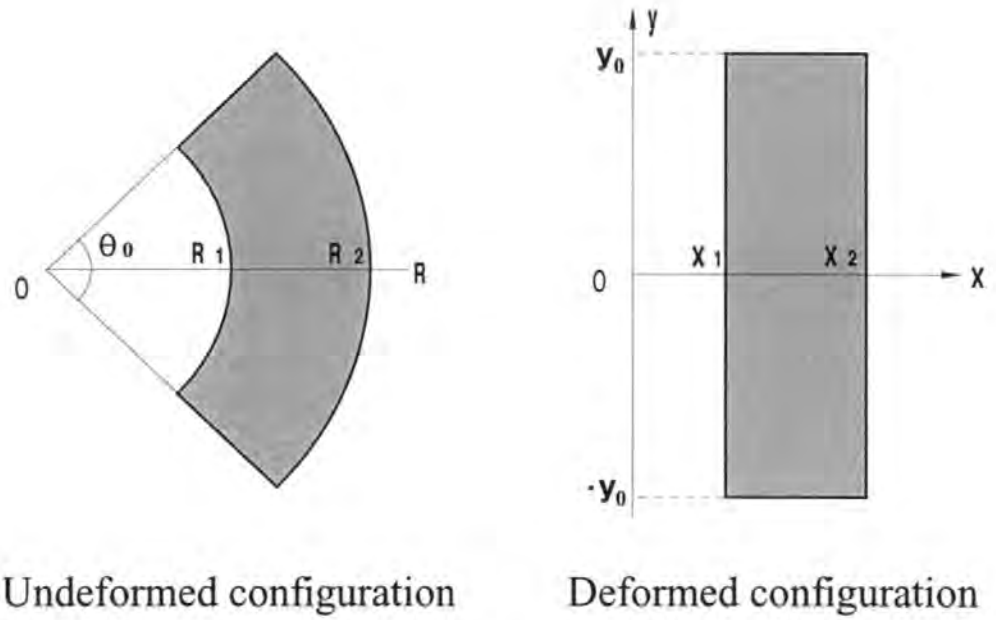

Figure 4.1: Straightening.

$$x = x(R),\ y = \alpha\Theta, \tag{4.1}$$

where, (x, y) are the Cartesian coordinates in the deformed configuration, (R, Θ) are the polar coordinates in the reference configuration, and α is a constant to be determined. The physical components of the deformation gradient are given by

$$[\mathbf{F}] = \begin{bmatrix} \mathrm{d}x/\mathrm{d}R & 0 \\ 0 & \alpha/R \end{bmatrix}. \tag{4.2}$$

Therefore, the principal stretches λ_i are

$$\lambda_1 = \frac{\mathrm{d}x}{\mathrm{d}R},\ \lambda_2 = \frac{\alpha}{R}. \tag{4.3}$$

On combining (2.27), (2.29) and (4.2) we obtain

$$T_{xx} = \frac{W_1}{\lambda_2} = \mu[1 - (\frac{\mathrm{d}R}{\mathrm{d}x})^{\beta+1} \cdot \frac{R}{\alpha}],\ T_{yy} = \frac{W_2}{\lambda_1} = \mu[1 - \frac{\mathrm{d}R}{\mathrm{d}x} \cdot (\frac{R}{\alpha})^{\beta+1}],\ T_{xy} = 0. \tag{4.4}$$

In view of (4.1) and (4.4), the equilibrium equation (see (2.96)) reduces to

$$\mathrm{d}T_{xx}/\mathrm{d}x = 0 \tag{4.5}$$

whose integration yields

$$x = C_1 R^{(\beta+2)/(\beta+1)} + C_2. \tag{4.6}$$

Here C_1, C_2 are arbitrary constants to be determined by boundary conditions. Note that the solution (4.6) is independent of the material parameter μ. On substituting (4.6) into (4.4) we find the non-vanishing components of Cauchy stresses as

$$T_{xx} = \mu[1 - \alpha^{-1} C_1^{-\beta-1} (\frac{\beta+1}{\beta+2})^{\beta+1}],\ T_{yy} = \mu[1 - \alpha^{-\beta-1} C_1^{-1} (\frac{\beta+1}{\beta+2}) R^{\frac{\beta(\beta+2)}{(\beta+1)}}]. \tag{4.7}$$

The analysis of the solution (4.6) will be carried out in the following section.

4.2 Boundary value problems

4.2.1 Boundary conditions of Place

We consider boundary conditions of place, that is

$$x = x_1, \text{ at } R = R_1;\ \ x = x_2, \text{ at } R = R_2;\ \ y = \pm y_0, \text{ at } \Theta = \pm\Theta_0, \tag{4.8}$$

where R_1, R_2 are the inner and outer radii of a sector of a circular tube in the reference configuration, and x_1, x_2 $(x_2 > x_1)$ are two prescribed values of the surfaces $R = R_1$ and $R = R_2$ after deformation.

Introducing the ratio of the radii

$$k \equiv R_2/R_1 > 1, \tag{4.9}$$

we find that, in view of (4.8) and (4.6), constants C_1, C_2, α can be determined as

$$\begin{aligned} C_1 &= \frac{x_2 - x_1}{k^{(\beta+2)/(\beta+1)} - 1} \cdot R_1^{-(\beta+2)/(\beta+1)}, \\ C_2 &= \frac{x_1 k^{(\beta+2)/(\beta+1)} - x_2}{k^{(\beta+2)/(\beta+1)} - 1}, \\ \alpha &= y_0/\Theta_0. \end{aligned} \tag{4.10}$$

The principal stretches (4.3) are then expressed as

$$\lambda_1 = \frac{(\beta+2)}{(\beta+1)[k^{(\beta+2)/(\beta+1)} - 1]} \cdot \frac{x_2 - x_1}{R_1} \cdot (\frac{R}{R_1})^{1/(\beta+1)}, \quad \lambda_2 = \frac{\alpha}{R}. \tag{4.11}$$

Clearly the principal stretches λ_i are always positive for any prescribed positive values x_1, x_2 with $x_2 > x_1$.

From (4.11) we obtain the ratio of the principal stretches as

$$w \equiv \frac{\lambda_1}{\lambda_2} = \frac{(\beta+2)(x_2 - x_1)}{(\beta+1)\alpha[k^{(\beta+2)/(\beta+1)} - 1]} \cdot (\frac{R}{R_1})^{(\beta+2)/(\beta+1)}. \tag{4.12}$$

Since w increases monotonically with R, the S-E condition (3.5) will be satisfied if and only if we have

$$t_E < w(R_1) \text{ and } w(R_2) < 1/t_E. \tag{4.13}$$

From (4.12) and (4.13) we find the following restrictions on the prescribed boundary values and the original geometry, which are equivalent to (4.13):

$$(\frac{\beta+1}{\beta+2})\alpha[k^{(\beta+2)/(\beta+1)} - 1]t_E < x_2 - x_1 < (\frac{\beta+1}{\beta+2})\alpha[1 - k^{-(\beta+2)/(\beta+1)}]t_E^{-1}. \tag{4.14}$$

For the condition (4.14) to hold, it is necessary that

$$k < t_E^{-2(\beta+1)/(\beta+2)} \tag{4.15}$$

and thus, if $k > k_{max} \equiv t_E^{-2(\beta+1)/(\beta+2)}$ the solution will be unstable. It is of interest to note that the inequality (4.15) gives the maximum thickness ($k_{max} \equiv t_E^{-2(\beta+1)/(\beta+2)}$) of the circular tube for which this deformation may be stable. Even if (4.15) holds, however, the solution is still unstable if the prescribed values x_1, x_2 in the deformed configuration are not in the range given by (4.14).

4.2.2 The traction boundary condition: Part I

The constants C_1 and α may also be determined by requiring that

$$T_{xx}(x_1) = 0,\ T_{xx}(x_2) = 0 \tag{4.16}$$

in which

$$x_1 \equiv x(R_1),\ x_2 \equiv x(R_2) \tag{4.17}$$

and by prescribing the load acting on the surfaces $\Theta = \pm\Theta_0$. For simplicity we require that

$$\int_{x_1}^{x_2} T_{yy} \mathrm{d}x = 0. \tag{4.18}$$

From (4.16) we find that

$$C_1 = (\frac{\beta+1}{\beta+2}) \cdot \alpha^{-1/(\beta+1)}, \tag{4.19}$$

which implies that $T_{xx} = 0$ for $x \in [x_1, x_2]$.

In view of (4.7), (4.18) and (4.19), we obtain

$$\alpha = R_1(\beta+1)^{-(\beta+1)/[\beta(\beta+2)]}\left[\frac{k^{(\beta+2)/(\beta+1)}-1}{k^{\beta+2}-1}\right]^{-(\beta+1)/[\beta(\beta+2)]} \tag{4.20}$$

where $k = R_2/R_1$. Consequently, the solution (4.6) now is determined in this way up to an arbitrary constant C_2 as

$$\begin{aligned} x &= (\frac{\beta+1}{\beta+2})\alpha^{-1/(\beta+1)}R^{(\beta+2)/(\beta+1)} + C_2 \\ &= \frac{(\beta+1)^{\frac{(\beta+1)^2}{\beta(\beta+2)}}}{(\beta+2)} \cdot \left[\frac{k^{(\beta+2)/(\beta+1)}-1}{k^{\beta+2}-1}\right]^{\frac{1}{\beta(\beta+2)}} \cdot (\frac{R}{R_1})^{\frac{\beta+2}{\beta+1}} \cdot R_1 + C_2. \end{aligned} \tag{4.21}$$

Here C_2 stands for a rigid movement of the rectangular block in the deformed configuration. When $\beta = 2$, the deformation (4.21) with $C_2 = 0$ is that obtained by Carroll and Horgan [17] for the Blatz-Ko material.

The only non-vanishing component of Cauchy stresses T_{yy} now is in the form

$$T_{yy} = \mu[1 - (\beta+1)\frac{k^{(\beta+2)/(\beta+1)}-1}{k^{\beta+2}-1}(\frac{R}{R_1})^{\beta(\beta+2)/(\beta+1)}], \tag{4.22}$$

which we re-write as

$$T_{yy} = \mu\{1 - (\beta+1)\frac{k^{(\beta+2)/(\beta+1)}-1}{k^{\beta+2}-1}\left[(k^{(\beta+2)/(\beta+1)}-1)\zeta + 1\right]^{\beta}\}, \tag{4.23}$$

where

$$\zeta \equiv (x - x_1)/(x_2 - x_1),\ x_1 \equiv x(R_1),\ x_2 \equiv x(R_2). \tag{4.24}$$

The ratio S/S_0, where S is the cross-sectional area in the deformed configuration and S_0 is the cross-sectional area in the reference configuration, is given by

$$\frac{S}{S_0} = \frac{2(\beta+1)^{(\beta+1)/(\beta+2)}(k^{(\beta+2)/(\beta+1)}-1)^{(\beta+1)/(\beta+2)}(k^{\beta+2}-1)^{1/(\beta+2)}}{(\beta+2)(k^2-1)}, \tag{4.25}$$

The moment M acting at the ends of the rectangular block is

$$M \equiv -\int_{x_1}^{x_2} T_{yy}(x - C_2)\mathrm{d}x, \tag{4.26}$$

which, together with (4.22) yields

$$\frac{M}{\mu R_1^2} = \frac{(\beta+1)^{\frac{(3\beta^2+6\beta+2)}{(\beta^2+2\beta)}}}{(\beta+2)^3} \cdot [k^{\frac{(\beta+2)^2}{(\beta+1)}} - 1][\frac{k^{\frac{(\beta+2)}{(\beta+1)}} - 1}{k^{\beta+2} - 1}]^{\frac{(\beta^2+2\beta+2)}{(\beta^2+2\beta)}}$$
$$-\frac{1}{2}\frac{(\beta+1)^{\frac{2(\beta+1)^2}{\beta(\beta+2)}}}{(\beta+2)^2} \cdot [k^{\frac{(2\beta+4)}{(\beta+1)}} - 1][\frac{k^{\frac{(\beta+2)}{(\beta+1)}} - 1}{k^{\beta+2} - 1}]^{\frac{2}{\beta(\beta+2)}}. \tag{4.27}$$

From (4.3), (4.20), and (4.21), the principal stretches can be determined as

$$\lambda_1 = (\beta+1)^{1/[\beta(\beta+2)]} \cdot \left[\frac{k^{(\beta+2)/(\beta+1)} - 1}{k^{\beta+2} - 1}\right]^{1/[\beta(\beta+2)]} (\frac{R}{R_1})^{1/(\beta+1)}, \quad \lambda_2 = \lambda_1^{-\beta-1}, \tag{4.28}$$

and their ratio is

$$w = (\beta+1)^{1/\beta} \cdot \left[\frac{k^{(\beta+2)/(\beta+1)} - 1}{k^{\beta+2} - 1}\right]^{1/\beta} (\frac{R}{R_1})^{(\beta+2)/(\beta+1)}. \tag{4.29}$$

Therefore, the S-E condition (3.5) is satisfied provided that

$$k^{\beta+2} - 1 < [k^{(\beta+2)/(\beta+1)} - 1](\beta+1)t_E^{-\beta}, \; 1 - k^{-\beta-2} > [1 - k^{-(\beta+2)/(\beta+1)}](\beta+1)t_E^{\beta}. \tag{4.30}$$

Numerical experiments with (4.30) indicate that $(4.30)_2$ holds for all $k > 1$ and $(4.30)_1$ implies that

$$k < k_E, \tag{4.31}$$

where k_E is a critical value of k, determined by

$$k_E^{\beta+2} = 1 + [k_E^{(\beta+2)/(\beta+1)} - 1](\beta+1)t_E^{-\beta}. \tag{4.32}$$

β	1/2	1	2	3	4
k_E	4.8972	4.5026	3.7884	3.2779	2.9157
k_{max}	10.3276	9.1808	7.21176	5.8736	4.9723
t_E	0.14289	0.1896	0.2679	0.3306	0.3820

Table 4.1: The values of k_E, k_{max}, t_E *vs.* β

Thus, it appears that if $k > k_E$ the solution is unstable for the traction boundary conditions considered here. The values of k_E, t_E, k_{max} for a range of β are shown numerically in Table 4.1. Note that k_E, k_{max} decrease with parameter β, and tend to unity as β tends to infinity. For any $\beta > 0$, $k_E < k_{max}$ holds always, which means that for $k \in (k_E, k_{max})$ we may have stability for boundary conditions of place whereas for boundary conditions of traction the solution is unstable.

From (4.21) and (4.28) we find that extreme values of the principal stretches occur on surfaces of the block since $\mathrm{d}\lambda_1/\mathrm{d}x = (\mathrm{d}\lambda_1/\mathrm{d}R)(\mathrm{d}R/\mathrm{d}x) > 0$ and $\mathrm{d}\lambda_2/\mathrm{d}x = (\mathrm{d}\lambda_2/\mathrm{d}R)(\mathrm{d}R/\mathrm{d}x) < 0$. The values of $\lambda_1(x_1), \lambda_1(x_2), \lambda_2(x_1), \lambda_2(x_2)$ for a range of β are given in Table 4.2. It can be seen that the body is deformed more severely near $x = x_1$. It is also interesting to note that the values of the principal stretch $\lambda_2(x_1)$ (regarded as a function of β), beyond which the strong-ellipticity condition is violated, are within the range $[2.2, 3.2]$ when β is given as $\beta = 1/2, 1, 2, 3, 4$ (see Table 4.3).

The plot S/S_0 *vs.* k is given in Figure 4.2, and this reveals that the area of the considered body becomes larger after deformation and it is an increasing function of β

k	β	$\lambda_1(x_1)$	$\lambda_1(x_2)$	$\lambda_2(x_1)$	$\lambda_2(x_2)$
1.2	1/2	.93743	1.05859	1.10177	.91814
	1	.95248	1.04339	1.10227	.91856
	2	.96770	1.02833	1.10353	.91961
	3	.97537	1.02086	1.10490	.92075
	4	.98000	1.01639	1.10631	.92193
2.9	1/2	.62116	1.26318	2.04268	.70437
	1	.69575	1.18481	2.06585	.71236
	2	.77849	1.11016	2.11954	.73088
	3	.82375	1.07497	2.17180	.74890
	4	.85263	1.05498	2.21914	.76522

Table 4.2: The values of $\lambda_1(x_1), \lambda_1(x_2), \lambda_2(x_1), \lambda_2(x_2)$ *vs.* β and k.

k_E	β	$\lambda_1(x_1)$	$\lambda_1(x_2)$	$\lambda_2(x_1)$	$\lambda_2(x_2)$
4.897	1/2	.459	1.324	3.214	.656
4.503	1	.574	1.219	3.031	.673
3.788	2	.719	1.122	2.685	.709
3.278	3	.801	1.078	2.424	.739
2.916	4	.852	1.055	2.230	.765

Table 4.3: The values of $\lambda_1(x_1), \lambda_1(x_2), \lambda_2(x_1), \lambda_2(x_2)$ *vs.* β and k_E.

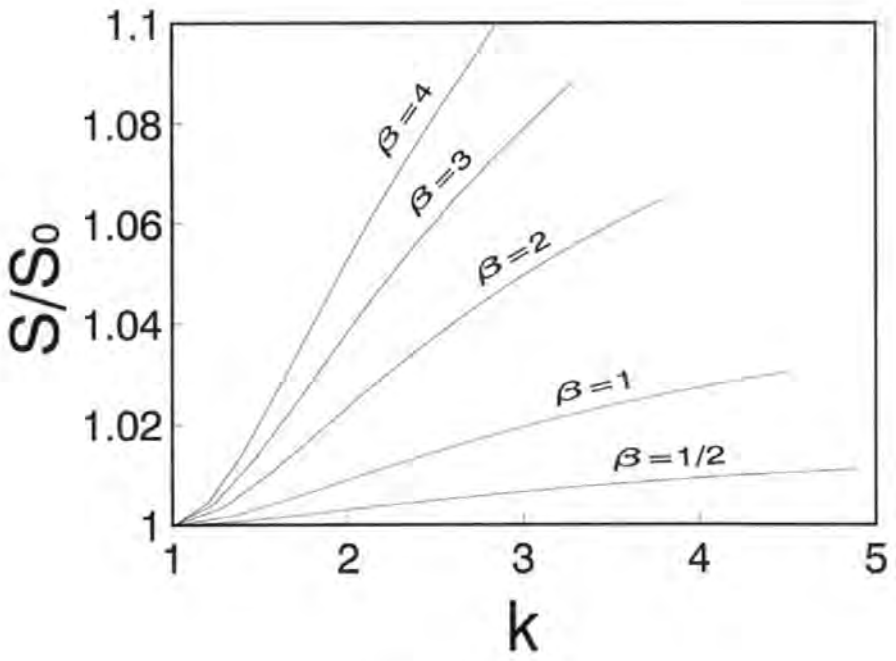

Figure 4.2: S/S_0 *vs.* k.

and k.

In view of (4.27), for a fixed value k, the moment M is a quadratic function of the inner radius R_1; but for a fixed value of the inner radius R_1, the moment M is an increasing function of the ratio k, as illustrated in Figure 4.3. Note that a larger moment M is needed for a prescribed value of k as β increases.

The distribution of the normal stress T_{yy} along the x-axis ($x \in [x_1, x_2]$, see (4.21)) is illustrated in Figure 4.4. It can be seen from Figure 4.4 that the normal stress T_{yy} decreases monotonically with x (cf. (4.23)). It is in tension at $x = x_1$ and in compression at $x = x_2$. As the thickness of the circular tube increases the magnitude of the Cauchy stress T_{yy} increases significantly (comparing Figure 4.4a and Figure 4.4b). As β increases, $T_{yy}(x_1)$ increases and tends to unity. It is interesting to note that

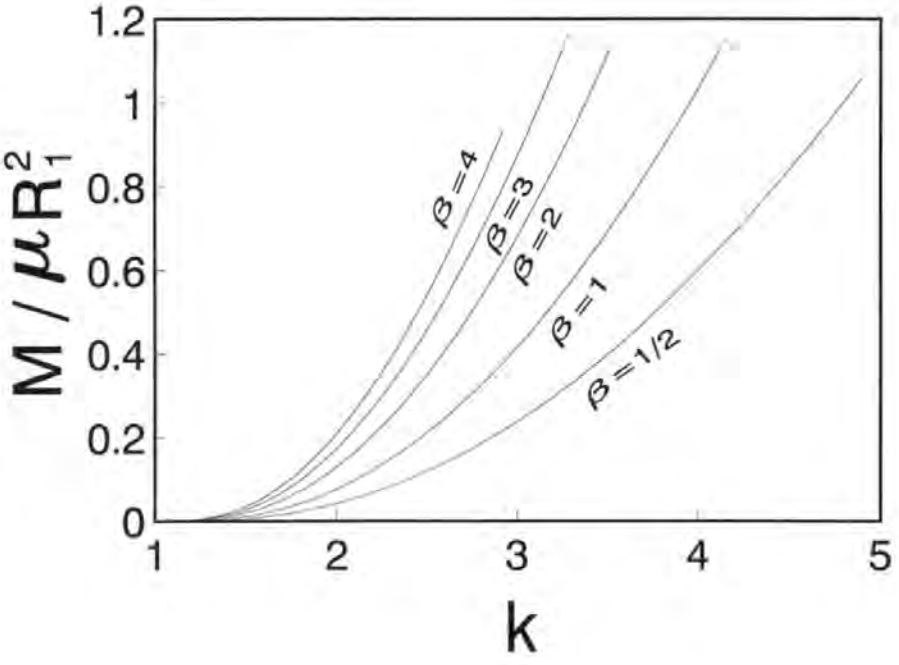

Figure 4.3: M *vs.* k.

regarded as a function of x, T_{yy} decreases faster with increasing values of β and the magnitude of T_{yy} increases as β increases. Therefore, the conjecture that the material becomes harder as β increases, drawn from considerations regarding homogeneous deformations in Chapter 3, is verified further here from considerations regarding this non-homogeneous deformation.

4.2.3 The traction boundary condition: Part II

Now we consider another boundary condition of traction to determine the constants C_1 and α. We still use the same prescriptions for the tractions on the surfaces $x = x_1$, $x = x_2$ as those in Section 4.2.2 (that is, (4.16)), but, instead of the resultant force acting on the surfaces $\Theta = \pm\Theta_0$, we prescribe the moment M given by (4.26). As before, we

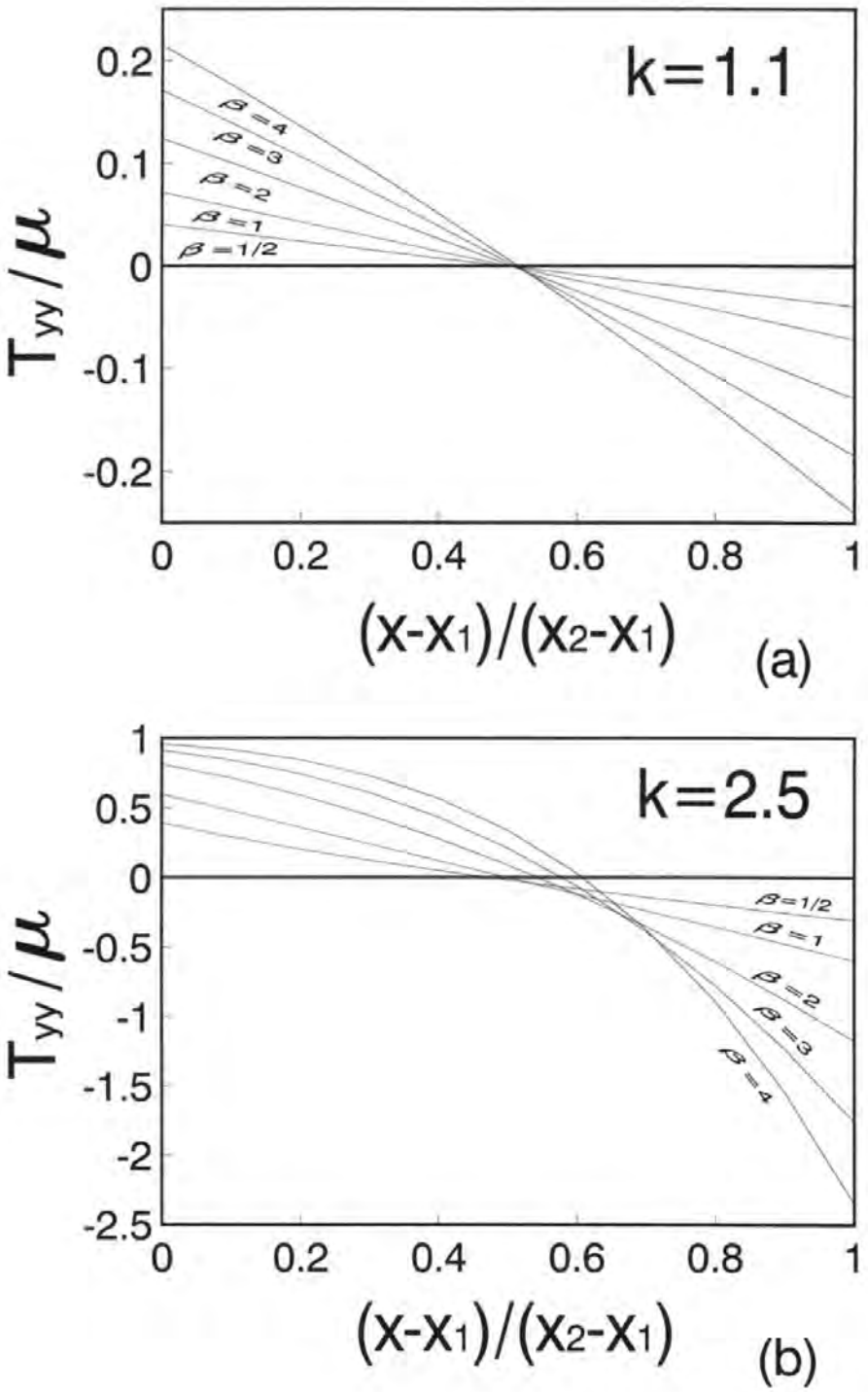

Figure 4.4: T_{yy} *vs.* x.

find that C_1 is given by (4.19) and thus we again have $T_{xx} = 0$ for $x \in [x_1, x_2]$.

On substituting (4.7) and (4.19) into (4.26), we find the following equation to determine R_1/α for any prescribed moment M as

$$\frac{M}{\mu R_1^2} = \frac{(\beta+1)^2}{2(\beta+2)^2}(\frac{R_1}{\alpha})^{2/(\beta+1)}[k^{2(\beta+2)/(\beta+1)} - 1]$$
$$-\frac{(\beta+1)^2}{(\beta+2)^3}(\frac{R_1}{\alpha})^{(\beta^2+2\beta+2)/(\beta+1)}[k^{(\beta+2)^2/(\beta+1)} - 1]. \tag{4.33}$$

The solution (4.6) is then determined in this way up to an arbitrary constant C_2 as

$$x = (\frac{\beta+1}{\beta+2})(\frac{R_1}{\alpha})^{1/(\beta+1)}(\frac{R}{R_1})^{(\beta+2)/(\beta+1)} \cdot R_1 + C_2 \tag{4.34}$$

in which R_1/α is determined by (4.33) and C_2 stands for a rigid movement of the rectangular block in the deformed configuration.

The only non-vanishing component of Cauchy stresses T_{yy} now is in the form

$$T_{yy} = \mu[1 - (\frac{R_1}{\alpha})^{\beta(\beta+2)/(\beta+1)} \cdot (\frac{R}{R_1})^{\beta(\beta+2)/(\beta+1)}], \tag{4.35}$$

or

$$T_{yy} = \mu\{1 - (\frac{R_1}{\alpha})^{\beta(\beta+2)/(\beta+1)}[1 + (k^{(\beta+2)/(\beta+1)} - 1)\zeta]^{\beta}\}, \tag{4.36}$$

where

$$\zeta \equiv (x - x_1)/(x_2 - x_1). \tag{4.37}$$

Naturally, we are concerned about the features of the moment M as a function of R_1/α. We introduce the notations

$$u \equiv (\frac{R_1}{\alpha})^{1/(\beta+1)} > 0, \; s \equiv k^{(\beta+2)/(\beta+1)} > 1,$$
$$\sigma(u) \equiv (\beta+2)(s^2-1)u^2 - 2(s^{\beta+2} - 1)u^{\beta^2+2\beta+2} \tag{4.38}$$

with the help of which (4.33) can be re-written as

$$\frac{M}{\mu R_1^2} = \frac{(\beta+1)^2}{2(\beta+2)^3}\sigma(u). \tag{4.39}$$

The first derivative of $\sigma(u)$ is

$$\sigma'(u) = 2(\beta+2)(s^2-1)u - 2(\beta^2+2\beta+2)(s^{\beta+2}-1)u^{\beta^2+2\beta+1}, \tag{4.40}$$

and thus, there are two stationary points for this function, given by

$$u_1 = 0,\ u_2^{\beta(\beta+2)} = \frac{(\beta+2)}{(\beta^2+2\beta+2)} \cdot \frac{(s^2-1)}{(s^{\beta+2}-1)} < 1, \tag{4.41}$$

and we also have

$$\sigma(u_1) = 0,\ \sigma(u_2) = \frac{\beta(\beta+2)^2(s^2-1)u_2^2}{\beta^2+2\beta+2} > 0. \tag{4.42}$$

Equation (4.40) can be rewritten as

$$\begin{aligned}\sigma'(u) &= 2(\beta+1)(s^2-1)u[1 - \frac{(\beta^2+2\beta+2)(s^{\beta+2}-1)u^{\beta(\beta+2)}}{(\beta+2)(s^2-1)}] \\ &= 2(\beta+1)(s^2-1)u[1 - (\frac{u}{u_2})^{\beta(\beta+2)}].\end{aligned} \tag{4.43}$$

Clearly we have

$$\sigma'(u) > 0,\ \text{for } 0 < u < u_2,\ \sigma'(u) < 0,\ \text{for } u > u_2. \tag{4.44}$$

By substituting $u = 1$ into (4.38) we find

$$\sigma(1) = (\beta+2)(s^2-1) - 2(s^{\beta+2}-1) \equiv \omega(s). \tag{4.45}$$

Since $\omega(1) = 0$, $\omega'(s) = 2(\beta+2)s(1-s^{\beta+1}) < 0$ for $s > 1$, we infer that

$$\sigma(1) = \omega(s) < 0,\ \text{for } s > 1. \tag{4.46}$$

Now we are ready to give a description of the moment M as a function of R_1/α: The moment M attains a maximum $M_{\max}$ at $R_1/\alpha = (R_1/\alpha)_m$, defined as

$$(\frac{R_1}{\alpha})_m \equiv \{\frac{(\beta+2)[k^{2(\beta+2)/(\beta+1)}-1]}{(\beta^2+2\beta+2)[k^{(\beta+2)^2/(\beta+1)}-1]}\}^{(\beta+1)/[\beta(\beta+2)]}. \tag{4.47}$$

When $0 < R_1/\alpha < (R_1/\alpha)_m$, M is a positive and steadily increasing function of R_1/α and reaches its only maximum M_{max} at $(R_1/\alpha)_m$ so that

$$\frac{M_{max}}{\mu R_1^2} \equiv \frac{\beta(\beta+1)^2(\beta+2)^{(2-2\beta-\beta^2)/[\beta(\beta+2)]}[k^{2(\beta+2)/(\beta+1)}-1]^{(\beta^2+2\beta+2)/[\beta(\beta+2)]}}{2(\beta^2+2\beta+2)^{(\beta^2+2\beta+2)/[\beta(\beta+2)]}[k^{(\beta+2)^2/(\beta+1)}-1]^{2/[\beta(\beta+2)]}}. \tag{4.48}$$

In contrast, when $R_1/\alpha > (R_1/\alpha)_m$, M decreases monotonically with R_1/α and tends to negative infinity as R_1/α tends to positive infinity. Using the fact that $\sigma(1) < 0$ we find that M has one root only given by

$$(\frac{R_1}{\alpha})_0 \equiv \{\frac{(\beta+2)[k^{2(\beta+2)/(\beta+1)}-1]}{2[k^{(\beta+2)^2/(\beta+1)}-1]}\}^{(\beta+1)/[\beta(\beta+2)]} \tag{4.49}$$

and we note that

$$(\frac{R_1}{\alpha})_m < (\frac{R_1}{\alpha})_0 < 1 \tag{4.50}$$

(see also the variation of M with R_1/α in Figure 4.5).

Thus we can draw conclusion on the solvability of (4.33) for any prescribed moment M: (i) if M is prescribed so that $M > M_{max}$ there is no solution to the boundary value problem; (ii) if M is given to be the value of M_{max}, that is, $M = M_{\max}$, there is only one solution to this problem and $R_1/\alpha = (R_1/\alpha)_m$; (iii) otherwise if M is given so that $M < M_{max}$ there are two solutions to the boundary value problem.

theory has also been found in other deformations (for example, the homogeneous deformation considered by Rivlin [63], the radial expansion of cylindrical and spherical shells by Chung & Horgan [16], the bending of a rectangular block of semi-linear material by Aron & Wang [32]; more examples can also be found in [64, 14] *et al*). In what follows we examine the stability of the solution by using the S-E criteria.

From (4.3) and (4.34), the principal stretches are given as

$$\lambda_1 = (\frac{R_1}{\alpha})^{1/(\beta+1)}(\frac{R}{R_1})^{1/(\beta+1)},\ \lambda_2 = \lambda_1^{-\beta-1}. \tag{4.51}$$

Hence, the S-E condition (3.5) is satisfied provided that

$$\frac{R_1}{\alpha} > t_E^{(\beta+1)/(\beta+2)},\ \frac{R_1}{\alpha} < k^{-1}t_E^{-(\beta+1)/(\beta+2)}. \tag{4.52}$$

The numerical experiments (using (4.49) and (4.52)) indicate that $k^{-1}t_E^{-(\beta+1)/(\beta+2)} > (R_1/\alpha)_0$ holds always, so we will omit $(4.52)_2$ henceforward. It follows also from the numerical examination that there exists a value of k, namely $\hat{k}_E(\beta)$, so that when $k > \hat{k}_E$ the S-E condition is always violated and so, the solution is unstable in the case. When $k < \hat{k}_E$ we can also conclude that the solution is unstable for certain values of k and $M/\mu R_1^2$. The values of $\hat{k}_E$ for a range of β are given in Table 4.4. As an example, in the case of $\beta = 3$, shown in Figure 4.5a, it follows that $\hat{k}_E = 0.3045$. When $k > 0.3045$ there are no stable solutions of this form. We may have one stable solution with $R_1/\alpha = .4753$ for $k = 2.5,\ \beta = 3,\ M/\mu R_1^2 = 0.3$ and also two solutions with $R_1/\alpha = .4137$ and $R_1/\alpha = 0.4577$ respectively for $k = 1.5,\ \beta = 3,\ M/\mu R_1^2 = 0.3264$, both of which may be infinitesimally stable (see also Figure 4.5b).

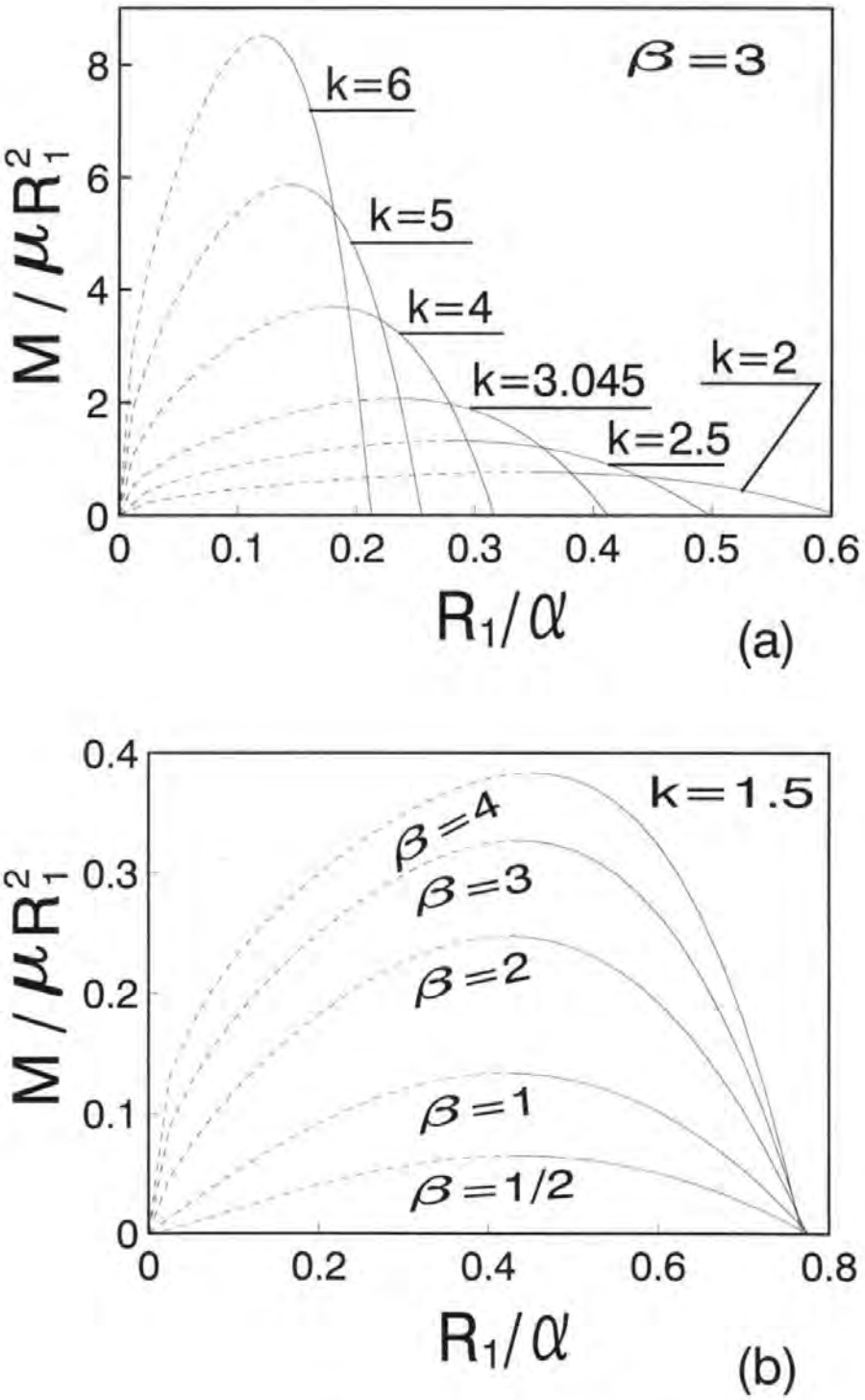

Figure 4.5: $M/\mu R_1^2$ *vs.* R_1/α.

β	1/2	1	2	3	4
t_E	0.14289	0.1896	0.2679	0.3306	0.3820
$t_E^{\frac{\beta+1}{\beta+2}}$	0.3112	0.3300	0.3724	0.4125	0.4484
$\hat{k}_E$	4.1703	3.9327	3.4350	3.0437	2.7507

Table 4.4: The values of $\hat{k}_E, t_E, t_E^{(\beta+1)/(\beta+2)}$ *vs.* β

To discriminate between multiple solutions we investigate the solution (4.34) further on physical grounds. For the convenience of discussion, We call one of the solutions, in which, M increases from 0 to M_{max} (for $0 < (R_1/\alpha) < (R_1/\alpha)_m$) as the first solution and the other, in which, M decreases from M_{max} to 0 (for $(R_1/\alpha)_m < (R_1/\alpha) < (R_1/\alpha)_0$) as the second solution. In figure 4.5, the first solution is denoted by dotted lines and the second by solid lines. For a sector of a circular tube with fixed geometric size values of R_1, R_2 and Θ_0, the physically realistic response should give us an increasing Cauchy stress T_{yy} with increasing moment M, that is

$$(T'_{yy} - T_{yy})(M' - M) > 0, \text{ if } M' \neq M. \tag{4.53}$$

It follows from (4.36) that

$$T'_{yy} - T_{yy} = \mu\{(\frac{R_1}{\alpha})^{\beta(\beta+2)/(\beta+1)} - [(\frac{R_1}{\alpha})']^{\beta(\beta+2)/(\beta+1)}\}(\frac{R}{R_1})^{\beta(\beta+2)/(\beta+1)}, \tag{4.54}$$

where (R_1/α) and $(R_1/\alpha)'$ are the values of (R_1/α) related to M and M' respectively. It can be readily verified that (4.53) only holds for the second solution due to the

monotonic decrease of M with (R_1/α) . Therefore we can reject the first solution on this physical ground.

Chapter 5

Bending of a rectangular block

In this chapter, we consider another simple non-homogeneous deformation in plane strain —the bending of a rectangular block into a sector of circular tube, which is the inverse of the deformation considered in Chapter 4. The solution of the considered deformation is presented in Section 5.1, and discussions follow in Section 5.2.

5.1 Solution of the problem

The non-homogeneous deformation with which we are concerned here is the bending of a rectangular block into a sector of circular tube and is illustrated in Figure 5.1. In plain strain framework, this deformation is usually sought in the form

$$r = r(X),\ -A \leq X \leq A;\ \ \theta = \alpha Y,\ -B \leq Y \leq B, \tag{5.1}$$

where, (r, θ) are the polar coordinates in the deformed configuration, (X, Y) are the Cartesian coordinates in the reference configuration, and α is a positive constant to be

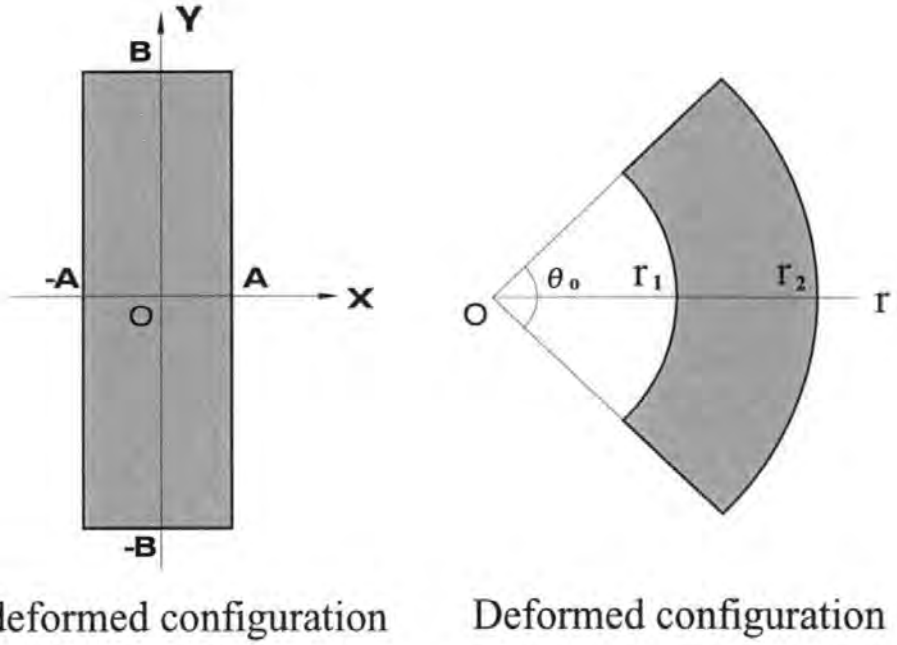

Figure 5.1: Bending.

determined. The rectangular block in the undeformed configuration is described as

$$-A \leq X \leq A,\ -B \leq Y \leq B,\ A, B = \text{constants}, \tag{5.2}$$

and the sector of circular tube in the deformed configuration is characterized by

$$r(-A) \leq r(X) \leq r(A),\ -\alpha B \leq \theta \leq \alpha B. \tag{5.3}$$

In view of (5.1), we have the physical components of the deformation gradient tensor $\mathbf{F}$ as

$$\mathbf{F} = \begin{bmatrix} \mathrm{d}r/\mathrm{d}X & 0 \\ 0 & \alpha r \end{bmatrix}. \tag{5.4}$$

For the deformation, the principal stretches λ_i are

$$\lambda_1 = \frac{\mathrm{d}r}{\mathrm{d}X},\ \lambda_2 = \alpha r, \tag{5.5}$$

and from $\alpha > 0$ we infer that a solution $r(X)$ to the bending problem must necessarily satisfy

$$r(X) > 0, \ \frac{\mathrm{d}r}{\mathrm{d}X} > 0. \tag{5.6}$$

Substitutions of (5.4) and (5.5) into the stress response equations (2.27), (2.29) give the components of the Cauchy stress $\mathbf{T}$ by

$$T_{rr} = \frac{W_1}{\lambda_2} = \mu[1-(\frac{\mathrm{d}X}{\mathrm{d}r})^{\beta+1}(\alpha r)^{-1}], T_{\theta\theta} = \frac{W_2}{\lambda_1} = \mu[1-\frac{\mathrm{d}X}{\mathrm{d}r}(\alpha r)^{-\beta-1}], T_{r\theta} = 0. \tag{5.7}$$

In view of (5.1) and (5.7), the radial equation of equilibrium (see (2.98))

$$\frac{\mathrm{d}T_{rr}}{\mathrm{d}r} + \frac{1}{r}(T_{rr} - T_{\theta\theta}) = 0 \tag{5.8}$$

thus reduces to

$$(\beta+1)\alpha^{\beta} r^{\beta+1} \frac{\mathrm{d}^2 X}{\mathrm{d}r^2} = (\frac{\mathrm{d}X}{\mathrm{d}r})^{1-\beta}. \tag{5.9}$$

A first integration leads to

$$(\beta+1)^{1/\beta}\alpha\frac{\mathrm{d}X}{\mathrm{d}r} = \frac{1}{r}(C_1 r^{\beta} - 1)^{1/\beta}, \tag{5.10}$$

where C_1 is a constant of integration. The second integration of the above equation yields a solution in the form

$$(\beta+1)^{1/\beta}\alpha X + C_2 = \int_{C_1^{-1/\beta}}^{r} \frac{(C_1 r^{\beta} - 1)^{1/\beta}}{r} dr, \tag{5.11}$$

where C_1, C_2 are arbitrary constants to be determined by boundary condition. The solution (5.11) was examined by Carroll & Horgan for the case of $\beta = 2$ [17]. On introducing

$$u \equiv (C_1 r^{\beta} - 1)^{1/\beta}, \ \eta(u) \equiv u - \int_0^u \frac{d\xi}{\xi^{\beta}+1}, \tag{5.12}$$

the solution (5.11) can be rewritten as

$$(\beta+1)^{1/\beta}\alpha X + C_2 = \eta(u). \tag{5.13}$$

Note that the solution (5.13) does not depend on the material parameter μ. Explicit expressions of the function η for some values of β are given in Table 5.1. The substitution

β	$\eta(u)$
1/2	$u - 2\sqrt{u} + 2\ln(\sqrt{u}+1)$
1	$u - \ln(u+1)$
2	$u - \arctan(u)$
3	$u - \frac{\arctan[(2u-1)/\sqrt{3}]}{\sqrt{3}} - \frac{1}{6}\ln[\frac{(u+1)^2}{(u^2-u+1)}] - \frac{\sqrt{3}\pi}{18}$
4	$u - \frac{\arctan(\sqrt{2}u+1)}{2\sqrt{2}} - \frac{\arctan(\sqrt{2}u-1)}{2\sqrt{2}} - \frac{\sqrt{2}}{8}\ln[\frac{u^2+\sqrt{2}u+1}{u^2-\sqrt{2}u+1}]$

Table 5.1: Explicit expressions of $\eta(u)$

of solution (5.11) into (5.7) leads to

$$\left.\begin{aligned} T_{rr} &= \mu[1-(\beta+1)^{-1-1/\beta}(\alpha r)^{-\beta-2}(C_1 r^\beta - 1)^{1+1/\beta}], \\ T_{\theta\theta} &= \mu[1-(\beta+1)^{-1/\beta}(\alpha r)^{-\beta-2}(C_1 r^\beta - 1)^{1/\beta}]. \end{aligned}\right\} \tag{5.14}$$

In view of (5.10) the principal stretches λ_i can now be expressed as

$$\lambda_1 = (\beta+1)^{1/\beta}\alpha r(C_1 r^\beta - 1)^{-1/\beta},\ \lambda_2 = \alpha r, \tag{5.15}$$

which are strictly positive for all $X \in [-A, A]$ provided that

$$v \equiv C_1[r(-A)]^\beta > 1. \tag{5.16}$$

5.2 Boundary value problem

5.2.1 The boundary condition of place

In the first instance we require that the following displacement boundary conditions be satisfied by the considered deformation:

$$r(-A) = r_1,\ r(A) = r_2,\ \ r_2 > r_1 > 0, \tag{5.17}$$

and

$$\theta = \pm\theta_0,\ \text{at}\ Y = \pm B,\ \ \theta_0 > 0, \tag{5.18}$$

where r_1, r_2 are given values of the inner and outer radii of the sector of circular tube in the deformed configuration (cf. Figure 5.1) and θ_0 is a prescribed angle of the sector of circular tube. For convenience of following discussion, we introduce the ratio of the prescribed radii

$$k \equiv r_2/r_1, \tag{5.19}$$

and in view of (5.12) and (5.16) denote

$$u_1 \equiv (C_1 r_1^{\beta} - 1)^{1/\beta} = (v-1)^{1/\beta},\ u_2 \equiv (C_1 r_2^{\beta} - 1)^{1/\beta} = (vk^{\beta} - 1)^{1/\beta}. \tag{5.20}$$

From (5.13) and (5.17) we then find that

$$\alpha = \theta_0/B \tag{5.21}$$

and

$$2(\beta+1)^{1/\beta}\alpha A = \eta(u_2) - \eta(u_1), \tag{5.22}$$

$$C_1 = v/r_1^{\beta},\ C_2 = [\eta(u_1) + \eta(u_2)]/2. \tag{5.23}$$

Clearly α is determined by (5.21) and once the parameter v is determined by the non-linear equation (5.22), constants C_1, C_2 can then be obtained from (5.23). On substituting (5.22) and (5.23) into (5.13) we can rewrite (5.13) as

$$[\eta(u_2) - \eta(u_1)]\frac{X}{A} + \eta(u_2) + \eta(u_1) = 2\eta(u),\ u = [v(\frac{r}{r_1})^{\beta} - 1]^{1/\beta}. \tag{5.24}$$

We note that v is a function of $\alpha A, k$ and β only, which implies that for a given value β the class of deformations with same values of αA and k will have the same solution. Therefore, we deduce that (5.24) with (5.20)-(5.22) represents the solution to the bending problem (5.9) and (5.17). The numerical examination of the solvability of (5.22) reveals that for any prescribed values of $\alpha A, k, \beta$, there always exists a positive value of v and that $v > 1$.

In view of (5.15) the S-E condition (3.5) is satisfied if and only if

$$(\beta+1)t_E^{\beta} + 1 < C_1 r^{\beta} < (\beta+1)t_E^{-\beta} + 1, \tag{5.25}$$

which are equivalent to

$$(\beta+1)t_E^{\beta} + 1 < C_1 r_1^{\beta} < C_1 r_2^{\beta} < (\beta+1)t_E^{-\beta} + 1. \tag{5.26}$$

On substituting (5.16) and (5.19) into (5.26) we obtain the specified S-E condition for the bending problem under the boundary condition of place in the form

$$(\beta+1)t_E^{\beta} + 1 < v < k^{-\beta}[(\beta+1)t_E^{-\beta} + 1], \tag{5.27}$$

which require that

$$k < k_{max} \equiv \{[(\beta+1)t_E^{-\beta}+1]/[(\beta+1)t_E^{\beta}+1]\}^{1/\beta}. \tag{5.28}$$

It is of interest to note that if $k > k_{max}$, i.e. (5.28) is violated, we do not expect that the deformed configuration of the body will be described by the equations (5.24) and (5.20)-(5.22) since this solution is unstable. Thus $k = k_{max}$ is the maximum value of the ratio r_2/r_1 for which the solution may be stable. The further numerical examination on (5.22), (5.27) and (5.28) reveals that for a fixed value of β, there exists a specific value of αA, namely $(\alpha A)_{max}$ so that for any value of $\alpha A > (\alpha A)_{max}$ the S-E condition is always violated. When αA takes the value of $(\alpha A)_{max}$, the S-E condition holds only for the value of $k = k_{max}$. Otherwise in the case when $\alpha A < (\alpha A)_{max}$, the S-E condition holds for a range of k, that is, for $k \in [k_1, k_2]$. Here, k_1 and k_2 are functions of αA and β and we have $k_1, k_2 < k_{max}$. The numerically computed values of k_{max} and $(\alpha A)_{max}$ for a range of β and the numerically computed values of k_1 and k_2 for a range of β and αA are shown in Table 5.2. We note that for a fixed value of αA $(< (\alpha A)_{max})$, k_{max} decreases with β, which implies that the thickness of the circular tube for which the solution may be stable decreases as β increases. Also we conclude that the range of thicknesses of the circular tube for which we may have a stable solution becomes smaller as β increases because k_1 increases with β, and k_2 decreases with β.

β	$(\alpha A)_{max}$	k_{max}	αA	k_1	k_2
1/2	2.429	10.05	0.50	1.171	3.791
			1.75	2.240	8.046
1	2.011	8.374	0.50	1.237	3.320
			1.75	3.506	7.540
2	1.449	5.934	0.60	1.483	3.205
			1.20	2.972	5.137
3	1.132	4.603	0.45	1.425	2.515
			0.90	2.510	3.895
4	0.935	3.820	0.40	1.441	2.254
			0.80	2.609	3.425

Table 5.2: The values of $(\alpha A)_{max}, k_{max}, k_1, k_2$ *vs.* β.

5.2.2 The boundary condition of traction

Now we determine the solution to the bending problem by prescribing boundary conditions of traction. We require that

$$T_{rr}(r_1) = T_{rr}(r_2) = 0, \tag{5.29}$$

and prescribe the moment acting on $\theta = \pm\theta_0$

$$M \equiv \int_{r_1}^{r_2} T_{\theta\theta} r \mathrm{d}r, \ M > 0, \tag{5.30}$$

where r_1 and r_2 are defined as

$$r_1 \equiv r(-A), \ \ r_2 \equiv r(A). \tag{5.31}$$

We note that (5.29) implies (see [50, Section 5.2.4])

$$\int_{r_1}^{r_2} T_{\theta\theta} \mathrm{d}r = 0. \tag{5.32}$$

The Cauchy stresses (5.14) can be rewritten as

$$\left.\begin{aligned} T_{rr} &= \mu\{1 - (\beta+1)^{-1-1/\beta}(\alpha r_1)^{-\beta-2}(\tfrac{r}{r_1})^{-\beta-2}[v(\tfrac{r}{r_1})^{\beta} - 1]^{1+1/\beta}\}, \\ T_{\theta\theta} &= \mu\{1 - (\beta+1)^{-1/\beta}(\alpha r_1)^{-\beta-2}(\tfrac{r}{r_1})^{-\beta-2}[v(\tfrac{r}{r_1})^{\beta} - 1)^{1/\beta}\}, \end{aligned}\right\} \tag{5.33}$$

and the substitution of $X = A$ and $X = -A$ into (5.13) leads to

$$C_2 = [\eta(u_1) + \eta(u_2)]/2, \ \ 2(\beta+1)^{1/\beta}\alpha A = \eta(u_2) - \eta(u_1), \tag{5.34}$$

in which u_1, u_2 are defined in (5.20) and $\eta(u)$ in (5.12). Thus (5.13) can be expressed as

$$[\eta(u_2) - \eta(u_1)]\frac{X}{A} + \eta(u_2) + \eta(u_1) = 2\eta(u), \ u = [v(\frac{r}{r_1})^{\beta} - 1]^{1/\beta}. \tag{5.35}$$

It is clear from (5.33) and (5.35) that once constants r_1, r_2, u_1, u_2, v and α are determined, the boundary value problem is solved. In what follows we will be discussing how these constants are to be determined by making use of (5.29) and (5.30).

From (5.29) we obtain

$$\left.\begin{aligned} \alpha r_1 &= u_1^{(\beta+1)/(\beta+2)}(\beta+1)^{-(\beta+1)/[\beta(\beta+2)]}, \\ \alpha r_2 &= u_2^{(\beta+1)/(\beta+2)}(\beta+1)^{-(\beta+1)/[\beta(\beta+2)]}. \end{aligned}\right\} \tag{5.36}$$

The substitution of $(5.36)_1$ into $(5.36)_2$ leads to

$$v = [k^{\beta(\beta+2)/(\beta+1)} - 1]/[k^{\beta(\beta+2)/(\beta+1)} - k^{\beta}], \tag{5.37}$$

and

$$u_1 = k^{-1}\{(1-k^{\beta})/[1-k^{\beta/(\beta+1)}]\}^{1/\beta}, \; u_2 = u_1 k^{(\beta+2)/(\beta+1)}. \tag{5.38}$$

With the help of $(5.34)_2$, r_1 and r_2 can then be expressed as

$$r_1 = \frac{2A(\beta+1)^{1/[\beta(\beta+2)]}u_1^{(\beta+1)/(\beta+2)}}{[\eta(u_2)-\eta(u_1)]}, \tag{5.39}$$

$$r_2 = k\frac{2A(\beta+1)^{1/[\beta(\beta+2)]}u_1^{(\beta+1)/(\beta+2)}}{[\eta(u_2)-\eta(u_1)]}. \tag{5.40}$$

Observe that $(5.34)_2$ and (5.37)-(5.40) express $u_1, u_2, v, \alpha, r_1, r_2$ in terms of the ratio $k = r_2/r_1$ which, in view of (5.30), is related with the prescribed moment M by

$$\frac{M}{2\mu A^2} = \frac{k^2 - 1 - 2(\beta+1)vu_1^{-\beta-1}\int_{u_1}^{u_2}\frac{\xi^{\beta}}{(\xi^{\beta}+1)^2}d\xi}{(\beta+1)^{-2/[\beta(\beta+2)]}[\eta(u_2)-\eta(u_1)]^2 u_1^{-2(\beta+1)/(\beta+2)}}. \tag{5.41}$$

Clearly once k is determined by (5.41) for a given moment M, then $\alpha, v, r_1, r_2, u_1, u_2$ can be easily obtained through $(5.34)_2$ and (5.37)-(5.40).

The expressions for the principal stretches (5.5) reduce to

$$\left.\begin{aligned}\lambda_1 &= (\beta+1)^{1/[\beta(\beta+2)]}u_1^{(\beta+1)/(\beta+2)}\cdot(\tfrac{r}{r_1})[v(\tfrac{r}{r_1})^\beta-1]^{-\frac{1}{\beta}},\\ \lambda_2 &= (\beta+1)^{-(\beta+1)/[\beta(\beta+2)]}u_1^{(\beta+1)/(\beta+2)}(\tfrac{r}{r_1}).\end{aligned}\right\} \tag{5.42}$$

Since (cf. (5.37))

$$\frac{\mathrm{d}v(k)}{\mathrm{d}k}<0,\ v(1)=\beta+2>2,\ v\to 1,\ k\to\infty, \tag{5.43}$$

it follows that $\lambda_1,\lambda_2>0$ for all $X\in[-A,A]$. The extreme values of the principal stretches (regarded as functions of r) occur on surfaces $r=r_1$ and $r=r_2$ due to the fact that

$$\frac{\mathrm{d}\lambda_1}{\mathrm{d}r}<0,\ \frac{\mathrm{d}\lambda_2}{\mathrm{d}r}>0. \tag{5.44}$$

Thus, the S-E condition (3.5) is satisfied if and only if

$$(\beta+1)t_E^{\beta}<\frac{k^\beta-1}{k^{\beta(\beta+2)/(\beta+1)}-k^\beta}\ \text{ and }\ (\beta+1)t_E^{-\beta}>\frac{k^{\beta(\beta+2)/(\beta+1)}-k^{\beta/(\beta+1)}}{k^{\beta/(\beta+1)}-1}. \tag{5.45}$$

The numerical examination on (5.45) indicates that $(5.45)_1$ holds always and $(5.45)_2$ reduces to

$$k<\tilde{k}_E \tag{5.46}$$

where $\tilde{k}_E$ is determined by

$$(\beta+1)t_E^{-\beta}=\frac{k^{\beta(\beta+2)/(\beta+1)}-k^{\beta/(\beta+1)}}{k^{\beta/(\beta+1)}-1}. \tag{5.47}$$

Numerical values of $\tilde{k}_E$ for $\beta=1/2,1,2,3,4$ are given in Table 5.3 (The values of $\tilde{k}_E$ are also shown by dots in Figure 5.2).

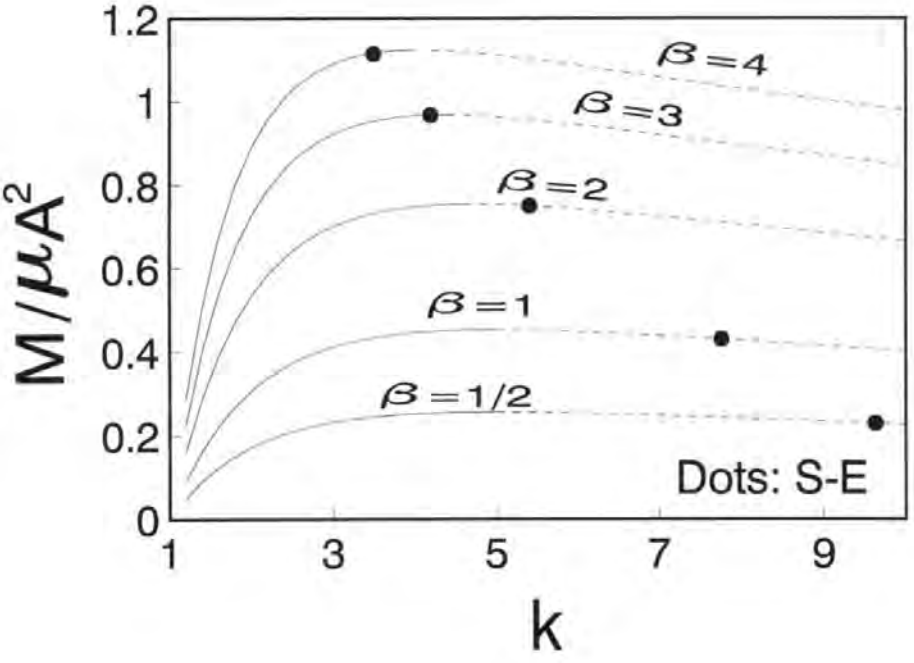

Figure 5.2: M *vs.* k

Naturally we would like to gain insight into the behaviour of $M = M(k)$. Hence we plot this function in Figure 5.2 with $\beta = 1/2, 1, 2, 3, 4$ and only for the range of $k < \tilde{k}_E$ since the solution is unstable when $k > \tilde{k}_E$.

β	1/2	1	2	3	4
t_E	0.14289	0.1896	0.2679	0.3306	0.3820
$\tilde{k}_E$	9.628	7.763	5.406	4.197	3.497
$\lambda_2(r_2)$	3.214	3.030	2.685	2.424	2.230

Table 5.3: The values of $t_E, \tilde{k}_E, \lambda_2(r_2)$ *vs.* β

Observe that M attains a maximum $M_{max} = M_{max}(\beta)$ at a certain value of $\bar{k}_m = \bar{k}_m(\beta)$. This observation implies that (i) if M is given so that $M > M_{max}$ there are no solutions to this problem and (ii) if M is prescribed so that $M < M_{max}$ there are two solutions to the bending problem. For convenience of further discussion, we denote the first of the two solutions, in which M increases from zero to M_{max} (for $1 < k < \bar{k}_m$) as the first solution and the other, in which M decreases from M_{max} (for $k > \bar{k}_m$), as the second solution. The two solutions are shown in Figure 5.2 by solid lines and dotted lines respectively. We note that non-uniqueness of this type also occurs for the straightening problem and was discussed in Section 4.2.3. We note that for certain values of M and β there could be two solutions, both of which may be stable (cf. Figure 5.2). In order to distinguish between these two possibilities, we check the solution (5.35) further on physical grounds. For a given rectangular block (with fixed values A, B), the expectation for a physically realistic response of Cauchy stresses of the block is that the Cauchy stresses should increase with the moment M. From this requirement we should have

$$[T'_{\theta\theta}(r_1) - T_{\theta\theta}(r_1)](M' - M) < 0, \text{ if } M' \neq M. \tag{5.48}$$

Here $T'_{\theta\theta}(r_1)$ and $T_{\theta\theta}(r_1)$ are the hoop Cauchy stress corresponding to prescribed values M' and M respectively. Thus from the expressions of the Cauchy stresses (5.33), which can be re-written as

$$\left.\begin{aligned} T_{rr} &= \mu\{1 - u_1^{-\beta-1}(\tfrac{r}{r_1})^{-\beta-2}[v(\tfrac{r}{r_1})^{\beta} - 1]^{1+\frac{1}{\beta}}\}, \\ T_{\theta\theta} &= \mu\{1 - (\beta+1)u_1^{-\beta-1}(\tfrac{r}{r_1})^{-\beta-2}[v(\tfrac{r}{r_1})^{\beta} - 1]^{\frac{1}{\beta}}\}, \end{aligned}\right\} \tag{5.49}$$

(5.48) reduces to

$$(\beta+1)[u_1^{-\beta-1}(v-1)^{1/\beta}-(u_1')^{-\beta-1}(v'-1)^{1/\beta}](M'-M)<0, \tag{5.50}$$

where u_1', v' are values which correspond to the moment M' and u_1, v are values which correspond to the moment M. The numerical examination of (5.37), (5.38) and (5.50) indicates that (5.50) holds only for the first solution, which is shown by the solid lines in Figure 5.2, due to the monotonical increase of M with k. Therefore we can reject the second solution, shown by dotted lines in Figure 5.2, on physical grounds.

The ratio S of the cross-sectional area of the body in the deformed configuration to the cross-sectional area of the body in the reference configuration is

$$S=(\beta+1)^{-1/(\beta+2)}\frac{(k^2-1)}{2[\eta(u_2)-\eta(u_1)]}u_1^{2(\beta+1)/(\beta+2)}. \tag{5.51}$$

The plot of S *vs.* k is shown in Figure 5.3. It can be seen from Figure 5.3 that the body expands after the deformation and S is an increasing function of β (for fixed k) and also k (for fixed β).

In view of the monotonical variations of the principal stretches along the r-axis (see (5.44)), the extreme values of the principal stretches at $r=r_1$ and $r=r_2$ are

$$\begin{aligned}
\lambda_1(r_1)&=(\beta+1)^{1/[\beta(\beta+2)]}u_1^{(\beta+1)/(\beta+2)}(v-1)^{-1/\beta},\\
\lambda_1(r_2)&=(\beta+1)^{1/[\beta(\beta+2)]}u_2^{(\beta+1)/(\beta+2)}(vk^\beta-1)^{-1/\beta},\\
\lambda_2(r_1)&=(\beta+1)^{-(\beta+1)/[\beta(\beta+2)]}u_1^{(\beta+1)/(\beta+2)},\\
\lambda_2(r_2)&=(\beta+1)^{-(\beta+1)/[\beta(\beta+2)]}u_2^{(\beta+1)/(\beta+2)}.
\end{aligned} \tag{5.52}$$

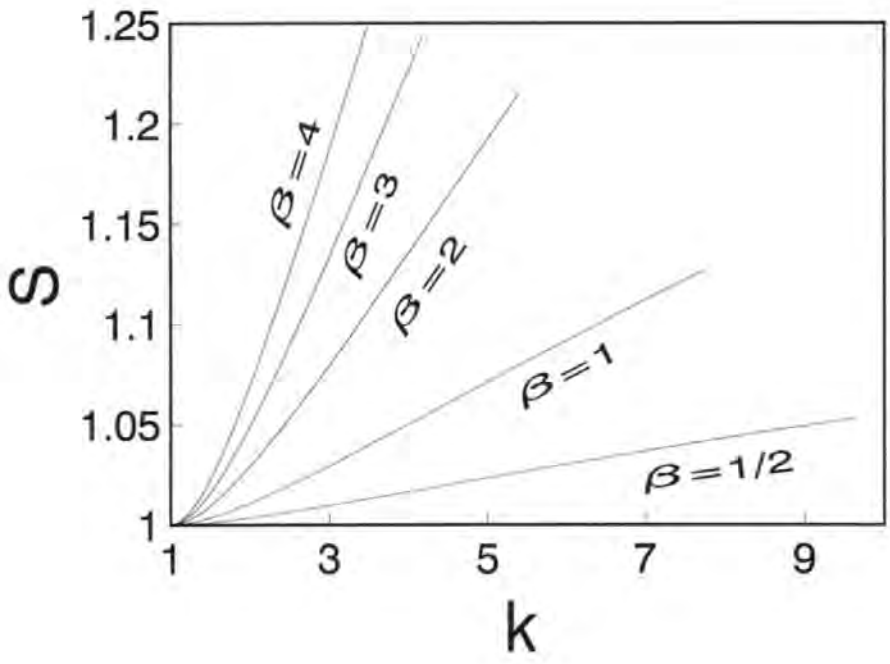

Figure 5.3: S *vs.* k.

The variations of $\lambda_1(r_1), \lambda_1(r_2), \lambda_2(r_1), \lambda_2(r_2)$ *vs.* k $(< \tilde{k}_E)$ are plotted in Figure 5.4. It can be seen from Figure 5.4 that $\lambda_1(r_1) > 1$, $\lambda_2(r_2) > 1$ and $\lambda_2(r_2) > \lambda_1(r_1)$. The values of $\lambda_2(r_2)$ when $k = \tilde{k}_E$, which represent the maximum values of the principal stretches beyond which the strong ellipticity condition will be violated, are given in Table 5.3. Comparison of Table 5.3 with Table 4.3 reveals that the values of $\lambda_2(r_2)$ when $k = \tilde{k}_E$ obtained here are the same as those obtained from the deformation of straightening.

The variations of $T_{rr}, T_{\theta\theta}$, as functions of r, are plotted in Figure 5.5. Clearly, T_{rr} is in compression for $r \in (r_1, r_2)$ and vanishes at $r = r_1$ and $r = r_2$. On the other hand, $T_{\theta\theta}$ is in compression at $r = r_1$ but is in tension at $r = r_2$. Also, we note that $T_{\theta\theta}(r_2) \to \mu$ as β increases. It is of interest to note that, for increasing values of β, $T_{\theta\theta}$

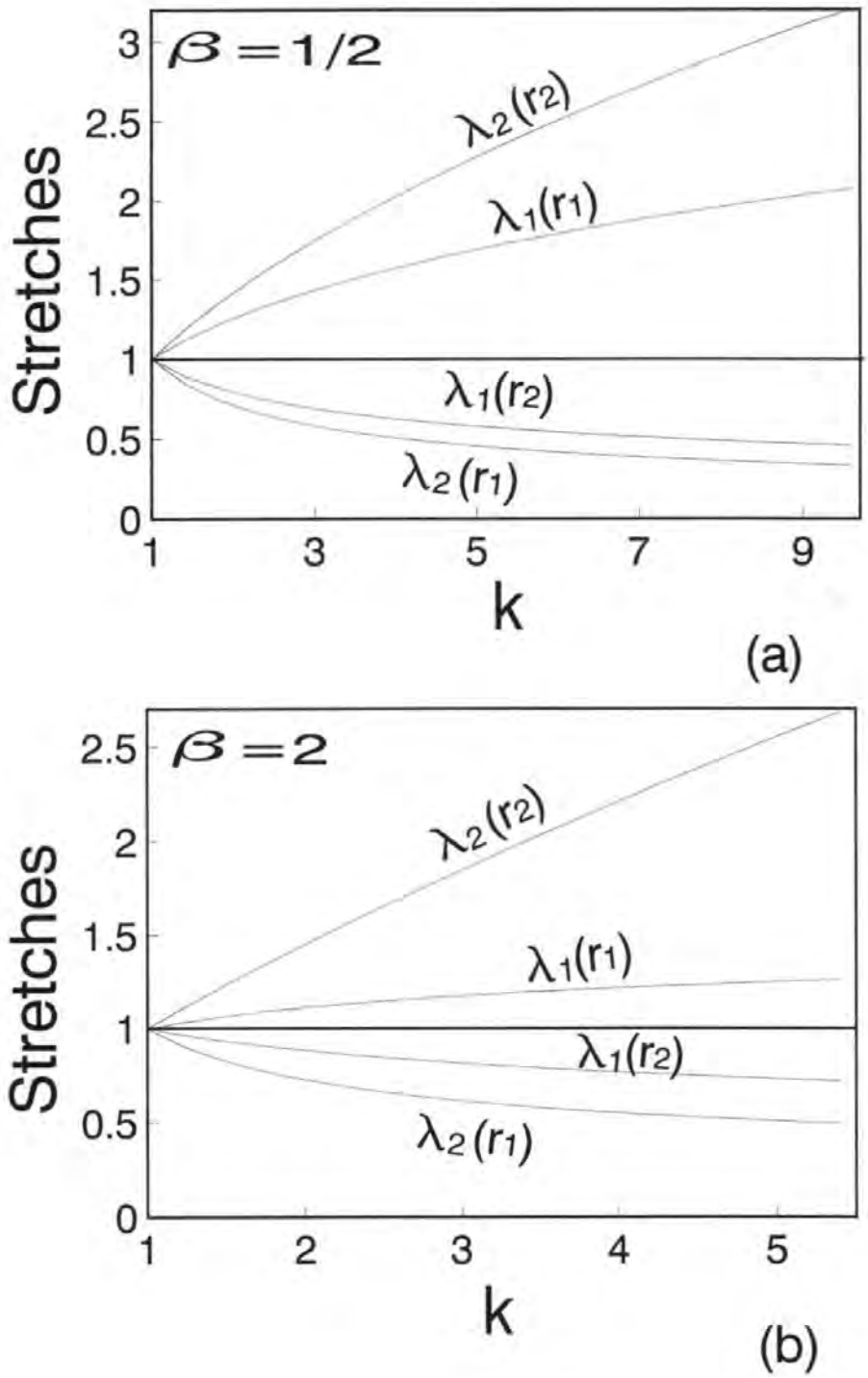

Figure 5.4: $\lambda_1(r_1), \lambda_1(r_2), \lambda_2(r_1), \lambda_2(r_2)$ *vs.* k.

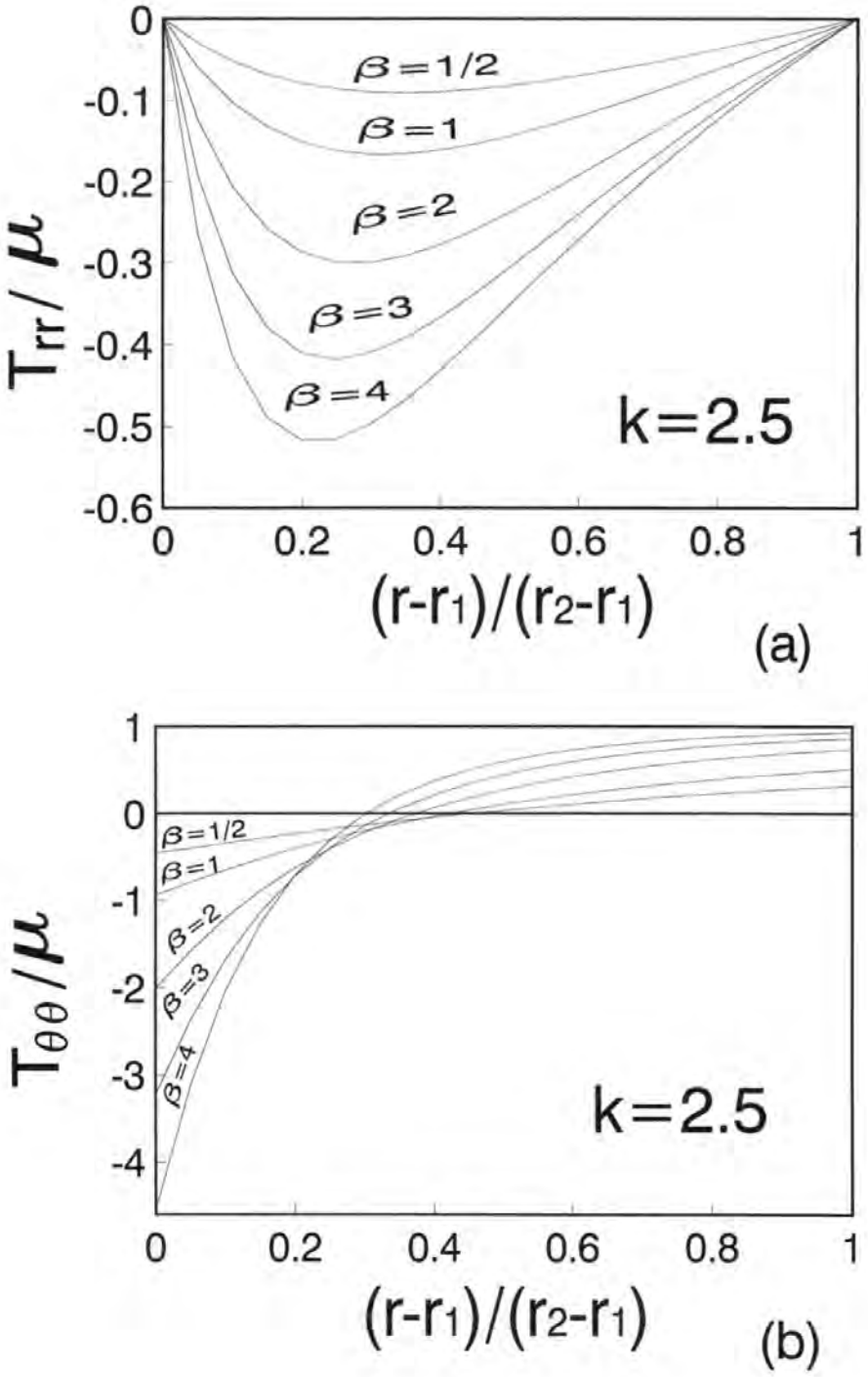

Figure 5.5: The distributions of $T_{rr}, T_{\theta\theta}$ along r.

increases faster along the r-axis and the magnitudes of $T_{\theta\theta}, T_{rr}$ become larger (for all $r \in [r_1, r_2]$) and that, otherwise, the distributions of Cauchy stresses are similar.

An examination of Figure 5.2 reveals that, as β increases, a larger value of M is needed in order to produce the same value of k. Once again, we can draw the conclusion that the material hardens as β increases.

Chapter 6

Eversion of cylindrical and spherical shells

The problem of eversion has been a particular interesting topic in the context of finite elastic theory since this eversion suggests that the equilibrium equations describing the problem should have at least two solutions, differing by more than a rigid displacement (see [65, 66]). However, although the problem has been formulated carefully in the 1950's (cf. Green & Adkins [67] and Truesdell & Noll [47]) and much work has been done for incompressible, elastic materials [68, 69, 66, 70, 72], many questions still remain open for isotropic, compressible elastic materials. In this chapter, we investigate the eversion of cylindrical and spherical shells composed of the material (3.1). In Section 6.1 we obtain exact solutions for the eversion of cylindrical shells, and then continue discussions paying special attention to the stability of the solution. In Section 6.2

we present results regarding the spherical eversion.

6.1 The eversion of cylindrical shells

We consider a cylindrical shell which, in the undeformed configuration, occupies the domain:

$$A \leq R \leq B,\ 0 \leq \Theta < 2\pi,\ 0 \leq Z \leq L \tag{6.1}$$

where (R, Θ, Z) are cylindrical polar coordinates and A, B, L are positive constants with $B > A$. This cylindrical shell is then everted into another cylindrical shell which occupies the region

$$a \leq r \leq b,\ 0 \leq \theta < 2\pi,\ -l \leq z \leq 0 \tag{6.2}$$

in which (r, θ, z) are cylindrical polar coordinates in the deformed configuration. Note that outer surface $R = B$ in the undeformed configuration is everted into the inner surface $r = a$ in the deformed configuration and that the inner surface $R = A$, in the undeformed configuration is everted into $r = b$, the outer surface in the deformed configuration. Here l is the length of the cylindrical shell after eversion. We assume that the deformation can be described as

$$r = r(R),\ \theta = \Theta,\ z = -\lambda Z \tag{6.3}$$

where $\lambda = l/L$. In view of (6.3) the deformation gradient tensor $\mathbf{F}$ is

$$\mathbf{F} = \frac{\mathrm{d}r}{\mathrm{d}R}\mathbf{e}_r \otimes \mathbf{e}_R + \frac{r}{R}\mathbf{e}_\theta \otimes \mathbf{e}_\Theta - \lambda \mathbf{e}_z \otimes \mathbf{e}_Z, \tag{6.4}$$

and this admits a polar decomposition $\mathbf{F} = \mathbf{VR}$ with rotation and left stretching tensors

$$\mathbf{R} = -\mathbf{e}_r \otimes \mathbf{e}_R + \mathbf{e}_\theta \otimes \mathbf{e}_\Theta - \mathbf{e}_z \otimes \mathbf{e}_Z \tag{6.5}$$

and

$$\mathbf{V} = -\frac{\mathrm{d}r}{\mathrm{d}R}\mathbf{e}_r \otimes \mathbf{e}_r + \frac{r}{R}\mathbf{e}_\theta \otimes \mathbf{e}_\theta + \lambda \mathbf{e}_z \otimes \mathbf{e}_z. \tag{6.6}$$

Thus, the principal stretches λ_i are given by

$$\lambda_r = -\frac{\mathrm{d}r}{\mathrm{d}R},\ \lambda_\theta = \frac{r}{R},\ \lambda_z = \lambda. \tag{6.7}$$

Since $\lambda > 0$ we infer that a solution $r(R)$ to the eversion problem must necessarily satisfy

$$r(R) > 0,\ \frac{\mathrm{d}r}{\mathrm{d}R} < 0. \tag{6.8}$$

The equilibrium equations for this deformation reduce to

$$\frac{\mathrm{d}T_{rr}}{\mathrm{d}r} + \frac{1}{r}(T_{rr} - T_{\theta\theta}) = 0, \tag{6.9}$$

where components of the Cauchy stress $\mathbf{T}$, (which can be obtained by substituting (3.1), (6.4) and (6.7) into the stress response equations (2.27), (2.29)), are

$$\begin{aligned}
T_{rr} &= \mu[1 - (-\frac{\mathrm{d}R}{\mathrm{d}r})^{\beta+1} \cdot (\frac{R}{r}) \cdot \frac{1}{\lambda}], \\
T_{\theta\theta} &= \mu[1 + (\frac{R}{r})^{\beta+1} \cdot \frac{\mathrm{d}R}{\mathrm{d}r} \cdot \frac{1}{\lambda}], \\
T_{zz} &= \mu[1 + \frac{R}{r} \cdot \frac{\mathrm{d}R}{\mathrm{d}r} \cdot \frac{1}{\lambda^{\beta+1}}], \\
T_{r\theta} &= T_{rz} = T_{z\theta} = 0.
\end{aligned} \tag{6.10}$$

Thus the substitution of (6.10) into (6.9) leads to the following nonlinear, second-order ordinary differential equation for $r(R)$:

$$(\beta+1)(\frac{\mathrm{d}R}{\mathrm{d}r})^{\beta-1}\cdot R\cdot\frac{\mathrm{d}^2R}{\mathrm{d}r^2}+(\frac{\mathrm{d}R}{\mathrm{d}r})^{\beta+1}+(-\frac{R}{r})^{\beta+1}=0. \tag{6.11}$$

We note that the equation (6.11) does not involve the axial stretch λ. By using the change of variable

$$w\equiv\frac{\lambda_r}{\lambda_\theta}=-\frac{R}{r}\cdot\frac{\mathrm{d}r}{\mathrm{d}R}>0, \tag{6.12}$$

introduced by Abeyaratne & Horgan [15, 23], the above differential equation can be shown to be equivalent to

$$(\beta+1)r\frac{\mathrm{d}w}{\mathrm{d}r}=-[\beta+2+(\beta+1)w+w^{\beta+1}] \tag{6.13}$$

or

$$(\beta+1)R\frac{\mathrm{d}w}{\mathrm{d}R}=w[\beta+2+(\beta+1)w+w^{\beta+1}]. \tag{6.14}$$

Solutions of this pair of parametric equations can be written in the form

$$r(w)=C_1\bar{r}(w),\ R(w)=C_2\bar{R}(w) \tag{6.15}$$

where C_1, C_2 (>0) are two constants of integration and functions $\bar{r}(w), \bar{R}(w)$ are defined by

$$\ln[\bar{r}(w)]\equiv-(\beta+1)\int 1/[\beta+2+(\beta+1)w+w^{\beta+1}]dw, \tag{6.16}$$

$$\ln[\bar{R}(w)]\equiv(\beta+1)\int 1/\{w[\beta+2+(\beta+1)w+w^{\beta+1}]\}dw. \tag{6.17}$$

We have found explicit expressions for (6.16) and (6.17) in the case when $\beta = 1/2, 1, 2, 3, 4$. As an example, in the case when $\beta = 1$, the expressions for $\bar{r}(w)$ and $\bar{R}(w)$ are

$$\bar{r}(w) = e^{-\sqrt{2}\arctan[(w+1)/\sqrt{2}]}, \tag{6.18}$$

$$\bar{R}(w) = e^{-\frac{\sqrt{2}}{3}\arctan[(w+1)/\sqrt{2}]} \cdot w^{\frac{2}{3}} \cdot (w^2 + 2w + 3)^{-\frac{1}{3}}. \tag{6.19}$$

In the case of $\beta = 2$, (6.16) and (6.17) reduce to

$$\bar{r}(w) = e^{-\frac{\sqrt{15}}{10}\arctan[(2w-1)/\sqrt{15}]} \cdot (w^2 - w + 4)^{\frac{1}{4}} \cdot (w+1)^{-\frac{1}{2}}, \tag{6.20}$$

$$\bar{R}(w) = e^{-\frac{\sqrt{15}}{20}\arctan[(2w-1)/\sqrt{15}]} \cdot w^{\frac{3}{4}} \cdot (w^2 - w + 4)^{-\frac{1}{8}} \cdot (w+1)^{-\frac{1}{2}}, \tag{6.21}$$

which are simply those obtained previously by Carroll & Horgan [17]. Exact analytical expressions for $\bar{r}(w)$ and $\bar{R}(w)$ in the case when $\beta = 1/2, 3, 4$ (where certain constants have been approximated for the sake of simplicity) are given in Table 6.1 and Table 6.2 respectively.

From (6.15) we can see that the solutions are now expressed as functions of the parameter w, which belongs to a certain range of $[w_A, w_B]$. Here w_A, w_B are the values of w at $R = A$ and $R = B$, that is,

$$R(w_A) = A,\ R(w_B) = B. \tag{6.22}$$

Also, we have

$$r(w_A) = b,\ r(w_B) = a. \tag{6.23}$$

We use the boundary condition of zero traction on the surfaces of the cylinder,

$$T_{rr}(a) = T_{rr}(b) = 0,\ 0 \le \theta < 2\pi,\ -l \le z \le 0, \tag{6.24}$$

β	$\ln[\bar{r}(w)]$
1/2	$-.7607 \arctan(.9453\sqrt{w} - .2735) - .4636 \ln(w - .5786\sqrt{w} + 1.2027)$ $+.9271 \ln(\sqrt{w} + 2.0786)$
3	$-.1656 \arctan(.6872w - .7551) - .9773 \arctan(1.8352w + 2.0163)$ $-.1760 \ln[(w^2 + 2.1974w + 1.5040)/(w^2 - 2.1974w + 3.3244)]$
4	$-.0926 \arctan(.9089w - 1.1588) - .4523 \arctan(.8123w + .6295)$ $+.1332 \ln(w^2 - 2.550w + 2.8358)$ $+.1168 \ln(w^2 + 1.550w + 2.1158) - \ln(w + 1)/2$

Table 6.1: Expressions of $\bar{r}(w)$ for $\beta = 1/2, 3, 4$.

β	$\ln[\bar{R}(w)]$
1/2	$-.1521 \arctan(.9453\sqrt{w} - .2735) - .4927 \ln(w - .5786\sqrt{w} + 1.2027)$ $+.6 \ln(w) - .2146 \ln(\sqrt{w} + 2.0786)$
3	$-.0993 \arctan(.6872w - .7551) - .5864 \arctan(1.8352w + 2.0163)$ $-.3056 \ln(w^2 + 2.1974w + 1.5040) - .0944 \ln(w^2 - 2.1974w + 3.3244)$ $+.8 \ln(w)$
4	$-.06174 \arctan(.9089w - 1.1588) - .3015 \arctan(.8123w + .6295)$ $-.07786 \ln(w^2 - 2.550w + 2.8358) - .08881 \ln(w^2 + 1.550w + 2.1158)$ $+.83333 \ln(w) - \ln(w + 1)/2$

Table 6.2: Expressions of $\bar{R}(w)$ for $\beta = 1/2, 3, 4$.

and, by considerations similar to those in [72, 68], we replace the point-wise end conditions

$$T_{zz} = 0 \text{ at } z = 0 \text{ and } z = -l,\ 0 \le \theta < 2\pi,\ a \le r \le b \tag{6.25}$$

with the averaged end conditions

$$N \equiv 2\pi \int_a^b r T_{zz} dr = 0, \text{ for } z = -l, 0. \tag{6.26}$$

Here N is the resultant force on the ends $z = -l$ or $z = 0$ and (6.26) means that the resultant force on the ends of the cylinder is zero. Note that the eversion problem is fully defined by (6.15) with (6.22), (6.24), and (6.26).

On substituting (6.10) and (6.15) into (6.22), (6.24), and (6.26) we obtain the following expressions to determine the unknown constants $C_1, C_2, w_A, w_B, \lambda$:

$$\bar{R}(w_B) = \frac{B}{A}\bar{R}(w_A), \tag{6.27}$$

$$w_A^{(\beta+1)/(\beta+2)} \cdot \frac{\bar{r}(w_A)}{\bar{R}(w_A)} = w_B^{(\beta+1)/(\beta+2)} \cdot \frac{\bar{r}(w_B)}{\bar{R}(w_B)}, \tag{6.28}$$

$$\lambda^{\beta(\beta+3)/(\beta+2)} = \frac{\bar{R}^2(w_B) - \bar{R}^2(w_A)}{\bar{r}^2(w_A) - \bar{r}^2(w_B)} \cdot [\frac{\bar{r}(w_A)}{\bar{R}(w_A)}]^2 \cdot w_A^{2(\beta+1)/(\beta+2)}, \tag{6.29}$$

$$C_1 = A w_A^{-(\beta+1)/(\beta+2)} [\bar{r}(w_A)]^{-1} \lambda^{-1/(\beta+2)}, \tag{6.30}$$

$$C_2 = A[\bar{R}(w_A)]^{-1}. \tag{6.31}$$

For any given value A/B, w_A, w_B can be determined by simultaneous equations (6.27) and (6.28). Then λ, C_1, C_2 can be easily found from (6.29) - (6.31). However, this determination can only be carried out numerically due to the high non-linearity of these equations. For certain values of A/B in the interval $[0.01, 0.99]$ and $\beta = 1/2, 1, 2, 3, 4$

we calculate the numerical values of w_A, w_B, λ from (6.27) - (6.29), which are plotted in Figure 6.1 and Figure 6.2. It can be seen that w_A is always less than unity and it is an increasing function of β (when A/B is fixed) and A/B for fixed β. When $A/B \to 1$, $w_A \to 1$ and $w_A \to 0$ as $A/B \to 0$. On the other hand, w_B is always greater than unity and decreases with β (for fixed A/B) and A/B when β is fixed. For fixed value β, when A/B tends to unity w_B tends to unity also (see Figure 6.1).

From Figure 6.2 we note that the axial stretch λ is an increasing function of A/B when β is fixed and $\lambda < 1$ holds always, which implies that the cylinder becomes shorter after being everted. This result is different from the results obtained by Haughton & Orr [72] for several incompressible materials (including the Varga material, the Neo-Hookean material and the three-term material, proposed by Ogden [56]) when it is shown that for these materials, the cylinder becomes longer after eversion. It should be borne in mind that neither shortening nor elongation are universal results since Chadwick has proved that shortening may accompany eversion for some Mooney-Rivlin materials also [69].

The ratio of the cross-sectional areas of the cylindrical shell before and after eversion is defined by

$$S \equiv \frac{\pi[r^2(w_A) - r^2(w_B)]}{\pi(B^2 - A^2)} = \lambda^{-\beta-1}, \tag{6.32}$$

which is plotted in Figure 6.3. It can be seen that S is an increasing function of A/B (when β is fixed) and of β (for fixed A/B) and that it is always greater than unity, which indicates that the cross section of the cylinder expands after eversion.

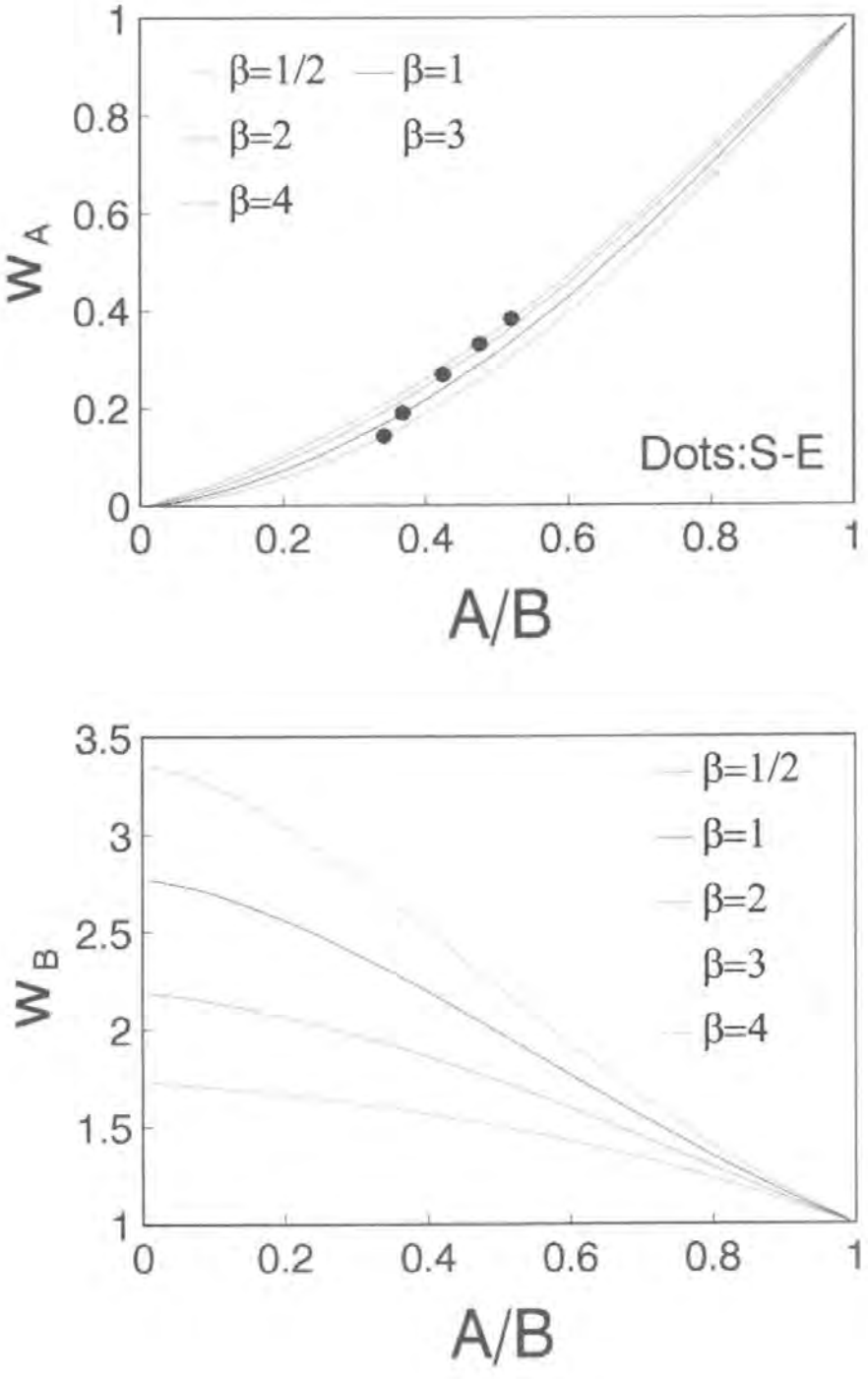

Figure 6.1: w_A, w_B *vs.* A/B in cylindrical eversion.

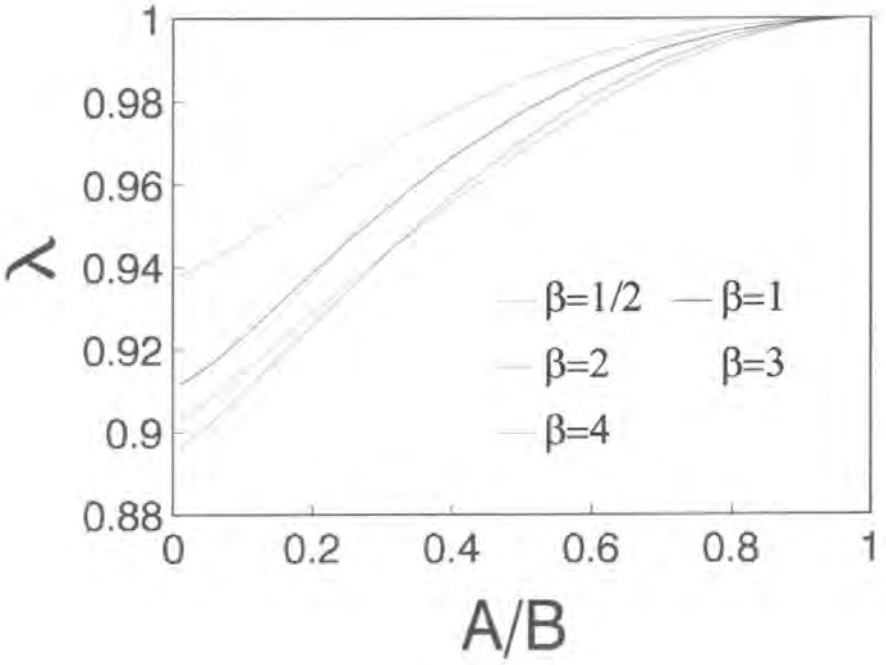

Figure 6.2: λ *vs.* A/B in cylindrical eversion.

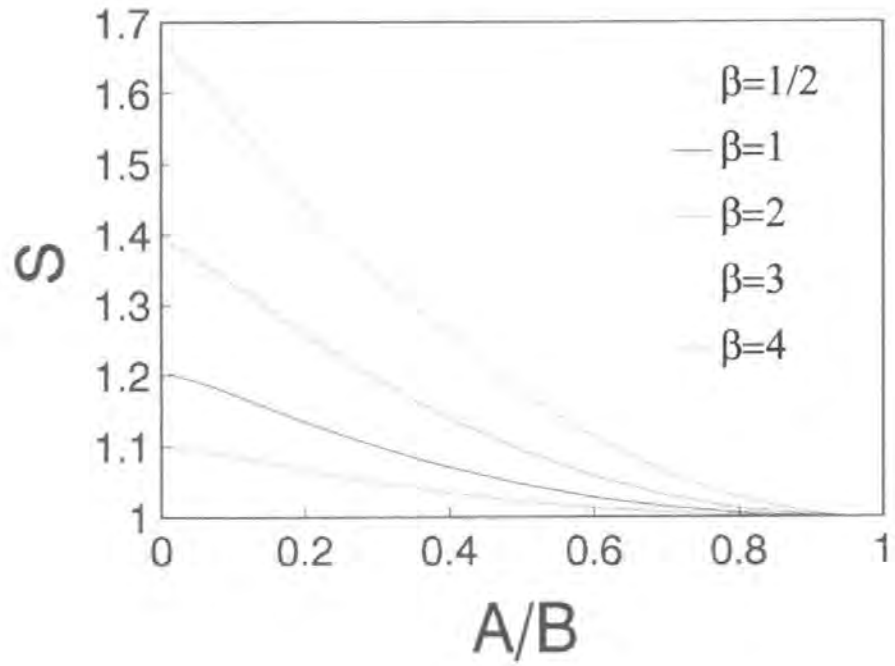

Figure 6.3: S *vs.* A/B in cylindrical eversion.

The deformed inner and outer radii a and b are given by

$$a = Bw_B^{-(\beta+1)/(\beta+2)}\lambda^{-1/(\beta+2)} \tag{6.33}$$

and

$$b = Aw_A^{-(\beta+1)/(\beta+2)}\lambda^{-1/(\beta+2)} \tag{6.34}$$

and numerical results obtained for $a/A, a/B, b/B$ (for certain values of A/B and β) are illustrated in Figure 6.4. These numerical results indicate that

$$A < a < B,\ b > B \tag{6.35}$$

which implies that the cylinder becomes thicker after eversion. It can be seen from Figure 6.4 that both a/A and b/B are decreasing function of A/B and we note that for $A/B \in (0, 0.1)$ the rate of decrease of a/A is much faster than that of b/B. For example, when $A/B = 0.01$, a is about 60 times larger than the radius A but b is only $(1.1 - 1.5)$ times larger than B. This phenomenon appears to contradict the intuition and it can be seen from the diagram of a/b *vs.* A/B also (Figure 6.5). These 'abnormal' phenomena remind us again that the existence of solution does not by itself guarantee that the solution is physically realistic, as pointed out by Aron & Wang [32].

In what follows we will be discussing the stability of the solution to the boundary value problem of traction with the help of the strong-ellipticity condition (3.5). We define

$$w_{rz} \equiv \frac{\lambda_r}{\lambda_z} = w\lambda^{-(\beta+3)/(\beta+2)}w_A^{-(\beta+1)/(\beta+2)} \cdot \frac{\bar{r}(w)\bar{R}(w_A)}{\bar{R}(w)\bar{r}(w_A)}, \tag{6.36}$$

$$w_{\theta z} \equiv \frac{\lambda_\theta}{\lambda_z} = \lambda^{-(\beta+3)/(\beta+2)}w_A^{-(\beta+1)/(\beta+2)} \cdot \frac{\bar{r}(w)\bar{R}(w_A)}{\bar{R}(w)\bar{r}(w_A)}, \tag{6.37}$$

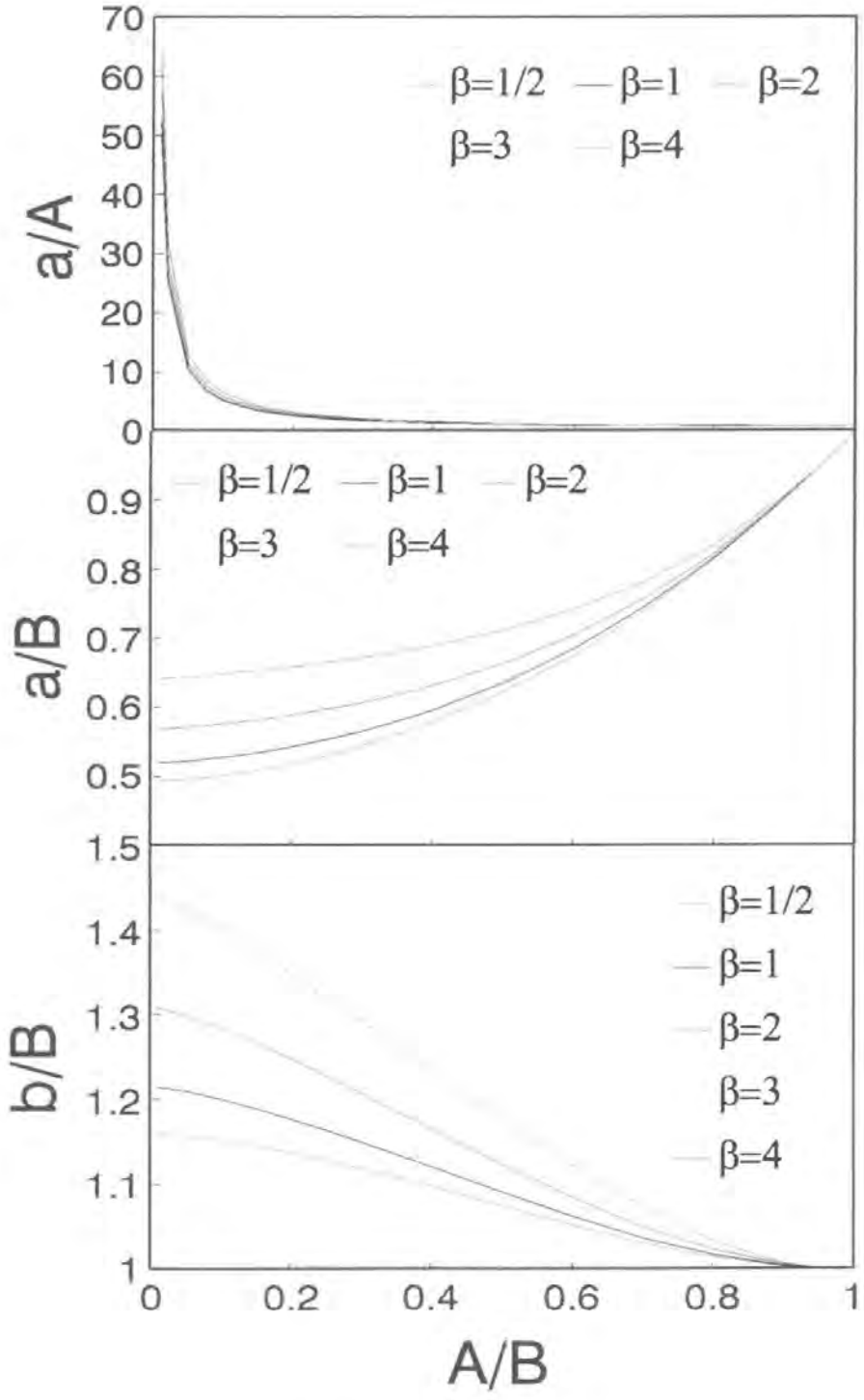

Figure 6.4: $a/A, a/B, b/B$ *vs.* A/B in cylindrical eversion.

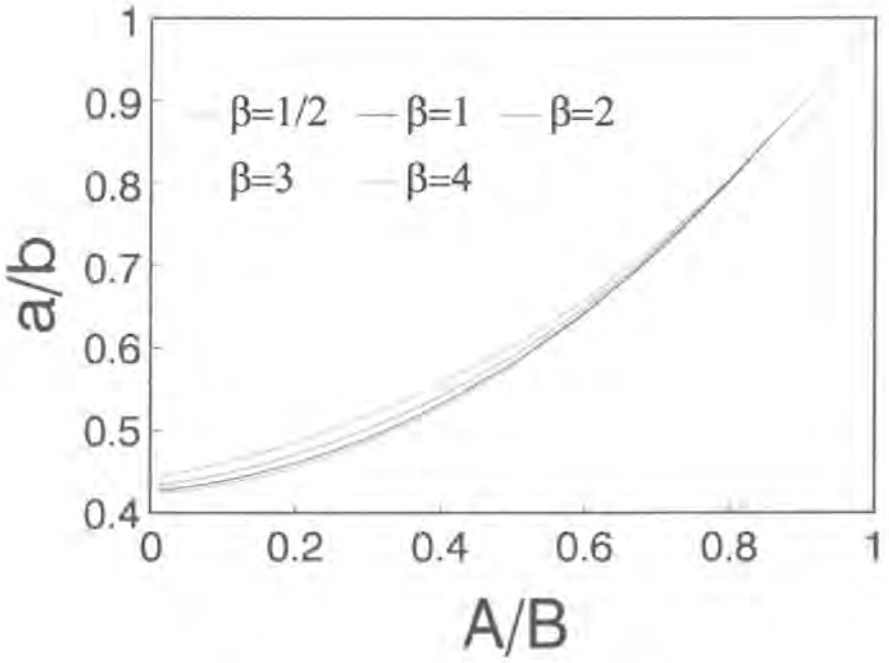

Figure 6.5: a/b *vs.* A/B in cylindrical eversion.

and recalling (6.12), we write the strong-ellipticity condition (3.5) in the form

$$t_E < w < 1/t_E, \quad t_E < w_{rz} < 1/t_E, \quad t_E < w_{\theta z} < 1/t_E. \tag{6.38}$$

Recalling (6.22) we find that $(6.38)_1$ is equivalent to

$$t_E < w_A \text{ and } w_B < 1/t_E. \tag{6.39}$$

Numerical examination on (6.39) reveals that: (i) for any given value of A/B in the interval of $[0.01, 0.99]$ and for $\beta = 1/2, 1, 2, 3, 4$, the condition $w_B < 1/t_E$ holds always and (ii) the condition $t_E < w_A$ yields the following restriction on A/B:

$$\frac{A}{B} > (\frac{A}{B})_E, \tag{6.40}$$

where $(\frac{A}{B})_E$ is a certain value in a range of $(0.3 \sim 0.6)$ which depends on β. Certain numerical values for $(A/B)_E$ are given in Table 6.3 and illustrated in Figure 6.1 by dots.

Numerical experiments indicate that when $\frac{A}{B}$ is prescribed such that $\frac{A}{B} > (\frac{A}{B})_E$, the

β	1/2	1	2	3	4
t_E	0.14289	0.1896	0.2679	0.3306	0.3820
$(\frac{A}{B})_E$	0.3416	0.3680	0.4245	0.4762	0.5203
$[(\frac{A}{B})_E]^{-1} - 1$	1.9277	1.7176	1.3559	1.1000	0.9220

Table 6.3: $(\frac{A}{B})_E$ *vs.* β in cylindrical eversion.

inequalities $(6.38)_2$ and $(6.38)_3$ are satisfied also. Thus $(6.39)_1$ appears to be a necessary condition for the stability of this solution. Since the range $((A/B)_E, 1)$ is different from the range for which a/A decreases very fast (see the comments on Figure 6.4), it follows that if the ratio A/B is such that $A/B > (A/B)_E$ the 'abnormal' phenomenon will not be observed in practice. It is of interest to note that the maximum thickness of the cylindrical shell for which we may have a stable solution to the considered problems, (given by $[(\frac{A}{B})_E]^{-1} - 1$), is less than twice that of the original inner radius and this maximum thickness becomes smaller as β increases. As an example, when $\beta = 4$ the maximum possible thickness of the cylindrical shell must be less than the inner radius A (see Table 6.3).

Also we are interested in the distributions of the Cauchy stresses $\mathbf{T}$. From (6.10) and (6.15) we find that

$$T_{rr} = \mu\{1 - (\frac{w_A}{w})^{\beta+1} \cdot [\frac{\bar{R}(w)\bar{r}(w_A)}{\bar{r}(w)\bar{R}(w_A)}]^{\beta+2}\} = \mu\{1 - (\frac{w_B}{w})^{\beta+1} \cdot [\frac{\bar{R}(w)\bar{r}(w_B)}{\bar{r}(w)\bar{R}(w_B)}]^{\beta+2}\},$$

$$T_{\theta\theta} = \mu\{1 - \frac{w_A^{\beta+1}}{w} \cdot [\frac{\bar{R}(w)\bar{r}(w_A)}{\bar{r}(w)\bar{R}(w_A)}]^{\beta+2}\} = \mu\{1 - \frac{w_B^{\beta+1}}{w} \cdot [\frac{\bar{R}(w)\bar{r}(w_B)}{\bar{r}(w)\bar{R}(w_B)}]^{\beta+2}\},$$
$$T_{zz} = \mu\{1 - w^{-1} \cdot [\frac{\bar{R}(w)}{\bar{r}(w)}]^2 \cdot \frac{\bar{r}^2(w_A) - \bar{r}^2(w_B)}{\bar{R}^2(w_B) - \bar{R}^2(w_A)}\}. \tag{6.41}$$

The distributions of $T_{rr}, T_{\theta\theta}, T_{zz}$ along the r-axis when $A/B = 0.5$ are plotted in Figure 6.6 (The distributions of the Cauchy stresses are similar for different values of A/B). Observe from Figure 6.6 that the radial stress T_{rr} is always in compression and vanishes at $r = a$ and $r = b$. The hoop stress $T_{\theta\theta}$ is in tension at $r = a$ and in compression at $r = b$ since $T_{\theta\theta}(a) = \mu(1 - w_B^{\beta}) < 0$ and $T_{\theta\theta}(b) = \mu(1 - w_A^{\beta}) > 0$. Both $T_{\theta\theta}$ and T_{zz} increase along the r-axis. It is of interest to note that, for increasing values of β, the stresses vary faster along the r-axis and that, otherwise, the distributions of the Cauchy stresses are similar when β takes different values ($\beta = 1/2, 1, 2, 3, 4$). Also, for a fixed value of A/B, greater magnitudes of the stresses correspond to larger values of β, and this verifies again the conjecture that the material becomes harder as β increases.

6.2 The eversion of spherical shells

In this section, we consider the eversion of a spherical shell. The region occupied by the spherical shell in the undeformed configuration is described by

$$A \leq R \leq B,\ 0 \leq \Theta \leq \Theta_0,\ 0 \leq \Phi < 2\pi \tag{6.42}$$

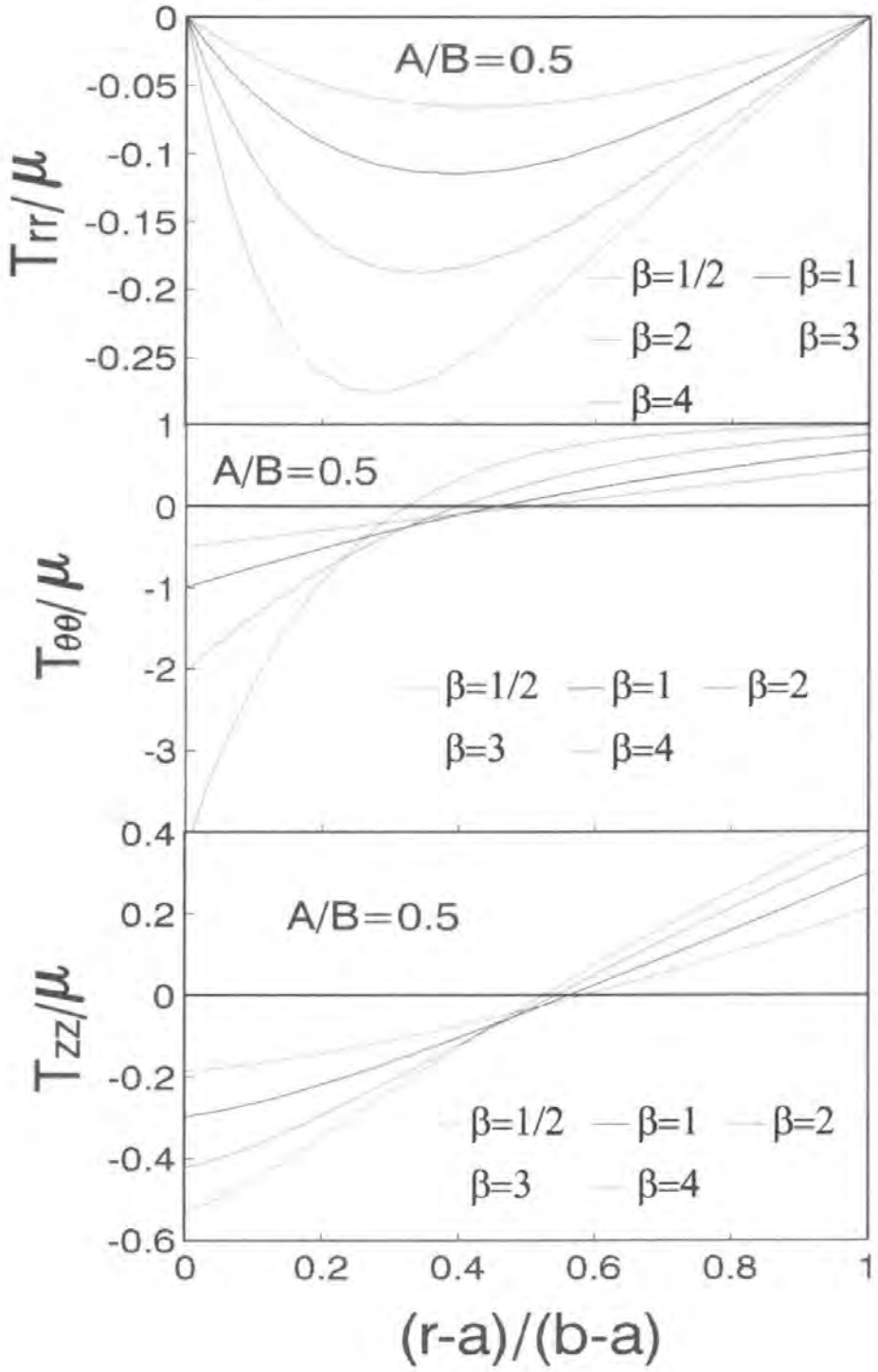

Figure 6.6: $T_{rr}, T_{\theta\theta}, T_{zz}$ along the r-axis.

where (R, Θ, Φ) are spherical polar coordinates and A, B, Θ_0 are positive constants. The spherical shell is everted into another spherical shell which occupies a domain

$$a \leq r \leq b,\ \pi - \Theta_0 \leq \theta \leq \pi,\ 0 \leq \phi < 2\pi. \tag{6.43}$$

in the deformed configuration. Here (r, θ, ϕ) are spherical polar coordinates also and a, b are the positions of the deformed inner and outer surfaces. We assume that the solution for this eversion problem is of the form

$$r = r(R),\ \theta = \pi - \Theta,\ \phi = \Phi. \tag{6.44}$$

With the help of (6.44) we find that

$$\mathbf{F} = \frac{\mathrm{d}r}{\mathrm{d}R}\mathbf{e}_r \otimes \mathbf{e}_R - \frac{r}{R}\mathbf{e}_\theta \otimes \mathbf{e}_\Theta + \frac{r}{R}\mathbf{e}_\phi \otimes \mathbf{e}_\Phi. \tag{6.45}$$

The polar decomposition $\mathbf{F} = \mathbf{VR}$ gives the rotation and left stretching tensors

$$\mathbf{R} = -\mathbf{e}_r \otimes \mathbf{e}_R - \mathbf{e}_\theta \otimes \mathbf{e}_\Theta + \mathbf{e}_\phi \otimes \mathbf{e}_\Phi \tag{6.46}$$

and

$$\mathbf{V} = -\frac{\mathrm{d}r}{\mathrm{d}R}\mathbf{e}_r \otimes \mathbf{e}_r + \frac{r}{R}\mathbf{e}_\theta \otimes \mathbf{e}_\theta + \frac{r}{R}\mathbf{e}_\phi \otimes \mathbf{e}_\phi. \tag{6.47}$$

Therefore, the principal stretches λ_i can then be written as

$$\lambda_r = -\frac{\mathrm{d}r}{\mathrm{d}R},\ \lambda_\theta = \lambda_\phi = \frac{r}{R}, \tag{6.48}$$

and we require that

$$r(R) > 0,\ \frac{\mathrm{d}r}{\mathrm{d}R} < 0. \tag{6.49}$$

For this deformation, components of the Cauchy stress $\mathbf{T}$ are

$$\begin{aligned} T_{rr} &= \frac{W_1}{\lambda_\theta \lambda_\phi} = \mu[1 - (-\frac{\mathrm{d}R}{\mathrm{d}r})^{\beta+1} \cdot (\frac{R}{r})^2], \\ T_{\theta\theta} = T_{\phi\phi} &= \frac{W_2}{\lambda_r \lambda_\theta} = \mu[1 + (\frac{R}{r})^{\beta+2} \cdot \frac{\mathrm{d}R}{\mathrm{d}r}], \\ T_{r\theta} &= T_{r\phi} = T_{\phi\theta} = 0, \end{aligned} \tag{6.50}$$

and the equilibrium equation

$$\frac{\mathrm{d}T_{rr}}{\mathrm{d}r} + \frac{2}{r}(T_{rr} - T_{\theta\theta}) = 0 \tag{6.51}$$

reduces to the following nonlinear, second-order ordinary differential equation for $r(R)$

$$(\beta+1)(\frac{\mathrm{d}R}{\mathrm{d}r})^{\beta-1} \cdot R \cdot \frac{\mathrm{d}^2R}{\mathrm{d}r^2} + 2(\frac{\mathrm{d}R}{\mathrm{d}r})^{\beta+1} + 2(-\frac{R}{r})^{\beta+1} = 0. \tag{6.52}$$

By making use of the substitution $w \equiv \lambda_r/\lambda_\theta = \lambda_r/\lambda_\phi$ [15, 23], equation (6.52) yields the following pair of parametric equations:

$$(\beta+1)r\frac{\mathrm{d}w}{\mathrm{d}r} = -[\beta + 3 + (\beta+1)w + 2w^{\beta+1}] \tag{6.53}$$

and

$$(\beta+1)R\frac{\mathrm{d}w}{\mathrm{d}R} = w[\beta + 3 + (\beta+1)w + 2w^{\beta+1}]. \tag{6.54}$$

As in the case of cylindrical eversion, solutions to these parametric equations can be written in the form

$$r(w) = C_1\check{r}(w), \;\; R(w) = C_2\check{R}(w) \tag{6.55}$$

where C_1, C_2 (> 0) are two constants of integration and the functions $\check{r}(w), \check{R}(w)$ are defined by

$$\ln[\check{r}(w)] \equiv -(\beta+1)\int 1/[\beta+3+(\beta+1)w+2w^{\beta+1}]dw, \tag{6.56}$$

$$\ln[\check{R}(w)] \equiv (\beta+1)\int 1/\{w[\beta+3+(\beta+1)w+2w^{\beta+1}]\}dw. \tag{6.57}$$

We have obtained explicit expressions for (6.56) and (6.57) for $\beta = 1/2, 1, 2, 3, 4$. For instance, in the case when $\beta = 1$, expressions of $\check{r}(w)$ and $\check{R}(w)$ are

$$\check{r}(w) = e^{-2\arctan[(2w+1)/\sqrt{7}]/\sqrt{7}}, \tag{6.58}$$

$$\check{R}(w) = e^{-\frac{\sqrt{7}}{14}\arctan[(2w+1)/\sqrt{7}]} \cdot w^{\frac{1}{2}} \cdot (w^2+w+2)^{-\frac{1}{4}}. \tag{6.59}$$

In the case of $\beta = 2$ (6.56) and (6.57) reduce to

$$\check{r}(w) = e^{-\arctan[(2w-1)/3]/3} \cdot (2w^2-2w+5)^{\frac{1}{6}} \cdot (w+1)^{-\frac{1}{3}}, \tag{6.60}$$

$$\check{R}(w) = e^{-2\arctan[(2w-1)/3]/15} \cdot w^{\frac{3}{5}} \cdot (2w^2-2w+5)^{-\frac{2}{15}} \cdot (w+1)^{-\frac{1}{3}}, \tag{6.61}$$

which are the same as those obtained previously by Carroll & Horgan [17]. The exact analytical expressions of $\check{r}(w)$ and $\check{R}(w)$ in the case when $\beta = 1/2, 3, 4$ (with approximate constants for simplicity) are given in Table 6.4 and Table 6.5 respectively.

In view of (6.55)-(6.57) we can see that the solutions for the eversion problem are now expressed as functions of the parameter w, which belongs to a certain range $[w_A, w_B]$. Here w_A, w_B are the values of w for which $R = A$ and $R = B$ respectively:

$$R(w_A) = A,\ R(w_B) = B. \tag{6.62}$$

Also, we have

$$r(w_A) = b,\ r(w_B) = a. \tag{6.63}$$

β	$\ln[\check{r}(w)]$
1/2	$-.5624\arctan(.9962\sqrt{w}-.3804)-.2468\ln(w-.7637\sqrt{w}+1.1534)$ $+.4935\ln(\sqrt{w}+1.5137)$
3	$-.5553\arctan(1.6234w+1.5444)-.1573\arctan(.8361w-.7954)$ $-.1393\ln[(w^2+1.9026w+1.2845)/(w^2-1.9027w+2.3356)]$
4	$-.3871\arctan(.8949w+.5547)-.09043\arctan(1.0603w-1.1874)$ $+.05426\ln(w^2+1.2396w+1.6329)$ $+.1124\ln(w^2-2.2396w+2.1434)-\ln(w+1)/3$

Table 6.4: Expressions of $\check{r}(w)$ for $\beta = 1/2, 3, 4$.

β	$\ln[\check{R}(w)]$
1/2	$-.07990\arctan(.9962\sqrt{w}-.3804)-.3219\ln(w-.7637\sqrt{w}+1.1534)$ $+.4296\ln(w)-.2153\ln(\sqrt{w}+1.5137)$
3	$-.2776\arctan(1.6234w+1.5444)-.07863\arctan(.8361w-.7954)$ $-.2363\ln(w^2+1.9026w+1.2845)-.09701\ln(w^2-1.9027w+2.3356)$ $+.6667\ln(w)$
4	$-.2212\arctan(.8949w+.5547)-.05168\arctan(1.0603w-1.1874)$ $-.1119\ln(w^2+1.2396w+1.6329)-.07862\ln(w^2-2.2396w+2.1434)$ $+.7143\ln(w)-\ln(w+1)/3$

Table 6.5: Expressions of $\check{R}(w)$ for $\beta = 1/2, 3, 4$.

The integration constants C_1 and C_2 can be determined by prescribing the traction to be zero on the surfaces of the spherical shell, that is

$$T_{rr}(a) = T_{rr}(b) = 0. \tag{6.64}$$

Thus, substitutions of (6.50) and (6.55) into (6.62) and (6.64) yields

$$\check{R}(w_B) = \frac{B}{A}\check{R}(w_A), \tag{6.65}$$

$$w_A^{(\beta+1)/(\beta+3)} \cdot \frac{\check{r}(w_A)}{\check{R}(w_A)} = w_B^{(\beta+1)/(\beta+3)} \cdot \frac{\check{r}(w_B)}{\check{R}(w_B)}, \tag{6.66}$$

$$C_1 = A w_A^{-(\beta+1)/(\beta+3)} [\check{r}(w_A)]^{-1}, \tag{6.67}$$

$$C_2 = A[\check{R}(w_A)]^{-1}. \tag{6.68}$$

For any given value of A/B, w_A, w_B can be determined by the two simultaneous equations (6.65) and (6.66). Then C_1, C_2 can be easily found from (6.67) and (6.68). For certain values of A/B in the interval of $[0.03, 0.99]$ and when β is prescribed such that $\beta = 1/2, 1, 2, 3, 4$, we have calculated the numerical values of w_A, w_B from (6.65) and (6.66), which are plotted in Figure 6.7. It can be seen that w_A is always less than unity and it is an increasing function of β (when A/B is fixed) and an increasing function of A/B for each fixed value of β. When $A/B \to 1$, $w_A \to 1$ and $w_A \to 0$ as $A/B \to 0$. On the other hand, w_B is always greater than unity, decreases with β for a given value A/B and also decreases with A/B when β is fixed. When A/B tends to unity w_B tends to unity also (see Figure 6.7).

The ratio of the volumes of the spherical shell before and after eversion is

$$V \equiv \frac{b^3 - a^3}{B^3 - A^3}. \tag{6.69}$$

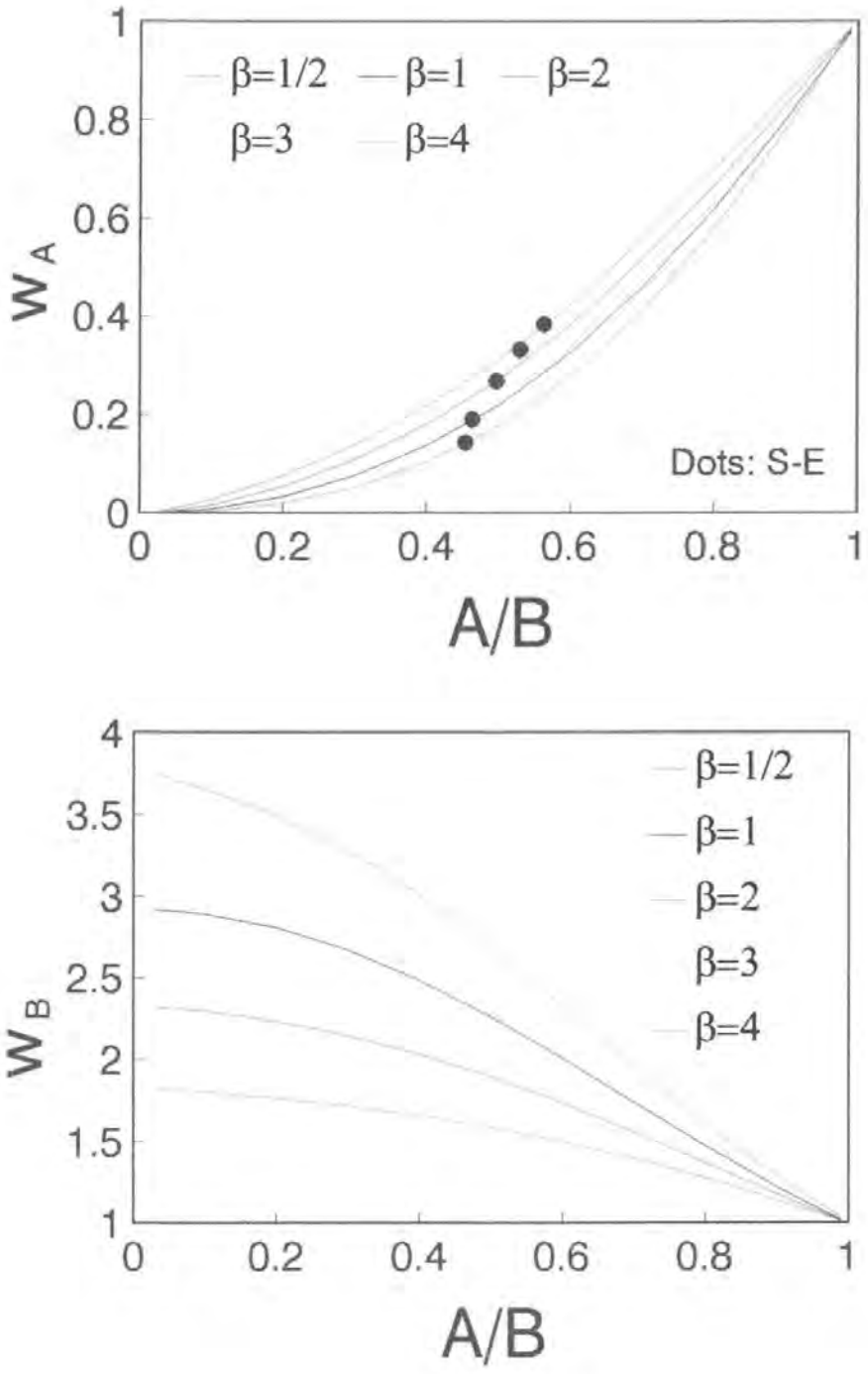

Figure 6.7: w_A, w_B *vs.* A/B in spherical eversion.

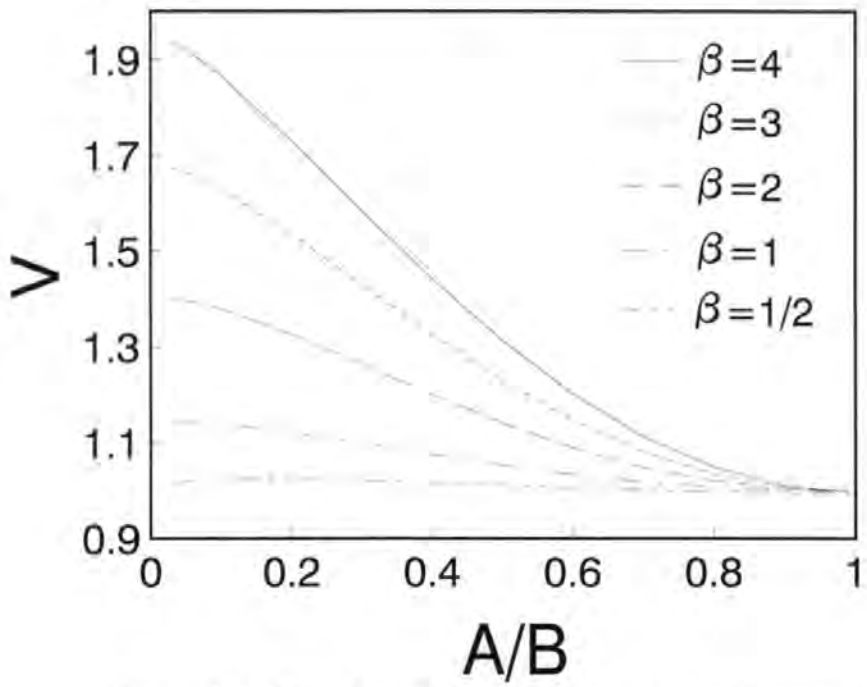

Figure 6.8: The plot of V *vs.* A/B in spherical eversion.

The variation of V with A/B for $\beta = 1/2, 1, 2, 3, 4$ is illustrated in Figure 6.8. It can be seen from Figure 6.8 that the values of A/B and β decide whether the deformation is compressive or tensile. We note that the monotonic decrease of the volume observed in cylindrical eversion ($V = \lambda^{-1}$), no longer holds in the case of spherical eversion.

The deformed inner and outer radii a and b are now given by

$$a = Bw_B^{-(\beta+1)/(\beta+3)} \tag{6.70}$$

and

$$b = Aw_A^{-(\beta+1)/(\beta+3)}, \tag{6.71}$$

which are plotted in Figure 6.9. Observe that features of the distributions shown by Figure 6.9 are different from those in the case of cylindrical eversion. The conclusions

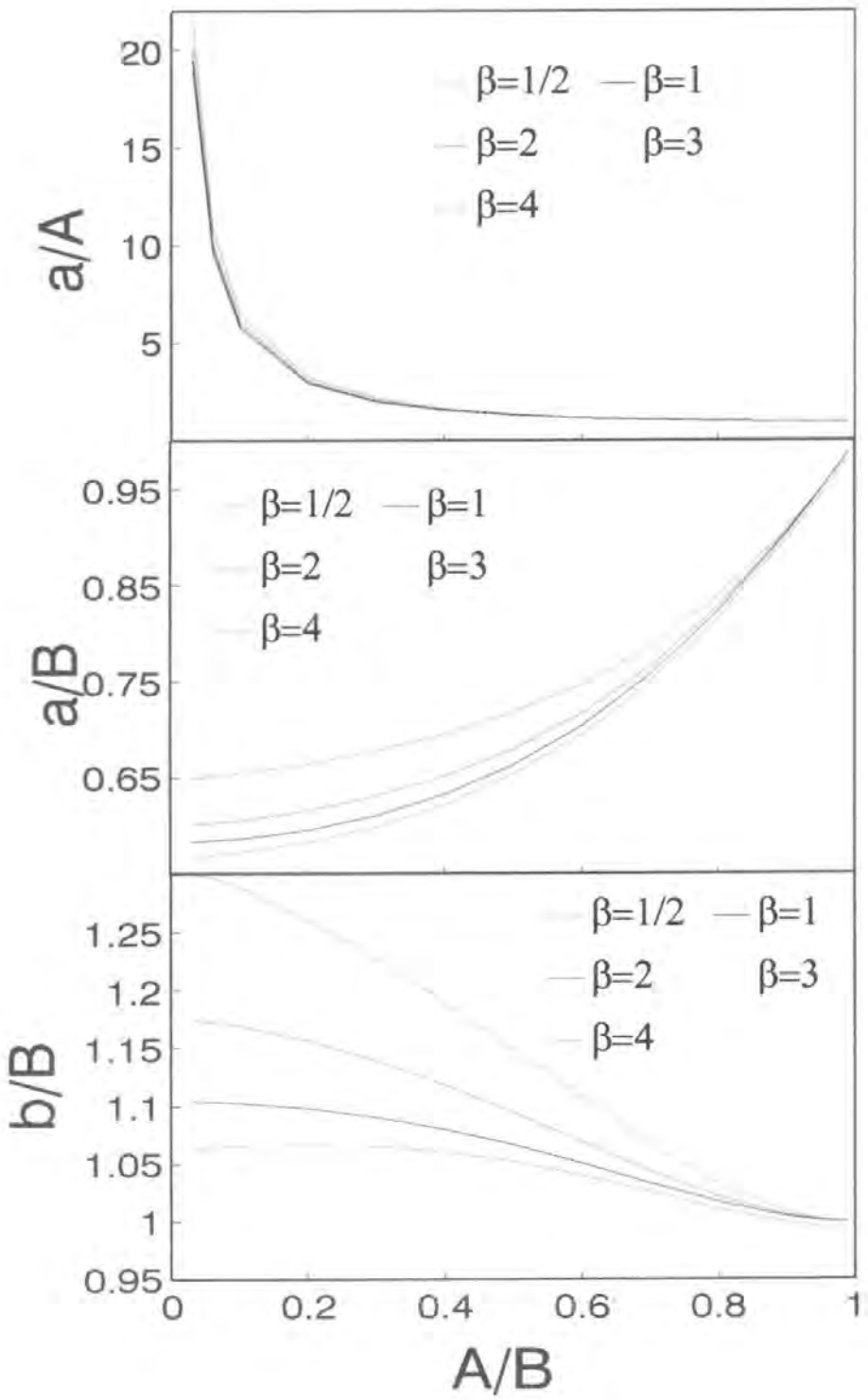

Figure 6.9: $a/A, a/B, b/B$ *vs.* A/B in spherical eversion.

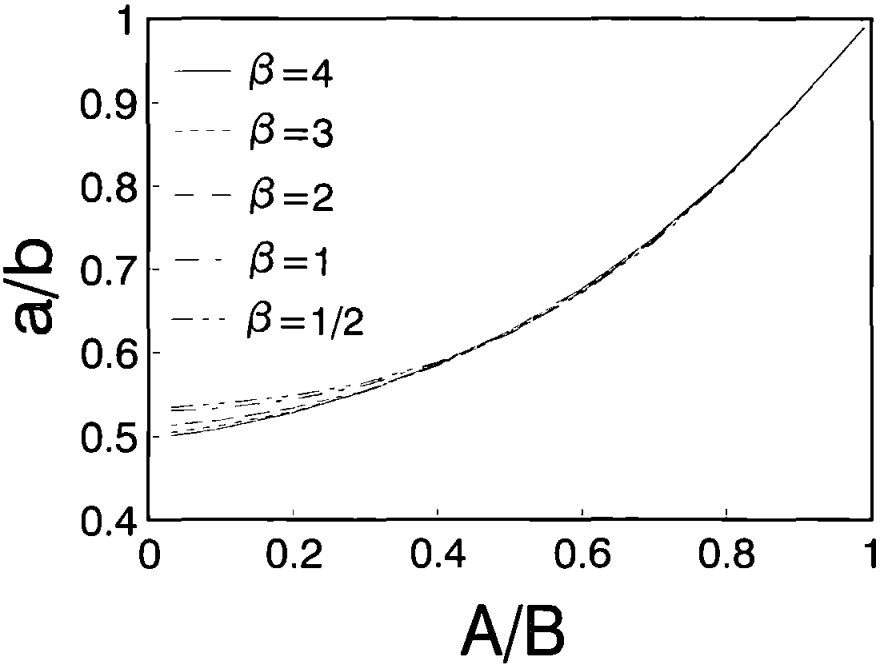

Figure 6.10: a/b *vs.* A/B in spherical eversion.

that $a/A > 1$ and $b/B > 1$, obtained for the cylindrical eversion, are no longer valid in this case. But the 'abnormal' phenomena, found by observations on Figure 6.4 and Figure 6.5, appears for this spherical eversion also (see Figure 6.9 and Figure 6.10). In view of the fact that $w = \lambda_r/\lambda_\theta = \lambda_r/\lambda_\phi$, the 3-dimensional S-E condition (3.5) reduces to the following restriction imposed upon the thickness of the spherical shell:

$$\frac{A}{B} > (\frac{A}{B})'_E \tag{6.72}$$

where $(\frac{A}{B})'_E$, regarded as a function of β, is an upper bound for the thickness of spherical shell and is given numerically in Table 6.6 (It is also shown in Figure 6.7 by dots). By comparing Table 6.3, (which gives the results for cylindrical eversion), with Table 6.6 we find that the maximum thickness of a spherical shell for which we may have a stable solution for the eversion problem is much smaller than the maximum thickness of a

β	1/2	1	2	3	4
l_E	0.14289	0.1896	0.2679	0.3306	0.3820
$(\frac{A}{B})'_E$	0.4547	0.4638	0.4970	0.5303	0.5629
$[(\frac{A}{B})'_E]^{-1} - 1$	1.1992	1.1562	1.0122	0.8859	0.7764

Table 6.6: $(\frac{A}{B})'_E$ *vs.* β in spherical eversion.

cylindrical shell for which the inverted configuration may be stable.

From (6.50) and (6.55) we find that

$$
\begin{aligned}
T_{rr} &= \mu\{1 - (\frac{w_A}{w})^{\beta+1} \cdot [\frac{\check{R}(w)\check{r}(w_A)}{\check{r}(w)\check{R}(w_A)}]^{\beta+3}\} = \mu\{1 - (\frac{w_B}{w})^{\beta+1} \cdot [\frac{\check{R}(w)\check{r}(w_B)}{\check{r}(w)\check{R}(w_B)}]^{\beta+3}\}, \\
T_{\theta\theta} &= \mu\{1 - \frac{w_A^{\beta+1}}{w} \cdot [\frac{\check{R}(w)\check{r}(w_A)}{\check{r}(w)\check{R}(w_A)}]^{\beta+3}\} = \mu\{1 - \frac{w_B^{\beta+1}}{w} \cdot [\frac{\check{R}(w)\check{r}(w_B)}{\check{r}(w)\check{R}(w_B)}]^{\beta+3}\}, \\
T_{\phi\phi} &= T_{\theta\theta}.
\end{aligned}
\tag{6.73}
$$

Variations of $T_{rr}, T_{\theta\theta}$ along the r-axis are plotted in Figure 6.11 and Figure 6.12 respectively. Comparing Figure 6.11 and Figure 6.12 with Figure 6.6, where we have illustrated the distribution of stresses for cylindrical eversion, we find that the distributions of T_{rr} and $T_{\theta\theta}$ in the spherical eversion are very similar to those in the cylindrical eversion. Also, as before, we can draw the conclusion that the material becomes harder as β increases since greater magnitudes of the Cauchy stresses correspond to larger values of β.

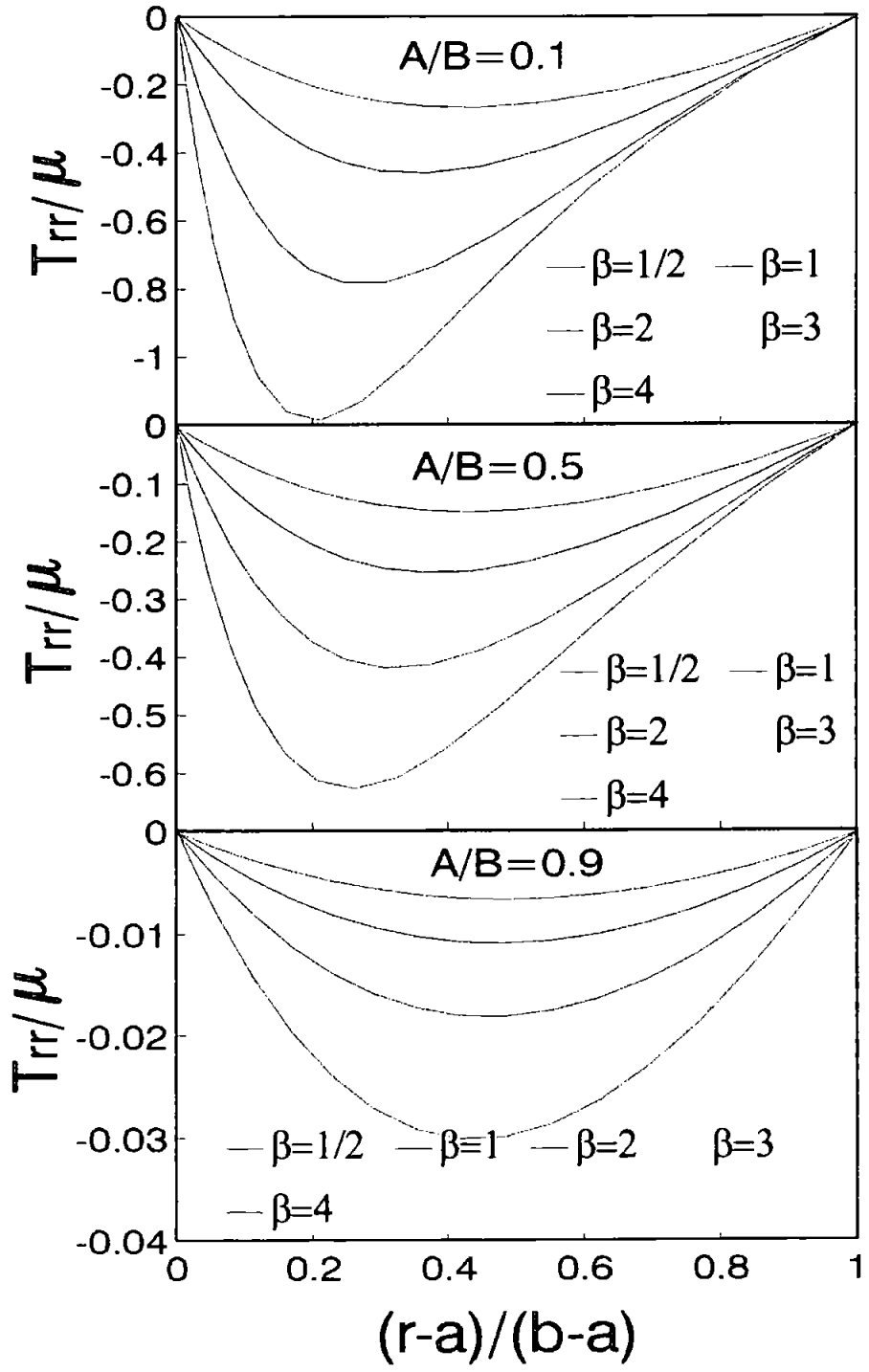

Figure 6.11: T_{rr} along the r-axis in spherical eversion.

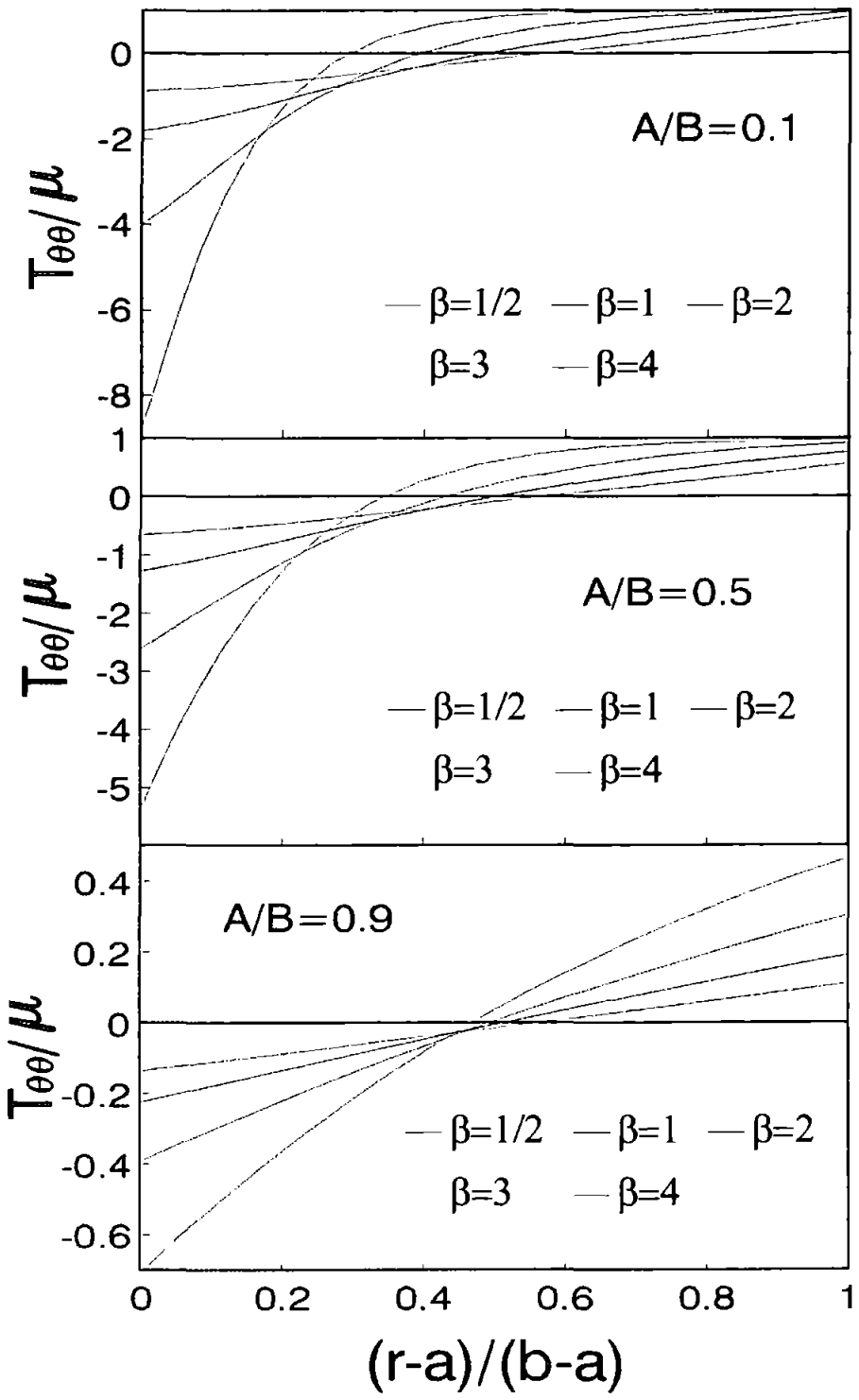

Figure 6.12: $T_{\theta\theta}$ along the r-axis in spherical eversion.

Chapter 7

Radial cylindrical expansions

In this chapter we consider radial cylindrical expansions. The formulation of the problem is presented In Section 7.1 and the solutions are given in Section 7.2. The discussion on the solution follows in Section 7.3 and Section 7.4.

7.1 Formulation of problem

We are concerned with a right circular cylinder in the reference configuration, whose cross-section is described by

$$A \leq R \leq B,\ 0 < \Theta \leq 2\pi, \tag{7.1}$$

where (R, Θ) are cylindrical polar coordinates and A, B stand for the inner and outer radii of the considered cylindrical shell respectively. Note that if B is given such that $B \to \infty$, (7.1) describes a cylindrical cavity in an infinite medium. The cylinder is

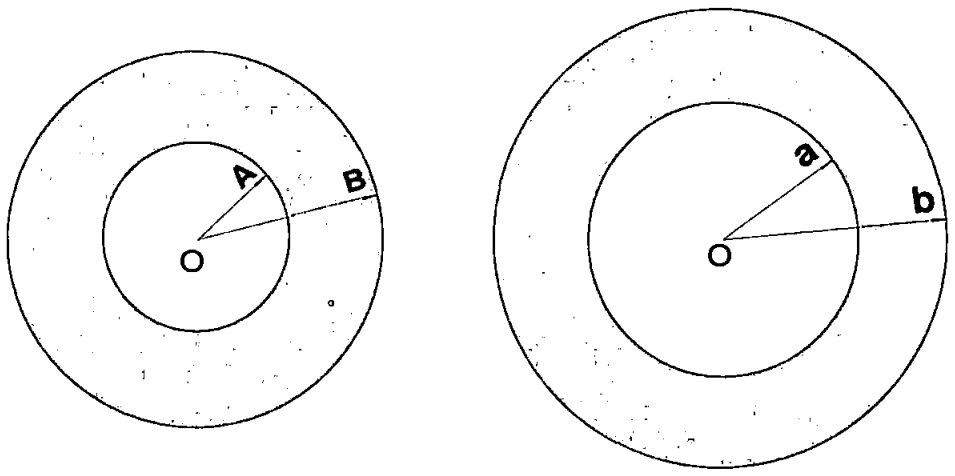

Figure 7.1: The illustration of cylindrical expansion.

subjected to an internal pressure P_A on its inner surface and an external pressure P_B on its outer surface. The deformation with which we are concerned maps a point with polar coordinates (R, Θ) in the undeformed configuration into a point with polar coordinates (r, θ) in the deformed configuration. The region occupied by the cylinder in the deformed configuration is

$$a \leq r \leq b,\ 0 < \theta \leq 2\pi \tag{7.2}$$

where a and b are the deformed inner and outer radii of the cylinder (The deformation is illustrated in Figure 7.1). We assume that a state of plane strain prevails and moreover, that the deformation is axisymmetric and can be sought in the form

$$r = r(R) > 0,\ \theta = \Theta, \tag{7.3}$$

where the positive function $r(R)$ is to be determined and is assumed to be twice continuously differentiable on $A \leq R \leq B$.

The polar components of the deformation gradient tensor $\mathbf{F}$ associated with (7.3) are given by

$$F_{rr} = \dot{r}(R),\ F_{\theta\theta} = r(R)/R,\ F_{r\theta} = F_{\theta r} = 0 \tag{7.4}$$

where the dot denotes differentiation with respect to the argument. The principal stretches associated with the radial deformation (7.3) are

$$\lambda_r = \dot{r}(R),\ \lambda_\theta = r(R)/R, \tag{7.5}$$

and they are required to be positive for $R \in [A, B]$. We assume that the cylinder is composed of the generalized Blatz-Ko material, whose strain energy function is given by (3.1). Thus, from (3.1), (2.29), (7.4) and (7.5) we obtain the following expressions for the Cauchy stress $\mathbf{T}$:

$$T_{rr} = \mu[1 - \frac{R}{r}(\frac{\mathrm{d}R}{\mathrm{d}r})^{\beta+1}],\ T_{\theta\theta} = \mu[1 - (\frac{R}{r})^{\beta+1}\frac{\mathrm{d}R}{\mathrm{d}r}],\ T_{r\theta} = 0. \tag{7.6}$$

In view of (7.6) the equilibrium equation reduces to

$$\frac{\mathrm{d}T_{rr}}{\mathrm{d}r} + \frac{1}{r}(T_{rr} - T_{\theta\theta}) = 0 \tag{7.7}$$

which can be expressed as the following second-order ordinary differential equation for $r(R)$:

$$(\beta+1)(\frac{\mathrm{d}R}{\mathrm{d}r})^{\beta-1} \cdot R \cdot \frac{\mathrm{d}^2R}{\mathrm{d}r^2} + (\frac{\mathrm{d}R}{\mathrm{d}r})^{\beta+1} - (\frac{R}{r})^{\beta+1} = 0. \tag{7.8}$$

From the prescribed boundary conditions of traction

$$T_{rr} = -P_A, \text{ at } r = a \text{ and } T_{rr} = -P_B, \text{ at } r = b, \tag{7.9}$$

the function $r(R)$ must also satisfy

$$r(A)[\dot{r}(A)]^{-\beta-1} = A(1 + P_A/\mu)^{-1},\ r(B)[\dot{r}(B)]^{-\beta-1} = B(1 + P_B/\mu)^{-1}. \tag{7.10}$$

Here we assume that

$$P_A \neq P_B. \tag{7.11}$$

The cylindrical expansion problem now consists of (7.8), (7.9) and (7.10) and in next section we will focus our attention to the finding of exact solutions for this boundary value problem.

7.2 Solution to the boundary value problem

By using the variable substitution proposed by Abeyaratne & Horgan [15, 23] and used in Chapter 6 of this thesis, namely,

$$w \equiv \frac{\lambda_r}{\lambda_\theta} = \frac{R}{r} \cdot \dot{r}, \tag{7.12}$$

the differential equation (7.8) can be shown to be equivalent to

$$(\beta + 1) r \frac{\mathrm{d}w}{\mathrm{d}r} = \beta + 2 - (\beta + 1)w - w^{\beta+1} \tag{7.13}$$

or

$$(\beta+1)R\frac{\mathrm{d}w}{\mathrm{d}R} = w[\beta+2-(\beta+1)w-w^{\beta+1}]. \tag{7.14}$$

Note that

$$\left.\begin{array}{l} \frac{\mathrm{d}r}{\mathrm{d}w} > 0,\ \frac{\mathrm{d}R}{\mathrm{d}w} > 0,\ \text{for } 0 < w < 1, \\ \frac{\mathrm{d}r}{\mathrm{d}w} < 0,\ \frac{\mathrm{d}R}{\mathrm{d}w} < 0,\ \text{for } w > 1. \end{array}\right\} \tag{7.15}$$

Here, we consider the possibility of $w(R)$ being identically equal to unity for the whole region of $A \leq R \leq B$. Note that $w(R) \equiv 1$ satisfies both (7.13) and (7.14) and, from (7.12), it follows that this situation corresponds to homogeneous deformation $r(R) = CR$ (C - constant), which yields (see (7.6)) $T_{rr} = T_{\theta\theta} = \mu(1 - C^{-\beta-2})$. This solution therefore cannot satisfy boundary conditions of the type we consider here (see (7.9)). According to the Proposition 6.4 in [71], if there exists a single value R_0 of R such that $w(R_0) = 1$, the only sufficiently regular solution of (7.13) and (7.14) is $r(R) = CR$. Consequently, we assume in what follows that $w \neq 1$ and we can confine our attention to finding non-homogeneous deformations which are solutions of (7.13) and (7.14). We consider this boundary value problem only for the cases when (i) β is an integer and (ii) β is a rational number of the form $\beta = 1/m$, where m is an integer.

CASE ONE: $\beta = n$ ($n \geq 1$, integer)

We rewrite (7.13) in the form

$$\frac{\mathrm{d}w}{\beta+2-(\beta+1)w-w^{\beta+1}} = \frac{\mathrm{d}r}{(\beta+1)r} \tag{7.16}$$

and from observation that $(1-w)$ is a factor of the denominator in the left hand side of (7.16), we find that

$$\beta+2-(\beta+1)w-w^{\beta+1}=(1-w)(\sum_{i=1}^{\beta}w^i+\beta+2). \tag{7.17}$$

We seek partial fractions for the coefficient of dw in (7.16) in the form

$$\frac{a_0}{1-w}+\frac{\sum_{i=1}^{\beta}a_iw^{\beta-i}}{\sum_{i=1}^{\beta}w^i+\beta+2}, \tag{7.18}$$

which, in view of (7.16) and (7.17), leads to

$$a_0=1/[2(\beta+1)],\ a_i=i/[2(\beta+1)],\ i=1,2,\cdots,\beta. \tag{7.19}$$

Thus, (7.16) reduces to

$$[\frac{1}{1-w}+\frac{\sum_{i=0}^{\beta-1}(\beta-i)w^i}{\sum_{i=1}^{\beta}w^i+\beta+2}]\mathrm{d}w=\frac{2\mathrm{d}r}{r}. \tag{7.20}$$

We define a function $h(w)$ as

$$h(w)\equiv\int_0^w\frac{\sum_{i=0}^{\beta-1}(\beta-i)u^i}{\sum_{i=1}^{\beta}u^i+\beta+2}\mathrm{d}u \tag{7.21}$$

and note that it satisfies

$$h(0)=0;\ h'(w)>0,\ h(w)>0,\ \text{for } w>0. \tag{7.22}$$

The solution of (7.13) can now be expressed as

$$r(w)=C_1e^{h(w)/2}|1-w|^{-1/2},\ w>0,\ w\neq 1, \tag{7.23}$$

where "| |" means the absolute value and C_1 is an integration constant.

Also, we can find the solution $R(w)$ of (7.14) along similar lines. Thus, with the help of (7.17)-(7.19), we rewrite (7.14) as

$$\{\frac{1}{w(1-w)}+\frac{\sum_{i=0}^{\beta-1}(\beta-i)w^i}{w[\sum_{i=1}^{\beta}w^i+\beta+2]}\}\mathrm{d}w=\frac{2\mathrm{d}R}{R}, \tag{7.24}$$

and, on assuming a partial fraction decomposition of the coefficient of dw in the left hand side of (7.24) of the form

$$\frac{1}{1-w}+\frac{1}{w}+\frac{b_0}{w}+\frac{\sum_{i=1}^{\beta}b_iw^{\beta-i}}{\sum_{i=1}^{\beta}w^i+\beta+2}, \tag{7.25}$$

we find that

$$b_0=\beta/(\beta+2);\ b_i=i-1-b_0,\ i=1,2,\cdots,\beta. \tag{7.26}$$

We define another function $g(w)$

$$g(w)\equiv\int_0^w\frac{\sum_{i=0}^{\beta-1}u^i}{\sum_{i=1}^{\beta}u^i+\beta+2}\mathrm{d}u \tag{7.27}$$

which has the same features as $h(w)$, i.e.

$$g(0)=0;\ g'(w)>0,\ g(w)>0,\ \text{for } w>0. \tag{7.28}$$

Therefore, we find the solution of (7.14) in the form

$$R(w)=C_2w^{(\beta+1)/(\beta+2)}e^{h(w)/2-(\beta+1)g(w)/(\beta+2)}|1-w|^{-1/2},\ w>0,\ w\neq 1, \tag{7.29}$$

where C_2 is an integration constant. We note that (7.23) with (7.21) and (7.29) with (7.27) provide parametric solutions to the differentiation equation (7.8) in the case when $\beta=n$.

Explicit expressions of $h(w)$ and $g(w)$ (see (7.21) and (7.27)) in the case when $\beta = 1$ are given by

$$h(w) = g(w) = \ln(w/3 + 1). \tag{7.30}$$

In the case of $\beta = 2$ (7.21) and (7.27) reduce to

$$h(w) = \frac{1}{2}\ln(w^2 + w + 4) + \frac{\sqrt{15}}{5}\arctan\frac{(2w+1)}{\sqrt{15}} - \ln 2 - \frac{\sqrt{15}}{5}\arctan\frac{1}{\sqrt{15}}, \tag{7.31}$$

and

$$g(w) = \frac{1}{2}\ln(w^2 + w + 4) + \frac{1}{\sqrt{15}}\arctan\frac{(2w+1)}{\sqrt{15}} - \ln 2 - \frac{1}{\sqrt{15}}\arctan\frac{1}{\sqrt{15}}, \tag{7.32}$$

which are the same as those previously obtained by Carroll & Horgan [54]. Explicit expressions of $h(w)$ and $g(w)$ in the case when $\beta = 3, 4$ are given in Table 7.1 and Table 7.2 with approximate constants for simplicity.

β	$h(w)$
3	$.8793\arctan(.6371w - .2807) + .3232\ln(w^2 - .8813w + 2.658)$ $+.3535\ln(w + 1.881) - .2987$
4	$.1852\arctan(.9089w + 1.1588) + .9046\arctan(.8123w - .6295)$ $+.2664\ln(w^2 + 2.5498w + 2.8358) + .2336\ln(w^2 - 1.5498w + 2.1158) - .1036$

Table 7.1: Expressions of $h(w)$ for $\beta = 3, 4$.

In view of (7.15) and the fact of $w \neq 1$, the parameter w should belong to the interval $[w_A, w_B]$, where either

$$0 < w_A < w < w_B < 1 \tag{7.33}$$

β	$g(w)$
3	$.2198 \arctan(.6371w - .2807) + .3308 \ln(w^2 - .8813w + 2.658)$ $+.3384 \ln(w + 1.881) - .4771$
4	$.03705 \arctan(.9089w + 1.1588) + .1809 \arctan(.8123w - .6295)$ $+.2533 \ln(w^2 + 2.5498w + 2.8358) + .2467 \ln(w^2 - 1.5498w + 2.1158) - .3791$

Table 7.2: Expressions of $g(w)$ for $\beta = 3, 4$.

or

$$1 < w_B < w < w_A \tag{7.34}$$

and w_A and w_B are values of w such that

$$R(w_A) = A,\ R(w_B) = B. \tag{7.35}$$

From (7.29), we see that the values w_A, w_B can be determined from the pair of equations

$$A = C_2\Phi(w_A),\ B = C_2\Phi(w_B), \tag{7.36}$$

where the auxiliary function $\Phi(w)$ is defined as

$$\Phi(w) = w^{(\beta+1)/(\beta+2)} e^{h(w)/2-(\beta+1)g(w)/(\beta+2)} |1 - w|^{-1/2}. \tag{7.37}$$

By using (7.6), (7.12), (7.23) and (7.29), the components of the Cauchy stresses T_{rr} and $T_{\theta\theta}$ can also be expressed in terms of w as

$$\left.\begin{aligned} T_{rr} &= \mu[1 - w^{-\beta-1}(\tfrac{R}{r})^{\beta+2}] = \mu[1 - (\tfrac{C_2}{C_1})^{\beta+2} e^{-(\beta+1)g(w)}], \\ T_{\theta\theta} &= \mu[1 - w^{-1}(\tfrac{R}{r})^{\beta+2}] = \mu[1 - (\tfrac{C_2}{C_1})^{\beta+2} w^{\beta} e^{-(\beta+1)g(w)}]. \end{aligned}\right\} \tag{7.38}$$

The substitution of (7.38) into (7.9) gives

$$\left.\begin{aligned}(1+\tfrac{P_B}{\mu})e^{(\beta+1)g(w_B)} &= (\tfrac{C_2}{C_1})^{\beta+2},\\ (1+\tfrac{P_A}{\mu})e^{(\beta+1)g(w_A)} &= (\tfrac{C_2}{C_1})^{\beta+2},\end{aligned}\right\} \tag{7.39}$$

which, when combined with (7.36), leads to the following equations to determine the unknown constants w_A, w_B, C_1, C_2:

$$B\Phi(w_A) = A\Phi(w_B), \tag{7.40}$$

$$g(w_B) = g(w_A) + \frac{1}{\beta+1}\ln(\frac{1+P_A/\mu}{1+P_B/\mu}), \tag{7.41}$$

$$C_2 = A/\Phi(w_A), \tag{7.42}$$

$$C_1 = C_2(1+P_A/\mu)^{-1/(\beta+2)}e^{-(\beta+1)g(w_A)/(\beta+2)}. \tag{7.43}$$

Note that (7.40) and (7.41) are simultaneous equations to determine w_A and w_B once P_A, P_B and B/A are given and that C_1, C_2 can be found easily from (7.42) and (7.43) afterwards. From (7.33), (7.34), (7.28) and (7.41) we find that

$$\begin{aligned}&0 < w_A < w < w_B < 1, \text{ for } P_A > P_B,\\ &1 < w_B < w < w_A, \text{ for } P_A < P_B.\end{aligned} \tag{7.44}$$

The substituting (7.39) into (7.38) leads to

$$\left.\begin{aligned}T_{rr} &= \mu\{1-(1+\tfrac{P_A}{\mu})e^{(\beta+1)[g(w_A)-g(w)]}\},\\ T_{\theta\theta} &= \mu\{1-(1+\tfrac{P_A}{\mu})w^{\beta}e^{(\beta+1)[g(w_A)-g(w)]}\}.\end{aligned}\right\} \tag{7.45}$$

From (7.23) and (7.29) we obtain the following expressions for the principal stretches λ_i:

$$\lambda_r = w^{1/(2+\beta)}(1+P_A/\mu)^{-1/(2+\beta)}e^{(1+\beta)[g(w)-g(w_A)]/(2+\beta)}, \tag{7.46}$$

$$\lambda_\theta = w^{-(1+\beta)/(2+\beta)}(1+P_A/\mu)^{-1/(2+\beta)}e^{(1+\beta)[g(w)-g(w_A)]/(2+\beta)}. \tag{7.47}$$

With the help of (7.28), (7.46) and (7.47) we find that

$$\frac{\mathrm{d}\lambda_r}{\mathrm{d}w} > 0, \ \frac{\mathrm{d}\lambda_\theta}{\mathrm{d}w} < 0, \tag{7.48}$$

which imply that the principal stretches vary monotonically along the r-axis.

From (7.6), (7.9) and (7.12) the ratio of the deformed inner radius a to the undeformed inner radius A is given by

$$\frac{a}{A} = w_A^{-(\beta+1)/(\beta+2)}(1 + P_A/\mu)^{-/(\beta+2)} \tag{7.49}$$

which is also the value of the hoop stretch λ_θ at $r = a$ (see (7.47)).

CASE TWO: $\beta = 1/m$ ($m \geq 2$, integer)

In the case when $\beta = 1/m$ we introduce the substitution

$$\zeta = w^{1/m}, \tag{7.50}$$

with the help of which (7.13) and (7.14) can be written as

$$(m+1)r\zeta^{m-1}\frac{\mathrm{d}\zeta}{\mathrm{d}r} = 2 + \frac{1}{m} - (1 + \frac{1}{m})\zeta^m - \zeta^{m+1} \tag{7.51}$$

and

$$(m+1)R\frac{\mathrm{d}\zeta}{\mathrm{d}R} = \zeta[2 + \frac{1}{m} - (1 + \frac{1}{m})\zeta^m - \zeta^{m+1}], \tag{7.52}$$

respectively. As before we can find exact solutions for (7.51) and (7.52) in the form

$$r(w) = C_1 e^{H(w^{1/m})/2}|1 - w^{1/m}|^{-1/2}, \ w > 0, \ w \neq 1 \tag{7.53}$$

and

$$R(w) = C_2 w^{(1+1/m)/(2+1/m)} e^{H(w^{1/m})/2-(1+1/m)G(w^{1/m})/(2+1/m)} |1 - w^{1/m}|^{-1/2}, \quad (7.54)$$

where C_1, C_2 are integration constants and $H(w), G(w)$ are two functions, defined by

$$H(w) \equiv \int_0^w \frac{u^{m-1}/(2+1/m) - \sum_{i=0}^{m-2}(i+1)u^i}{u^m/(2+1/m) + \sum_{i=0}^{m-1} u^i} \mathrm{d}u \quad (7.55)$$

and

$$G(w) \equiv \int_0^w \frac{m^2 u^{m-1}/(2m+1)}{u^m/(2+1/m) + \sum_{i=0}^{m-1} u^i} \mathrm{d}u. \quad (7.56)$$

We have

$$H(0) = 0 \quad (7.57)$$

and the function $G = G(w)$ satisfies

$$G(0) = 0;\ G'(w) > 0,\ G(w) > 0, \text{ for } w > 0. \quad (7.58)$$

We note that (7.53) and (7.54) with (7.55) and (7.56) are parametric solutions to the differential equation (7.8) for the case when $\beta = 1/m$. Explicit expressions of $H(w)$ and $G(w)$ can be found by integrating (7.55) and (7.56) for a specific number m. As an example, in the case when $\beta = 1/2$ ($m = 2$) we find that

$$H(w) = \frac{1}{2}\ln(\frac{2}{5}w^2 + w + 1) - \sqrt{15}\arctan\frac{(4w+5)}{\sqrt{15}} + \sqrt{15}\arctan\frac{\sqrt{15}}{3}, \quad (7.59)$$

and

$$G(w) = \ln(\frac{2}{5}w^2 + w + 1) - \frac{2\sqrt{15}}{3}\arctan\frac{(4w+5)}{\sqrt{15}} + \frac{2\sqrt{15}}{3}\arctan\frac{\sqrt{15}}{3}. \quad (7.60)$$

The range of the parameter w is given by (7.33) or (7.34) and, in view of (7.54), w_A, w_B can be found from

$$A = C_2\Psi(w_A),\ B = C_2\Psi(w_B) \tag{7.61}$$

where the auxiliary function $\Psi(w)$ is defined as

$$\Psi(w) = w^{(1+1/m)/(2+1/m)}e^{H(w^{1/m})/2-(1+1/m)G(w^{1/m})/(2+1/m)}|1-w^{1/m}|^{-1/2}. \tag{7.62}$$

By making use of (7.6), (7.12), (7.53) and (7.54), the components of the Cauchy stress tensor $T_{rr}, T_{\theta\theta}$ can be then expressed in terms of w as

$$\left.\begin{aligned} T_{rr} &= \mu[1-(\tfrac{C_2}{C_1})^{2+1/m}e^{-(1+1/m)G(w^{1/m})}], \\ T_{\theta\theta} &= \mu[1-(\tfrac{C_2}{C_1})^{2+1/m}w^{1/m}e^{-(1+1/m)G(w^{1/m})}]. \end{aligned}\right\} \tag{7.63}$$

Then the combination of (7.9) and (7.61) with (7.63) gives

$$B\Psi(w_A) = A\Psi(w_B), \tag{7.64}$$

$$G(w_B^{1/m}) = G(w_A^{1/m}) + \frac{1}{1+1/m}\ln(\frac{1+P_A/\mu}{1+P_B/\mu}), \tag{7.65}$$

$$C_2 = A/\Psi(w_A), \tag{7.66}$$

$$C_1 = C_2(1+P_A/\mu)^{-1/(2+1/m)}e^{-(1+1/m)G(w_A^{1/m})/(2+1/m)}. \tag{7.67}$$

and the substitution of (7.66) and (7.67) into (7.63) leads to

$$\left.\begin{aligned} T_{rr} &= \mu\{1-(1+\tfrac{P_A}{\mu})e^{(1+1/m)[G(w_A^{1/m})-G(w^{1/m})]}\}, \\ T_{\theta\theta} &= \mu\{1-(1+\tfrac{P_A}{\mu})w^{1/m}e^{(1+1/m)[G(w_A^{1/m})-G(w^{1/m})]}\}. \end{aligned}\right\} \tag{7.68}$$

In view of (7.53) and (7.54) the principal stretches can now be rewritten as

$$\lambda_r = w^{1/(2+1/m)}(1+P_A/\mu)^{-1/(2+1/m)}e^{(1+1/m)[G(w^{1/m})-G(w_A^{1/m})]/(2+1/m)}, \tag{7.69}$$

$$\lambda_\theta = w^{-(1+1/m)/(2+1/m)}(1+P_A/\mu)^{-1/(2+1/m)}e^{(1+1/m)[G(w^{1/m})-G(w_A^{1/m})]/(2+1/m)}. \tag{7.70}$$

From (7.6), (7.9) and (7.12) the ratio of the deformed inner radius a to the undeformed inner radius A is given by

$$\frac{a}{A} = w_A^{-(1+1/m)/(2+1/m)}(1 + P_A/\mu)^{-1/(2+1/m)} \tag{7.71}$$

By comparing (7.23) with (7.53), (7.29) with (7.54), (7.21) with (7.55) and (7.27) with (7.56), we find that the solutions in the case when $\beta = 1/m$ are similar to those in the case when $\beta = n$ and these can be obtained from the latter by replacing $h(w)$ with $H(w)$, $g(w)$ with $G(w)$ and w with $w^{1/m}$. Moreover, in the case when $\beta = 1/m$, the equations used to determine the constants w_A, w_B, C_1, C_2 ((7.40) - (7.43)), the expressions for the Cauchy stresses (7.68) and the expressions for the principal stretches ((7.46) and (7.47)) can also be obtained from the corresponding expressions in the case $\beta = n$ in the same manner as indicated above. This similarity will enable us to simplify our following discussions. For this reason, the discussion which follows will be mainly confined to the case when $\beta = n$, and only occasionally we will also comment upon the case when $\beta = 1/m$.

7.3 Discussion on the expansion of a cylindrical cavity in an infinite medium

In this section we assume that $B \to \infty$ and replace the boundary conditions (7.9) with

$$T_{rr} = -P_A, \text{ at } r = a, \text{ and } T_{rr} \to -P_B, \ r \to \infty. \tag{7.72}$$

Since $w \to 1$ as $r \to \infty$, we have $w_B = 1$ in this case. The equations used to determine the unknown constants C_1, C_2 and w_A in solutions (7.23) and (7.29) are therefore (7.41), (7.42) and (7.43) with $w_B = 1$. If (7.41) can be solved for a w_A such that

$$0 < w_A < 1, \text{ for } P_A > P_B,$$

$$w_A > 1, \text{ for } P_A < P_B, \tag{7.73}$$

then, (7.42) and (7.43) should provide positive constants C_1 and C_2, which ensure parametric solutions (7.23) and (7.29) being positive.

In order to verify the solvability of (7.41), we observe that the auxiliary function $F(w)$, defined by

$$F(w) \equiv g(w) - g(1) - \frac{1}{\beta + 1} \ln \left(\frac{1 + P_B/\mu}{1 + P_A/\mu} \right), \tag{7.74}$$

is monotonically increasing due to the fact that $F'(w) > 0$. It follows that (7.41) has a unique root w_A, such that

$$0 < w_A < 1, \text{ if } P_B < P_A < P_{max},$$

$$w_A > 1, \text{ if } P_A < P_B, \tag{7.75}$$

where

$$P_{max} \equiv \mu[(1 + P_B/\mu)e^{(1+\beta)g(1)} - 1] \tag{7.76}$$

is an increasing function of the external pressure P_B. In view of the monotonical increase of functions $F(w)$ and $g(w)$ we also find that: (i) w_A, which is the value of the parameter w at the wall of the cavity, tends to unity as P_A tends to P_B and (ii)

for any prescribed positive value P_B, when $P_A \to P_{max}$, $w_A \to 0$, the deformed inner radius $a \to \infty$ and the hoop stress $T_{\theta\theta}$ on the inner surface ($r = a$) tends to μ.

The differentiation of $(7.45)_1$ (with $w_B = 1$) with respect to r yields

$$\frac{\mathrm{d}T_{rr}}{\mathrm{d}r} = \frac{\mathrm{d}w}{\mathrm{d}r}\mu(1+\beta)(1+\frac{P_A}{\mu})g'(w)e^{(\beta+1)[g(w_A)-g(w)]} \tag{7.77}$$

which implies that

$$\begin{aligned} &\frac{\mathrm{d}T_{rr}}{\mathrm{d}r} > 0, \text{ for } P_B < P_A < P_{max}, \\ &\frac{\mathrm{d}T_{rr}}{\mathrm{d}r} < 0, \text{ for } P_A < P_B. \end{aligned} \tag{7.78}$$

Consequently, the radial stress T_{rr} increases monotonically from $-P_A$ along the r-axis and tends to $-P_B$ as $r \to \infty$ when $P_B < P_A < P_{max}$; but decreases monotonically from $-P_A$ with r and tends to $-P_B$ when $r \to \infty$ for $P_A < P_B$.

The derivative of the hoop stress $T_{\theta\theta}$ with respect to r (see $(7.45)_2$) is

$$\frac{\mathrm{d}T_{\theta\theta}}{\mathrm{d}r} = \frac{\mathrm{d}w}{\mathrm{d}r}\mu(1+\frac{P_A}{\mu})w^{\beta}e^{(\beta+1)[g(w_A)-g(w)]}[(1+\beta)g'(w)-\beta/w]. \tag{7.79}$$

Introducing

$$\sigma(w) \equiv [(1+\beta)wg'(w)-\beta](\sum_{i=1}^{\beta} w^i + \beta + 2) \tag{7.80}$$

and with the help of (7.27) we find that

$$\frac{\mathrm{d}\sigma}{\mathrm{d}w} > 0,\ \sigma(0) = -\beta^2 - 2\beta < 0,\ \sigma(1) = -\beta^2 - \beta < 0. \tag{7.81}$$

In view of (7.44), (7.79) and (7.81), we can draw following conclusions: (i) when P_A is given such that $P_B < P_A < P_{max}$, we have $\mathrm{d}T_{\theta\theta}/\mathrm{d}r < 0$. The hoop stress $T_{\theta\theta}$ has its

maximum value on the cavity wall $r = a$

$$(T_{\theta\theta})_{max} = \mu[1 - (1 + \frac{P_A}{\mu})w_A^{\beta}], \tag{7.82}$$

then, $T_{\theta\theta}$ decreases monotonically with r and tends to $-P_B$ as $r \to \infty$ ($w \to 1$); (ii) when P_A and P_B are given such that $P_A < P_B$, there exists a certain value w_0 such that at $w = w_0$ we have

$$\frac{\mathrm{d}T_{\theta\theta}}{\mathrm{d}w}(w_0) = 0, \text{ for } P_A < P_B \tag{7.83}$$

and

$$\begin{aligned} &\frac{\mathrm{d}T_{\theta\theta}}{\mathrm{d}r} > 0, \ 1 < w < w_0, \\ &\frac{\mathrm{d}T_{\theta\theta}}{\mathrm{d}r} < 0, \ w > w_0. \end{aligned} \tag{7.84}$$

It is easy to verify that $w_0 = 3$ when $\beta = 1$, $w_0 = (\sqrt{33} - 1)/2$ if $\beta = 2$ and *etc.*, so we conjecture that w_0 is a decreasing function of β. Thus, when $w > w_0$, which is equivalent to $r < r(w_0)$, $T_{\theta\theta}$ increases monotonically along r and arrives at its maximum value at $w = w_0$ ($r = r(w_0)$), then decreases monotonically with r for $1 < w < w_0$ (i.e., $r > r(w_0)$). Note that this is true only if the value w_A, determined by the prescribed values P_A, P_B, ensures that $w_A > w_0$. Otherwise, if P_A, P_B are prescribed such that $P_A < P_B$ and the resultant value w_A is less than w_0, $T_{\theta\theta}$ will start from its maximum value at $r = a$, the wall of the cavity, and decreases monotonically along the r-axis.

Now we turn our attention to the strong ellipticity of the solutions. Recall that for the generalized Blatz-Ko material the strong ellipticity condition will be violated when the ratio of the principal stretches are not in the range of $(t_E, 1/t_E)$, where $t_E \in (0, 1)$ is

a critical value determined by (3.6) (cf. (3.5)). For convenience, this strong-ellipticity condition is cited here as

$$t_E < w < 1/t_E. \tag{7.85}$$

Since we have either $w > 1$ or $0 < w < 1$ in our present solutions, it follows that the right hand side of the inequality (7.85) holds for $0 < w < 1$, whereas the left hand side of the inequality may be violated for certain boundary values; and vice versa when $w > 1$.

In view of the monotonic increasing (decreasing) character of w with r when $w_A < w < 1$ (or $1 < w < w_A$, see (7.15)), it follows that the strong ellipticity is first lost at $r(w_A) = a$ and moreover, that it occurs when $w_A = t_E$ for $P_B < P_A < P_{max}$ or $w_A = 1/t_E$ for $P_A < P_B$, which impose following restrictions upon the pressures P_A and P_B

$$\begin{aligned} &P_A < P_B < P_E^B \equiv \mu\{(1 + P_A/\mu)e^{(1+\beta)[g(1/t_E)-g(1)]} - 1\}, \\ &P_B < P_A < P_E^A \equiv \mu\{(1 + P_B/\mu)e^{(1+\beta)[g(1)-g(t_E)]} - 1\}. \end{aligned} \tag{7.86}$$

Comparison of P_E^A with P_{max} reveals that P_E^A is less than P_{max}. It is of interest to note that P_E^A is a linear function of P_B/μ, P_E^B is a linear function of P_A/μ and the coefficients of the linear equations are functions of the material parameter β only, which are shown to be increasing functions of β by numerical experiments. For any values of P_A, P_B, given within the range of $P_E^A < P_A < P_{max}$ or $P_B > P_E^B$, the existence of the smooth solutions obtained here is still ensured. However, there is now an annular

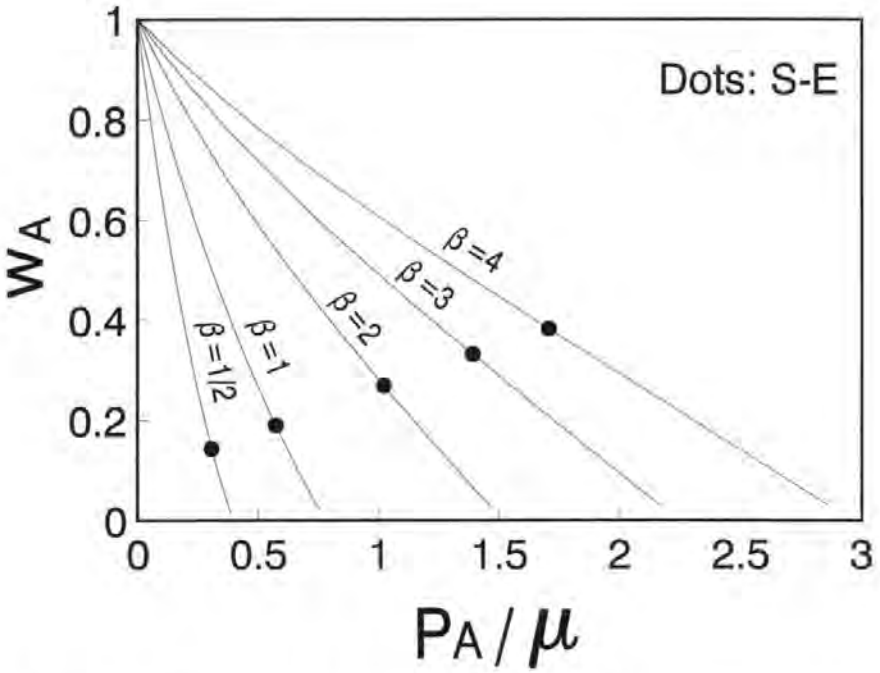

Figure 7.2: w_A *vs.* P_A for a cylindrical cavity in an infinite medium.

zone $A \leq R \leq R_E$, on which the equilibrium equation (7.7) is no longer elliptic at the solutions, while for $R > R_E$, the strong ellipticity holds. The radius R_E at the interface between the elliptic and non-elliptic regions is given by (7.29), (7.41), (7.43) and (7.42) with $R = R_E$, $w_B = 1$ and $w = t_E$ (or $w = 1/t_E$) as

$$R_E = A\left(\frac{1-w_A}{1-t_E}\right)^{\frac{1}{2}}\left(\frac{t_E}{w_A}\right)^{\frac{1+\beta}{2+\beta}} e^{\frac{1}{2}[h(t_E)-h(w_A)]+\frac{1+\beta}{2+\beta}[g(w_A)-g(t_E)]}, \quad P_E^A < P_A < P_{max} \quad (7.87)$$

or

$$R_E = A\left(\frac{1-w_A}{1-1/t_E}\right)^{\frac{1}{2}}\left(t_E w_A\right)^{-\frac{1+\beta}{2+\beta}} e^{\frac{1}{2}[h(1/t_E)-h(w_A)]+\frac{1+\beta}{2+\beta}[g(w_A)-g(1/t_E)]}, \quad P_E^B < P_B. \quad (7.88)$$

When the external pressure P_B is given to be zero, which represents an internally pressurized cylindrical cavity in an infinite medium, the plot of w_A *vs.* P_A is illustrated in Figure 7.2, where the dots correspond to values of P_E^A and the graphs are interrupted

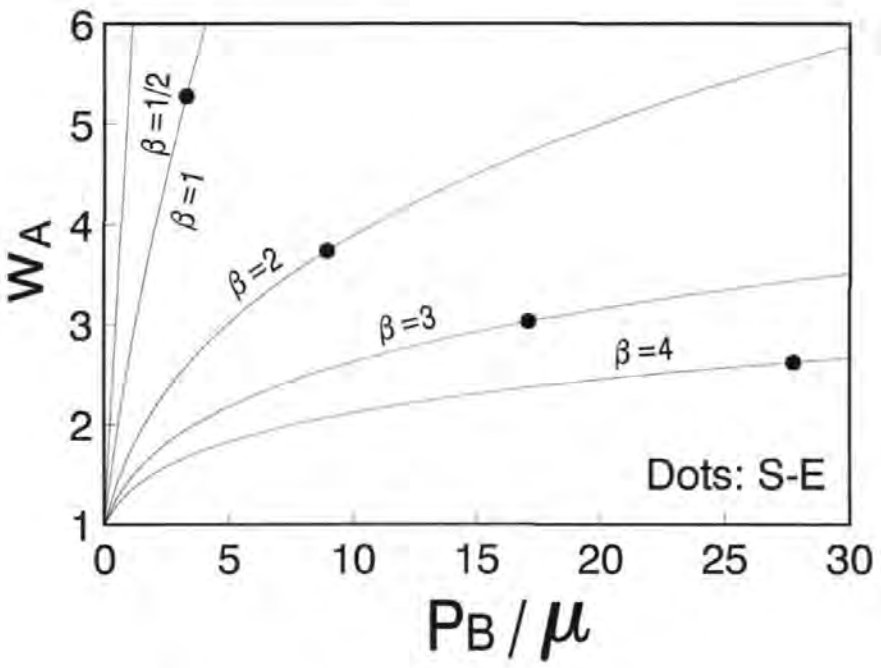

Figure 7.4: w_A *vs.* P_B for a cylindrical cavity in an infinite medium.

When the internal pressure P_A is assumed to be zero, we have an externally pressurized cylindrical cavity in an infinite medium. The plot of w_A *vs.* P_B (with $P_A = 0$) is given in Figure 7.4 where the dots indicate values corresponding to P_E^B. It can be seen from the diagram that for any prescribed value P_B, there always exists a corresponding value w_A. But when P_B is given such that $P_B > P_E^B$, in which P_E^B is the pressure corresponding to that $w_A = t_E$ and is an increasing function of β, the strong-ellipticity condition will be violated. It can be seen from (7.46) to (7.48) that for the externally pressurized cylindrical cavity, the hoop stretch λ_θ has its minimum value $w_A^{-(1+\beta)/(2+\beta)} < 1$ at $r = a$, then increases monotonically with r and tends to its maximum value $(1 + P_B/\mu)^{-1/(2+\beta)} < 1$ as $r \to \infty$; the radial stretch λ_r decreases from its maximum value $w_A^{1/(2+\beta)} > 1$ at $r = a$ and tends to its minimum

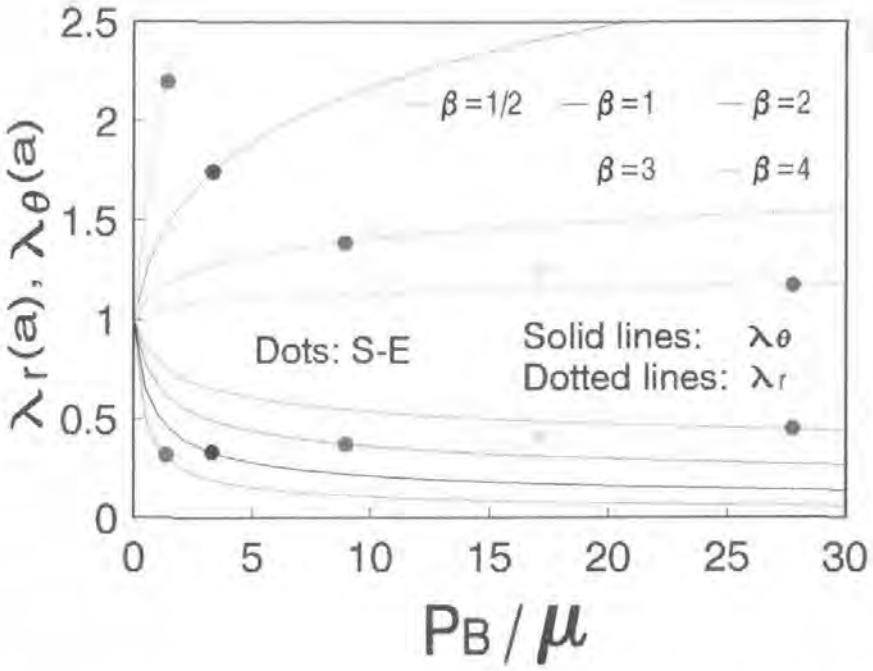

Figure 7.5: $\lambda_r(a), \lambda_\theta(a)$ *vs.* P_B for a cylindrical cavity in an infinite medium.

value $(1 + P_B/\mu)^{-1/(2+\beta)} < 1$ as $r \to \infty$. The plot of $\lambda_r(a), \lambda_\theta(a)$ *vs.* P_B (Figure 7.5, in which the dots stand for values corresponding to P_E^B) also reveals that when β is given by $\beta = 1/2, 1, 2, 3, 4$, the values of the principal stretch $\lambda_r(a)$, beyond which the strong-ellipticity condition will be violated, are within the range of $[1.2, 2.2]$ and that the values of the principal stretch $\lambda_\theta(a)$, beyond which the strong-ellipticity condition no longer holds, are within the range of $[.32, .45]$.

7.4 Discussions on the expansion of an internally pressurized cylindrical shell

Now we examine our solutions (7.23) and (7.29) for another specific situation of the cylindrical expansion, that is, the radial expansion of an internally pressurized hollow cylinder. Here the inner and outer radii A, B are given as positive constants (see (7.1)) and the outer surface of the considered hollow cylinder is assumed to be free of traction ($P_B = 0$) whereas the inner surface is subjected to a prescribed pressure $P_A > 0$ (see (7.9)). Therefore, once B/A and P_A are given, the unknown constants w_A, w_B, C_1, and C_2 in (7.23) and (7.29) can be determined from (7.40)-(7.43) with $P_B = 0$. Note that we can solve the simultaneous equations (7.40) and (7.41) only numerically and according to (7.44) we have

$$0 < w_A < w < w_B < 1. \tag{7.89}$$

We plot the numerical results of w_A, w_B *vs.* P_A in Figure 7.6 and Figure 7.7, in which B/A is given as $B/A = 2$ and $B/A = 10$ respectively. It can be seen from Figure 7.6 and Figure 7.7 that there exists a maximum value of the internal pressure P_A, namely P_{max}, which is an increasing function of β (for a fixed A/B) and of B/A when β is fixed. If the pressure P_A is given such that $P_A > P_{max}$ there are no solutions to these radial expansion problems. Otherwise if P_A is prescribed as $P_A < P_{max}$ we would have two solutions to these boundary-value problems. We use dotted and solid lines to represent the two solutions shown in Figure 7.6 and Figure 7.7 respectively.

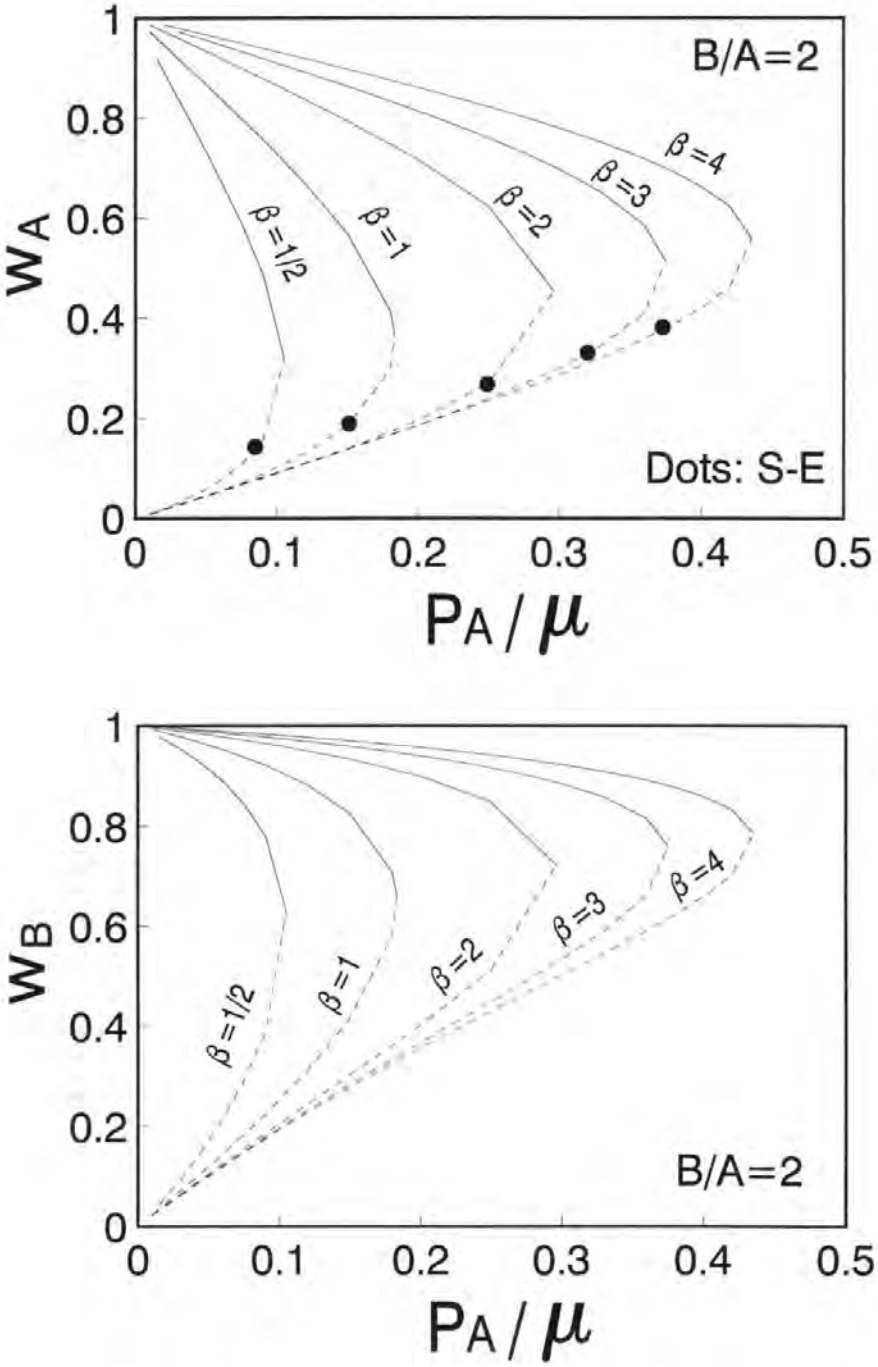

Figure 7.6: w_A, w_B *vs.* P_A for a cylindrical shell with $B/A = 2$.

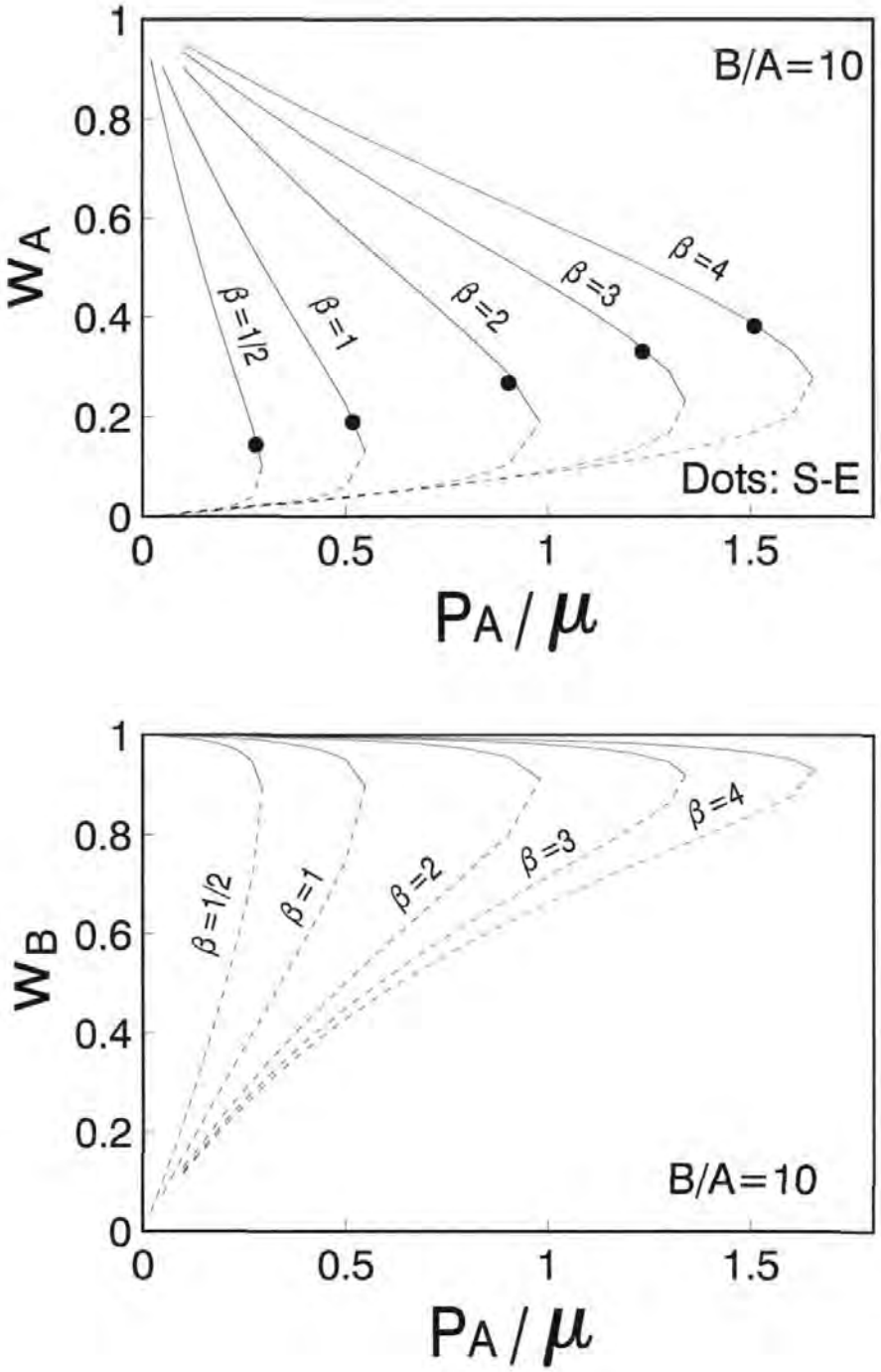

Figure 7.7: w_A, w_B *vs.* P_A for a cylindrical shell with $B/A = 10$.

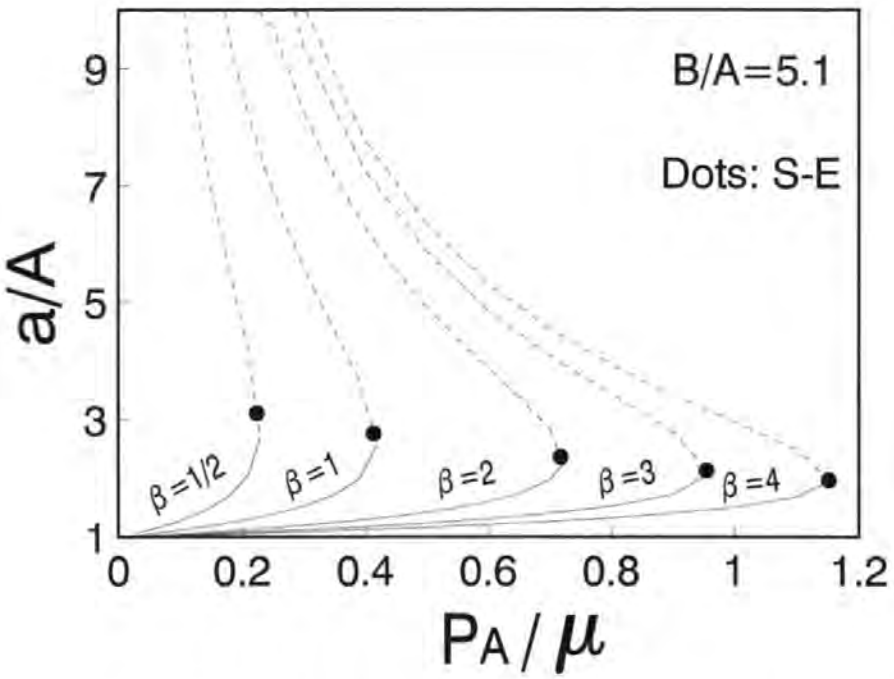

Figure 7.8: a/A *vs.* P_A for a cylindrical shell with $B/A = 5.1$.

For each of the two solutions, $w_A < w_B$ holds, which can also be verified by (7.41). w_A and w_B decrease with P_A for the solid lines' solutions but increase with P_A for the dotted lines' ones. In order to distinguish the two possibilities we give the plot of a/A *vs.* P_A in Figure 7.8 and the plot of $T_{\theta\theta}(a)$ *vs.* P_A in Figure 7.9. For physically realistic solutions, we expect both the inner radius a and the magnitude of $T_{\theta\theta}(a)$ to increase with pressure P_A. Examination of Figure 7.8 and Figure 7.9 indicates that the features of $a, T_{\theta\theta}(a)$ shown by the solid lines' solutions are coincident with this expectation. In contrast, for the dotted lines' solutions, a increases as P_A decreases and tends to infinity when P_A tends to zero (see Figure 7.8); $T_{\theta\theta}(a)$ decreases with P_A and tends to μ when P_A tends to zero (Figure 7.9). Such characteristics of a and $T_{\theta\theta}(a)$ are physically unrealistic. Therefore, on these physical grounds, we can reject

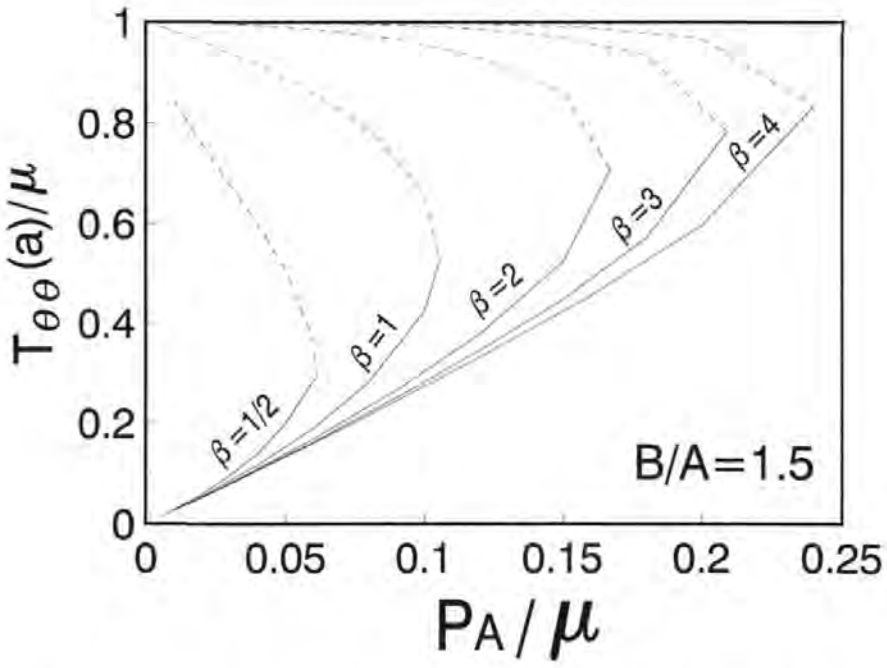

Figure 7.9: $T_{\theta\theta}(a)$ *vs.* P_A for a cylindrical shell with $B/A = 1.5$.

the dotted lines' solutions and we will consider the solid lines' solutions only in the following discussion.

Recalling that in plane strain the strong ellipticity condition holds for the material if and only if (7.85) holds and since we have $w < 1$ at the present problem (see (7.89)), the right hand side of the inequality (7.85) is satisfied for any given boundary values, but the left hand side of (7.85) may be violated for certain boundary values. By virtue of the monotonic increase of w with r (see (7.15)), it follows that the strong-ellipticity is first lost at $r = a$ and occurs when $w_A = t_E$ and that the corresponding value P_A, say P_E, can then be found by (7.41). These values of P_E are represented by dots in Figures 7.6 to 7.8 and Figure 7.10. We plot a/A *vs.* P_A when B/A is given within the range of $[1.05, 100]$ and $\beta = 1$ in Figure 7.10 (the results for $\beta = 1/2, 2, 3, 4$ are similar

to those shown in Figure 7.10). As an example, it can be seen from Figure 7.10 that for $B/A = 1.05$ and for $P_A < P_{max}$, the strong ellipticity holds for all $r \in [a, b]$ since the values of w_A represented by the solid lines are greater than t_E. For $B/A = 10$, however, the strong ellipticity is lost for $P_E < P_A < P_{max}$. It then follows that there is a certain value of B/A, say $(B/A)_E$, so that if $B/A < (B/A)_E$ the strong ellipticity holds for all values of $P_A < P_{max}$, whereas if $B/A > (B/A)_E$ then the strong ellipticity is violated for $P_E < P_A < P_{max}$. In the case when $\beta = 1$ the value of $(B/A)_E$ is approximately 5.96 (in the case when $\beta = 2$, $(B/A)_E \approx 5.1$, a value determined previously by Chung *et al.* [16]).

With the help of (7.41) and the fact that $P_B = 0$, the principal stretch λ_r (7.46) can be rewritten as

$$\lambda_r = w^{1/(2+\beta)} e^{(1+\beta)[g(w)-g(w_B)]/(2+\beta)} \tag{7.90}$$

which, in view of (7.28) and the fact that $0 < w < 1$, indicates that $\lambda_r < 1$. Thus, from (7.48) and (7.90) we find that the minimum value of λ_r and the maximum value of λ_θ occur at $r = a$. Numerical examination of $\lambda_\theta(a) = a/A$ reveals that the values of the principal stretch λ_θ, beyond which the strong ellipticity no longer holds, are within the range of $[1.9, 3.2]$ when β is given by $\beta = 1/2, 1, 2, 3, 4$ and B/A is within the interval $[1.05, 100]$ (cf. Figure 7.8 and Figure 7.10).

Because of

$$\frac{\mathrm{d}T_{rr}}{\mathrm{d}r} = \frac{\mathrm{d}w}{\mathrm{d}r}\mu(1+\beta)(1+\frac{P_A}{\mu})g'(w)e^{(\beta+1)[g(w_A)-g(w)]} > 0 \tag{7.91}$$

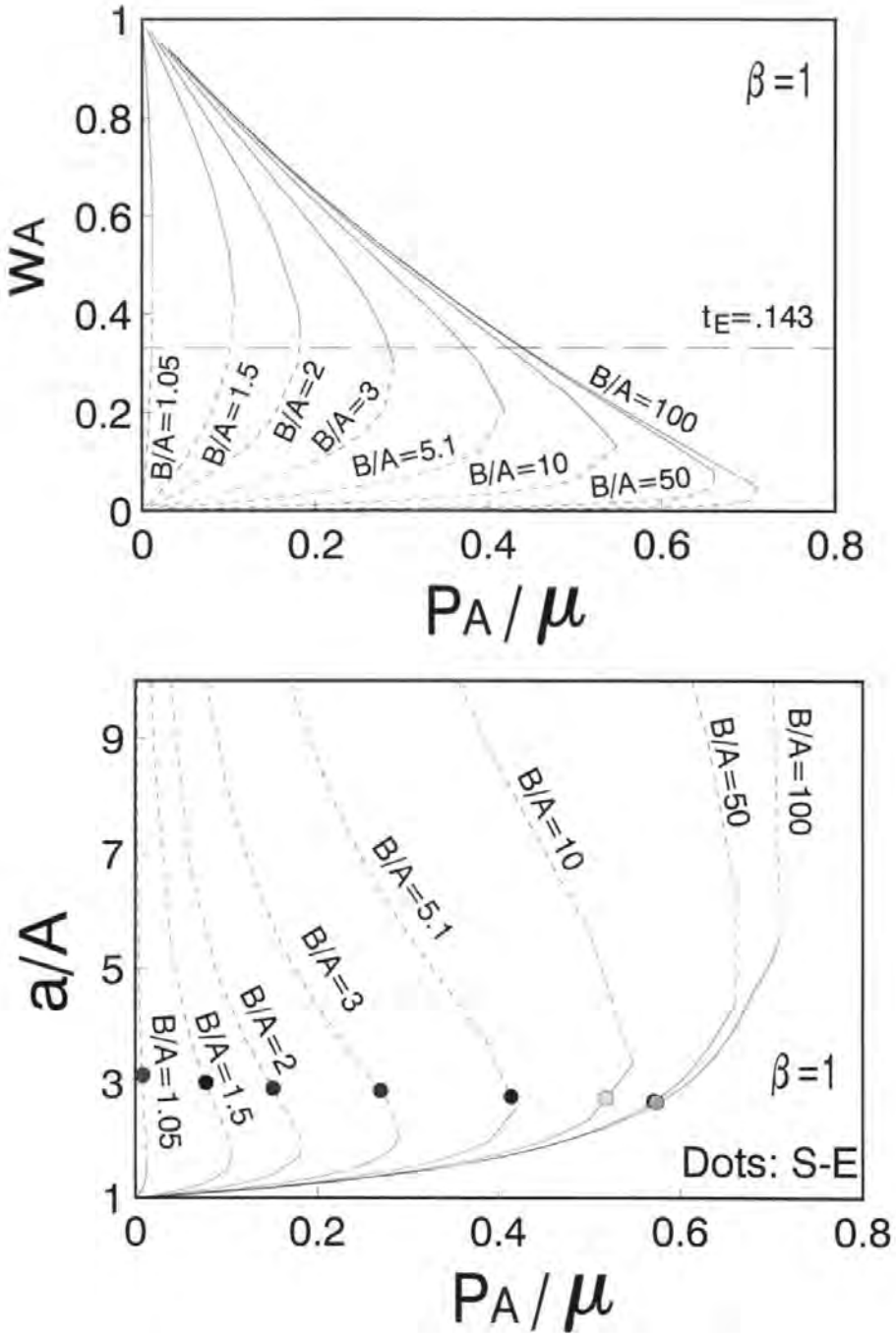

Figure 7.10: w_A and a/A *vs.* P_A for a cylindrical shell with $\beta = 1$.

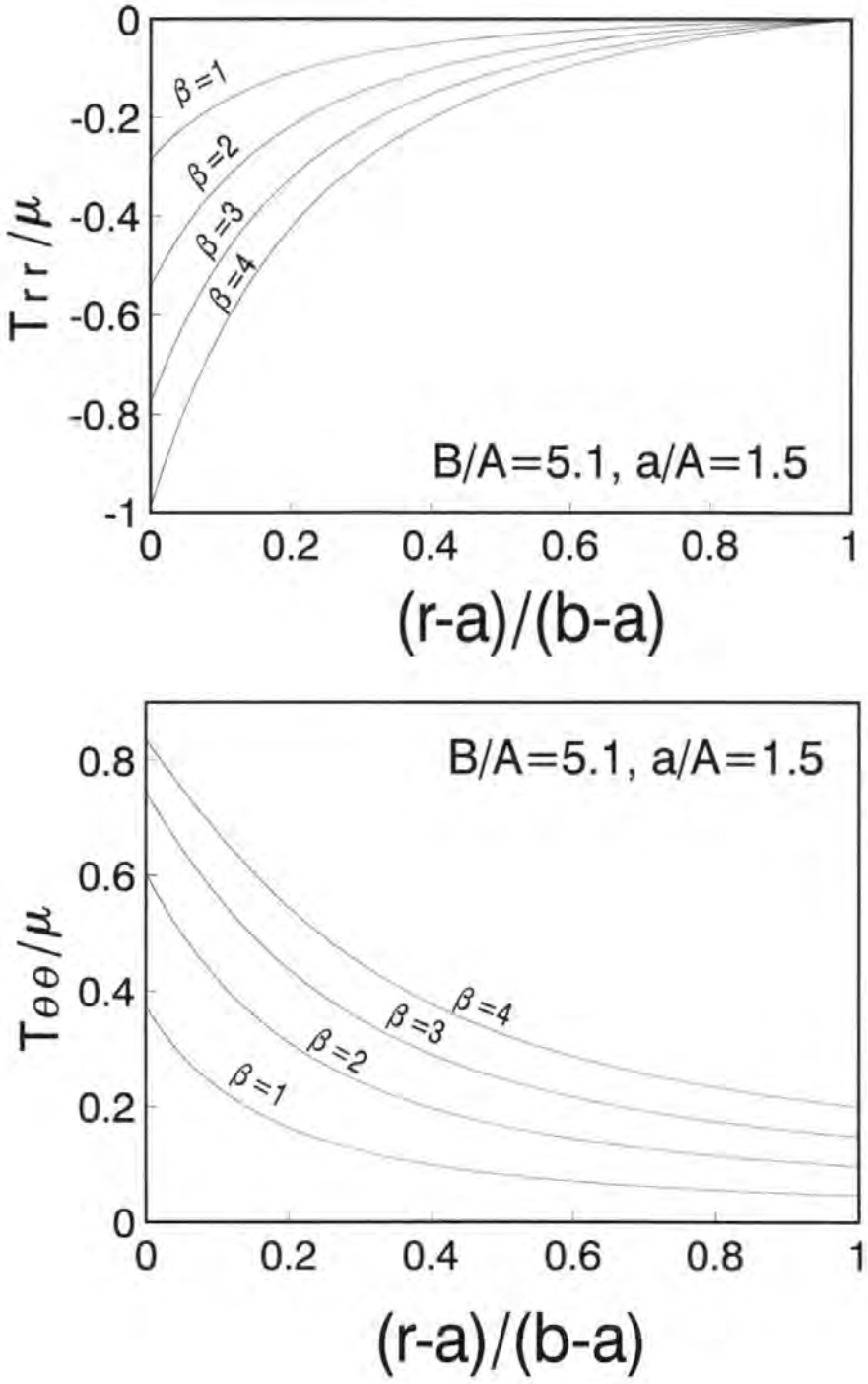

Figure 7.11: $T_{rr}, T_{\theta\theta}$ *vs.* r for a cylindrical shell.

and

$$\frac{\mathrm{d}T_{\theta\theta}}{\mathrm{d}r} = \frac{\mathrm{d}w}{\mathrm{d}r}\mu(1+\frac{P_A}{\mu})w^{\beta}e^{(\beta+1)[g(w_A)-g(w)]}[(1+\beta)g'(w)-\beta/w] < 0 \tag{7.92}$$

(see (7.45), (7.80) and (7.81) for details), we infer that the radial stress T_{rr} is a negative increasing function of r (which belongs to the interval $(-P_A, 0)$); the hoop stress $T_{\theta\theta}$ decreases monotonically from the inner surface to the outer surface of the cylinder and the maximum value of $T_{\theta\theta}$ occurs on the inner surface. These features of T_{rr} and $T_{\theta\theta}$ can be seen from Figure 7.11 also. It is of interest to note from Figure 7.11 that the distributions of Cauchy stresses are similar for all values of $\beta > 0$ and moreover that the greater magnitudes of the Cauchy stresses correspond to the larger values of β. Thus, as before, we can conclude that the metarial becomes harder as β increases.

Chapter 8

Radial spherical expansions

In this chapter we consider radial spherical expansions. The formulation of the problem is presented in Section 8.1 and solutions are given in Section 8.2. The discussion follows in Section 8.3 and Section 8.4.

8.1 Formulation of the problem

We consider the radial expansion of a spherical shell which occupies the domain

$$A \leq R \leq B,\ 0 < \Theta \leq 2\pi,\ 0 < \Phi \leq \pi, \tag{8.1}$$

in the reference configuration. Here, (R, Θ, Φ) are spherical polar coordinates and A, B are the inner and outer radii of the considered spherical shell. The spherical shell is subjected to an internal pressure P_A on its inner surface and an external pressure P_B on its outer surface. We assume that the body preserves its spherical shape after

expansion and that in the deformed configuration the body occupies the region

$$a \leq r \leq b,\ 0 < \theta \leq 2\pi,\ 0 < \phi \leq \pi, \tag{8.2}$$

where (r, θ, ϕ) are spherical polar coordinates and a, b are the deformed inner and outer radii of the considered spherical shell. We consequently seek the deformation of the shell in the form

$$r = r(R) > 0,\ \theta = \Theta,\ \phi = \Phi, \tag{8.3}$$

where the positive function $r(R)$ that is to be determined is assumed to be twice continuously differentiable on $A \leq R \leq B$.

The polar components of the deformation gradient tensor $\mathbf{F}$ associated with (8.3) are given by

$$F_{rr} = \dot{r}(R),\ F_{\theta\theta} = F_{\phi\phi} = r(R)/R,\ F_{r\theta} = F_{\theta r} = F_{r\phi} = F_{\phi r} = F_{\theta\phi} = F_{\phi\theta} = 0 \tag{8.4}$$

where the dot denotes differentiation with respect to the argument. The principal stretches associated with this radial deformation (8.3) are

$$\lambda_r = \dot{r}(R),\ \lambda_\theta = \lambda_\phi = r(R)/R. \tag{8.5}$$

The function $r(R)$ must necessarily satisfy

$$r(R) > 0,\ \dot{r}(R) > 0, \text{ for } A \leq R \leq B. \tag{8.6}$$

We assume that the spherical shell is composed of the generalized Blatz-Ko material, whose strain energy function is given by (3.1). Thus, by using (3.1), (2.29), (8.4) and

(8.5) we obtain the expressions for the Cauchy stress $\mathbf{T}$ as

$$T_{rr} = \mu[1 - (\frac{R}{r})^2(\frac{\mathrm{d}R}{\mathrm{d}r})^{\beta+1}],\ T_{\theta\theta} = T_{\phi\phi} = \mu[1 - (\frac{R}{r})^{\beta+2}\frac{\mathrm{d}R}{\mathrm{d}r}],$$

$$T_{r\theta} = T_{r\phi} = T_{\theta\phi} = 0. \tag{8.7}$$

In view of (8.7) the equilibrium equation reduces to

$$\frac{\mathrm{d}T_{rr}}{\mathrm{d}r} + \frac{2}{r}(T_{rr} - T_{\theta\theta}) = 0 \tag{8.8}$$

which can be expressed as the following second-order ordinary differential equation for $r(R)$:

$$\frac{\beta+1}{2}(\frac{\mathrm{d}R}{\mathrm{d}r})^{\beta-1} \cdot R \cdot \frac{\mathrm{d}^2R}{\mathrm{d}r^2} + (\frac{\mathrm{d}R}{\mathrm{d}r})^{\beta+1} - (\frac{R}{r})^{\beta+1} = 0. \tag{8.9}$$

We prescribe the tractions on surfaces of the considered spherical shell by

$$T_{rr} = -P_A, \text{ at } r = a, \text{ and } T_{rr} = -P_B, \text{ at } r = b, \tag{8.10}$$

in which we assume that

$$P_A \neq P_B. \tag{8.11}$$

8.2 Solution of the problem

The variable substitution of

$$w \equiv \frac{\lambda_r}{\lambda_\theta} = \frac{\lambda_r}{\lambda_\phi} = \frac{R}{r} \cdot \dot{r} > 0, \tag{8.12}$$

proposed by Abeyaratne & Horgan [15, 23] and used in Chapter 6 and Chapter 7 of this thesis, into (8.9) yields the following pair of first-order parametric equations (which are equivalent to (8.9)):

$$(\beta+1)r\frac{\mathrm{d}w}{\mathrm{d}r} = \beta+3-(\beta+1)w-2w^{\beta+1} \tag{8.13}$$

and

$$(\beta+1)R\frac{\mathrm{d}w}{\mathrm{d}R} = w[\beta+3-(\beta+1)w-2w^{\beta+1}]. \tag{8.14}$$

Note that

$$\left.\begin{array}{l} \frac{\mathrm{d}r}{\mathrm{d}w}>0,\ \frac{\mathrm{d}R}{\mathrm{d}w}>0,\ \text{for } 0<w<1, \\ \frac{\mathrm{d}r}{\mathrm{d}w}<0,\ \frac{\mathrm{d}R}{\mathrm{d}w}<0,\ \text{for } w>1. \end{array}\right\} \tag{8.15}$$

By considerations similar to those in Section 7.1, we assume that $w \neq 1$. We first treat the case when the material parameter β is given as an integer ($\beta = n,\ n \geq 1$).

We rewrite (8.13) in the form

$$\frac{\mathrm{d}w}{\beta+3-(\beta+1)w-2w^{\beta+1}} = \frac{\mathrm{d}r}{(\beta+1)r}, \tag{8.16}$$

where $\beta = n$, and from the observation that $(1-w)$ is a factor of the denominator in the left hand side of (8.16), we find that

$$\beta+3-(\beta+1)w-2w^{\beta+1} = (1-w)(\sum_{i=1}^{\beta} 2w^i+\beta+3). \tag{8.17}$$

We seek partial fractions for the coefficient of $\mathrm{d}w$ in (8.16) of the form

$$\frac{a_0}{1-w}+\frac{\sum_{i=1}^{\beta} a_i w^{\beta-i}}{\sum_{i=1}^{\beta} 2w^i+\beta+3}, \tag{8.18}$$

which, from (8.16), (8.17) and (8.18) leads to

$$a_0 = 1/[3(\beta+1)],\ a_i = 2i/[3(\beta+1)],\ i = 1, 2, \cdots, \beta. \tag{8.19}$$

Thus, (8.16) reduces to

$$[\frac{1}{1-w} + \frac{\sum_{i=0}^{\beta-1}(\beta-i)w^i}{\sum_{i=1}^{\beta} w^i + (\beta+3)/2}]\mathrm{d}w = \frac{3\mathrm{d}r}{r}. \tag{8.20}$$

Upon integrating (8.20) we find that

$$r(w) = C_1 e^{\hat{h}(w)/3}|1-w|^{-1/3},\ w > 0,\ w \neq 1 \tag{8.21}$$

where "| |" means the absolute value, C_1 is an integration constant and the function $\hat{h}(w)$ is defined by

$$\hat{h}(w) \equiv \int_0^w \frac{\sum_{i=0}^{\beta-1}(\beta-i)u^i}{\sum_{i=1}^{\beta} u^i + (\beta+3)/2}\mathrm{d}u. \tag{8.22}$$

Note that $\hat{h}(w)$ satisfies

$$\hat{h}(0) = 0;\ \hat{h}'(w) > 0,\ \hat{h}(w) > 0,\ \text{for } w > 0. \tag{8.23}$$

Along similar lines we can find the solution $R(w)$ for (8.14). Thus, by making use of (8.17) - (8.19) we rewrite (8.14) as

$$\{\frac{1}{w(1-w)} + \frac{\sum_{i=0}^{\beta-1}(\beta-i)w^i}{w[\sum_{i=1}^{\beta} w^i + (\beta+3)/2]}\}\mathrm{d}w = \frac{3\mathrm{d}R}{R}, \tag{8.24}$$

and, on assuming a partial fraction decomposition of the coefficient of $\mathrm{d}w$ in the left hand side of (8.24) of the form

$$\frac{1}{1-w} + \frac{1}{w} + \frac{b_0}{w} + \frac{\sum_{i=1}^{\beta} b_i w^{\beta-i}}{\sum_{i=1}^{\beta} w^i + (\beta+3)/2}, \tag{8.25}$$

we find that

$$b_0 = 2\beta/(\beta+3);\ b_i = i - 1 - b_0,\ i = 1, 2, \cdots, \beta. \tag{8.26}$$

Thus, with the help of (8.26), the integration of (8.25) leads to

$$R(w) = C_2 w^{(\beta+1)/(\beta+3)} e^{\hat{h}(w)/3 - (\beta+1)\hat{g}(w)/(\beta+3)} |1-w|^{-1/3},\ w > 0,\ w \neq 1, \tag{8.27}$$

where C_2 is an integration constant and the function $\hat{g}(w)$ is defined by

$$\hat{g}(w) \equiv \int_0^w \frac{\sum_{i=0}^{\beta-1} u^i}{\sum_{i=1}^{\beta} u^i + (\beta+3)/2} \mathrm{d}u. \tag{8.28}$$

Function $\hat{g}(w)$ has the same features as $\hat{h}(w)$, i.e.,

$$\hat{g}(0) = 0;\ \hat{g}'(w) > 0,\ \hat{g}(w) > 0,\ \text{for } w > 0. \tag{8.29}$$

Explicit expressions of $\hat{h}(w)$ and $\hat{g}(w)$ in the case when $\beta = 1$ are

$$\hat{h}(w) = \hat{g}(w) = \ln(w/2 + 1). \tag{8.30}$$

In the case when $\beta = 2$ $\hat{h}(w)$ and $\hat{g}(w)$ are given by

$$\hat{h}(w) = \frac{1}{2}\ln(2w^2 + 2w + 5) + \arctan\frac{(2w+1)}{3} - \frac{1}{2}\ln 5 - \arctan\frac{1}{3}, \tag{8.31}$$

and

$$\hat{g}(w) = \frac{1}{2}\ln(2w^2 + 2w + 5) + \frac{1}{3}\arctan\frac{(2w+1)}{3} - \frac{1}{2}\ln 5 - \frac{1}{3}\arctan\frac{1}{3}, \tag{8.32}$$

which are the same as those obtained previously by Carroll & Horgan [54]. Explicit expressions of $\hat{h}(w)$ and $\hat{g}(w)$ in the case when $\beta = 3, 4$ are given in Table 8.3 and Table 8.4 with approximate constants for simplicity.

β	$\hat{h}(w)$
3	$1.1355 \arctan(.7407w - .2129) + .2797 \ln(w^2 - .5747w + 1.9052)$ $+.4405 \ln(w + 1.5747) - .1422$
4	$.2713 \arctan(1.0603w + 1.18735) + 1.1612 \arctan(.8949w - .5547)$ $+.3372 \ln(w^2 + 2.2396w + 2.1434) + .1628 \ln(w^2 - 1.2396w + 1.6329) + .01489$

Table 8.1: Expressions of $\hat{h}(w)$ when $\beta = 3, 4$.

β	$\hat{g}(w)$
3	$.2839 \arctan(.7407w - .2129) + .3199 \ln(w^2 - .5747w + 1.9052)$ $+.3601 \ln(w + 1.5747) - .3102$
4	$.05426 \arctan(1.0603w + 1.1873) + .2322 \arctan(.8949w - .5547)$ $+.2674 \ln(w^2 + 2.2396w + 2.1434) + .2326 \ln(w^2 - 1.2396w + 1.6329) - .2476$

Table 8.2: Expressions of $\hat{g}(w)$ when $\beta = 3, 4$.

We note that (8.21) with (8.22) and (8.27) with (8.28) provide parametric solutions to the differentiation equation (8.9) in the case when $\beta = n$ (integer), in which two constants C_1, C_2 are to be determined by boundary conditions and the parameter w is within the range of $[w_A, w_B]$. Here $[w_A, w_B]$ are the values of w on the surfaces of the considered spherical shell, that is,

$$R(w_A) = A, \; R(w_B) = B \tag{8.33}$$

which, in view of (8.27), are equivalent to

$$A = C_2\hat{\Phi}(w_A), \; B = C_2\hat{\Phi}(w_B). \tag{8.34}$$

Here, the auxiliary function $\hat{\Phi}(w)$ is defined by

$$\hat{\Phi}(w) = w^{(\beta+1)/(\beta+3)}e^{\hat{h}(w)/3-(\beta+1)\hat{g}(w)/(\beta+3)}|1-w|^{-1/3}. \tag{8.35}$$

From (8.15) and the fact of $w \neq 1$, we find that

$$0 < w_A < w < w_B < 1 \tag{8.36}$$

or

$$1 < w_B < w < w_A. \tag{8.37}$$

The components of the Cauchy stress $T_{rr}, T_{\theta\theta} = T_{\phi\phi}$ can be expressed in terms of w by using (8.7), (8.12), (8.21) and (8.27) as

$$\left.\begin{aligned} T_{rr} &= \mu[1 - w^{-\beta-1}(\tfrac{R}{r})^{\beta+3}] = \mu[1 - (\tfrac{C_2}{C_1})^{\beta+3}e^{-(\beta+1)\hat{g}(w)}], \\ T_{\theta\theta} &= \mu[1 - w^{-1}(\tfrac{R}{r})^{\beta+3}] = \mu[1 - (\tfrac{C_2}{C_1})^{\beta+3}w^{\beta}e^{-(\beta+1)\hat{g}(w)}]. \end{aligned}\right\} \tag{8.38}$$

which, with the help of (8.10), yield

$$\left.\begin{aligned}(1+\tfrac{P_B}{\mu})e^{(\beta+1)\hat{g}(w_B)} &= (\tfrac{C_2}{C_1})^{\beta+3},\\ (1+\tfrac{P_A}{\mu})e^{(\beta+1)\hat{g}(w_A)} &= (\tfrac{C_2}{C_1})^{\beta+3}.\end{aligned}\right\} \tag{8.39}$$

By combining (8.34) with (8.39) we obtain the following equations for the determination of the unknown constants w_A, w_B, C_1, C_2:

$$B\hat{\Phi}(w_A) = A\hat{\Phi}(w_B), \tag{8.40}$$

$$\hat{g}(w_B) = \hat{g}(w_A) + \frac{1}{\beta+1}\ln\left(\frac{1+P_A/\mu}{1+P_B/\mu}\right), \tag{8.41}$$

$$C_2 = A/\hat{\Phi}(w_A), \tag{8.42}$$

$$C_1 = C_2(1+P_A/\mu)^{-1/(\beta+3)}e^{-(\beta+1)\hat{g}(w_A)/(\beta+3)}. \tag{8.43}$$

Note that (8.40) and (8.41) are simultaneous equations to determine w_A and w_B once P_A, P_B and B/A are given and that C_1, C_2 can be then found from (8.42) and (8.43) easily afterwards. The inspection of (8.36), (8.37), (8.29) and (8.41) reveals that

$$\begin{aligned}&0 < w_A < w < w_B < 1, \text{ for } P_A > P_B,\\ &1 < w_B < w < w_A, \text{ for } P_A < P_B.\end{aligned} \tag{8.44}$$

On substituting (8.39) into (8.38) the components of the Cauchy stress can now be rewritten as

$$\left.\begin{aligned}T_{rr} &= \mu\{1-(1+\tfrac{P_A}{\mu})e^{(\beta+1)[\hat{g}(w_A)-\hat{g}(w)]}\},\\ T_{\theta\theta} &= \mu\{1-(1+\tfrac{P_A}{\mu})w^{\beta}e^{(\beta+1)[\hat{g}(w_A)-\hat{g}(w)]}\}.\end{aligned}\right\} \tag{8.45}$$

From (8.21) and (8.27) we find the following expressions for the principal stretches λ_i:

$$\lambda_r = w^{2/(\beta+3)}(1+P_A/\mu)^{-1/(\beta+3)}e^{(1+\beta)[\hat{g}(w)-\hat{g}(w_A)]/(\beta+3)}, \tag{8.46}$$

$$\lambda_\theta = \lambda_\phi = w^{-(1+\beta)/(3+\beta)}(1+P_A/\mu)^{-1/(3+\beta)}e^{(1+\beta)[\hat{g}(w)-\hat{g}(w_A)]/(3+\beta)}. \tag{8.47}$$

With the help of (8.28), (8.46) and (8.47) it is readily to verify that

$$\frac{\mathrm{d}\lambda_r}{\mathrm{d}w} > 0, \ \frac{\mathrm{d}\lambda_\theta}{\mathrm{d}w} < 0, \tag{8.48}$$

which indicate that the principal stretches vary monotonically along the r-axis. From (8.7), (8.10) and (8.12) the ratio of the deformed inner radius a to the undeformed inner radius A is given by

$$\frac{a}{A} = w_A^{-(\beta+1)/(\beta+3)}(1 + P_A/\mu)^{-/(\beta+3)} \tag{8.49}$$

which is also the value of the hoop stretch λ_θ at $r = a$ (see (8.47)).

Along similar lines, we can find exact solutions for (8.13) and (8.14) in the case when the material parameter β is given as a fraction. For example, when $\beta = 1/2$ we find that

$$r(w) = C_1 e^{\hat{H}(w^{1/2})/3}|1 - w^{1/2}|^{-1/3}, \ w > 0, \ w \neq 1 \tag{8.50}$$

and

$$R(w) = C_2 w^{3/7} e^{\hat{H}(w^{1/2})/3 - 3\hat{G}(w^{1/2})/7}|1 - w^{1/2}|^{-1/3}, \ w > 0, \ w \neq 1, \tag{8.51}$$

where C_1, C_2 are integration constants and functions $\hat{H}(w), \hat{G}(w)$ are defined by

$$\hat{H}(w) = \frac{1}{2}\ln\left(\frac{4}{7}w^2 + w + 1\right) - \sqrt{7}\arctan\frac{\sqrt{7}(8w+7)}{21} + \sqrt{7}\arctan\frac{\sqrt{7}}{3} \tag{8.52}$$

and

$$\hat{G}(w) = \ln\left(\frac{4}{7}w^2 + w + 1\right) - \frac{2\sqrt{7}}{3}\arctan\frac{\sqrt{7}(8w+7)}{21} + \frac{2\sqrt{7}}{3}\arctan\frac{\sqrt{7}}{3} \tag{8.53}$$

respectively.

By comparing this section with Section 7.2 we note that the equations obtained here for the spherical expansion are similar to those obtained in Section 7.2 for the cylindrical expansion.

8.3 Discussions on radial expansion of a spherical cavity in an infinite medium

In this section we assume that $B \to \infty$ and replace the boundary conditions (8.10) with

$$T_{rr} = -P_A, \text{ at } r = a, \text{ and } T_{rr} \to -P_B, \text{ as } r \to \infty. \tag{8.54}$$

Since $w \to 1$ as $r \to \infty$, we have $w_B = 1$ in this case. Hence, equations used to determine the unknown constants C_1, C_2 and w_A in (8.21) and (8.27) are therefore (8.41), (8.42) and (8.43) but with $w_B = 1$. If (8.41) can be solved for a w_A such that

$$\begin{aligned} &0 < w_A < 1, \text{ for } P_A > P_B, \\ &w_A > 1, \text{ for } P_A < P_B, \end{aligned} \tag{8.55}$$

then, (8.42) and (8.43) should provide positive constants C_1, C_2, which ensure that the parametric solutions (8.21) and (8.27) are positive.

In order to verify the solvability of (8.41), we observe that the auxiliary function $\hat{F}(w)$, defined by

$$\hat{F}(w) \equiv \hat{g}(w) - \hat{g}(1) - \frac{1}{\beta + 1} \ln\left(\frac{1 + P_B/\mu}{1 + P_A/\mu}\right), \tag{8.56}$$

is monotonically increasing due to the fact that $\hat{F}'(w) > 0$. It follows that (8.41) can be solved for a unique root w_A, such that

$$0 < w_A < 1, \text{ if } P_B < P_A < \hat{P}_{max} \equiv \mu[(1 + P_B/\mu)e^{(1+\beta)\hat{g}(1)} - 1],$$

$$w_A > 1, \text{ if } P_A < P_B \tag{8.57}$$

where $\hat{P}_{max}$ is an increasing function of the external pressure P_B. In view of the monotonic character of function $\hat{F}(w)$ and $\hat{g}(w)$ we also find that: (i) w_A, which is the value of the parameter w at the wall of the cavity and is given by (8.41), tends to unity as P_A tends to P_B and (ii) for any prescribed positive value P_B, when $P_A \to \hat{P}_{max}$, we have that $w_A \to 0$, the deformed inner radius $a \to \infty$ and the hoop stress $T_{\theta\theta}$ on the inner surface ($r = a$) tends to μ.

The differentiation of $(8.45)_1$ (with $w_B = 1$) with respect to r yields

$$\frac{\mathrm{d}T_{rr}}{\mathrm{d}r} = \frac{\mathrm{d}w}{\mathrm{d}r}\mu(1+\beta)(1+\frac{P_A}{\mu})\hat{g}'(w)e^{(\beta+1)[\hat{g}(w_A)-\hat{g}(w)]} \tag{8.58}$$

which indicates that

$$\frac{\mathrm{d}T_{rr}}{\mathrm{d}r} > 0, \text{ for } P_B < P_A < \hat{P}_{max},$$
$$\frac{\mathrm{d}T_{rr}}{\mathrm{d}r} < 0, \text{ for } P_A < P_B. \tag{8.59}$$

Consequently, the radial stress T_{rr} increases monotonically from $-P_A$ along the r-axis and tends to $-P_B$ as $r \to \infty$ when $P_B < P_A < \hat{P}_{max}$; but it decreases monotonically from $-P_A$ along the r-axis and tends to $-P_B$ when $r \to \infty$ for $P_A < P_B$.

The derivative of the hoop stress $T_{\theta\theta}$ with respect to r (see $(8.45)_2$) is

$$\frac{\mathrm{d}T_{\theta\theta}}{\mathrm{d}r} = \frac{\mathrm{d}w}{\mathrm{d}r}\mu(1+\frac{P_A}{\mu})w^{\beta}e^{(\beta+1)[\hat{g}(w_A)-\hat{g}(w)]}[(1+\beta)\hat{g}'(w) - \beta/w]. \tag{8.60}$$

Introducing

$$\hat{\sigma}(w) \equiv [(1+\beta)w\hat{g}'(w) - \beta][\sum_{i=1}^{\beta} w^i + (\beta+3)/2] \tag{8.61}$$

and with the help of (8.28) we find that

$$\frac{\mathrm{d}\hat{\sigma}}{\mathrm{d}w} > 0,\ \hat{\sigma}(0) = -(3+\beta)\beta/2 < 0,\ \hat{\sigma}(1) = -(1+\beta)\beta/2 < 0. \tag{8.62}$$

In view of (8.44), (8.60) and (8.62), we find that when P_A is given such that $P_B < P_A < \hat{P}_{max}$, we have $\mathrm{d}T_{\theta\theta}/\mathrm{d}r < 0$. Thus the hoop stress $T_{\theta\theta}$ attains its maximum value on the cavity wall $r = a$, and this is given by

$$(T_{\theta\theta})_{max} = \mu[1 - (1 + \frac{P_A}{\mu})w_A^{\beta}]. \tag{8.63}$$

$T_{\theta\theta}$ then decreases monotonically with r and tends to $-P_B$ as $r \to \infty$ $(w \to 1)$. The equations (8.44), (8.60) and (8.62) also show that when P_A, P_B are given such that $P_A < P_B$, there exists a certain value $w_0 > 1$ such that at $w = w_0$ we have

$$\frac{\mathrm{d}T_{\theta\theta}}{\mathrm{d}w}(w_0) = 0, \text{ for } P_A < P_B, \tag{8.64}$$

and

$$\frac{\mathrm{d}T_{\theta\theta}}{\mathrm{d}r}(w - w_0) < 0,\ w > 1. \tag{8.65}$$

It is easy to verify that $w_0 = 2$ when $\beta = 1$, $w_0 = (\sqrt{21} - 1)/2$ if $\beta = 2$ and *etc.*, so we conjecture that w_0 is a decreasing function of β. Thus, when $w > w_0$, which is equivalent to $r < r(w_0)$, $T_{\theta\theta}$ increases monotonically along r and attains its maximum value at $w = w_0$ $(r = r(w_0))$, it then decreases monotonically with r for $1 < w < w_0$

(i.e., $r > r(w_0)$). Note that this is true only if the value w_A, determined by the prescribed values P_A, P_B, is such that $w_A > w_0$. Otherwise, if P_A, P_B are prescribed such that $P_A < P_B$ and the resultant value w_A of w is less than w_0, $T_{\theta\theta}$ will start from its maximum value at $r = a$, the wall of the cavity, and decrease monotonically along the r-axis.

Now we turn to analyzing the strong ellipticity for the solution with the boundary condition of traction. In view of (8.12) the strong ellipticity condition (3.5) reduces to

$$t_E < w < 1/t_E \tag{8.66}$$

where $t_E \in (0,1)$ is a critical value determined by (3.6). Since we have either $w > 1$ or $0 < w < 1$ in our present solutions, it follows that when the pressures P_A, P_B are prescribed such that $P_A > P_B$ (i.e. $0 < w < 1$), the right hand side of the inequality (8.66) holds always, whereas the left hand side of the inequality may be violated for certain boundary values. When P_A, P_B are given such that $P_A < P_B$ (i.e. $w > 1$), the opposite of the above situation holds true.

In view of the monotonic increasing (decreasing) character of w with r when $w_A < w < 1$ (or $1 < w < w_A$; see (8.15)), it follows that the strong ellipticity is first lost at $r(w_A) = a$ and moreover, that it occurs when $w_A = t_E$ for $P_B < P_A < \hat{P}_{max}$ or $w_A = 1/t_E$ for $P_A < P_B$, which impose the following restrictions upon the pressures P_A and P_B

$$\begin{aligned} &P_A < P_B < \hat{P}_E^B \equiv \mu\{(1 + P_A/\mu)e^{(1+\beta)[\hat{g}(1/t_E)-\hat{g}(1)]} - 1\}, \\ &P_B < P_A < \hat{P}_E^A \equiv \mu\{(1 + P_B/\mu)e^{(1+\beta)[\hat{g}(1)-\hat{g}(t_E)]} - 1\}. \end{aligned} \tag{8.67}$$

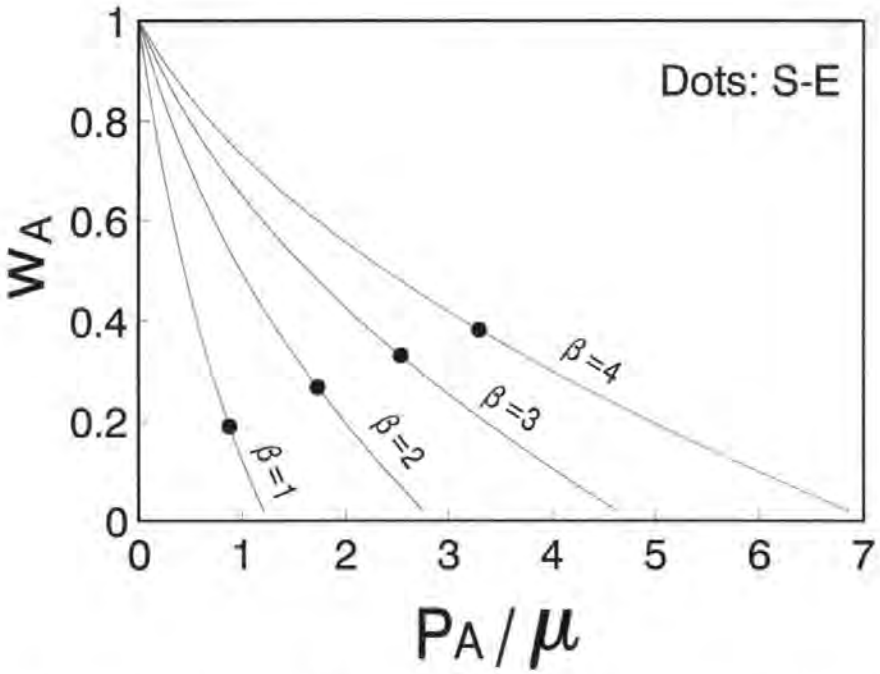

Figure 8.1: w_A *vs.* P_A for a spherical cavity in an infinite medium.

Comparison of $\hat{P}_E^A$ with $\hat{P}_{max}$ reveals that $\hat{P}_E^A$ is less than $\hat{P}_{max}$. It is also of interest to note that $\hat{P}_E^A$ is a linear function of P_B/μ, $\hat{P}_E^B$ is a linear function of P_A/μ and the coefficients of the linear equations are functions of the material parameter β only, which are shown to be increasing functions of β by numerical experiments.

When the external pressure P_B is given to be zero, which represents an internally pressurized spherical cavity in an infinite medium, the plot of w_A *vs.* P_A is illustrated in Figure 8.1, where dots correspond to values of $\hat{P}_E^B$ and the graphs are interrupted at $\hat{P}_{max}$. As before, we can see that w_A decreases with P_A and tends to zero when P_A tends to $\hat{P}_{max}$ and moreover that, both $\hat{P}_E^A$ and $\hat{P}_{max}$ increase with the parameter β. The principal stretches at $r = a$, regarded as a function of P_A, are plotted in Figure 8.2. Here the dots indicate the values of $\hat{P}_E^B$. Recalling from (8.46) to (8.48) that λ_θ

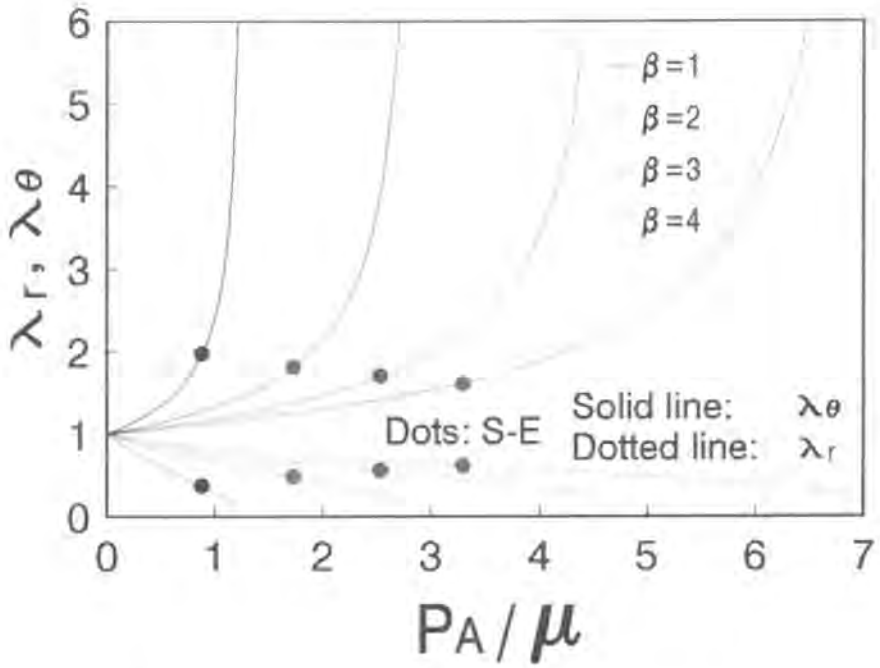

Figure 8.2: $\lambda_r(a), \lambda_\theta(a)$ *vs.* P_A for a spherical cavity in an infinite medium.

attains its maximum value at $r = a$ and λ_r attains its minimum value at $r = a$, we find from Figure 8.2 that $\lambda_\theta(a)$ increases with P_A (for fixed β) and with β (for fixed P_A); whereas $\lambda_r(a)$ decreases with P_A and β. We note that the values of the principal stretch $\lambda_\theta(a)$, beyond which the strong-ellipticity condition will be violated, are within the range $[1.58, 1.98]$ when β is given by $\beta = 1, 2, 3, 4$, which are less than those obtained previously from the radial expansion of an internally pressurized cylindrical cavity (see Figure 7.3).

When the internal pressure P_A is assumed to be zero, we have an externally pressurized spherical cavity in an infinite medium. The plot of w_A *vs.* P_B (with $P_A = 0$) is given in Figure 8.3, where the dots represent the values P_E^B. It can be seen from the diagram that for any prescribed value P_B, there always exists a corresponding value

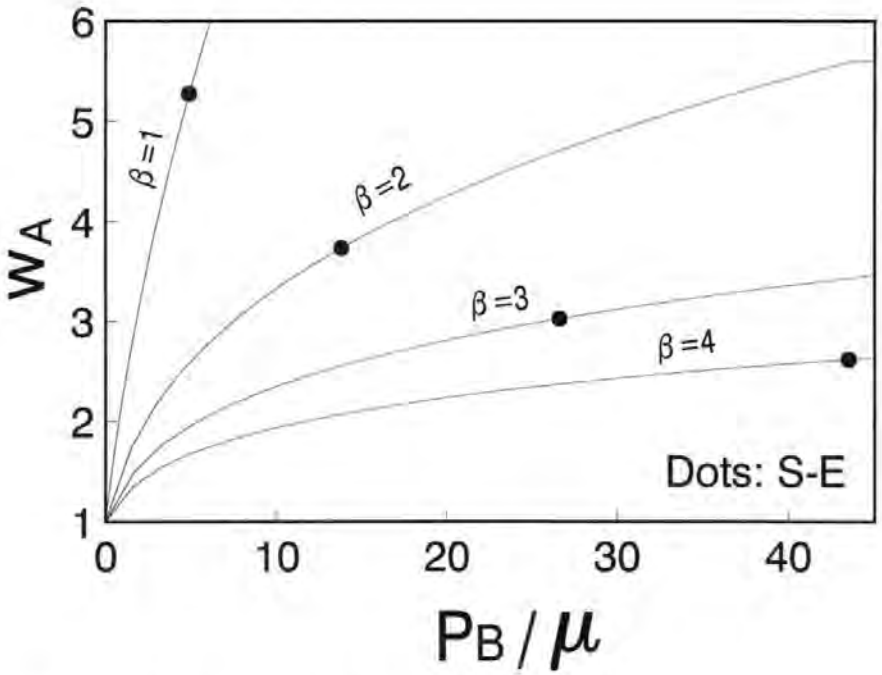

Figure 8.3: w_A *vs.* P_B for a spherical cavity in an infinite medium.

w_A. But when P_B is given such that $P_B > \hat{P}_E^B$, where $\hat{P}_E^B$ is the pressure corresponding to that $w_A = t_E$, the strong-ellipticity condition will be violated. In view of (8.46)-(8.48) we conclude that for an externally pressurized spherical cavity, the hoop stretch λ_θ has its minimum value $w_A^{-(1+\beta)/(3+\beta)} < 1$ at $r = a$ and then increases monotonically with r and tends to its maximum value $(1 + P_B/\mu)^{-1/(3+\beta)} < 1$ as $r \to \infty$; the radial stretch λ_r decreases from its maximum value $w_A^{1/(3+\beta)} > 1$, at $r = a$, and tends to its minimum value $(1+P_B/\mu)^{-1/(3+\beta)} < 1$ as $r \to \infty$. From the plot of $\lambda_r(a), \lambda_\theta(a)$ *vs.* $\hat{P}_B$, see Figure 8.4, where dots stand for the values of P_E^B, we find that the values of $\lambda_r(a)$, beyond which the strong-ellipticity condition no longer holds, are within the range of $[1.32, 2.30]$ when β is given by $\beta = 1, 2, 3, 4$ and the values of λ_θ, beyond which the strong ellipticity no longer holds, are within the range of $[0.44, .50]$ for $\beta = 1, 2, 3, 4$.

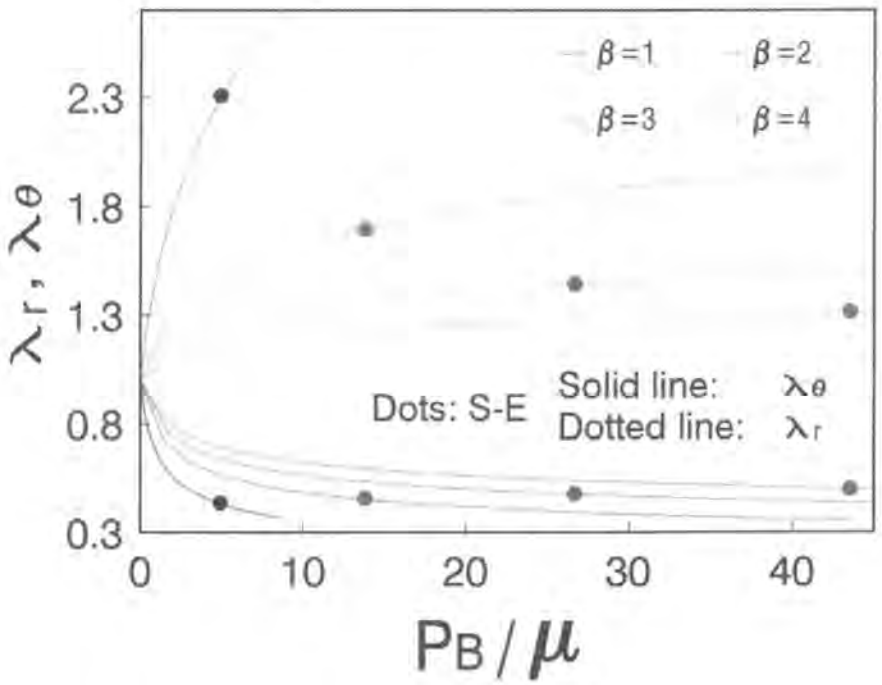

Figure 8.4: $\lambda_r(a), \lambda_\theta(a)$ *vs.* P_B for a spherical cavity in an infinite medium.

8.4 Discussions on the expansion of an internally pressurized spherical shell

In this section, we examine our solutions (8.21) and (8.27) for the radial expansion of an internally pressurized spherical shell. Here the inner and outer radii A, B are given as positive constants (see (8.1)) and the outer surface of the considered shell is assumed to be free of traction ($P_B = 0$) whereas the inner surface is subjected to a prescribed pressure $P_A > 0$ (see (8.10)). Therefore, once B/A and P_A are given, the unknown constants w_A, w_B, C_1 and C_2 in (8.21) and (8.27) can be determined from (8.40)-(8.43) with $P_B = 0$. Note that we can solve the simultaneous equations (8.40) and (8.41) only

numerically and according to (8.44) we have

$$0 < w_A < w < w_B < 1. \tag{8.68}$$

We plot the numerical results of w_A, w_B *vs.* P_A in Figure 8.5 and Figure 8.6, where B/A is given as $B/A = 2$ and $B/A = 10$ respectively. It can be seen from Figure 8.5 and Figure 8.6 that there exists a maximum value of the internal pressure P_A, namely $\hat{P}_{max}$, which is an increasing function of β and B/A. If the pressure P_A is given such that $P_A > \hat{P}_{max}$ there are no solutions to this spherical expansion problem. Otherwise if P_A is prescribed as $P_A < \hat{P}_{max}$ we have two solutions to this boundary-value problem. We use dotted lines and solid lines to represent the two solutions shown in Figure 8.5 and Figure 8.6. For each of the two solutions, $w_A < w_B$ holds, which can also be verified by (8.41). w_A and w_B decrease with P_A for the solid lines' solutions but increase with P_A for the dotted lines' ones. In order to distinguish between the two possibilities we plot a/A *vs.* P_A in Figure 8.7 and $T_{\theta\theta}(a)$ *vs.* P_A in Figure 8.8. For physically realistic solutions, we expect that the inner radius a and $T_{\theta\theta}(a)$ will be increasing functions of the pressure P_A. Examination of Figure 8.7 and Figure 8.8 reveals that the solid lines' solutions behave according to this expectation. In contrast, for the dotted lines' solutions, a/A increases as P_A decreases and tends to infinity when P_A tends to zero (see Figure 8.7). Also for these solutions, $T_{\theta\theta}(a)$ decreases with P_A and tends to μ when P_A tends to zero (Figure 8.8). Such kind of behaviour appears to be physically unrealistic and therefore, on these physical grounds, we can reject the dotted lines' solutions. The discussion which follows will be confined accordingly to the solid lines'

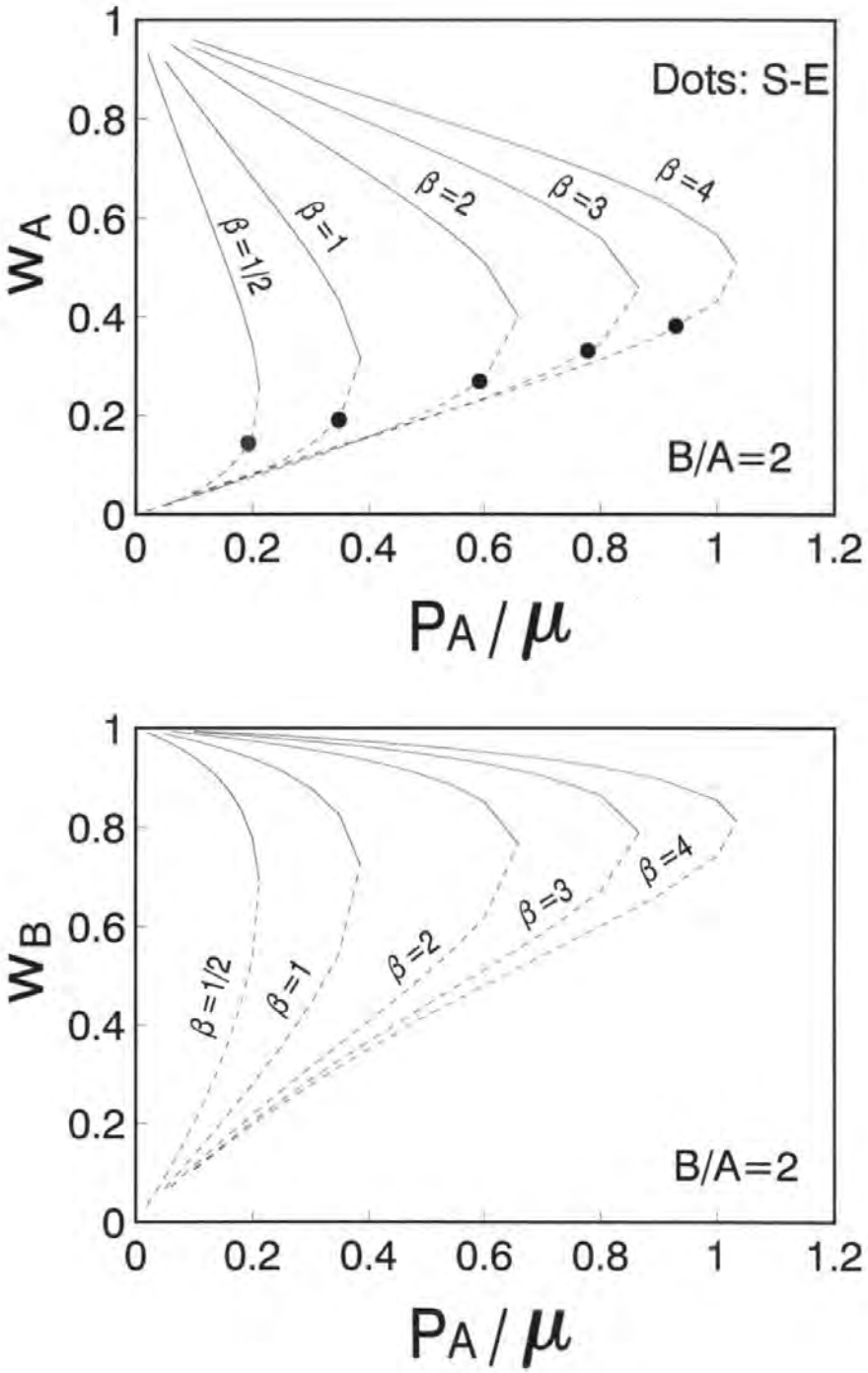

Figure 8.5: w_A, w_B *vs.* P_A for a spherical shell with $B/A = 2$.

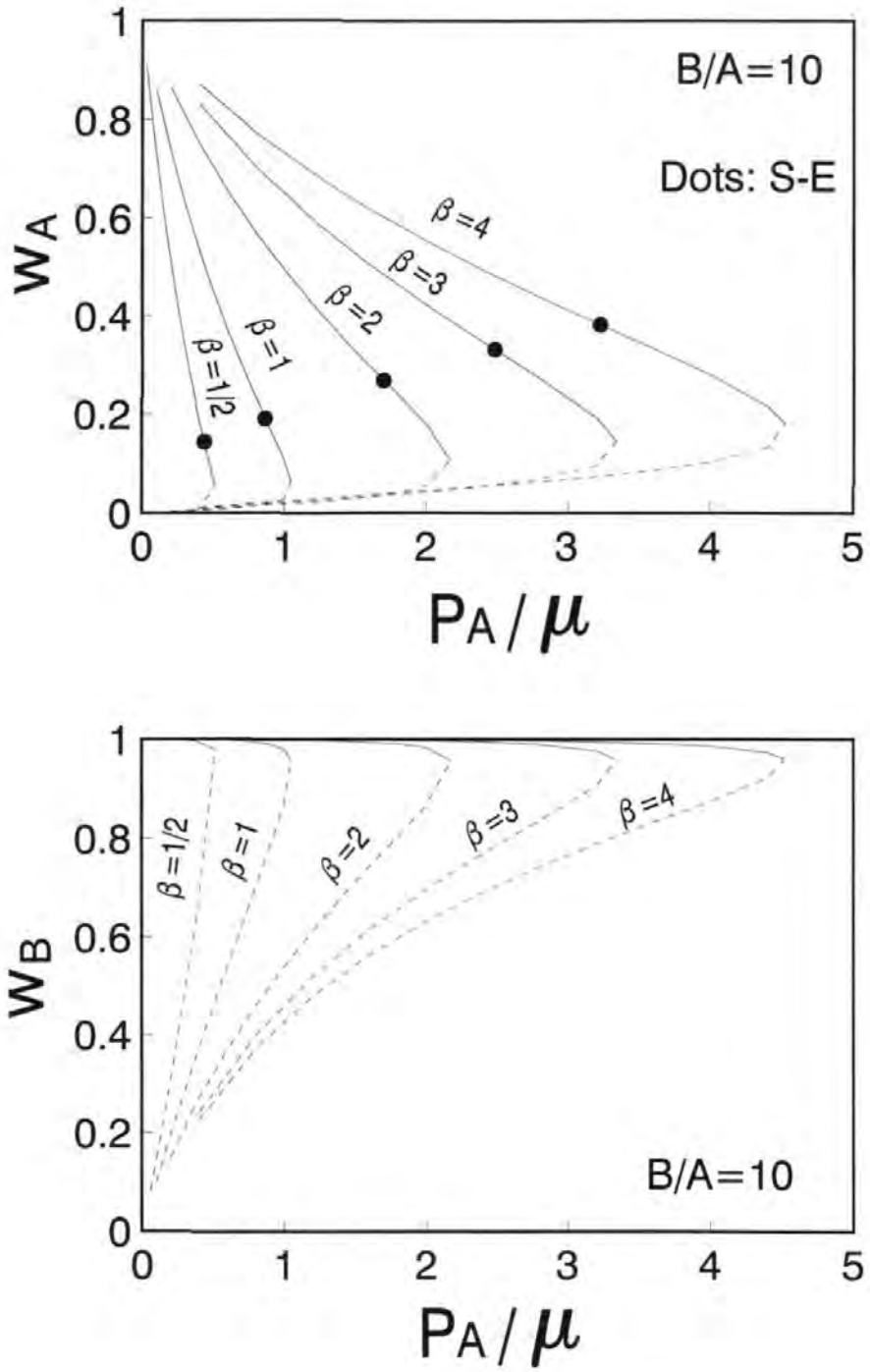

Figure 8.6: w_A, w_B *vs.* P_A for a spherical shell with $B/A = 10$.

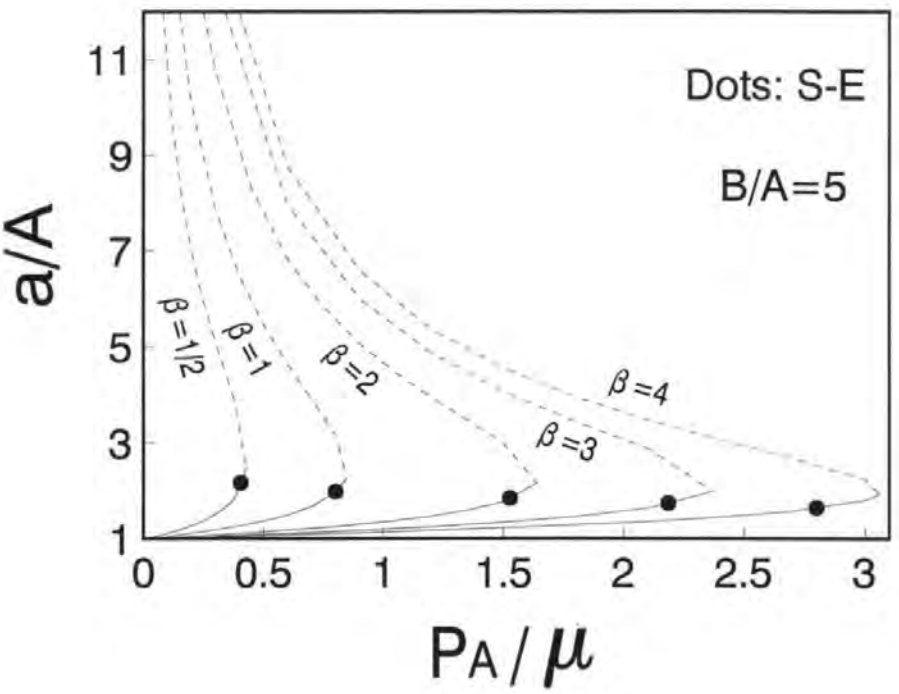

Figure 8.7: a/A *vs.* P_A for a spherical shell with $B/A = 5$.

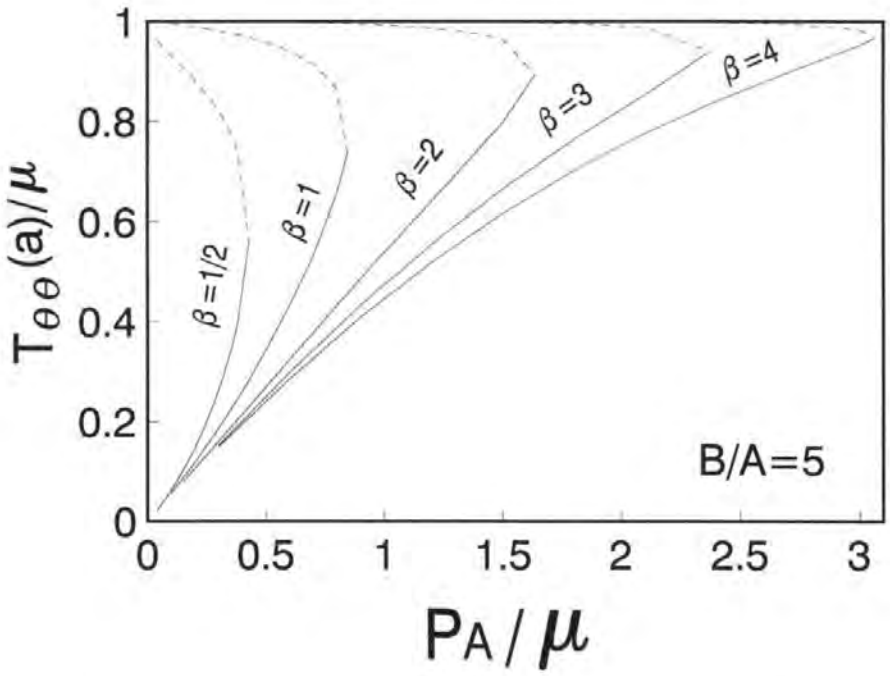

Figure 8.8: $T_{\theta\theta}(a)$ *vs.* P_A for a spherical shell with $B/A = 5$.

solutions.

Since we have $w < 1$ for the present problem (see (8.68)), the right hand side inequality in (8.66) is satisfied for any given boundary values, but the left hand side inequality in (8.66) may be violated for certain boundary values. We recall that (8.66) is the strong-ellipticity condition for the material. By virtue of the monotonic increase of w with r (see (8.15)), it follows that the strong-ellipticity is first lost at $r = a$ and occurs when $w_A = t_E$ and that the corresponding values of P_A, say $\hat{P}_E$, can then be found by (8.41), which are represented by dots in Figure 8.5 to Figure 8.7. In Figure 8.9 we plot w_A and a/A *vs.* P_A when B/A is prescribed within the range of $[1.1, 100]$ and when β is fixed as $\beta = 3$ (The results for different values of β are similar). Here the dots correspond to the values of $\hat{P}_E$. When B/A is given as $B/A = 2$, for example, the value w_A is greater than t_E and, therefore, for any prescribed value $P_A < \hat{P}_{max}$ the strong-ellipticity condition holds. On the other hand, when B/A is given as $B/A = 10$, the value w_A is greater than t_E only if P_A is given as $P_A < \hat{P}_E$ $(< \hat{P}_{max})$. Thus, according to the numerical examination we conclude that when the thickness of a spherical shell is less than a certain value, namely $(B/A)_E$, the strong-ellipticity condition holds for any prescribed value $P_A < \hat{P}_{max}$. However, when the thickness of the considered spherical shell exceeds this value, i.e., $B/A > (B/A)_E$, the strong-ellipticity condition holds only if the internal pressure P_A is prescribed such as $P_A < \hat{P}_E < \hat{P}_{max}$. The value of $(B/A)_E$ is approximately 3.54 when $\beta = 3$ and 3.25 when $\beta = 2$. The latter was previously obtained by Chung [16]. Comparing the values of $(B/A)_E$ in this spherical expansion

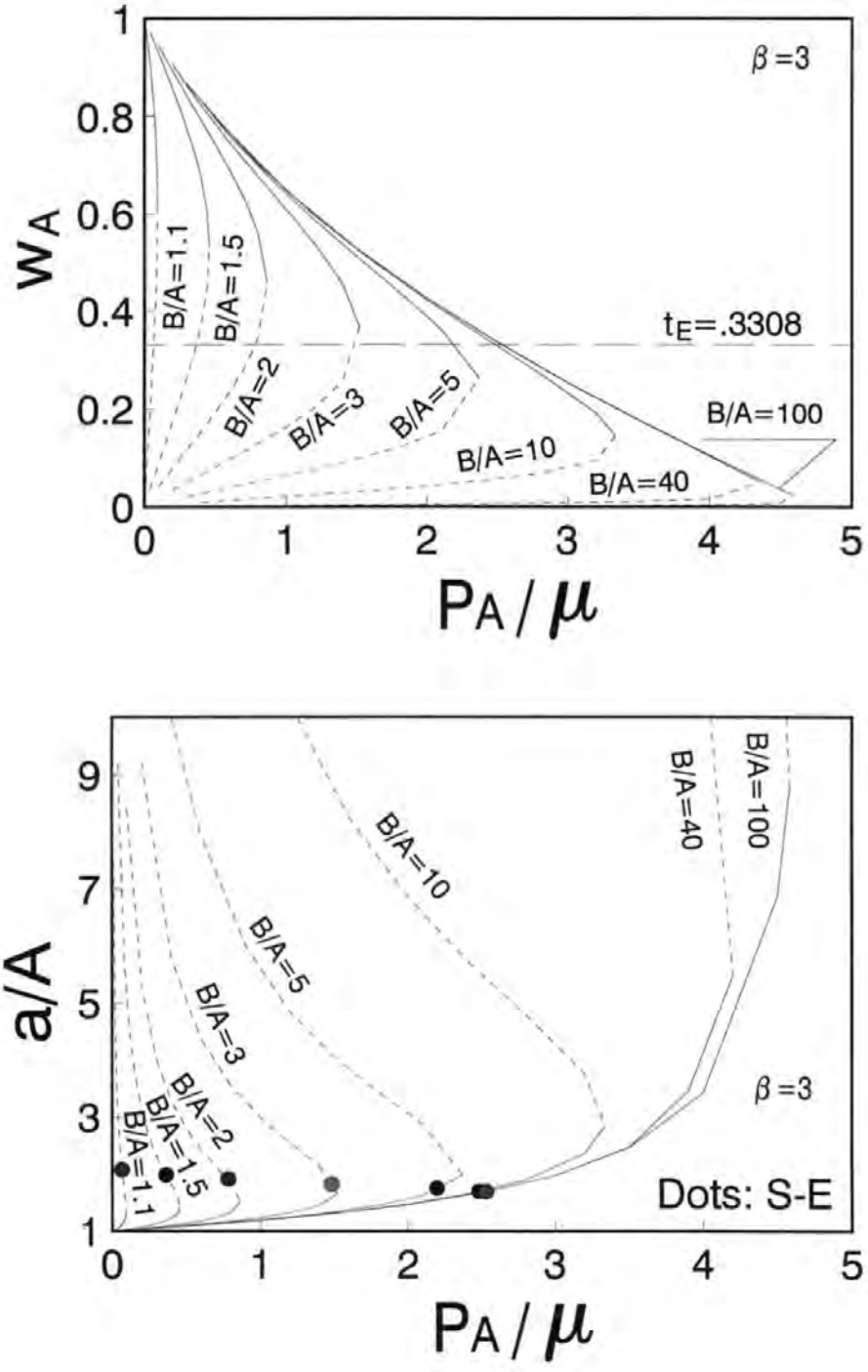

Figure 8.9: $w_A, a/A$ *vs.* P_A for a spherical shell with $\beta = 1$.

with those in the case of cylindrical expansion (see Section 7.4) we find that the values of $(B/A)_E$ in this spherical expansion are smaller.

With the help of (8.41) and the fact that $P_B = 0$, the principal stretch λ_r given by (8.46) can be rewritten as

$$\lambda_r = w^{2/(3+\beta)} e^{(1+\beta)[\hat{g}(w)-\hat{g}(w_B)]/(3+\beta)} \tag{8.69}$$

which, in view of (8.29) and the fact that $0 < w < 1$, induces the conclusion that $\lambda_r < 1$. Thus, from (8.48) we find that the minimum value of λ_r and the maximum value of λ_θ occur at $r = a$. Numerical examinations on $\lambda_r(a)$, which is obtained by substituting w in (8.46) with w_A, and of $\lambda_\theta(a)$, which equals to a/A, reveal that the values of the principal stretch $\lambda_\theta(a) = a/A$, beyond which the strong-ellipticity condition no longer holds are within the range $[1.6, 2.0]$, which is smaller than those obtained from the radial expansion of an internally pressurized cylindrical shell.

Because of

$$\frac{\mathrm{d}T_{rr}}{\mathrm{d}r} = \frac{\mathrm{d}w}{\mathrm{d}r}\mu(1+\beta)(1+\frac{P_A}{\mu})g'(w)e^{(\beta+1)[\hat{g}(w_A)-\hat{g}(w)]} > 0 \tag{8.70}$$

and

$$\frac{\mathrm{d}T_{\theta\theta}}{\mathrm{d}r} = \frac{\mathrm{d}w}{\mathrm{d}r}\mu(1+\frac{P_A}{\mu})w^\beta e^{(\beta+1)[\hat{g}(w_A)-\hat{g}(w)]}[(1+\beta)\hat{g}'(w) - \beta/w] < 0 \tag{8.71}$$

(see (8.45), (8.61) and (8.62) for details), we infer that the radial stress T_{rr} is a negative, steadily increasing function of r, within the range of $(-P_A, 0)$; the hoop stress $T_{\theta\theta}$ decreases monotonically from the inner surface to the outer surface and the maximum value of $T_{\theta\theta}$ occurs on the inner surface. These features of T_{rr} and $T_{\theta\theta}$ can be seen

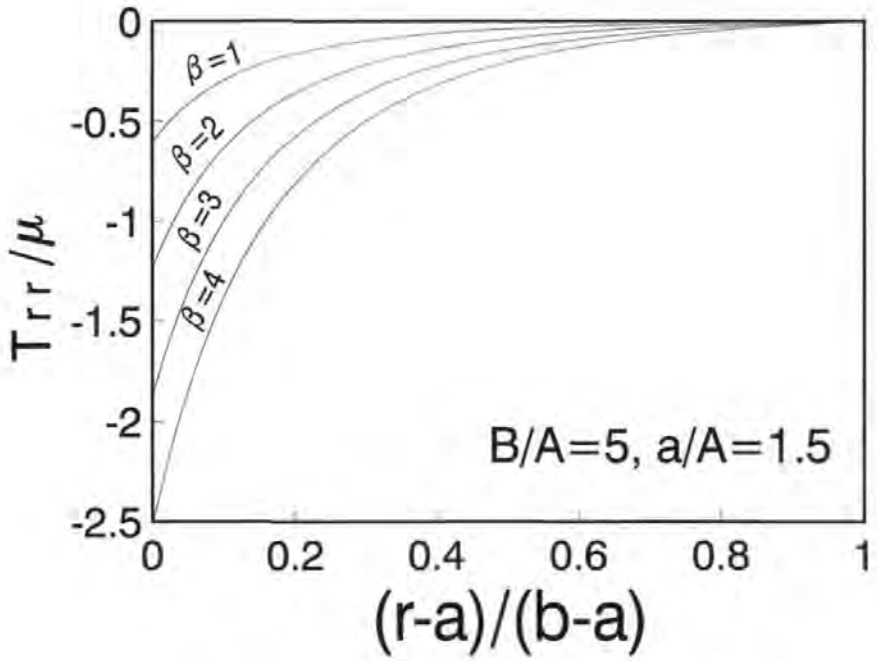

Figure 8.10: T_{rr} *vs.* r for a spherical shell.

from Figure 8.10 and Figure 8.11 also. It is of interest to note from Figure 8.10 and Figure 8.11 that the Cauchy stresses change faster as β increases and otherwise, the distributions of the Cauchy stresses are similar to each other for different values of β. From the previous work on the other non-homogeneous deformations considered in this thesis, we have drawn the conclusion that the material hardens as the material parameter β increases. It can be seen that this conclusion is valid for the present deformation also since for a fixed value P_A, the greater magnitudes of T_{rr} and $T_{\theta\theta}$ are corresponding to the larger values of β (see Figure 8.10 and Figure 8.11).

It is interesting to analyze the response of very thin spherical shells (balloons). By making use of Willson & Myers' results [37] which are valid for all isotropic compressible materials, we find that for the generalized Blatz-Ko material the asymptotic relation

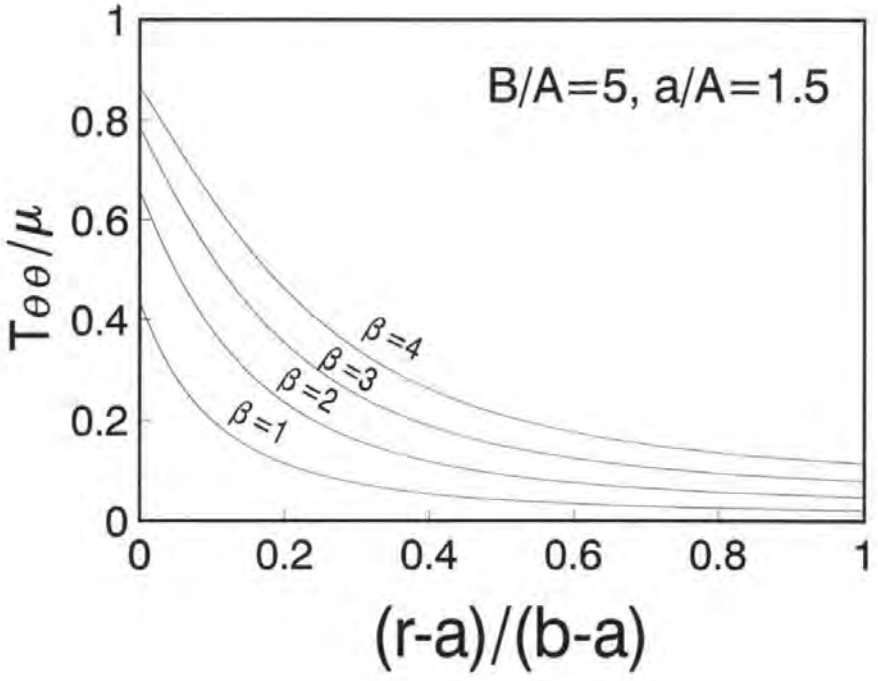

Figure 8.11: $T_{\theta\theta}$ *vs.* r for a spherical shell.

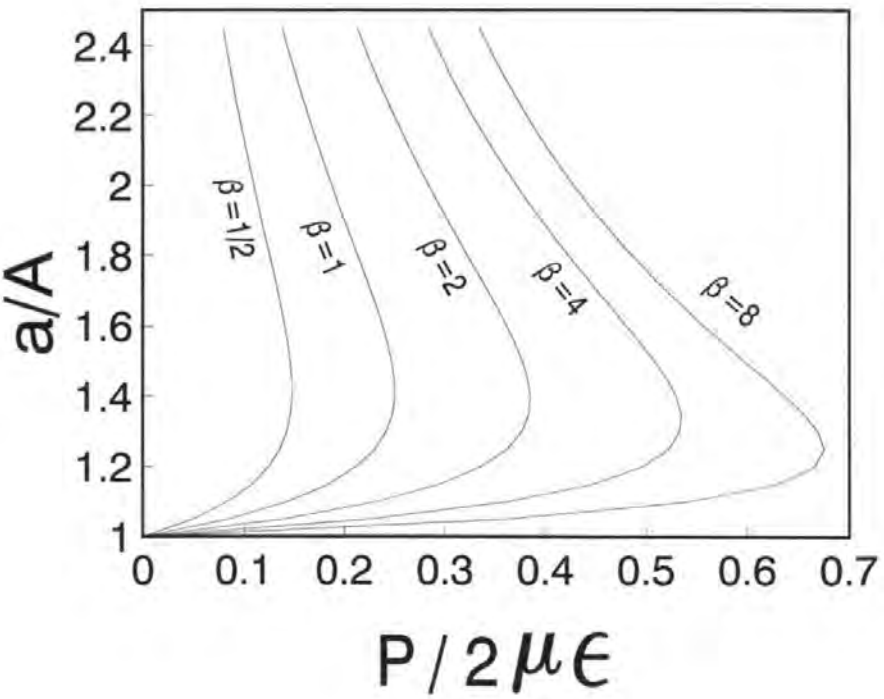

Figure 8.12: Balloon

between applied pressure and deformed radius of thin-wall spherical shells reduces to

$$P_A = 2\mu\epsilon(\alpha - \alpha^{\beta+1}) \tag{8.72}$$

in which $\epsilon = (B - A)/A$ and α is given by

$$\alpha = (\frac{A}{a})^{(\beta+3)/(\beta+1)}. \tag{8.73}$$

The plot of pressure-radius relations when $\beta = 1/2, 1, 2, 3, 4$ is given in Figure 8.12. Note that each curve in the plot (which is very similar to the plot in Figure 8.9 obtained without this simplifying assumption) has only one turning point, and it does not admit a pressure at which the balloon bursts (as observed by Chung *et al.* , Murphy [28], and Beatty [14] for the Blatz-Ko material). Clearly a larger pressure is needed to produce the same deformation as β increases.

Chapter 9

Conclusions

In this dissertation we have investigated the mechanical features of the materials (1.13) with $\beta \neq 2$ and comparison has been made with the mechanical features of the Blatz-Ko material. This has been achieved by considering the response of these materials when subjected to both homogeneous and non-homogeneous deformations. We have first compared the material characteristics of the generalized Blatz-Ko material with those of the Blatz-Ko material by considering homogeneous deformations. Specifically, we discussed the isotropic extension, the isotropic plane stress, the uni-axial tension, the isotropic plane strain, the plane-strain uni-axial tension, and the simple shear deformation. From the analysis of these homogeneous deformations we have obtained the following conclusions:

(i) For all values of $\beta > 0$, the distributions of Cauchy and Piola stresses are qualitatively similar in the isotropic extension, the uni-axial tension, the isotropic plane strain,

and the plane-strain uni-axial tension and they indicate that the material hardens as β increases.

(ii) For all values of $\beta > 1$, the distributions of Piola stresses in isotropic plane stress are qualitatively similar and they indicate that the material hardens as β increases. For $\beta \leq 1$, however, the distributions of Piola stresses corresponding to this deformation are qualitatively different from the distributions in the case when $\beta > 1$, although they still indicate that the material hardens as β increases.

(iii) For all values of $\beta \geq 2$, the distributions of Cauchy stresses in the simple shear deformation are qualitatively similar and they indicate that the material hardens as β increases. For $\beta < 2$, however, the distributions of Piola stresses corresponding to this deformation are qualitatively different from the distributions in the case when $\beta \geq 2$. In particular for $\beta < 2$, we can no longer conclude that the material hardens as β increases.

Further we have carried out the comparison by considering non-homogeneous deformations. We have used the semi-inverse method and, by generalizing the work of Carroll & Horgan [17], Abeyarante & Horgan [15], and Chung, Horgan & Abeyaratne [16], we have obtained closed-form solutions to the equilibrium equations for the non-homogeneous deformations describing the straightening of a sector of a circular tube, the bending of a rectangular block into a sector of a circular tube, the eversion of cylindrical and spherical shells, and the cylindrical and spherical expansions. Additionally, using both analytical and numerical methods we have investigated a number

of associated boundary value problems and, by means of a qualitative analysis, we have concluded that in respect of these deformations the materials in this class become harder as the material parameter β increases, but that otherwise they all behave in a similar manner.

Also, in this dissertation we have paid special attention to considerations on stability, non-existence and non-uniqueness of solutions. In order to describe the situations in which the solutions become unstable, we have reformulated the conditions for the strong ellipticity of the equilibrium equations for non-linearly elastic materials so as to be expressible in terms of the derivatives of the strain-energy function regarded as a function of the principal stretches. By using these conditions we have obtained necessary and sufficient conditions, in terms of restrictions upon the principal stretches, for the strong ellipticity of the generalized Blatz-Ko material (thereby generalizing the results obtained by Knowles & Sternberg [13] for the Blatz-Ko material) and found that for the six considered non-homogeneous deformations, the solutions become unstable when the loadings become larger than certain critical values. Conditions, in terms of boundary data, in which solutions of the pre-assigned form do not exist, have been also described and instances of non-uniqueness of solution have been dealt with by selecting on physical grounds the solution which appears to be the most plausible.

On the basis of the qualitative analysis involving both homogeneous and non-homogeneous deformations we conclude that all of the materials (1.13) for which $\beta \geq 2$ behave in the same manner and, consequently, that the materials (1.13) for which $\beta > 2$

also represent foam rubbers of the type described by the Blatz-Ko material ($\beta = 2$), the Blatz-Ko material being the softest material in the subclass defined by $\beta \geq 2$.

List of symbols

β — The material constant for the generalized Blatz-Ko material.

λ_i — Principal stretches.

μ — The material constant for the generalized Blatz-Ko material.

$\Im_0$ — Reference configuration.

$\Im$ — Deformed configuration.

τ_i — Principal stresses.

a — Inner radius of a cylindrical or spherical shell in the deformed configuration.

A — Inner radius of a cylindrical or spherical shell in the reference configuration.

$\mathbf{A}$ — Elasticity tensor.

$\mathbf{b}$ — Body force.

b — Outer radius of a cylindrical or spherical shell in the deformed configuration.

B — Outer radius of cylindrical or spherical shell in the reference configuration.

$\mathbf{B}$ — Left Cauchy-Green strain tensor.

$\mathbf{C}$ — Right Cauchy-Green strain tensor.

C_1, C_2 — Integration constants.

d_{ij} — Ratio of λ_i to λ_j.

$\mathbf{e}^i$ — An orthonormal vector basis in an Euclidean space.

$\mathbf{F}$ — Deformation gradient.

I_i — Principal invariants.

J — Jacobian determinant.

M — Moment.

$\mathbf{O}$ — An origin point in an Euclidean space.

P_A, P_B — Inner and external pressures.

(r, θ, z) — The cylindrical polar coordinates in the deformed configuration.

(r, θ, ϕ) — The spherical polar coordinates in the deformed configuration.

r_1, r_2 — Inner and outer radii of a sector of a circular tube in the deformed configuration.

(R, Θ, Z) — The cylindrical polar coordinates in the reference configuration.

(R, Θ, Φ) — The spherical polar coordinates in the reference configuration.

R_1, R_2 — Inner and outer radii of a sector of a circular tube in the reference configuration.

$\mathbf{R}$ — Rotation tensor.

$\mathbf{S}$ — Piola stress tensor.

$\mathbf{T}$ — Cauchy stress tensor.

t_E — Critical value of the strong ellipticity condition for the generalized Blatz-Ko material.

$\mathbf{U}$ — Right stretching tensor.

$\mathbf{V}$ — Left stretching tensor.

$\{\mathbf{v}^i\}$ — Principal axes of stretch.

w — Ratio of λ_1 to λ_2.

w_A — The value of w at $R = A$.

w_B — The value of w at $R = B$.

W — Strain energy function.

W_i — Partial derivative of W with respect to λ_i.

W_{ij} — Second partial derivative of W with respect to λ_i and λ_j.

$\mathbf{X}$ — A position vector in the reference configuration.

X_i — Components of $\mathbf{X}$.

$\mathbf{x}$ — A position vector in the deformed configuration.

x_i — Components of $\mathbf{x}$.

Bibliography

[1] R.S. Rivlin and D.W. Saunders. Large elastic deformations of isotropic materials VII: Experiments on the deformation of rubber. *Phil. Trans. Roy. Soc. Lond*, A 243:251–288, 1951.

[2] Y.C.B. Fung. Elasticity of soft tissues in simple elongation. *Am J. Physiology*, 213:1532–1544, 1967.

[3] P.J. Blatz and W.L. Ko. Application of finite elasticity to the deformation of rubbery materials. *Trans. Soc. Rheol.*, 6:223–251, 1962.

[4] D.R. Veronda and R.A. Westmann. Mechanical characterization of skin-finite deformations. *J. Biomechanics*, 3:111–124, 1970.

[5] R.M. Christensen. A two material constant, nonlinear elastic stress constitutive equation including the effect of compressibility. *Mechanics of Materials*, 7:155–162, 1988.

[6] J. Fong and W. Penn. Construction of a strain-energy function for an isotropic elastic material. *Trans. Society of Rheology*, 19:99–113, 1975.

[7] P. Flory and Y. Tatara. The elastic free energy and the elastic equation of state: elongation and swelling of polydimethylsiloxane network. *J. Polymer Science (Physics)*, 13:683, 1975.

[8] R.W. Ogden. Volume changes associated with the deformations of rubber-like solids. *J. Mech. Phys. Solids*, 24:313–338, 1976.

[9] S. Peng and R. Landel. Stored energy function and compressibility of compressible materials under large strain. *J. Applied Physics*, 46:2599–2604, 1975.

[10] L.R.G. Treloar. The elasticity and related properties of rubbers. *Rep. Prog. Phys.*, 36:755–826, 1973.

[11] R.W. Ogden. *Elastic deformations of rubberlike solids. Mechanics of Solids.* Eds. H.G. Hopkins and K.J. Sewell, Pergamon Press, 1982.

[12] R.J. Atkin and N. Fox. *An Introduction to the Theory of Elasticity.* Longman, London and New York, 1980.

[13] J.K. Knowles and E. Sternberg. On the ellipticity of the equations of nonlinear elastostatics for a special material. *J. Elasticity*, 5:341–361, 1975.

[14] M.F. Beatty. Topics in finite elasticity: Hyperelasticity of rubber, elastomers, and biological tissues – with examples. *Appl. Mech. Rev*, 40(12):1699–1734, 1987.

[15] R. Abeyaratne and C.O. Horgan. Initiation of localized plane deformations at a circular cavity in an infinite compressible nonlinearly elastic medium. *J. Elasticity*, 15:243–256, 1985.

[16] D.T. Chung C.O. Horgan and R. Abeyarate. The finite deformations of internally pressurized hollow cylinders and spheres for a class of compressible elastic materials. *Int. J. Solid Structures*, 22(12):1557–1570, 1986.

[17] M.M. Carroll and C.O. Horgan. Finite strain solutions for a compressible elastic solid. *Quart. Appl. Math.*, 48(4):767–780, 1990.

[18] C.O. Horgan and D.A. Polignone. A note on the pure torsion of a circular cylinder for a compressible nonlinearly elastic material with nonconvex strain-energy. *J. Elasticity*, 37(2):167–178, 1995.

[19] Y. Wang and M. Aron. Radial deformations of cylindrical and spherical shells composed of a generalized Blatz-Ko material. *J. Appl. Math. Mech. (ZAMM)*. in press.

[20] J.K. Knowles and E. Sternberg. On the failure of ellipticity of the equations for finite elastostatic plane strain. *Arch. Rational Mech. Anal.*, 63:321–336, 1977.

[21] M.F. Beatty and D.O. Stalnaker. The Poisson function of finite elasticity. *J. Appl. Mech., Trans. ASME*, 53:807–813, 1986.

[22] C.O. Horgan and R. Abeyaratne. A bifurcation problem for a compressible nonlinearly elastic medium: growth of a micro-void. *J. Elasticity*, 16:189–200, 1986.

[23] C.O. Horgan. Some remarks on axisymmetric solutions in finite elastics for compressible materials. *Proc. Roy. Irish Acad.*, A89:185–193, 1989.

[24] D.A. Polignone and C.O. Horgan. Axisymmetric finite anti-plane shear of compressible nonlinear elastic circular tubes. *Quart. J. Appl. Math.*, 50(2):323–341, 1992.

[25] D.A. Polignone and C.O. Horgan. Pure torsion of compressible nonlinearly elastic circular cylinders. *Quart. J. Appl. Math.*, 49(3):591–607, 1991.

[26] Q. Jiang and M.F. Beatty. On compressible materials capable of sustaining axisymmetric shear deformations. Part 1: Anti-plane shear of isotropic hyperelastic materials. *J. Elasticity*, 39:75–95, 1995.

[27] D.A. Polignone and C.O. Horgan. Pure azimuthal shear of compressible nonlinearly elastic circular tubes. *Quart. J. Appl. Math.*, 52(1):113–131, 1994.

[28] J.G. Murphy. Some new closed-form solutions describing spherical inflation in compressible finite elasticity. *IMA J. Appl. Math.*, 48:305–316, 1992.

[29] D.M. Haughton and K.A. Lindsay. The second-order deformation of a finite compressible isotropic elastic annulus subjected to circular shearing. *Proc. Roy. Soc. Lond.*, A442:621–639, 1993.

[30] D.M. Haughton. Circular shearing of compressible elastic cylinders. *Quart. J. Mech. Appl. Math.*, 51:471–486, 1993.

[31] M. Levinson and I.W. Burgess. A comparison of some simple constitutive relations for slightly compressible rubber-like materials. *Int. J. Mech. Sci.*, 13:563–572, 1971.

[32] M. Aron and Y. Wang. Remarks concerning the flexure of a compressible nonlinearly elastic rectangular block. *J. Elasticity*, 40:99–106, 1995.

[33] O.H. Varga. *Stress-strain behaviour of elastic materials.* Wiley, New York, 1966.

[34] D.M. Haughton. Inflation and bifurcation of thick-walled compressible elastic spherical shells. *IMA J. Appl. Math.*, 39:259–272, 1987.

[35] F. John. Plane strain problems for a perfectly elastic material of harmonic type. *Commun. Pure Appl. Math*, 13:239–296, 1960.

[36] A.J. Willson and P.J. Myers. A generalization of Ko's strain-energy function. *Int. J. Engng. Sci.*, 26:509–517, 1988.

[37] A.J. Willson and P.J. Myers. On the finite elastostatic deformation of thin-walled spheres and cylinders. *Int. J. Solids Structures*, 26:369–373, 1990.

[38] S.A. Silling. Creasing singularities in compressible elastic materials. *J. Appl. Mech., Trans. ASME*, 58:70–74, 1991.

[39] R. Hill. *Aspects of invariance in solid mechanics. In Advances in Applied Mechanics*, volume 18. Ed. C.-S. Yih, Academic Press, New York, 1978.

[40] B. Storakers. On material representation and constitutive branching in finite compressible elasticity. *J. Mech. Phys. Solids*, 34:125–145, 1986.

[41] D.M. Haughton. Cavitation in compressible elastic membranes. *Int. J. Engng. Sci.*, 28(2):162–168, 1990.

[42] S. Biwa. Critical stretch for formation of a cylindrical void in a compressible hyperelastic material. *Int. J. Non-linear Mech.*, 30(6):899–914, 1995.

[43] M. Aron and S. Aizicovici. Two new universal relations in nonlinear elasticity and some related matters. *J. Appl. Mech., Trans. ASME*, 61:784–787, 1994.

[44] J.L. Ericksen. Deformations possible in every isotropic, incompressible, perfectly elastic body. *J. Appl. Mech. Phys.(ZAMP)*, 5:466–489, 1954.

[45] J.L. Ericksen. Deformations possible in every compressible,isotropic,perfectly elastic material. *J. Math. Phys.*, 34:126–128, 1955.

[46] M Singh and A.C. Pipkin. Note on Ericksen's problem. *J. Appl. Mech. Phys.(ZAMP)*, 16:706–709, 1965.

[47] C. Truesdell and W. Noll. *The non-linear field theories of mechanics, Handbuch der Physik*, volume III/3. Ed. S. Flugge, Springer, Berlin Heidelberg New York, 1965.

[48] C. Truesdell. *The Elements of Continuum Mechanics.* Springer-Verlag, Berlin Heidelberg New York, 1966.

[49] A.J.M. Spencer. *Continuum Mechanics.* Longman, London and New York, 1980.

[50] R.W. Ogden. *Nonlinear Elastic Deformations.* Wiley, New York, 1984.

[51] E. Sternberg and J.K. Knowles. On the existence of an elastic potential for a simple material without memory. *Arch. Rational Mech. Anal.*, 70:19–30, 1979.

[52] J.K. Knowles and E. Sternberg. On the singularity induced by certain mixed boundary condition in linearized and nonlinear elastostatics. *Int. J. Solids Structures*, 11:1173–1201, 1975.

[53] A.H. Jafari R. Abeyaratne and C.O. Horgan. The finite deformation of a pressurized circular tube for a class of compressible materials. *J. Appl. Mech. Phys.(ZAMP)*, 35:227–246, 1984.

[54] M. M. Carroll. Finite strain solutions in compressible isotropic elasticity. *J. Elasticity*, 20:65–92, 1988.

[55] M. Aron. On a class of plane radial deformations of compressible nonlinear elastic solids. *IMA J. Appl. Math.*, 52:289–296, 1994.

[56] R.W. Ogden. Large deformation isotropic elasticity-on the correlation of theory and experiment for compressible rubberlike solids. *Phil. Roy. Soc. Lond.*, A328:567–583, 1972.

[57] H.C. Simpson and S.J. Spector. On copositive matrices and strong ellipticity for isotropic elastic materials. *Arch. Rational Mech. Anal.*, 84:55–68, 1983.

[58] P. Rosakis. Ellipticity and deformations with discontinuous gradients in finite elastostatics. *Arch. Ration. Mech. Anal.*, 109:1–37, 1990.

[59] L.M. Zubov and A.N. Rudev. An effective method of verifying Hadamard's condition for a non-linearly elastic compressible medium. *J. Appl. Math. Mech*, 52:252–260, 1992.

[60] R. Hill. On the theory of plane strain in finitely deformed compressible materials. *Math. Proc. Camb. Phil. Soc*, 86:161–178, 1979.

[61] G. Aubert and R. Tahraoui. Sur la faible fermeture de certains ensembles de containes en elasticite' non-lineaire plane. *Arch. Ration. Mech. Anal.*, 97:33–59, 1987.

[62] P.J. Davies. A simple derivation of necessary and sufficient conditions for the strong ellipticity of isotropic hyperelastic materials in plane strain. *J. Elasticity*, 26(3):291–296, 1991.

[63] R.S. Rivlin. Stability of pure homogeneous deformations of an elastic cube under dead loading. *Quart. J. Appl. Math.*, 32:265–272, 1974.

[64] M.E. Gurtin and S.J. Spector. On stability and uniqueness in finite elasticity. *Arch. Rational Mech. Anal*, 70:153–165, 1970.

[65] S.S. Antman. The eversion of thick spherical shells. *Arch. Ration. Mech. Anal.*, 70:113–123, 1979.

[66] C. Truesdell. *Some challanges offered to analysis by rational thermodynamics. in Contemporary developments in continuum mechanics and pratial differential equations.* Eds. G.M. De La Penha and L.A. Medeiros, Springer, Berlin Heidelberg New York, 1978.

[67] A.E. Green and J.E. Adkins. *Large elastic deformations.* Clarendon Press, Oxford, 1960.

[68] R.S. Rivlin. Large elastic deformations of isotropic materials VI: Further results in the theory of trosion, shear and flexure. *Phil. Trans. Roy. Soc. Lond*, A 242:173–195, 1949.

[69] P. Chadwick. The existence and uniqueness of solutions of two problems in the Mooney-Rivlin theory for rubber. *J. Elasticity*, 2:123–128, 1972.

[70] S.A. Adeleke. On the problem of eversion for incompressible elastic materials. *J. Elasticity*, 13:23–69, 1983.

[71] J.M. Ball. Discontinuous equilibrium solutions and cavitation in nonlinear elasticity. *Phil. Trans. Roy. Soc.*, A306:557–611, 1982.

[72] D.M. Haughton and A. Orr. On the eversion of incompressible elastic cylinders. *Int. J. Non-linear Mech.*, 30(2):81–95, 1995.